Universidad Rey Juan Carlos

DOCTORAL THESIS

Environmental and economic assessment and optimization of a novel technology for furfural production through life cycle tools

Author:

Jorge Blanco Cejas

Supervisors:

Jovita Moreno Vozmediano
María Linares Serrano

Doctoral Program in Industrial Technologies: Chemical, Environmental, Energy, Electronic, Mechanic and Materials

International Doctoral School

2024

Jovita Moreno Vozmediano, Profesora Titular de Universidad en el área de Ingeniería Química del Departamento de Tecnología Química y Ambiental, de la Universidad Rey Juan Carlos,

y

María Linares Serrano, Profesora Titular de Universidad en el área de Ingeniería Química del Departamento de Tecnología Química, Energética y Mecánica, de la Universidad Rey Juan Carlos.

Certifican:

Que el presente trabajo de investigación titulado "*Environmental and economic assessment and optimization of a novel technology for furfural production through life cycle tools*" constituye la memoria que presenta el Ingeniero Jorge Blanco Cejas para aspirar al grado de Doctor por la Universidad Rey Juan Carlos, y ha sido realizado en el Grupo de Ingeniería Química y Ambiental de la Universidad Rey Juan Carlos bajo nuestra dirección.

Y para que así conste, firmamos el presente certificado en Móstoles, a de de 2024.

Fdo: Jovita Moreno Vozmediano Fdo: María Linares Serrano

Agradecimientos

RESUMEN

ANTECEDENTES

La crisis ambiental es uno de los principales retos de nuestra era. En una sociedad dependiente del sistema productivo, la industria juega un papel determinante. Así, la transición hacia una economía consciente de las capacidades de carga del planeta resulta primordial. Este cambio de paradigma precisa políticas claras que establezcan objetivos ambiciosos a distintos horizontes temporales. En la Unión Europea, la principal herramienta para la diseminación y activación de acciones concretas es el Pacto Verde Europeo (PVE). El PVE está constituido por un conjunto de iniciativas que tratan de cubrir tres objetivos generales: alcanzar la neutralidad de emisiones netas de CO_2 para el año 2050, desvincular el crecimiento económico del consumo de recursos, y proteger la biodiversidad disminuyendo los niveles de contaminación.

Cualquiera de estos objetivos pasa por la integración de la bioeconomía circular como modelo dominante del tejido industrial europeo. Esto supone disminuir la dependencia de los combustibles fósiles, mitigar el problema en la gestión de residuos, y descarbonizar uno de los sectores más relevantes del territorio. La biomasa lignocelulósica se postula en este sentido como una materia prima estratégica debido a su abundancia, su bajo coste y su versatilidad para producir diversos productos químicos o combustibles. Además, durante su crecimiento esta biomasa absorbe CO_2. A diferencia de en el caso de los combustibles fósiles, este carbono forma parte del ciclo biogeoquímico, por lo que su emisión o secuestro no suponen un incremento neto del carbono atmosférico.

El aprovechamiento de la biomasa se lleva a cabo en instalaciones industriales análogas a las refinerías convencionales. Estas plantas se enfrentan a retos principalmente relacionados con la recalcitrancia y la fluctuación estacional de la biomasa. No obstante, su penetración en el mercado es una realidad, con más de 2000 biorrefinerías operando en Europa en la actualidad.

La fuerza impulsora para el establecimiento de estas tecnologías es el valor añadido de los productos que pone a disposición del mercado. Este valor no es únicamente monetario, si no que añade una componente ambiental que ha de traducirse en una ventaja competitiva. Este trabajo pone el foco en la producción a escala comercial de furfural, debido a su destacado interés como molécula plataforma. Desde hace décadas, la producción de furfural está relegada a países con una legislación ambiental relativamente laxa por su elevado consumo energético y la producción de residuos ácidos. Sin embargo, su demanda sigue siendo elevada y se espera que incremente en los próximos

años, por lo que el impacto no desaparece si no que se externaliza. El desarrollo de alternativas tecnológicas para la producción de furfural, supondría la deslocalización de la producción y por tanto disminuiría las dependencias comerciales.

La sustitución a nivel industrial tiene que venir precedida de unos índices de rentabilidad competitivos y una mejora ambiental que permita la operación dentro de las fronteras comunitarias. Asegurar estas mejoras comienza por conocer los detalles de los procesos convencionales a fin de contar con una referencia válida para la comparación. La metodología más completa disponible para observar la implicación de todas las entradas y salidas en un sistema de producto el análisis de ciclo de vida (ACV). El ACV permite la comparación rigurosa de dos sistemas y la identificación de los cuellos de botella que restringen la implantación de un proceso. La integración de este análisis en la fase de diseño permite la optimización de la producción a nivel económico y ambiental.

OBJETIVOS

Esta tesis doctoral se centra en evaluar la viabilidad de un proceso novedoso para la producción de furfural en base a su desempeño económico y ambiental, así como identificar los puntos críticos que dificultan su implantación. Este objetivo general se acomete desde la consecución de los siguientes objetivos parciales:

- Identificación de las mejores prácticas metodológicas para el análisis de la sostenibilidad medioambiental en el contexto de la tesis.
- Generación de un inventario de tecnologías de referencia mediante la simulación rigurosa de los datos bibliográficos existentes.
- Asegurar condiciones de simulación y ACV comparables para operar dentro del mismo marco metodológico en el caso de las tecnologías convencionales y la tecnología propuesta.
- Análisis del ciclo de vida de la tecnología propuesta para sustituir la producción convencional de furfural.
- Comparación del perfil ambiental obtenido mediante ACV con el de las tecnologías de referencia para evaluar las divergencias, los puntos críticos y los potenciales aspectos de mejora.

- Evaluar un caso de estudio sobre la construcción de una planta de producción de furfural en España empleando la nueva tecnología propuesta e incluyendo el diseño y optimización de la cadena de suministro en función de parámetros económicos y medioambientales.

METODOLOGÍA

Para la consecución de estos objetivos se han empleado las tres herramientas computacionales que se enumeran a continuación.

La obtención de todas las entradas y salidas de los procesos comerciales y del proceso propuesto como alternativa tecnológica se obtuvieron mediante la simulación en Aspen Plus. Los datos para construir estas simulaciones fueron obtenidos a partir de literatura en el caso de los procesos convencionales. Para la simulación del proceso alternativo se emplearon datos procedentes de la colaboración con otros grupos de investigación.

El análisis de ciclo de vida de todos los procesos se llevó a cabo empleando la herramienta de código abierto Brightway. Para el manejo de Brightway se empleó la interfaz Activity Browser. Los datos del sistema de background fueron obtenidos de la base de datos de Ecoinvent (v3.9), usando la configuración de modelado APOS ('At the Point Of Substitution') para capturar todos los flujos del sistema.

Por último, el modelo algebraico para la optimización de la cadena de suministro fue implementado en GAMS (v45.7). El solver utilizado para la resolución del sistema lineal de ecuaciones fue el CPLEX.

RESULTADOS

Se llevó a cabo la revisión bibliográfica de los estudios de ACV publicados hasta la fecha sobre las biomoléculas de mayor relevancia. Esto permitió identificar las decisiones metodológicas con mayor influencia sobre los resultados en este tipo de sistemas de producto. Con ello, se propuso la consideración del secuestro del carbono biogénico en estudios de la cuna a la puerta. Para identificar y reportar la incertidumbre de procesos de baja madurez tecnológica, se propuso el empleo de la matriz de Pedigree para la determinación de la variabilidad de las entradas. Como método preferido para la propagación de esta incertidumbre se propone el muestreo por Monte Carlo. Por último, para afrontar la multifuncionalidad se propone el enfoque consecuencial como primera alternativa. En caso de que la baja disponibilidad

de datos favorezca el uso de la perspectiva atribucional, se refiere a la jerarquía establecida en la ISO 14044.

En segundo lugar, se simuló de manera rigurosa la producción de furfural en los procesos con mayor implantación: el proceso Quaker Oats, y el proceso chino por lotes. Se determinó que, si bien los residuos ácidos resultan tratables, el principal problema de su uso reside en los problemas de corrosión. El aumento en el espesor de la pared del reactor fuerza a calentar el reactor mediante la condensación de vapor inyectado directamente. Esto disminuye significativamente la eficiencia, y genera un elevado impacto por la quema de combustibles para la generación del caudal de vapor requerido.

Se observó también que los impactos del proceso chino son más elevados por la mayor dilución del ácido. Esto mejora la cinética de reacción, pero implica una entrada de agua de dilución muy superior en este proceso. Consecuentemente, el tamaño de los equipos aumenta y por tanto sus requerimientos energéticos. Asimismo, obliga a una recuperación de calor más ineficiente en la primera columna de destilación, lo que resulta uno de los puntos críticos del sistema.

Por último, se pudo comprobar cómo una de las mayores ineficiencias del proceso viene del desaprovechamiento del 90% de la biomasa de partida, ya que sólo parte de la fracción hemicelulósica (<40%) es aprovechada. Ambos procesos consumen residuos, lo que ayuda significativamente a la minimización de los impactos por ocupación de terreno. Esto resulta un punto interesante para futuros procesos basados en biomasa. Se determinó que el proceso alternativo para la producción de furfural, basado en el fraccionamiento de biomasa lignocelulósica, produce un menor impacto en diez categorías ambientales de las dieciséis contempladas en la normativa europea. Los problemas en el calentamiento del reactor y en la eficiencia en el uso de biomasa son ampliamente superados, si bien los consumos energéticos asociados a la recuperación de disolvente (ɣ-valerolactona, GVL) son excesivos.

La recuperación de GVL resulta en un ahorro de costes muy significativo, por lo que los objetivos económico y ambiental van en sentidos opuestos. El diseño actual opera en el máximo económico, puesto que se busca minimizar el riesgo financiero al tratarse de un proceso totalmente nuevo. No obstante, operando dentro del margen de rentabilidad, es posible reducir la emisión de hasta dos toneladas por hora de CO_2 equivalente.

El proceso de fraccionamiento obtiene como coproductos celulosa y lignina. Los costes anualizados de cubrir la demanda pueden reducirse de forma

significativa con respecto al escenario actual. Las funciones ambientales sin embargo se encuentran severamente restringidas. Esto hace que en el mejor de los casos se consiga un ahorro del 24% de los costes anualizados y un 2% en los impactos sobre la salud humana. A cambio, la afección a la biodiversidad y el consumo de recursos naturales aumentarían en un 26% y un 21% respectivamente. El primero de los casos está dominado por la mayor ocupación de terreno de la biomasa de partida, al provenir de un cultivo forestal dedicado en lugar de ser residual. El aumento en el consumo de recursos deriva del elevado requerimiento energético de la recuperación de GVL.

CONCLUSIONES

De forma general, esta tesis ha permitido analizar en detalle el perfil ambiental de los procesos convencionales de producción de furfural mediante la construcción de inventarios inexistentes en la literatura. Estos sistemas se han empleado como referencia para evaluar el desempeño económico y ambiental de un proceso alternativo de producción basado en una tecnología de fraccionamiento Organosolv y en el aprovechamiento integral de todas las fracciones de la corriente de biomasa. El estudio realizado ha permitido identificar los principales puntos críticos que deberían ser abordados para la posible implantación de esta nueva tecnología productiva en Europa.

SUMMARY

BACKGROUND

The environmental crisis is one of the main challenges of our era. In a society dependent on the production system, industry plays a decisive role. Thus, the transition to an economy aware of the planet's carrying capacities is paramount. This paradigm shift requires clear policies that set ambitious goals at different time horizons. In the European Union, the main tool for the dissemination and activation of tangible actions is the European Green Deal (EUGD). The EUGD is made up of a set of initiatives that aim to cover three general objectives: achieve net-zero emissions by 2050, decouple economic growth from resource consumption, and protect biodiversity by reducing pollution levels.

Any of these objectives involves the integration of the circular bioeconomy as the dominant model of the European industry. This means reducing dependence on fossil fuels, mitigating the problem in waste management, and decarbonizing one of the most relevant sectors of the territory. Lignocellulosic biomass is postulated in this sense as a strategic raw material due to its abundance, low cost, and versatility to produce various chemicals or fuels. In addition, during its growth, the biomass absorbs CO2. Unlike in the case of fossil fuels, this carbon is part of the biogeochemical cycle, so its emission or sequestration does not imply a net increase in atmospheric carbon.

The use of biomass is carried out in industrial facilities similar to conventional refineries. These plants face challenges mainly related to the recalcitrance and seasonal fluctuation of biomass. However, its penetration in the market is a reality, with more than 2000 biorefineries operating in Europe today.

The driving force for the establishment of these technologies is the value of the products they produce. This value is not only monetary but encompasses an environmental component that must be translated into a competitive advantage. This work focuses on the commercial-scale production of furfural, due to its outstanding interest as a platform molecule. For decades, the production of furfural has been relegated to countries with relatively lax environmental legislation due to its high energy consumption and the production of acidic waste. However, its demand remains high and is expected to increase in the coming years, so the impact does not disappear but is externalized. The development of technological alternatives for the production of furfural would mean the delocalization of production and therefore would decrease commercial dependencies.

Industrial substitution must be preceded by competitive profitability indices and an environmental improvement that allows operation within the European borders. Ensuring these improvements begins by acknowledging the details of conventional processes in order to have a valid reference for comparison. The most complete methodology we have to observe the implication of all inputs and outputs in a product system is the life cycle analysis (LCA). The LCA allows the rigorous comparison of two systems and the identification of the bottlenecks that restrict the implementation of a process. The integration of this analysis in the design phase allows the optimization of production at an economic and environmental level.

OBJECTIVES

This doctoral thesis focuses on evaluating the viability of a novel process for the production of furfural based on its economic and environmental performance, as well as identifying the critical points that hinder its implementation. This objective is tackled from the achievement of the following partial objectives:

- Identification of the best methodological practices for the analysis of environmental sustainability in the context of the thesis.
- Generation of an inventory of reference technologies through rigorous simulation of existing bibliographic data.
- Ensure comparable simulation and LCA conditions operate within the same methodological framework in the case of conventional technologies and the proposed technology.
- Life cycle analysis of the proposed technology to replace conventional furfural production.
- Comparison of the environmental profiles obtained by LCA with those corresponding to the reference technologies to evaluate divergences, critical points, and improvement potentials.
- Assessment of a case study on the construction of a furfural production plant in Spain using this new technology, including the design and optimization of the supply chain based on economic and environmental parameters.

METHODOLOGY

To achieve these objectives, the following computational tools have been used.

All inputs and outputs of commercial and proposed processes were obtained through simulation in Aspen Plus. The data to build these simulations were obtained from literature in the case of conventional processes. For the simulation of the alternative process, data from collaboration with other research groups were used.

The life cycle analysis of all processes was carried out using the open-source tool Brightway. The Activity Browser interface was used to handle Brightway. The background system data were obtained from the Ecoinvent database (v3.9), using the APOS ('At the Point Of Substitution') modelling configuration to capture all system flows.

Finally, the algebraic model for the optimization of the supply chain was implemented in GAMS (v45.7). The solver used to solve the linear system of equations was CPLEX.

RESULTS

A bibliographic review was conducted on the LCA studies published to date on the most relevant biomolecules. This allowed the identification of the methodological decisions with the greatest influence on the results in this type of product system. With this, the consideration of the sequestration of biogenic carbon in cradle-to-gate studies was proposed. To identify and report the uncertainty of low technological maturity processes, the use of the Pedigree matrix was proposed to determine the variability of the inputs. Monte Carlo sampling is selected as the preferred method for propagating this uncertainty. Finally, to address multifunctionality, the consequential approach is proposed as the first alternative. In case the low availability of data favours the use of the attributional perspective, the hierarchy established in ISO 14044 should be followed.

Secondly, the production of furfural in the most widely implemented processes was rigorously simulated: the Quaker Oats process, and the Chinese batch process. It was determined that, while acidic waste is treatable, the main problem with acid use lies in corrosion issues. The increase in the thickness of the reactor wall forces the reactor to be heated by the condensation of directly injected steam. This significantly decreases efficiency and generates a high impact due to the burning of fuels for the generation of this fluid.

It was also observed that the impacts of the Chinese process are higher due to the larger dilution of the acid. This improves the reaction kinetics, but implies a greater dilution water input in this process. Consequently, the size of the equipment increases and therefore its energy requirements. Furthermore,

it also forces a more inefficient heat recovery in the first distillation column, which is one of the critical points of the system.

Finally, it was found that one of the largest inefficiencies of the process comes from the losses of 90% of the starting biomass, as only part of the hemicellulosic fraction (<40%) is used. Both processes consume agricultural residues, which significantly helps to minimize the impacts of land occupation, which is an interesting point for future biomass-based processes.

Relative to the alternative process for the production of furfural, based on the fractionation of lignocellulosic biomass, it was determined that it produces a lower impact in ten environmental categories of the sixteen contemplated in the European regulations. The problems in heating the reactor and in the efficiency in the use of biomass are widely overcome, although the energy consumption associated with the recovery of solvent (ɣ-valerolactone, GVL) is excessive. The recovery of GVL results in a very significant cost saving, so the economic and environmental objectives go in opposite directions. The current design operates at the economic maximum, as it seeks to minimize financial risk as it is a completely new process. However, operating within the profitability margin, it is possible to reduce the emission of up to two tons per hour of equivalent CO_2.

The fractionation process obtains cellulose and lignin as co-products. The annualized costs of meeting demand can be significantly reduced compared to the current scenario. Environmental functions, however, are severely constrained. This means that in the best case, a saving of 24% of the annualized costs and a 2% impact on human health is achieved. In return, the impact on biodiversity and the consumption of natural resources would increase by 26% and 21% respectively. The first impact is dominated by the greater occupation of land by biomass, as it comes from dedicated forest crops instead of being residual. The increase in resource consumption derives from the high energy requirement of GVL recovery.

CONCLUSIONS

In conclusion, this doctoral thesis has facilitated to analyse in detail the environmental profile of conventional processes for furfural production through the construction of inventories that are not present in the existing literature. These have been utilised as benchmark to assess the environmental performance of an alternative production process based on an Organosolv fractionation technology that leads to an integral use of all fractions of the

biomass stream. This study has allowed to identify critical points that should be overcame for a feasible implementation in Europe.

TABLE OF CONTENTS

INTRODUCTION

Today's society faces a multitude of pressing environmental challenges. While this is not unique in history, the urgency and potential consequences of these challenges demand timely and precise solutions as never before. These solutions inevitably involve adaptation of the production system to a context focused on sustainability. A representative example is the chemical industry, one of the world's dominant economic sectors. According to previous studies, less than 1% of the compounds manufactured are produced in a way that respects the carrying capacity of the planet [1].

Among the most critical aspects to deal with are climate change and the consumption of natural resources. A promising alternative to address both issues together is the substitution of fossil-based raw materials and fuels with bio-based ones. Biomass is an attractive alternative as it is an abundant, renewable source and integrates a part of the carbon cycle. Therefore, this thesis focuses on the use of biomass to produce bulk chemicals. Specifically, furfural production, a commodity with a large market volume, is proposed as a case study given its relevance.

Suggesting technological developments to speed up this transition implies prospecting among several alternatives so that the best options can be selected from the early stages of design. Process design, coupled with life cycle assessment (LCA), allows the environmental impacts of different candidates to be systematically explored, supporting and accelerating decision-making.

This introduction section is focused on contextualizing the current picture of our productive system, its needs of adaptation and how a bio-based chemical industry could contribute to reduce our environmental footprint. Thus, Section 1.1 describes the current environmental landscape in detail, with a strong focus on legislative developments and standards promoted by the European Community.

Taking this paradigm as a framework, Section 1.2 provides an overview of the state of the art of biorefineries, their importance and the logistical challenges influencing their development.

Section 1.3 presents a dissertation on furfural, its main characteristics and expected market forecasts. In this section, particular emphasis is placed on production processes, as this is one of the main focuses of this work.

1.1. Current environmental situation and policymaking

1.1.1. Current environmental situation

Human-induced global warming is a widely acknowledged and thoroughly documented phenomenon. Rather than focusing on distant future effects, we are now confronted with ongoing changes. For instance, the global average temperature over the past decade has exceeded that of the period between 1850 and 1900 by 1.1°C [2]. These rising temperatures have led to a proliferation of adverse phenomena, affecting the natural environment (e.g., droughts, loss of biodiversity), society (e.g., human health, vulnerable populations), and the economy (e.g., impacts on infrastructure and agriculture), as categorized by the European Commission. Furthermore, according to the World Health Organization (WHO), climate change is expected to cause an additional 250,000 deaths per year between 2030 and 2050 due to malnutrition, malaria, diarrhoea, and heat stress [3].

This increase in temperature is primarily attributed to the elevated concentrations of carbon dioxide (CO_2) and methane (CH_4) in the atmosphere [4]. In 2019, the primary sources of these greenhouse gases (GHGs) were the combustion of fossil fuels for energy production (20 Gt CO_2-eq) and industrial activities (14 Gt CO_2-eq) [2]. However, the consequences of this overreliance on fossil fuels extend beyond GHG emissions. Fossil fuel reserves are not only physically finite but also economically constrained, with most conventional gas, oil, and coal deposits projected to be depleted by 2100, according to Höök et al. [5]. Furthermore, the localized nature of these reserves leads to geopolitical dependencies and potential conflicts, as witnessed in recent events in Europe

[6]. This *de facto* implies that any environmental issue will inevitably lead to social and economic consequences. For instance, the economic costs of climate change are staggering. According to the National Bureau of Economic Research, unmitigated climate change could result in a 10.5% loss in GDP by 2100 [7]. In this sense, developing countries are disproportionately affected due to their geographical location and limited adaptive capacity [8].

While the urgency to address these issues is clear, it's essential to recognize that the scope of challenges goes far beyond climate change. The intricate interconnections within ecosystems and planetary dynamics mean that even slight imbalances can trigger chain reactions with indirect consequences. This was emphasized by Lenton et al. [9], who identified critical tipping points that, if crossed, could lead to irreversible consequences. Furthermore, the concept of planetary boundaries introduced by Richardson et al. [10] include other critical environmental issues such as biosphere integrity, land-system change, or altered biogeochemical cycles among others (see Figure 1.1).

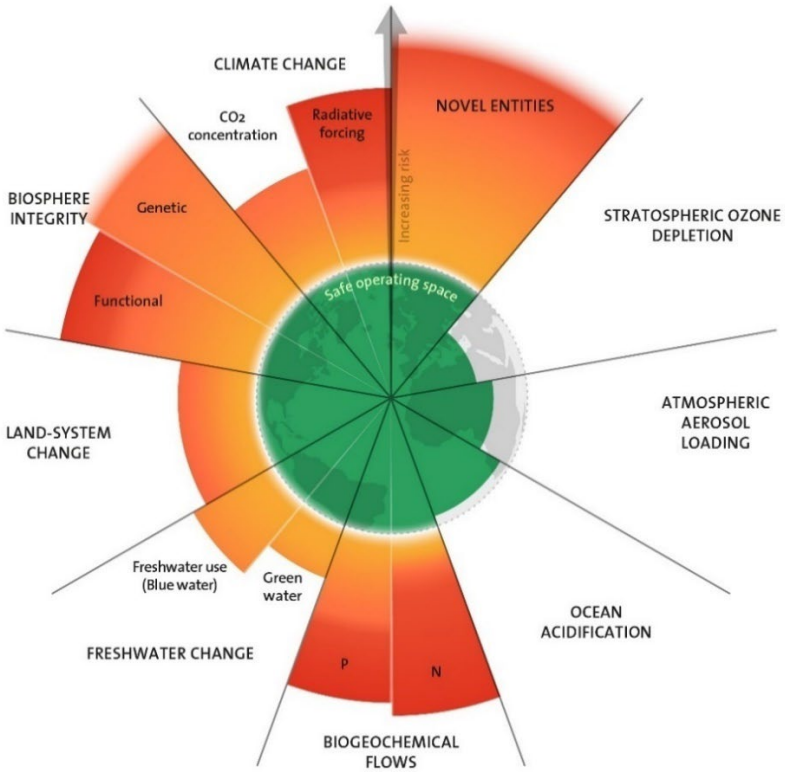

Figure 1.1 Planetary boundaries identified and measured in in Richardson et al. 2023 [10].

Transgressing these boundaries could lead to a state of the Earth system that is inhospitable to human societies and many other life forms. Currently, six of the nine identified and measured indicators have already been surpassed. Besides, according to the authors the pressure exerted on these environmental compartments is increasing in all cases except for the ozone depletion.

This situation underscores the urgency of transitioning to a renewable and clean production system [11] which, undoubtedly, involves major challenges. The intermittent nature of renewable energy sources, the requirement for energy storage and grid infrastructure upgrades, and the social and economic implications of moving away from fossil fuel industries are all significant obstacles that must be addressed [12]. The section 1.1.2 focuses on European legislation and policy-making efforts. This regional perspective provides context for the ensuing discussions, acknowledging the role of European policies in the global response to all these challenges.

1.1.2. Environmental legislation and policies in the European context

European environmental policy is structured in a fairly understandable way. There is a core policy based on objectives that is periodically renewed, and from these guidelines all concrete actions and plans are derived. These objectives are formulated as strategic documents that set out objectives and a roadmap for achieving them over a given period. These documents are the Environmental Action Plans (EAPs). The first EAP was published in 1973, while the latest, the 8th EAP, covers the period from 2022 to 2030. In 2015, during the validity period of the seventh EAP, the United Nations (UN) published the Sustainable Development Goals (SDGs), which are part of the 2030 Agenda also developed by the UN. The European Union (EU) played a crucial role in defining these goals. Therefore, the 8th EAP, published seven years after the SDGs, was intentionally aimed at achieving them. However, the scope of these environmental actions is not sufficient to meet the social and economic needs set out in the SDGs. Given this lack of alignment, in 2019 the EU published a much more ambitious plan in terms of targets and time horizon. This plan is the European Green Deal (EUGD), a roadmap for achieving sustainability in the European Union by 2050. This section outlines the main objectives and policies promoted by the EUGD, as it is the most comprehensive and detailed instrument currently active.

The European Green Deal has three core objectives, from which more specific goals are derived. These are: achieving net-zero greenhouse gas

emissions by 2050, decoupling economic growth from resource use, and ensuring "no person or place is left behind". To achieve the proposed goals, various areas of work are distinguished, such as climate change, industries, energy, and environment amongst others. In the field of climate change, the European Union has set the ambitious goal of achieving climate neutrality across Europe by 2050. To ensure that this goal is not merely aspirational, the Commission has introduced the European Climate Law, which legally enshrines this objective. The law also establishes a more aggressive target of reducing net greenhouse gas emissions by a minimum of 55% by 2030, relative to 1990 levels. The Commission has committed to the European Climate Pact and pledged to achieve climate neutrality in its operations by 2030. As a part of its Communication and action plan on Greening the Commission, adopted in April 2022, the Commission aims to gradually reduce its greenhouse gas emissions by at least 60% compared to 2005 levels. Any remaining emissions in 2030 will be offset with high-quality certified carbon removals. Additionally, in February 2024, the Commission announced an interim climate target for the EU for 2040. This target aims to achieve a 90% reduction in net greenhouse gas emissions compared to 1990 levels.

To achieve the decarbonisation target, it is essential to reduce emissions across all sectors. To this end, the transition to a circular economy is one of the fundamental building blocks of the existing actions. This plan is allocated within the work area of 'Environment and Oceans', and its results are key in an economy-driven context. The doctoral thesis presented here focuses on sustainable process design and its life cycle evaluation within the context of the circular economy, so discussion hereafter is pointed towards this specific work area given its relevance.

I. Circular Bioeconomy

The circular economy is a production and consumption model that aims to extend the life cycle of products and minimise waste. When a product reaches the end of its life, its materials are recycled and reused to create further value. This model departs from the traditional linear economic model and aims to address global challenges, such as climate change, biodiversity loss, waste, and pollution, by decoupling economic activity from the consumption of finite resources. This is exemplified in Figure 1.2.

In March 2020, the European Commission introduced the new Circular Economy Plan, which is considered one of the main pillars for the development of the EUGD. The plan aims to enhance the environment, stimulate the economy, and generate employment opportunities, thereby

integrating the three dimensions of sustainability. It adopts a comprehensive approach and is founded on the life cycle of production processes, encompassing every stage from design to end-of-life. The plan comprises a catalogue of 35 measures, which can be accessed at [13]. These measures include legislative and non-legislative instruments, which are monitored over time to ensure their proper implementation. The actions outlined in the Plan are translated into specific policies and tools, such as sustainable products, critical raw materials, eco-labelling, and environmental footprint methodology.

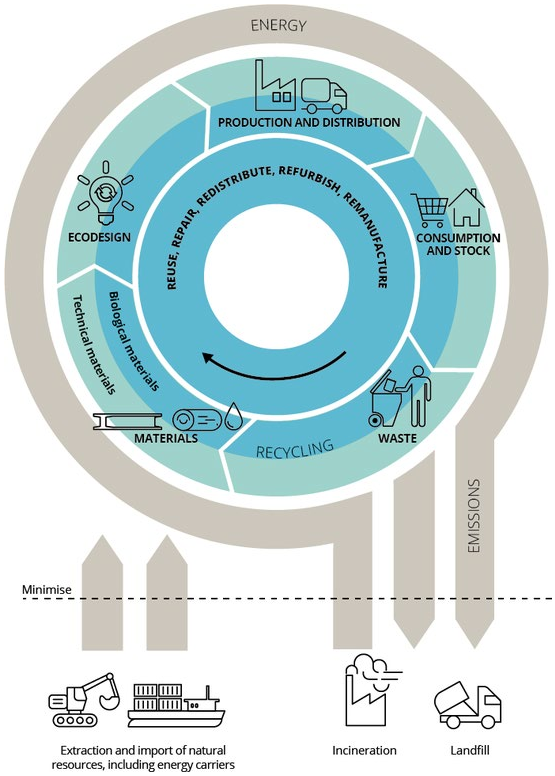

Figure 1.2. Circular economy framework.

When coupled with the substitution of fossil resources for biomass, the concept of a circular bioeconomy is introduced. This framework proposes closed loops of cascading biomass use and is directly tied to the biorefinery concept developed in Section 1.2 [14, 15]. The EU strongly supports this model through the EUGD framework. It evaluates, proposes strategies, and monitors their implementation based on the unique characteristics of each EU territory [16]. The relevance of this industry is easily perceived through its figures. When examining data as early as 2021, the bioeconomy in the EU had an overall value of approximately €2 trillion in annual turnover, with over 18 million people

employed. It contributed €621 billion in added value, which is equivalent to 4.2% of the EU's GDP [17].

II. Funding

The size of the goals implies funding of the same magnitude. Understanding the structure provides opportunities to contribute to the aforementioned objectives. Therefore, it is relevant to mention this budget model in this section as separate information. The European Commission has committed to mobilising a minimum of €1 trillion in sustainable investments over the next decade to finance the European Green Deal [18]. This funding is expected to come from a variety of sources, including the EU budget, national funds, and private sector investments. At the European level, €600 billion of the €1.8 trillion from the NextGenerationEU (NGEU) Recovery Plan and the EU budget for the next seven years is expected to finance the European Green Deal [19]. These funds are intended to be deployed between 2021 and 2027. Aside from that, the Cohesion Policy is the European Union's primary investment policy, aimed at reducing economic, social, and territorial disparities among regions. This initiative aims to support job creation, business competitiveness, economic growth, sustainable development, and improvements to citizens' quality of life in all regions of the European Union. An additional €118 billion from the Cohesion Policy until 2027 has been earmarked to support the EUGD [20].

At the national level, EU countries are required to allocate a minimum of 37% of the funding received from the €672.5 billion Recovery and Resilience Facility to investments and reforms that promote climate objectives. All investments and reforms must be aligned with the EU's environmental objectives. The Commission, acting on behalf of the EU, plans to generate 30% of the funds under NGEU by issuing green bonds [18].

For the channelling of these funds, the EU has a fair distribution mechanism known as the Just Transition Mechanism (JTM). It supports the regions most affected by the transition and aims to mobilise at least €100 billion from 2021 to 2027 [21]. In addition to the EU's budget contributions through all transition-relevant instruments, this support is provided. The JTM consists of three main financing sources. The first one in thought fresh EU funds that will contribute to The Just Transition Fund with €7.5 billion. Secondly, Member States are committed to matching their budget from the Just Transition Fund with funds from the European Regional Development Fund and the European Social Fund Plus, as well as additional national resources. This approach is expected to provide funding between €30 and €50 billion.

Finally, a just transition scheme dedicated to InvestEU [22] aims to mobilise up to €45 billion of investments. This scheme aims to attract private investments. A loan facility for the public sector has been established with the European Investment Bank, supported by the EU budget. The facility is expected to generate investments of between €25 and €30 billion.

Regarding the private sector, it has a crucial role to play in the successful implementation of the European Green Deal. Its active participation is essential to meet the EUGD's climate neutrality goal as it is responsible for over 80% of greenhouse gas emissions in the EU. Private sector contributions to the European Green Deal come in various forms, such as direct investments in green and sustainable projects, technological innovations, and the development of sustainable business practices. The private sector is expected to leverage the funding provided by the EU through various mechanisms, such as the JTM and InvestEU, to mobilise additional investments. The European Commission has implemented various measures to promote private sector investment in green and sustainable projects, including the Taxonomy Regulation for classifying green investments [18]. The objective is to establish a regulatory and financial environment that encourages private sector entities to align their business strategies with the goals of the EUGD.

The bioeconomy is a sector that is particularly relevant to achieving climate targets. In this regard, the Circular Bio-based Europe Joint Undertaking (CBE-JU) is a key initiative for promoting the use of bio-based materials. Its creation is aimed at advancing the development of a circular economy in Europe. The CBE-JU is a €2 billion partnership between the EU and the Bio-based Industries Consortium (BIC). Under Horizon Europe, the EU's research and innovation programme, it supports projects that promote competitive circular bio-based industries, and it is considered a strategic financial instrument for Europe's biotech and biomanufacturing sector. In 2022, the CBE JU developed the Strategic Research and Innovation Agenda (SRIA) for the 2022-2030 period [23]. The SRIA serves as a roadmap, providing clear direction for the partnership's activities to ensure that the CBE-JU remains focused on its objectives and contributes effectively to the EUGD. More information on this can be found in the following section. In June 2022, the CBE-JU launched its first call for project proposals with a budget of €120 million. The call received over 125 applicants. In 2024, this budget has increased up to €213 million shared by Innovation Actions at flagship level (€60 millions), Innovation Actions (€105 millions), Research and Innovation Actions (€38 millions), and Coordination and Support Actions (€10 millions) [24]. That shows that the opportunities in this sector are trending upwards.

1.2. Biorefineries and lignocellulose

Summarising Section 1.1, we are currently in a transitional phase. The scarcity of fossil resources, their dwindling availability, and the environmental impacts linked to their exploitation and consumption are the primary pressures responsible for this situation. The biorefinery, a concept that has been around for nearly two decades, is emerging as a solution within this context. As defined by the IEA (International Energy Agency): "Biorefining is the sustainable processing of biomass into a spectrum of marketable products and energy" [25].

Analogous to conventional refineries, biorefineries aim to extract the elemental constituents of biomass. Similarly to crude oil's long carbon polymers, lignocellulosic biomass consists of three structural molecules: cellulose, hemicellulose, and lignin. These complex polymers are degraded into their elementary components (monomers), e.g. glucose in the case of cellulose. Once the most basic molecules are released, they are conveniently rearranged to produce products of interest, mainly biofuels, bioproducts or energy. Depolymerisation can be accomplished by a number of processes. Broadly speaking, these can be divided into chemical, thermochemical and biological transformations. In these processes, degradation is caused respectively by a chemical agent such as an acid or base, by the action of temperature and pressure, or by enzymatic digestion. In Section 1.2.1, these processes are described in detail along with the most commonly used types of biomass.

1.2.1. Biorefineries state of the art

Biomass is the feedstock used in these systems and, by so, the cornerstone of their operation. It refers to organic matter produced by living things, which absorb carbon from the environment during their life cycle. The most common example is plants and atmospheric CO_2 fixation. That contrasts with fossils that fixed carbon millions of years ago. So, in the first situation, the natural carbon cycle is being considered, whereas the second situation involves the release of "extra" carbon that has been stored until now. Because biomass is produced from living organisms, its controlled use makes it a potentially unlimited and delocalised source. That is extremely attractive, although it has some drawbacks, such as competition with food products or the recalcitrance of some biomasses to be degraded. Over time, technological concepts have been refined, leading to the use of more complex feedstocks such as lignocellulosic biomass. Today, the ideal situation is for biorefineries to operate flexibly with different inputs, although these can still be differentiated

according to general characteristics. That has led to one of the most common classifications of biorefinery types, which is outlined below.

- First-generation biorefineries use sugar, starch or oil crops as feedstock, such as corn, sugarcane, soybean, and rapeseed. These crops are rich in readily fermentable sugars or oils that can be converted into biofuels or bioproducts. However, these crops also compete with food and feed production [26].
- Second-generation biorefineries use lignocellulosic biomass as a feedstock, such as agricultural and forest residues, energy crops and grasses. These biomass sources are abundant, renewable, and do not compete with food and feed production. However, they require more complex and costly processes to break down the lignin and cellulose components into fermentable sugars [27].
- Third-generation biorefineries use algal biomass as a feedstock. Such biomass is highly productive, has a high oil content and can grow in a wide range of environments [28].

Although this classification is useful at a general level, the definition of biomass type is unclear. Biomass can be classified by origin and composition, as shown in Table 1.1. [29, 30]. A brief explanation of each type is included below.

Table 1.1. Feedstock classification according to its origin and composition.

Feedstock origin	Feedstock composition
Energy crops	Triglycerides
Agricultural residues	
Forestry residues	Sugars and Starch
Industrial wastes	
Municipal wastes	Lignocellulose
Sewage sludge	

Further elaborating on the classification attending to its **origin**:

- Energy crops are those grown specifically for energy purposes. They can be divided into herbaceous, woody, aquatic, and agricultural crops. Herbaceous crops include grasses such as switchgrass, miscanthus and sorghum, and provide high biomass yields with low water and fertiliser requirements. Wood crops, which include trees like poplar, willow, or eucalyptus, have high energy density and can be harvested several times. Aquatic crops consist of both micro and macroalgae. Farm crops consist of food crops like corn, sugar cane, soybean, and rapeseed [31].

- Agricultural residues are the by-products of agricultural activities. They include crop residues, such as straw, stalks, husks, and bagasse, that are left in the fields after harvesting; and animal wastes, such as manure, dung, and litter, that are produced by livestock and poultry [32].

- Forestry residues are the by-products of forest-related activities such as logging, thinning, and pruning. The forestry industry generates two types of waste: forest residue consisting of branches, tops, needles, and leaves, left after silviculture operations; and wood waste, like pallets, crates, and furniture, produced by the wood products sector.

- Finally, human activities generate organic waste from both industrial and municipal sources. Moreover, treating domestic and industrial wastewater yields potentially valuable sewage sludge [33].

Now, focusing on the classification attending to its **composition**:

- Triglycerides feedstock are biomass sources containing esters of glycerol and fatty acids. They include waste cooking oils, such as used frying oil collected from restaurants and households; animal fats, such as tallow, lard, and butter, that derive from animal tissues; and microalgal oils, such as lipids produced by microalgae [34]. Another important source for triglycerides feedstock are vegetable oils. Vegetable oils are composed of C8 - C24 fatty acids, and they can either be edible (e.g., rapeseed, coconut, sunflower) or non-edible (e.g., jatropha, mahua, karanja).

- Sugar and starchy feedstock refer to biomass with a high content of carbohydrates in the form of oligomers (sugars) or glucose polymers (starch). They include sucrose-containing biomass, such as sugar beet or sugarcane, and starchy biomass, such as wheat, corn, or barley [35].

- Lignocellulosic biomass consists of cellulose and hemicellulose polysaccharides and lignin, a complex polymer consisting of various aromatic groups. It is the most abundant of the above resources and the feedstock for second-generation biorefineries. A detailed commentary on this type of biomass can be found in Section 1.2.2.

The composition of the biomass used determines the applicable treatment. For example, treating fatty acids from cooking oil will differ significantly from digesting the plant cell wall matrix of lignocellulosic biomass. That is a key factor in the approach to each utilisation route. While it is not the aim of this work to explore all these routes, a summary of some of the more prominent routes according to the type of biomass used is presented in Table 1.2 [36].

Table 1.2. Biomass classification attending to its composition, and fitting valorisation routes for each type.

Biomass composition	Valorisation route
Triglycerides	Transesterification. Reaction of triglycerides with an alcohol (usually methanol) to produce biodiesel and glycerol. Hydrolysis. Reaction of triglycerides with water to produce glycerol and fatty acids. Hydrodeoxygenation. Removal of oxygen from triglycerides or fatty acids to produce hydrocarbons, such as diesel or jet fuel. Pyrolysis. Thermal decomposition of triglycerides or fatty acids to produce syngas, bio-oil, or biochar. Reforming. Reaction of triglycerides or fatty acids with steam or carbon dioxide to produce syngas, which can be further converted into fuels or chemicals by catalytic upgrading.
Sugar & Starch	Fermentation. Transformation of sugars into alcohols or organic acids by microorganisms or enzymes. This method can produce ethanol, lactic acid, or succinic acid. Catalytic upgrading. Conversion of sugars to aromatics or alkanes such as benzene, toluene, xylene, or hexane using heterogeneous catalysts in water. Aqueous phase reforming. Conversion into hydrogen by using heterogeneous catalysts in water Dehydrocyclation. Transformation of sugars into furan derivatives like 5-hydroxymethylfurfural (5-HMF[4]) or furfural through acid catalysts.
Lignocellulose	Chemical processes. Use of catalysts and solvents to degrade the biomass into smaller molecules such as sugars, phenols, and furans. Thermochemical processes. Use of heat and pressure to convert biomass into syngas, bio-oil or biochar. Biological processes. Use of microorganisms or enzymes to ferment the biomass into value added products as ethanol, butanol, or biogas.

Before these processes occur, lignocellulosic biomass typically requires an additional pretreatment to remove impurities and increase reactivity. Pretreatment techniques involve physical, chemical, biological, or combined methods, like milling, acid hydrolysis, steam explosion, or organosolv processes.

Commercial interest in this type of processes has been a fact of life in established economies for years. In the European context, the bioeconomy generated €2 trillion and meant the creation of 18.5 million jobs as depicted in Section 1.1.2. The demand for biorefinery products is largely well-established and is therefore a low-risk market. Many of the intermediates produced in these refineries are analogues of existing chemicals. These are known as drop-in

chemicals, and their penetration of the current market is only cushioned by the existing supply, which will be gradually superseded by the regulatory environment. Forecasts from projects such as "S2Biom" put the estimated market volume for bioproducts in 2030 at around €50 billion. To meet this demand, 476 million tonnes of lignocellulosic biomass will need to be secured [37].

1.2.2. Lignocellulosic biomass as a feedstock

Lignocellulosic biomass may be the most promising alternative to replace current fossil resources among the sources described. That is mainly because it is the most common and renewable source of biomass on Earth [38]. Plus, it is easily accessible and inexpensive in most regions. Every year, agricultural and food-processing industries generate large amounts of organic waste that is lignocellulosic in nature. It is estimated that for every ton of cereals harvested, two to three tons of lignocellulose-rich residues are produced [39].

Its chemical complexity comes with challenges. Its recalcitrant nature creates a bottleneck for the processes scale-up as it requires large amounts of energy to decompose. That results in increased costs and environmental impacts. However, this intricated structure also enables the manufacture of a diverse range of products. As described above, lignocellulose is composed of cellulose, hemicellulose, and lignin. These polymers have a high structural complexity. The first two are carbohydrates, while lignin is a polymer composed of phenolic groups. As shown in Figure 1.3, cellulose is the main component of the microfibres that weave the structural wall, while hemicellulose and lignin have functions related to the packing and stiffness of these fibres.

Cellulose is the predominant component in both hardwoods and softwoods, with an average content of around 42% [40]. Cellulose is an organic polysaccharide consisting of a linear chain of hundreds to thousands of β(1→4) linked d-glucopyranoside residues in the $^4C_1$ chair conformation. These cellulose chains are usually highly ramified, linked together by hydrogen bonds (Figure 1.4). That gives the microfibres a strong stability in the cell wall of which they are a part. This cross-linking causes cellulose to be poorly soluble in both water and organic solvents [41]. That is a double-edged sword, as it makes it difficult to process, but favours the obtention of fibres with high purity under the right conditions (severe operating conditions lead to shorter fibres due to bond cleavage).

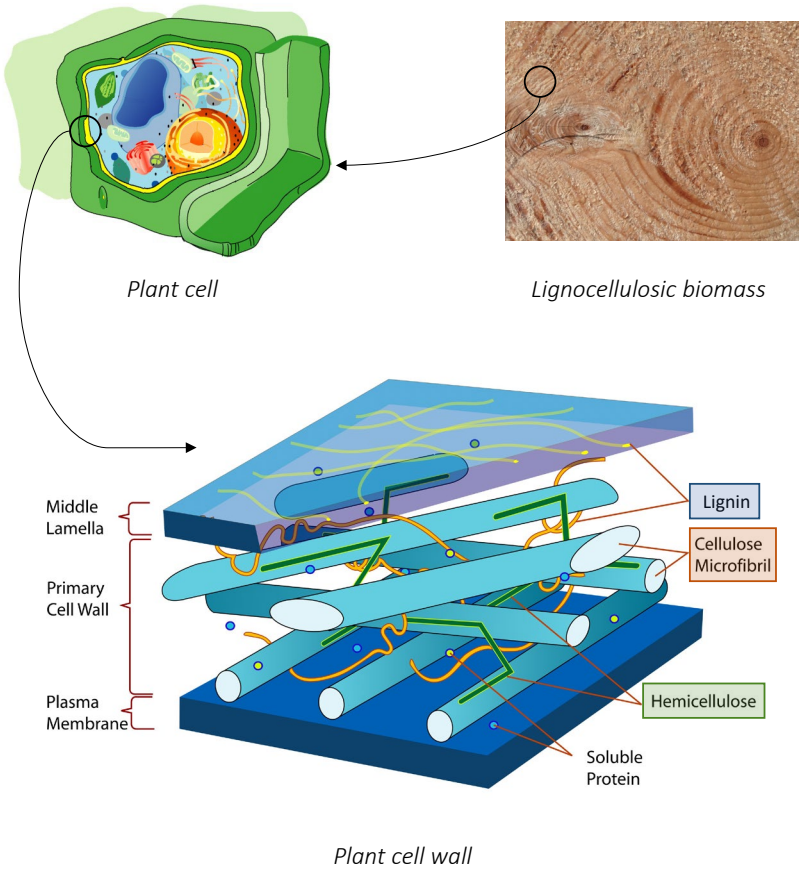

Figure 1.3. Lignocellulosic biomass composition, from the macro to the microscale.

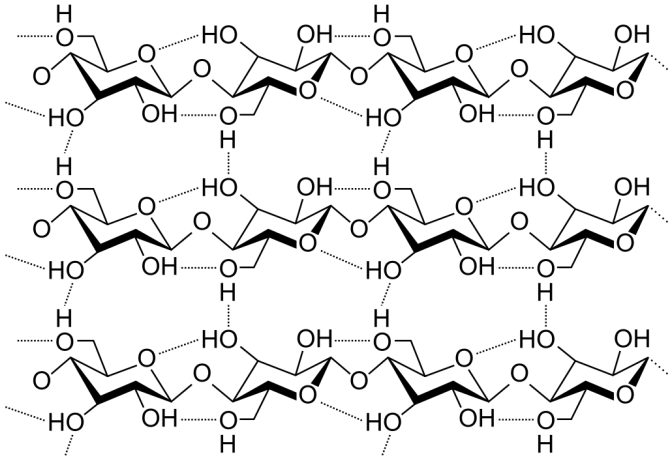

Figure 1.4. Cellulose reticulate polymer composed of linear branches linked by hydrogen bonds.

Hemicellulose is a heteropolysaccharide that differs from cellulose in that it is much more branched, has a much lower degree of polymerisation [42], lacks crystalline regions, and is composed of different sugars such as glucose, xylose, arabinose, mannose or galacturonic and glucuronic acids [43]. These sugars are also linked by glycosidic bonds, resulting in different structures depending on the backbone and side chains, as in Figure 1.5 These structures are related to the plant species, cell type and developmental stage of the species [44].

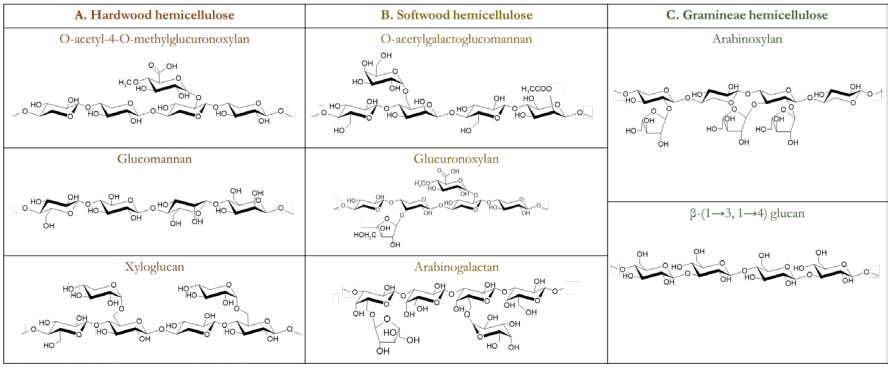

Figure 1.5. Structural formulae of hemicellulose in hardwood (O-acetyl-4-O-methylglucuronoxylan, glucomannan, and xyloglucan); softwood (O-acetylgalactoglucomannan, glucuronoxylan, and arabinogalactan); and Gramineae (arabinoxylan and β-(1→3, 1→4) glucan). Adapted from [44].

Lignin is a complex organic polymer composed mainly of three types of phenylpropane units: p-coumaryl alcohol, coniferyl alcohol and sinapyl alcohol [45]. These units are linked together by various types of linkages such as β-O-4, β-5, β-β, 5-5 and 4-O-5 [46]. Lignin provides stiffness and strength to cell walls and assists in water transport in plants. Its conformation varies slightly depending on the type of lignocellulose. Thus, softwood lignin consists exclusively of coniferyl alcohol, hardwood lignin consists mainly of coniferyl alcohol and sinapyl alcohol, and grass lignin has all three types of monomers (coniferyl, sinapyl and p-coumaryl alcohols) [47]. Lignin is the most recalcitrant and persistent polymer found in plant cell walls [48].

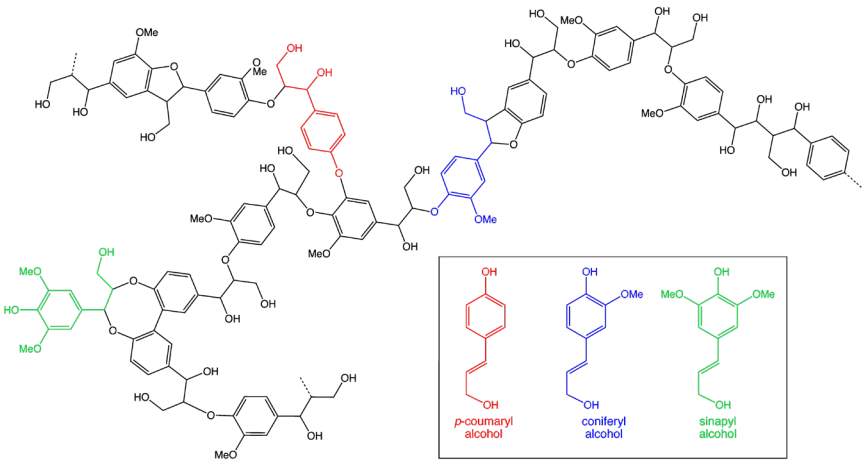

Figure 1.6. Chemical structure of lignin. Its main monolignols are represented in colour, as described in the figure legend.

I. Lignocellulose pretreatment

This difficulty in decomposing lignocellulosic biomass is one of the main factors slowing down its use, which in recent years has led to the search for processes that facilitate this transformation. Pre-treatment of the lignocellulose is an unavoidable step that allows the lignin to be removed, making the sugars in the holocellulose more accessible [49]. There are there are three types of pre-treatments: physical, chemical, and physicochemical. These are described in detail below.

Physical pre-treatment. This method generally involves the size reduction of biomass by mechanical means, such as milling, grinding, shredding, or chipping. The main advantage of this method is that it effectively increases the surface area and porosity of the biomass, making it more accessible to enzymes and chemicals. The main disadvantage is that it requires high energy input and does not remove lignin [50]. Other significant processes are the extrusion [51], the use of microwaves [52], or the ultrasound pretreatment [53]. Extrusion is a thermo-mechanical pretreatment process that uses a single or twin-screw extruder to continuously process lignocellulosic biomass at high solids loading. The extruder applies high temperature, pressure, and shear forces to the biomass, causing physical and chemical changes in its structure and composition. Microwave pretreatment of lignocellulose is a process that uses electromagnetic radiation to disrupt the biomass structure by interacting with polar molecules or ions. That leads to an increased temperature and the subsequent modification of the structural components of the lignocellulose. The ultrasound process uses ultrasonic

waves to induce cavitation, which disrupts the cell wall structure of the biomass, increasing its specific surface area and reducing the degree of polymerisation. The effects of ultrasound can be influenced by parameters such as ultrasonic frequency and reactor geometry and type.

Physicochemical pre-treatment**.** These processes often combine the application of heat and/or high pressure with the use of chemicals or solvents. The most widespread technologies include steam explosion, ammonia fibre explosion and hot liquid water treatment. Steam explosion involves injecting high-pressure steam into a reactor where it comes into contact with the biomass for a few minutes. The temperature in this first phase is between 170 and 210°C, which favours the rupture of the cell wall matrix. This is followed by rapid decompression, which causes the steam to expand and weaken the polymer chains [54]. Ammonia Fibre Expansion (AFEX) is a physicochemical pretreatment process that uses ammonia at high temperatures and pressure to break down the complex structure of biomass. The optimum conditions for this process are typically around 100°C with an ammonia-to-dry matter ratio of 1:1, a moisture content of 80% (dry weight basis) and a residence time of 5 minutes [55]. Hot Liquid Water (HLW) pretreatment is a hydrothermal process that uses water at high temperatures to disrupt the complex structure of biomass, resulting in the solubilisation of xylan, the reduction of hemicellulose molecular weights and the degree of polymerisation of cellulose, and the cleavage of alkyl-aryl ether bonds in lignin [56].

Chemical pre-treatment. These methods use acids, bases, or organic solvents to break down the lignin and hemicellulose bonds in the biomass. Acid pretreatment uses different acids such as sulphuric acid (H_2SO_4) or hydrochloric acid (HCl). The application of the acid can be achieved by mixing it with the biomass in a bed system, spraying it onto the biomass, or stirring the acid solution with the biomass in a reactor. The slurry is then heated either directly through the vessel walls or indirectly by steam injection [57]. Alkali pretreatment involves the use of alkaline solutions such as NaOH, $Ca(OH)_2$ or ammonia to remove lignin and part of the hemicelluloses, thereby increasing the accessibility to cellulose. Typically, the alkali is mixed with the biomass and the resulting slurry is heated [58]. Organosolv pretreatment uses organic solvents to separate cellulose, hemicellulose and lignin with minimal structural modification [59]. Organosolv processes use bio-based solvents such as gamma-valerolactone (GVL), acetone or 2-methyltetrahydrofuran, being the first one of the most promising alternatives [60].

II. ɣ-Valerolactone as a solvent for lignocellulose treatment

The complex lignocellulose structure makes it difficult to control the degree of fractionation of the different biomass components, resulting in a wide range of products and by-products. This is because for a given set of reaction conditions, some fractions will be more recalcitrant than others, while others break down rapidly. If short-chain molecules are released into the reaction medium at the start of the reaction, they can repolymerise uncontrollably, resulting in the formation of condensation products such as humins. The use of GVL in the reaction medium facilitates control over undesired reactions as it acts as a stabilizing agent, preventing the rapid and uncontrolled condensation reactions [60 - 62]. Additionally, GVL's solvent properties allow it to dissolve the lignin and hemicellulose fractions, thereby reducing the recalcitrance of the biomass and enhancing the efficiency of the depolymerization process. Humins are also soluble in GVL, which prevents the accumulation of solids in the reactor and thus allows for high biomass loading. Another benefit of using GVL is its ability to enable continuous feeding of biomass due to its low vapour pressure. Overall, it has the capacity to facilitate clean component fractionation under mild process conditions, making downstream processing of component streams within the solvent effective and avoiding expensive separations [63].

Gamma-valerolactone can be produced from biomass through two main routes. The most commonly reported route involves levulinic acid (LA) as an intermediate. LA is first hydrogenated to 4-hydroxypentoic acid (4-HPA) and then dehydrated to GVL, as shown in Figure 1.7. Theoretically, this could result in significant cost reductions as the solvent could be produced on-site.

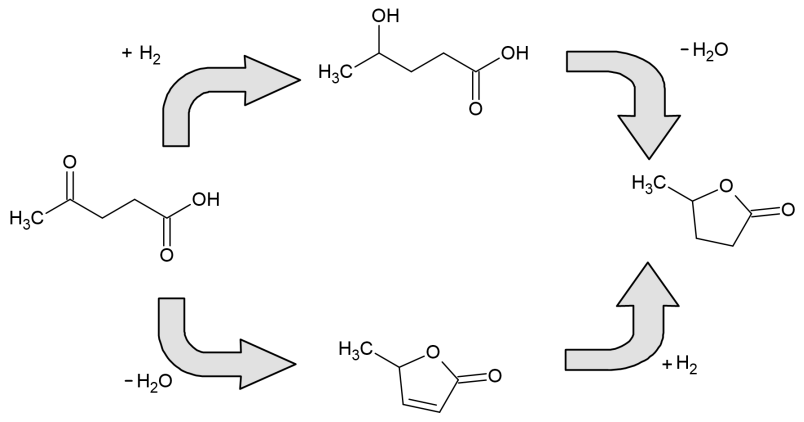

Figure 1.7. Gamma-valerolactone synthesis route from levulinic acid.

1.2.3. Biorefineries design and implementation in Europe

Lignocellulosic biorefineries in Europe are a growing industry, with more than 2150 such facilities currently operating according to [64] and the official tool hosted at the knowledge4policy web portal. Of these, 489 plants are focused on chemical production, 77.5% of which operate on a commercial scale. France and Germany lead the way in the number of installations dedicated to using agricultural biomass as the preferred feedstock, as depicted in Figure 1.8.

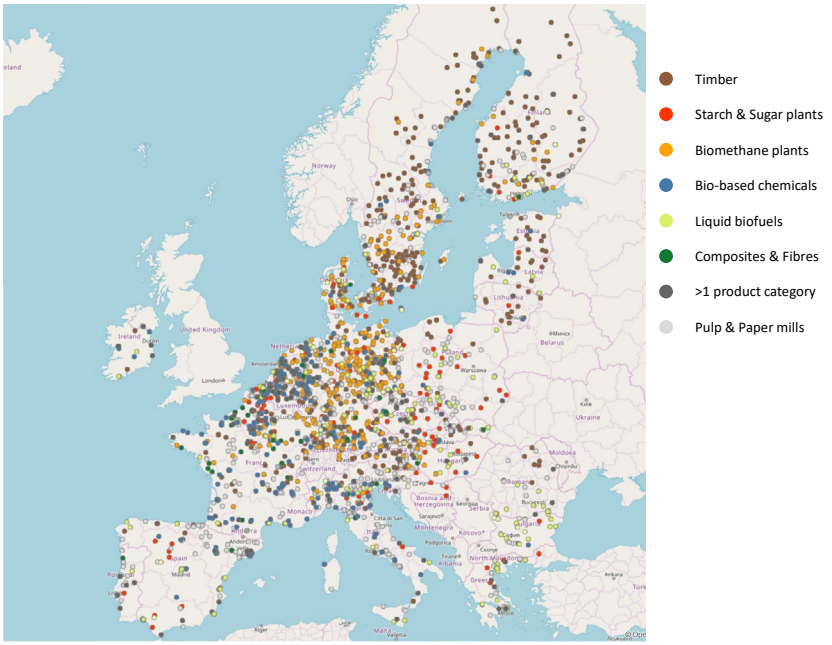

Figure 1.8. Biorefineries distribution in Europe and classification by output (2023).

Furthermore, it is anticipated that this demand will continue to rise throughout the course of this decade. According to [65], the consumption of bio-based chemicals could reach 16 million tonnes by 2030. The most pessimistic scenario is outlined in the report 'WP 5 - Market prospects for biorefineries to 2030 - demand scenarios' by Fachagentur Nachwachsende Rohstoffe (FNR). This study suggests that demand would be approximately half, which would still result in an annual growth of 3% compared to consumption in 2021.

According to the 2030 Biorefinery Outlook [66], bio-based chemicals and materials hold immense promise for a sustainable future, but several challenges hinder their widespread adoption. The first and most evident barrier

is the economic viability: Biorefineries producing large-volume commodities face a significant gap between market willingness to pay for bio-based products and their actual production costs. Factors such as limited willingness to pay more for renewable or low-carbon alternatives, competitive fossil-derived equivalents, and high production costs contribute to this challenge. Furthermore, some EU biorefineries struggle to compete due to higher energy costs, labour expenses, taxes, and limited access to low-cost biomass feedstocks.

Another important challenge is the feedstock supply. All bio-based chemical and material-driven biorefineries share concerns about certified sustainable feedstock availability. While the EU has substantial biomass potential from primary crops, agricultural residues, and post-consumer waste, demand exists across various sectors. Properly balance the biomass flows between and within regions is both a political and logistic dispute. Currently, agricultural by-products and wastes are the most widespread feedstock, although forestry outputs are rapidly growing. Figure 1.9 illustrates the refineries currently in operation for the production of chemicals derived from biomass. The data includes the number of operational plants, categorized by both feedstock and country, with the figures provided in brackets. Noteworthy, France and Germany are at the forefront, boasting the highest number of operational facilities. A significant majority of these facilities primarily utilize agricultural residues.

Finally, bio-based products are expected to offer environmental advantages, such as reducing greenhouse gas emissions by substituting fossil-based counterparts. Additionally, some bio-based polymers exhibit superior characteristics, like biodegradability. To ensure these benefits, quantitative evidence is required. A comprehensive life cycle assessment (LCA) is essential to demonstrate the environmental advantages of bio-based products, as reflected in the EUGD. The life cycle assessment is a systematic and holistic approach that considers the environmental aspects and potential impacts associated with a product, process, or system from the extraction of raw materials, through production, use, and end-of-life treatment, to the final disposal or recycling. LCA can help identify the environmental hotspots, trade-offs, and improvement opportunities along the life cycle, as well as support decision-making and policymaking.

To scale up biomass-based technologies, it is crucial to improve their sustainability, both operationally and in the supply chain [67]. Therefore, integrating LCA from the design stages is essential. This integrated framework

is a discipline that has gained significant importance in recent years [68]. Furthermore, the combination of LCA with other tools, such as Integrated Assessment Models (IAMs), allows the creation of future scenarios that aid decision-making in a dynamic context with significant uncertainty [69]. Connecting data science techniques with advances in this field of study enables the identification of the most sustainable alternatives [70, 71] at any given time, ensuring an optimal transition towards a more sustainable context [72].

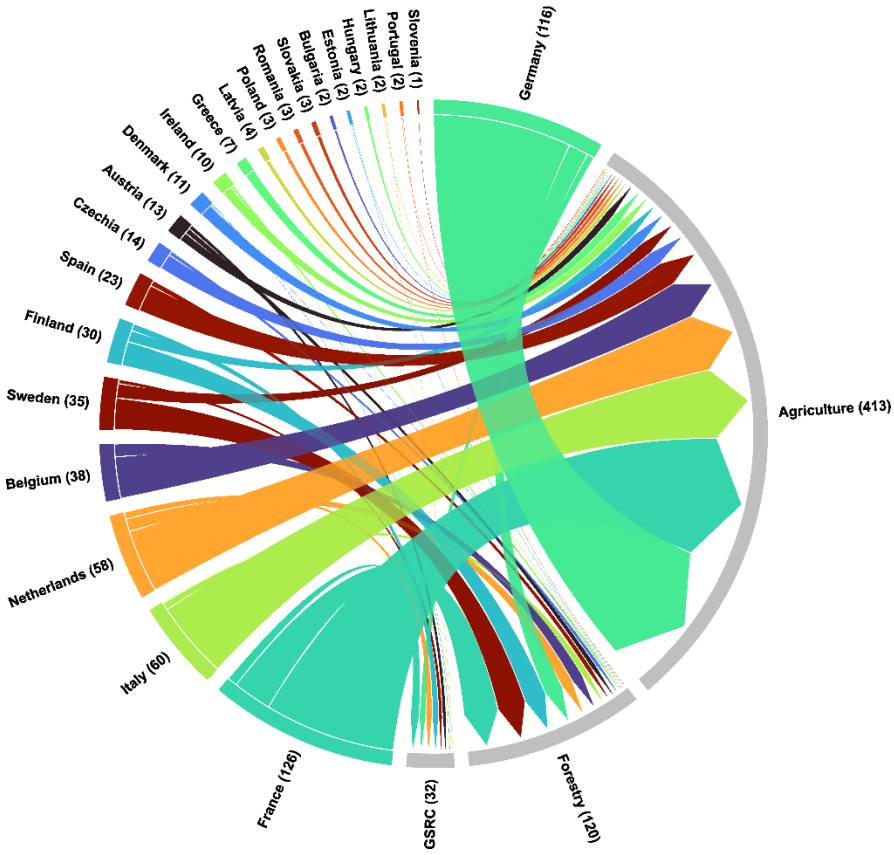

Figure 1.9. European countries with lignocellulosic biorefineries operating on a commercial scale and main feedstocks used in each region. GSRC: Grasses and Short-rotation Coppice. Figures in brackets show the number of operating plants.

1.3. State of the art on furfural production

In the context of biorefineries, the question of which molecules to target arises. In 2004, the National Renewable Energy Laboratory (NREL) generated a list of the 10 compounds with the highest potential added value [73]. This list was revised and refined in 2010 by one of the authors of the first report, Joseph J. Bozell, updating the criteria related to the technology needed to produce these molecules [74]. The complete list is as follows: ethanol, furfural, 5-hydroxymethylfurfural (HMF), 2-furandicarboxylic acid (FDCA), glycerol, isoprene, biohydrocarbons, lactic acid, succinic acid, hydroxypropionic acid, levulinic acid, sorbitol, and xylitol.

In all cases, the molecules targeted are referred to as building blocks. This term is used because they are intermediate compounds between more nonspecific platform molecules (such as syngas and sugars) and somewhat niche secondary chemicals (such as ammonia and diesel). The value of these building blocks lies in the fact that many of them can be easily obtained from only a few platform molecules, and each of them serves as the basis for the synthesis of a large number of secondary chemicals.

1.3.1. Furfural chemistry and properties

One of the compounds of greatest interest is furfural or 2-furfuraldehyde due to its rising market outlook in the coming years. Moreover, it has already been produced on a commercial scale for about a century, so it has a well-established and potentially unconstrained market. It is a highly versatile chemical, as it can be used for synthesising other building blocks, as illustrated in Figure 1.10.

Furfural is a colourless liquid with a pungent almond odour [75]. It was first isolated by the German chemist Johann W. Döbereiner as a by-product of formic acid. In 1840 [76], John Stenhaus succeeded in determining its empirical formula: $C_5H_4O_2$. Chemically speaking, furfural is an organic compound consisting of a furanic ring with an aldehyde group in the 2-position. Some of its main properties are summarized in Table 1.3. It is commonly synthesized by hydrolysing pentosans (5-carbon sugars) to pentoses and then dehydrating them. These pentosans are derived from the hemicellulosic fraction of plant residues, such as maize cobs or sugar cane bagasse.

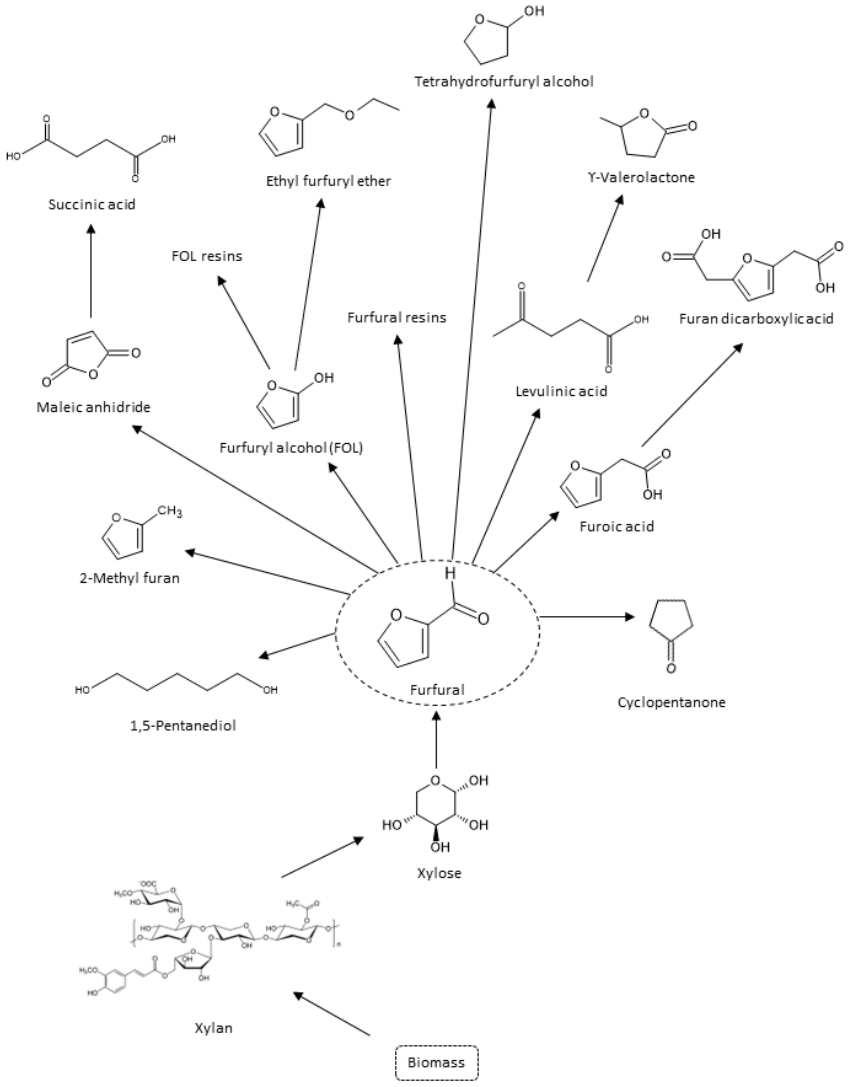

Figure 1.10. Furfural as a building block chemical.

Table 1.3. Furfural properties.

Property	Value
Molecular weight	96.08 g/mol
Boiling point	161.7 °C
Melting point	-36.5 °C
Solubility in water	Partially soluble
Density	1.16 g/cm³
Standard Formation Enthalpy (ΔH_f°)	-110 kJ/mol
Combustion Enthalpy (ΔH_c)	-1,360 kJ/mol
Vaporization Enthalpy (ΔH_{vap})	40 kJ/mol

The process for obtaining furfural involves two steps. Initially, the pentosans present in the hemicellulose are hydrolysed to release the sugar monomers, primarily xylose and arabinose. Subsequently, these pentoses undergo cyclodehydration to produce furfural. The reaction follows the stoichiometry outlined below:

(1) Hydrolysis of pentosans:

$$\text{Pentosan} + n\cdot\text{Water} \rightarrow n\cdot\text{Pentose}$$

$$(C_5H_8O_4)n + n\ H_2O \rightarrow n\ C_5H_{10}O_5$$

$$n\cdot 132.114 + n\cdot 18.016 \rightarrow n\cdot 150.130$$

(2) Dehydration of pentoses:

$$\text{Pentose} - 3\cdot\text{Water} \rightarrow \text{Furfural}$$

$$C_5H_{10}O_5 - 3\ H_2O \rightarrow C_5H_4O_2$$

$$150.130 - 54.048 \rightarrow 96.082$$

Based on these molecular ratios, the theoretical maximum yield for furfural is calculated to be 0.727.

The main compound in the pentosan skeleton is xylan, specifically β-D-xylopyranoside. Xylan has α-L-arabinofuranose groups at different positions, as illustrated in Figure 1.11, and is therefore referred to as arabinoxylans. Figure 1.11 to Figure 1.18 are adapted from [77].

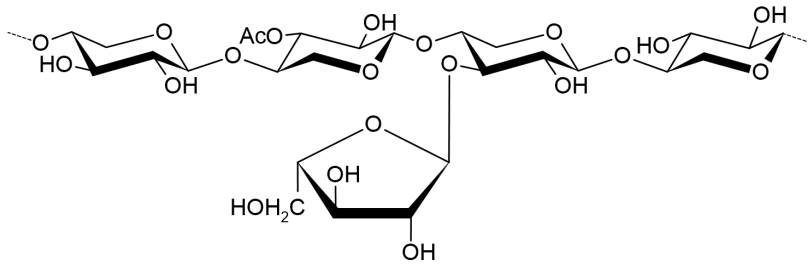

Figure 1.11. Arabinoxylans present in the hemicellulose.

The initial acid hydrolysis step breaks down the arabinoxylans into four monosaccharides: arabinofuranose/L-arabinose; and D-xylopyranose/D-xylose. The hydrolysis process is conducted in the presence of a highly diluted mineral catalyst, typically sulphuric acid. The reason for diluting the acid before adding it is because hemicellulose is more easily hydrolysed than cellulose, so a low acid concentration allows the extraction of pentoses and prevents their subsequent degradation. Besides, high acidity of the medium leads to greater environmental and corrosion issues. However, this low acid concentration may increase residence times.

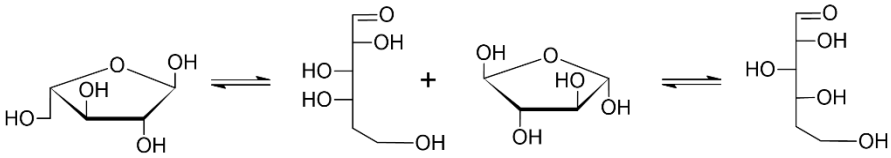

Figure 1.12. Monomers released upon the arabinoxylan hydrolysis.

In certain processes, the presence of water vapour and organic acids can facilitate protonation even without a catalyst. Protonation of the oxygen in the ether bonds results in the formation of a trivalent oxygen. Hydrolysis at this bond produces a carbocation on one side and a hydroxyl on the other. The carbocation reacts with water to form a hydroxyl group while releasing a proton into the medium.

Part of the hydroxyl groups of arabinoxylan (Figure 1.11) are acylated by short-chain fatty acids such as acetic acid. These esters give rise to their corresponding carboxylic acids (formic, acetic...) during hydrolysis. Additionally, certain pentosans may contain methyl groups at positions 1 or 5, which also leads to the production of methanol. The corresponding sugars, when dehydrated, produce 2-acetylfuran and 5-methylfurfural, which are typical by-products of commercial furfural, comprising less than 1% by weight.

During the second stage, the monosaccharides shown in Figure 1.12 undergo dehydration to form furfural ($-3H_2O$). This stage is the limiting factor of the process, with a rate 50 times lower than that of hydrolysis. In the first stage, both xylose and arabinose adopt the 1,2-enediol conformation (Figure 1.13, a). The molecule undergoes protonation from the acidic medium (Brønsted acidity) at position 3 (Figure 1.13, b).

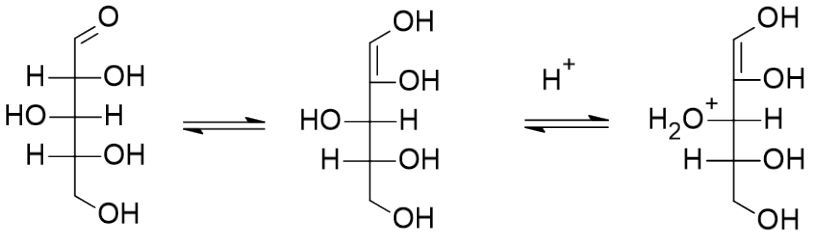

(a) (b)

Figure 1.13. (a) 1,2-enediol conformation of xylan and arabinan. (b) Molecule protonation at C3.

The water molecule is then removed, resulting in the formation of 3-deoxy-D-xylosulose in its enolic form (Figure 1.14).

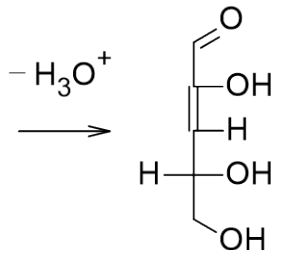

Figure 1.14. 3-deoxi-D-xilosulose formed after first dehydration.

The same occurs at position 4, resulting in 3,4-dideoxy-D-xyl-3-pentenosulose (Figure 1.15).

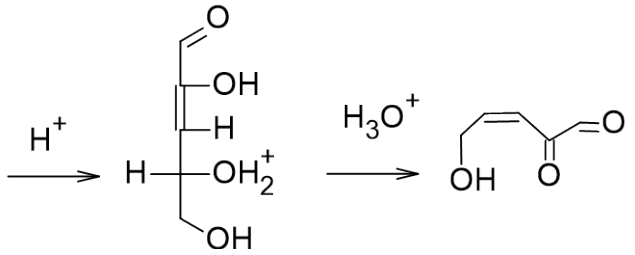

Figure 1.15. 3,4-dideoxi-D-xilo-3-pentenosulose formed after second dehydration.

This species again accepts a proton from the medium, forming a cyclic acetal, which undergoes a third and final dehydration to form furfural (Figure 1.16).

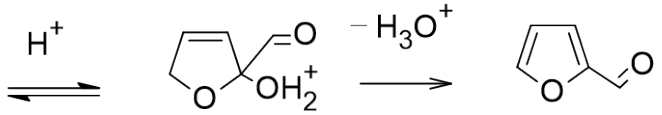

Figure 1.16. Furfural formed after third dehydration step.

Some of the most common side reactions have already been discussed. The formation of carboxylic acids (high boilers) is usually stopped by extracting them from the bottom of a first distillation column. Other elements of smaller molecular size (low boilers), mainly methanol, are removed in the same column at the head. 2-Acetylfuran and 5-methylfurfural are frequently present as impurities in the final product due to their low concentrations. Distillation of these impurities is often not cost-effective due to their equilibrium with the main product. Some feedstocks may contain coniferyl aldehyde, which can be digested into acetaldehyde under acidic conditions. This acetaldehyde can be oxygenated in the presence of oxygen in radical form under industrial conditions, resulting in the production of 2,3-butanedione and 2,3-pentanedione. If they are produced, they are usually recovered from the final furfural stream by distillation due to their high value. One of the main challenges in the industrial production of furfural is its limited yield, which is only 55% of the theoretical maximum (see Section 1.3.3). This is because the furfural formed in the medium spends time in the liquid phase, where condensation and resinification reactions occur. The main condensation reaction that takes place is the acetalization of pentoses with furfural (Figure 1.17).

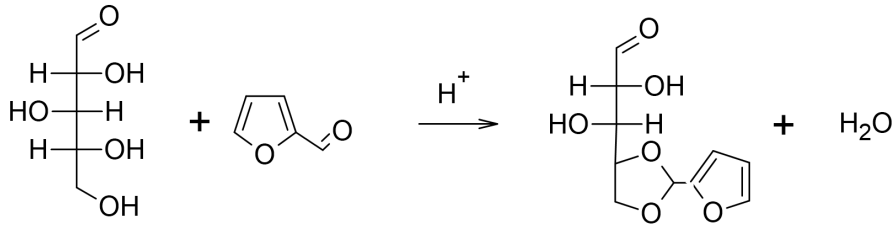

Figure 1.17. Condensation reaction of furfural with free pentoses in the reaction medium.

Furfural is also prone to resinification, and especially at low temperatures it undergoes self-condensation due to the entropic effect, as in the schemes in Figure 1.18.

Detailed information about the kinetics is provided in the Section 3.1.3.

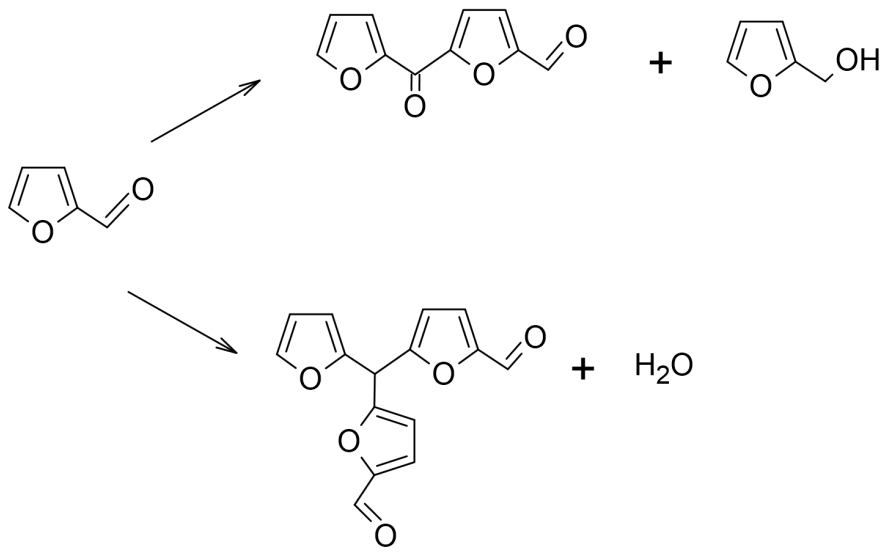

Figure 1.18. Common resinification reaction in furfural formation.

1.3.2. Furfural markets

The global furfural market volume in 2022 was USD556.74 million. Moreover, its projections are favourable as consumption of its derivatives is expected to increase over the next decade. Until 2030, a compound annual growth rate (CAGR) between 6.5% to 7% is expected depending on the source consulted [78, 79]. The estimated market volume for that year is expected to be USD923.89 million [78, 79]. Although more up-to-date data is not available, in 2012 the global production of furfuraldehyde production was 300Kton/year [80], and since then it has continued to increase. China (many different producers, [81]), the Dominican Republic (Central Romana Corporation, [82]), and South Africa (Illovo Sugar Africa (Pty.) Ltd., [83]) have been the largest producers of furfural for over a decade [82]. However, China dominates the market with a revenue share ranging from 74.5% to 82% [78, 79], mostly through small-scale manufacturers. The Section 1.3.3 provides an in-depth review of the commercial and non-commercial processes used for the industrial-scale production of furfural.

In Europe, Belgium and the Netherlands dominate imports of furfural through the company *TransFurans*. Much of the furfural purchased comes from China and the Dominican Republic, although it is not limited to this supplier as it would not cover the entire demand on its own. Other major consumers such as France purchase this furfural and the derived furfuryl alcohol (FOL) through these primary importers. Production in Europe is very limited in

comparison, and only Slovenia (*Tanin Sevnica d.d.*, [84]) and Austria (*Lenzing*, [85]) produce and export furfural in significant quantities. The company *Silvateam S.P.A.* in Italy also produces furfural but in a smaller scale [86]. Table 1.4 shows a traceability matrix connecting the main furfural exporters and importers, eliminating intermediaries. This allows for observation of net flows of furfural into Europe. The matrix calculations are based on global import and export data for the year 2022, as reported in the Observatory of Economic Complexity (OEC) webpage.

Table 1.4. Traceability matrix connecting furfural international exporters to European importers. Flows are represented from countries in rows to countries in columns in million USD. Cells marked with 'NS' indicate non-representative flows. AU: Austria; BE: Belgium; CN: China; CZ: Czech Republic; DO: Dominican Republic; FR: France; GR: Germany; IR: Israel; IT: Italy; NT: Netherlands; PL: Poland; PT: Portugal; SL: Slovenia; ZA: South Africa; SP: Spain; CH: Switzerland; US: United States.

	BE	**CZ**	**FR**	**GR**	**IT**	**NT**	**PL**	**PT**	**SP**	**CH**
AU		0.01		0.48				0.19		
CN	15.01	NS	0.01	0.03		3.53	0.003		0.02	0.001
DO	9.16		0.	0.03		2.64	NS			
IR			0.52			2.88			0.16	
SL	0.03				0.85	1.90	0.39		0.04	
ZA	1.19	NS				2.83			0.04	
US		0.001	0.005	0.04		2.22	NS			0.02

Furfural is primarily used as a feedstock for producing furfuryl alcohol (FOL). The consumption of FOL is expected to increase in the next decade, which will be the main driver boosting the demand for furfural in the coming years. Furfural is also widely used as a solvent, particularly in oil refining, and in the manufacture of adhesives and lubricants Additionally, it finds application in the paint and coatings industry. Finally, furfural use is very extended in the pharmaceutical, agricultural, and food industries, as well as in the production of biofuels.

An important use of FOL is the production of industrial resins in foundries to be used as a binder for sands. Additionally, its demand in refractory materials, such as bricks, fiberglass, and ceramic composites, is expected to increase due to the growing construction industry. With the advancement of environmental legislation, it is projected that bio-products will be increasingly favoured over fossil-based products, meaning that FOL will increasingly be produced preferably from furfural.

1.3.3. Commercial-scale furfural production

Its commercial production has a century-long history. The company Quaker Oats was the first to produce it on an industrial scale in the early 1920s, and since then many ventures have been developed, with more or less success. Table 1.5 lists some of the most prominent technological developments of recent decades and their main (and simplified) characteristics. Although the number is large, only a few have survived in the market. Currently, the most widely established technologies are the Quaker Oats (batch), the Chinese batch and continuous processes (Huaxia), and the Rosenlew process. Some more modern processes, such as SupraYield or Vedernikovs, also operate at an industrial scale, although their production is much lower globally.

There is a common constraint that prevents further competition between these processes. Traditionally, these processes depolymerise the biomass by adding large amounts of acid. At elevated temperatures, the corrosive capacity of this medium is very high. That is mitigated in different ways depending on the technology. For example, the Quaker Oats Process (QOP) uses a refractory brick lining inside the reactor, while the Chinese Batch Process (CBP) uses mild steels about 50 mm thick. In any case, none of these reactors are jacketed, as heat transfer through these surfaces would be extremely inefficient. The common solution is therefore to heat the reactor by injecting medium or high-pressure steam. This steam serves a dual purpose. On the one hand, it releases latent heat to raise the temperature during condensation, and on the other, it acts as a stripping agent to remove the furfural formed in the liquid phase. However, this heat is not sufficient to bring the pentose-rich medium to its boiling point. An explanation to this phenomenon is provided hereafter. Pentoses are polyhydroxylated sugars that can be either aldoses (if they have an aldehyde group) or ketoses (if they have a ketone group). Pentoses can be cyclized by the reaction of the carbonyl carbon of the aldehyde or ketone function with a secondary hydroxyl group to form cyclic hemiacetals. The presence of multiple hydroxyl (-OH) groups on pentoses can increase the ability of these molecules to form hydrogen bonds with each other. Hydrogen bonds are weak interactions, but when formed in large numbers, this cross-linking can increase the amount of energy required to boil the medium. Since the medium does not reach the boiling point, the furfural formed remains in the liquid phase long enough to undergo condensation and resinification reactions before being carried away by the stripping steam. Therefore, although the operational yield of this reaction would be 100%, industrial processes are limited to about 50% of the stoichiometric maximum (72%).

Table 1.5. Summary of the main production processes for furfural on a commercial or semi-commercial scale. Data are simplified for clarity.

Name	Op. Temperature		Operation		Input	Catalyst
	< 200 ˚C	> 200 ˚C	Batch	Cont.		
Quaker Oats	X		X		SCB[1]	H_2SO_4
Quaker Oats		X		X	Oat Hulls	H_3PO_4, H_2SO_4
Chinese Batch	X		X		Corn Cobs	H_2SO_4
Huaxia (Westpro)	X			X	Corn Cobs	H_2SO_4
SupraYield		X	X		SCB	H_2SO_4
Biofine		X	X		Paper sludge	H_2SO_4
Vedernikovs		X	X		Cellulose wastes	H_2SO_4 + salts
MTC		X		X	Wheat straw	HCl, NaCl
Esher Wyss	X			X	LCB[3]	H_2SO_4, Acetic ac.
Rosenlew	X			X	SCB	Autocat.[2]
CIMV		X		X	Wheat Straw	Acetic, Formic
Lignol	X			X	Wood	Enzimes
Agrifurane	X		X		Corn Bran	H_2SO_4
Supratherm		X			SCB	H_2SO_4
Stake		X			Wood	Autocat.

1. *Sugarcane Bagasse*; 2. *Autocatalytic process. 3. Lignocellulosic Biomass.*

As a result, the amount of steam needed to produce furfural is enormous. Consequently, the amount of energy required to produce it is also very large. This, together with the high concentrations of acid required to break down the structure of the biomass, makes these processes environmentally harmful. Therefore, furfural production is currently almost exclusively confined to regions with lax environmental legislation. The dominant processes on the market are at present the Quaker Oats batch process in the Dominican Republic, the Chinese batch and Huaxia (modified by Westpro) processes in China, and the Rosenlew process in South Africa. In particular, the Chinese batch process (CBP) currently has 82% of the market share [78, 87]. However, this is far from solving the problem in Europe, one of the world's largest consumers of furfural. Instead, it simply shifts environmental pressures with a regional dimension while ignoring others of a global nature, such as climate change.

The processes listed in Table 1.5 are briefly described below to provide an overview of current furfural production. The descriptions hereby provided are summarised from Zeitsch [75], and the Ullman's Encyclopaedia [77] unless an alternative reference is provided.

Quaker Oats batch process. The Quaker Oats batch process uses cylindrical digesters rotating on a longitudinal axis in which raw materials and sulphuric acid are mixed and heated to 153°C for 5 hours by steam injection. The digesters are lined with carbon bricks, which are sealed with acid-resistant cement to withstand the process conditions. The yield of furfural depends on the initial water content. Brownlee's study found that the optimum initial water content was 25.4%, resulting in a furfural yield of 62.2% of the theoretical yield, although part of it is lost in the discharged residue. However, the process has its drawbacks, including a long residence time due to low temperature, high sulphuric acid requirements, corrosion problems and difficulties in processing fines. Despite these challenges, the process is still in use today.

Quaker Oats continuous Process. After 50 years of operation, Quaker Oats developed the process in continuous. This process was in use for 30 years before it was abandoned due to poor profitability. The main difference from the original process was the continuous operation and the injection of superheated steam to reach temperatures of up to 184°C. This allowed similar yields to be achieved with up to 5 times shorter residence times.

Chinese batch Process. The Chinese batch Process is a simplified version of the Quaker Oats batch process. It uses unlined mild steel reactors with a wall thickness of 50mm, which are protected against corrosion by furfural-derived polymers that naturally form on the inner wall. The reactors are filled to approximately 75% with ground maize cobs, which have been sieved to remove fines and sprayed with 4% aqueous sulphuric acid. The mixture is then heated with steam at 6 to 7 atm for 4 to 5 hours. The residue is rapidly discharged by opening a flap valve at the bottom of the reactor. The process differs from the Quaker Oats method in that the reactor vapour is passed directly through the reboiler of the azeotropic distillation column and most of the low boilers are vented to the atmosphere before distillation begins. Despite these differences, the furfural yield in the distillate is similar at around 50%.

Huaxia process. The Huaxia furfural technology is a continuous process with fixed bed reactors and dynamic refining. This process, modified by Westpro in 2004, begins with the pre-treatment of raw materials, typically crushed corncobs, which are then hydrolysed in steel reactors. The furfural

formed is removed with steam and refined by continuous dynamic azeotropic distillation. Valuable by-products such as acetic acid and levulinic acid can be recovered [88].

SupraYield. This process uses a method called delayed decompression, where water is heated above its atmospheric boiling point under elevated pressure, then gradually decompressed to maintain boiling. This allows for rapid initial heating by steam condensation without fouling issues. The process involves heating a well-insulated reactor charged with raw material to a primary temperature, then gradually decompressing to produce a steady small flow of product vapor. Depending on the primary temperature, the process can be run with or without a foreign acid. If a foreign acid is used, it should not be sulfuric acid due to its known losses by sulfonation. Instead, orthophosphoric acid is used to avoid side reactions.

Biofine. In the Biofine process, the biomass feedstock is first shredded to an optimal size and then mixed with recycled dilute sulphuric acid in a tank before passing through two different acid-catalysed stages. The first stage focuses on the hydrolysis of carbohydrate polysaccharides into soluble intermediates such as HMF. This is achieved in a plug flow reactor under specific conditions (210-220°C, 25 bar pressure and a residence time of 12 seconds). The rapid removal of products allows for a small reactor diameter. The second stage carried out under less stringent conditions (190-200°C, 14 bar), favours the reaction sequence leading to levulinic acid (LA). This stage requires a larger reactor due to the longer residence time (approximately 20 minutes). Furfural is typically recovered at this point as a by-product, with a yield from 5-carbon sugars around 70% of the theoretical value [89].

Vedernikov's process. Vedernikov developed a one-step furfural production process that simultaneously hydrolyses and dehydrates lignocellulosic biomass to furfural using a dilute sulphuric acid solution. This process limits the presence of excess pentoses in the solution, reducing side reactions and by-product formation. As a result, a higher proportion of pentoses are converted to furfural, with a yield of 75% over the theoretical maximum. The process also preserves biomass cellulose, facilitating its use in the production of other value-added chemicals such as ethanol. Despite the higher furfural yield, the process generates a significant amount of acidic waste, which is an environmental concern. The technology has been evaluated in the former Soviet Union, Slovenia, Hungary, and Finland [82].

Muti-Turbine Column (MTC) process. The MTC, developed at TU Delft in the Netherlands, is a one-step process in which pre-hydrolysed

straw is acid hydrolysed to furfural in a continuous reactor. A 5% (w/w) aqueous solution containing pentosans is used as the feedstock and is fed directly to the column. Furfural is produced in water inside the reactor and simultaneously transferred to the vapour phase. The use of different acids and salts has been shown to affect the selectivity, yield and separation of furfural production. Under optimum conditions, furfural yields in excess of 83% have been achieved with purities in excess of 99%. One of the advantages of this process is the minimal formation of by-products. As a continuous reactor and distillation tower, the MTC process also features low energy consumption, making it a more suitable alternative to traditional batch processes. However, this technology is still at an early stage of development and further in-depth analysis is required before it can be commercialised [90].

Escher Wyss process. The Escher Wyss process, now abandoned, was a continuous process for the production of furfural using a fluidised bed system. In this process, the raw material passed through a rotary feeder and fell into a central tube where it was sprayed with aqueous sulphuric acid, providing 3% of this catalyst in the moisture content of the feed. Steam from a rotary distributor maintained the raw material in a state of suspension (fluidized bed) in the lower half of the reactor, facilitating the desired hydrolysis and dehydration reactions. The process was operated at a temperature of 170°C and had an average residence time of 45 minutes.

Rosenlew. In the Rosenlew process, which typically uses bagasse, the feedstock is screened to remove fines, with approximately 40% of the incoming bagasse being rejected. The remaining coarse fraction enters the reactor from the top and moves slowly downwards by gravity, while superheated steam at 10 bar is introduced at the bottom and flows upwards. This countercurrent operation allows the steam to react with the feedstock, pick up volatile reaction products and exit at the top. The process operates as an autocatalytic system where no foreign acid is added, and the catalyst is a mixture of acetic acid, formic acid and small amounts of higher carboxylic acids formed from the feedstock. The Rosenlew reactor can be viewed as a stripping column energised by steam injection at the bottom, with carboxylic acids injected at the top where these acids are formed in the reactor.

CIMV. The process of the *Compagnie Industrielle de la Matière Végétale* (CIMV), launched in 2008, is a continuous fractionation of biomass (specifically wheat straw) under acidic conditions (using acetic and formic acid at 185°C–210°C) in a pilot-scale lignocellulosic biorefinery facility located in France. The fractionated components, namely lignin, cellulose and

hemicelluloses, are directed along different pathways. Hemicelluloses are converted into xylitol, furfural and furfuryl alcohol. Cellulose is converted to bleached pulp, which has properties similar to hardwood pulp. Lignin is used to make resins and adhesives [82].

Lignol. Lignol Innovations Corporation developed a continuous biorefinery process that uses an organosolv pretreatment step to separate lignin, hemicellulose and extractives from the biomass matrix. The process is designed to produce ethanol by enzymatic cellulose hydrolysis followed by fermentation. The liquor obtained from the Organosolv pre-treatment is further processed to produce furfural, xylose, acetic acid, lipophilic extractives and lignin. The underlying philosophy of this process is that ethanol-only production is not economically viable, especially for operations on the scale of a typical sawmill (~100 tons/day of dry wood) [91].

Agrifurane. The Agrifurane process, also known as the Petro Chimie process, uses a series of batch reactors to process a slurry of raw material and filtrate from a belt filter press. The process involves a series of reactors, each receiving a mixture of primary and secondary steam, with the steam from each reactor being fed into the next. This countercurrent operation allows the reaction and collection of volatile products. However, the process has significant drawbacks, including a costly valve control system, an expensive belt filter press to dewater the residue, and the need for a drier to make the belt filter cake combustible. Due to these high costs, the process is considered obsolete.

Supratherm. The Supratherm process is a continuous hydrolysis process that uses high temperatures (200-240°C) to simplify the reactor to a pipe. Crushed bagasse is mixed with a liquid recycle fraction and dilute sulphuric acid to form a slurry, which is then converted into a pulp. This pulp is heated to 230°C in a continuous flow reactor, which initiates rapid hydrolysis. The reacted pulp is then separated into a vapour fraction rich in furfural and a residual slurry in a cyclone operated at reduced pressure. This process significantly increases the furfural yield and avoids the encrustation problems associated with conventional furfural plants. The cyclone underflow filtrate, consisting of water with low concentrations of sulphuric acid, furfural, and by-products, is recycled to prepare the feed slurry. This recycling scheme allows most of the sulphuric acid to be recovered and reused, with the only loss being the amount contained in the cake. However, the process has a significant disadvantage: the high investment and maintenance costs for the belt filter press and a dryer to make the cake combustible.

Stake. The Stake Technology process, also known as Staketech Biomass Conversion (SBC), is a continuous hydrolysis process involving three stages: high temperature/high-pressure hydrolysis of the feedstock without chemicals, water extraction of the hydrolysed feedstock to produce a crude xylose-xylan solution, and dilute alkali extraction to remove the lignin and leave the cellulose. The process uses a screw conveyor to feed the raw material into a coaxial cylindrical chamber where it undergoes hydrolysis to furfural and is then flashed into a blow bin where the residue is separated from a product vapour rich in furfural. The residue is transferred to a rotary dryer driven by superheated steam. The exiting vapour, cleaned of entrained particles by a cyclone, enters a partial condenser, producing an aqueous effluent and a small vapour fraction containing some furfural. Despite its advantages, the process requires a significant amount of water to produce furfural, which can dilute the acid catalyst and reduce the calorific combustion benefit of the residue.

All the processes described and listed in Table 1.5 require further purification of the furfural downstream of the reactor. Furthermore, it is common practice for these processes to treat the liquid effluent prior to its discharge into natural watercourses. The following sections (1.3.3.I and 1.3.3.II) provide an overview of the purification train and water treatment approaches commonly applied in these processes.

I. Furfural purification

As there are many similarities between commercial and semi-commercial scale processes, the purification train used in these processes is also quite similar. The most common processes for obtaining furfural with purities of 98.5-99.5% are described below.

The furfural stream leaving the reactor consists mainly of water (over 90%), furfural (up to 6%) and various by-products. This stream is condensed before distillation, which is often used to produce secondary vapour. In addition, it is usually subjected to filtration or centrifugal separation of solids. The resulting product stream is fed to a distillation unit as shown in Figure 1.19.

The distillation unit uses an azeotropic distillation column (A) operating at atmospheric pressure to receive the condensed product. This column uses the water/furfural azeotrope, characterised by an atmospheric boiling point of 97.85°C and a water content of 65%, to separate the water/furfural mixture from substances with lower boiling points, such as

methanol, and those with higher boiling points, including carboxylic acids such as acetic acid.

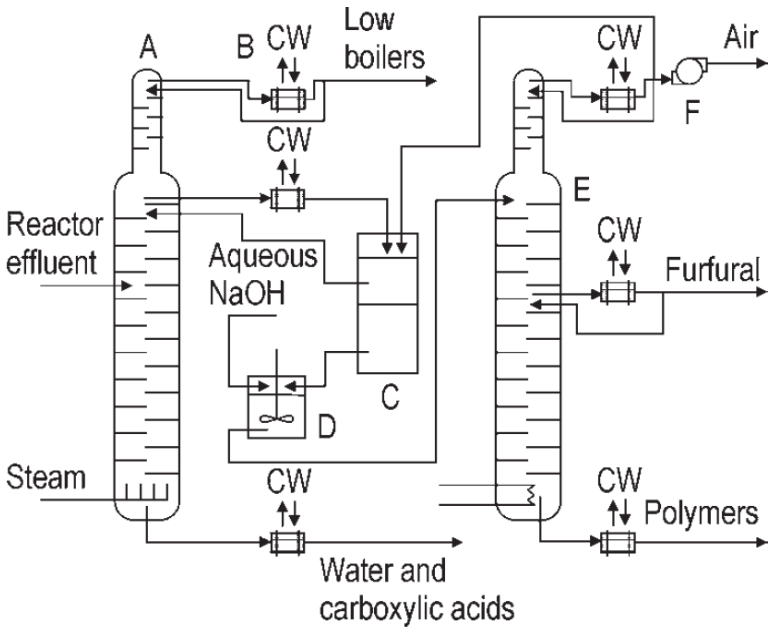

Figure 1.19. Furfural distillation scheme, from [77].

A fraction close to the azeotrope is withdrawn from the column as a liquid side stream and fed to a decanter (C). Here it separates into two liquid phases: a light phase, rich in water and containing a small amount of furfural, and a heavy phase, rich in furfural (typically 94 wt.%). The light phase is refluxed back into the azeotropic column, while the heavy phase is neutralised with an alkali (D) before being subjected to a further vacuum distillation (E) to recover pure anhydrous furfural. The bottom fraction of the azeotropic column, loaded with carboxylic acids (mainly acetic acid), can be discharged into the sea or a wastewater treatment plant, or further processed.

The top fraction of the vacuum column, containing the water-furfural azeotrope, is recycled to the static decanter. The bottom fraction, which contains a small amount of furfural polymers, is typically discarded. In this configuration, furfural is once again removed as a side stream. However, the objective of operating at low pressures is to reduce polymer formation. Consequently, many columns are capable of operating without three outflows and recovering the furfural at the base of the column.

II. Wastewater treatment

The following subsection has been adapted from Reference [75], as it describes the wastewater treatment process in great detail on an industrial scale.

The wastewater from all furfural production plants contains a variety of carboxylic acids, with acetic acid being the main component at 1 to 5% by weight. Furfural is also present in concentrations up to 600 ppm. The concentration of furfural depends on the efficiency of the first distillation column, with superior columns reducing the concentration to 50 ppm. If the concentration of acetic acid is insufficient to justify the installation of an acid recovery facility, the most common approach is to directly discharge the effluent, although this practice is expected to be abandoned.

In light of these developments, anaerobic digestion of wastewater has become the preferred method (Figure 1.20). Methanogenic bacteria not only thrive on acetic acid but also consume furfural at the concentrations found. These bacteria, which are known to convert acetic acid into methane and carbon dioxide according to the reaction $CH_3COOH \rightarrow CH_4+CO_2$, are used as "filters" that retain the methane bacteria, especially for the low concentrations of acetic acid in furfural wastewater.

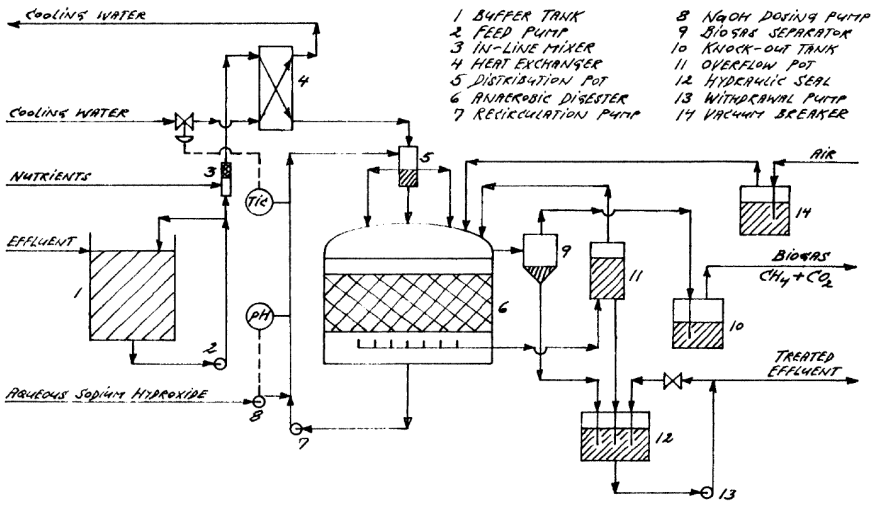

Figure 1.20. Industrial anaerobic wastewater treatment plant for a furfural production plant, from [75].

An industrial furfural wastewater treatment plant, described in Zeitsch's book [75], is shown schematically in Figure 1.20. After 90% of the chemical oxygen demand (COD) has been removed by anaerobic treatment,

the remaining 10% can be eliminated by subsequent aerobic treatment, as it relates to substances that cannot be metabolised by methanogenic bacteria. It should be noted, however, that the aerobic removal of the last 10% of COD requires a larger plant than the anaerobic removal of the first 90%. In addition to its considerable size, subsequent aerobic treatment has two other drawbacks: the rapid proliferation of microorganisms, resulting in sludge problems, and a significant amount of electrical energy required to oxygenate the water.

As previously outlined, there is a clear necessity for a shift in the production of strategic chemical compounds in Europe towards more sustainable strategies. The following chapters of this doctoral thesis will evaluate the environmental and economic viability of a new furfural production process, in line with the sustainable development objectives set for the coming decades.

OBJECTIVES

This doctoral thesis is situated within the framework of the bioeconomy. In particular, the thesis seeks to implement new lignocellulosic biorefinery models that move towards a circular system. This transition is only beneficial if it ensures an improvement in sustainability concerning existing processes. To achieve this, it is essential to integrate tools for life cycle assessment from the design phase onwards.

The driving force behind this circular bioeconomy is the market penetration of bio-based products that replace conventional products. In order to achieve this, these products must be economically competitive. This work is focused on the production of furfural due to its commercial relevance as a platform molecule.

In this context, this thesis sets out to achieve two general objectives (G.O.). First, to outline the environmental profile of a new technological development in furfural production (G.O. 1). The majority of furfural production occurs in countries with fewer environmental restrictions. Consequently, the implementation of a process that complies with both current and future European legislation would serve to attract production and stimulate the economy. The indicators measured provide relative information; therefore, it is necessary to contrast them with existing benchmarks. Accordingly, the second objective of this thesis is to compare the sustainability metrics with the results obtained by conventional technologies (G.O. 2).

To achieve these two general objectives, the following specific objectives (E.O.) are set out. The specific objectives are shown in chronological order, relating them to the general objective they serve.

E.O. 1: Identification of methodological best practices for the LCA in the context of the thesis.	**G.O. 1-2**
E.O. 2: Generation of an inventory of benchmark technologies through rigorous simulation of existing literature data.	**G.O. 2**
E.O. 3: Ensure comparable simulation conditions and LCA choices to operate within the same methodological framework in the case of conventional technologies and the proposed technology.	**G.O. 2**
E.O. 4: Life cycle analysis of proposed technology to replace conventional furfural production.	**G.O. 1**
E.O. 5: Case study on the construction of a furfural production plant in Spain. Design and optimisation of the supply chain based on economic and environmental parameters.	**G.O. 1**

Results are presented in Chapters I to II within the results block, ordered according to these objectives. Consequently, Chapter I establishes the foundation for standardising the decision-making process regarding the LCA methodology. This helps ensure comparability and elucidate the most appropriate choices in the context of bio-based products (E.O.1).

Chapter II presents the simulation and LCA results of the reference technologies for furfural production. This provides a rigorous benchmark to compare the results of any alternative process (E.O.2).

Chapter II provides a detailed account of the design, techno-economic analysis and LCA of a novel process for furfural production. The results are contrasted with those obtained in Chapter II, based on the criteria defined in Chapter I (E.O. 3 and 4). Finally, a case study is proposed for the construction of a furfural production plant in Spain based on this technology. The supply chain optimisation results based on economic and environmental criteria are presented (E.O.5).

METHODOLOGY

The methodology section presents the rationale, limitations, and assumptions of the software tools used for the development of this thesis. The tools used were Aspen Plus for process simulation in Chapters II and III, the Activity Browser in Chapters II and III for life cycle analysis, and GAMS for biomass supply chain formulation and optimization shown in Chapter III.

Most of the information on the applied procedures is provided within each appropriate results chapter for in-context clarification. Notwithstanding, the methodology provides more general information as a reference for the following sections.

3.1. Process simulation with Aspen Plus

Data to complete the consumption and emissions inventory required for the life cycle analysis of the furfural production systems were obtained using the software Aspen Plus (v12.1). Aspen Plus is a leading chemical process simulator used by engineers to model a wide range of chemical processes. For a given process design and an appropriate selection of a thermodynamic model, Aspen Plus uses mathematical reasoning to predict the performance of the process. It does this by solving the material and energy balances of all the unit operations included in that design. The calculation is done sequentially so that the output of one unit is the input to the next unit downstream. Aspen uses different convergence methods to ensure that the overall calculation meets given tolerances before returning a solution.

This section describes the main definitions and assumptions in the models shown in Chapter II.

3.1.1. Components definition

Given the complexity of biomass, the definition of compounds is a laborious process. In the present work, the definition of biomass was carried out systematically through the most abundant components of its structure: cellulose, hemicellulose, and lignin. In addition, the inert compounds were considered in the form of ashes, while the oleaginous fraction was discarded when dealing with the kinetics, as its role in the process is of minor significance, both quantitatively and functionally. Finally, a percentage of the biomass was populated with acetyl and formyl groups, which contribute significantly to the formation of acetic and formic acids in the reactor, according to the literature [75]. The pentosan chains of the raw material are dotted to varying degrees with acetyl, formyl and similar groups. The ratio of acetyl to formyl groups is typically 10:1. In a characteristic hardwood pentosan, the distribution of acetyl is such that 58% of the rings have no acetyl groups, 24% are acetylated on C-3, 12% on C-2 and the remaining 6% have acetyl groups on both C-3 and C-2 [75]. All these compounds were described as conventional solids in Aspen Plus.

Some of these compounds are readily available in the databases associated with Aspen Plus, such as cellulose. For solids not present in these databases, such as pentosans, the definition provided by the National Renewable Energy Laboratory (NREL) in [92] has been adopted. A full list of the compounds included in the simulations is given in Table 3.1, although the specific composition is further defined for each process separately (see 5.1.1

and 5.1.2). In the case sugars, acids, and other soluble compounds, the definition is taken directly from databases.

Table 3.1. Components included in the Aspen Plus simulations.

Name	Type	Comment
Cellulose	Solid	
Xylan		Solid xylose modified based on [92]
Arabinan		
Lignin		Vanillin modified based on [92]
Ash		Solid calcium oxide
Acetyl groups		Solid acetic acid modified based on [92]
Formyl Groups		Solid acetic formic modified based on [92]
Tar (type 1)		Solid xylose modified based on [93]
Tar (type 2)		
Glucose	Conventional	Dextrose
Xylose		
Arabinose		Xylose
Xylose intermediates		Xylose as a proxy for intermediates (see 1.3.1)
Furfural		
Acetic acid		
Formic acid		
Methanol		
Water		
Sulfuric acid		
Calcium oxide		
Sodium carbonate		
Sodium acetate		
Methane		
Carbon dioxide		

3.1.2. Thermodynamic model selection

One of the primary challenges in furfural production processes is purification, specifically the separation of the azeotrope furfural-water [94 - 96]. Accurately modelling the complex equilibrium relationships is necessary for this purpose. The non-random two-liquid (NRTL) model is commonly used due to its ability to predict vapour-liquid equilibria (VLE) and liquid-liquid equilibria (LLE) of mixtures with strong non-idealities. This method is also used and recommended by NREL in previous publications for similar mixtures [97]. Additionally, the Redlich-Kwong (RK) equation of state (EOS) was introduced. The RK equation is endorsed for describing the carboxylic acids interaction in the gas phase. It is a simplification of the Hayden-O'Connell (HOC) EOS, since it captures a lower number of interactions. This

generalization is valid since the system operates at pressures below 10 atm, as stated in the Aspen manual.

A singular feature of any furfural production process is the separation of the azeotrope formed with water (see 1.3.3.I). It is of paramount importance to accurately predict this equilibrium to correctly model the interactions in the first distillation column. Figure 3.1 displays the Txy diagram for the furfural-water mixture, accurately predicting the azeotrope at 97.46°C and 65 wt.% water, consistent with the findings in [75]. The diagram was obtained from the simulations presented in Chapters II and III of this doctoral thesis.

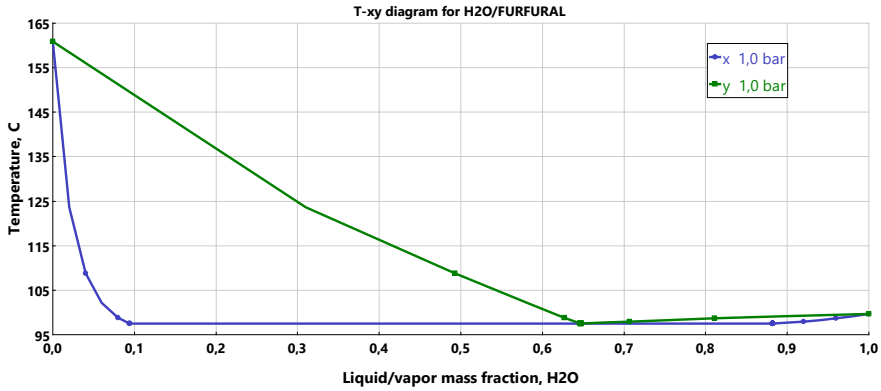

Figure 3.1. Txy diagram for the water-furfural binary mixture at P = 1 atm.

3.1.3. Kinetic model for furfural production

As described in Section 1.3.1, the reaction conditions characteristic of these processes benefit from the easier conversion of the hemicellulosic fraction compared to cellulose. Conventional processes therefore operate under mild conditions of pressure and temperature. In this way, the cellulose is not degraded into smaller oligomers, which are more difficult to separate, and retains its structure almost intact. For this reason, the reaction cascade from cellulose to compounds such as lactic and formic acids was considered to be only partially active and does not extend beyond glucose. Lignin also remains unaltered under these conditions and is therefore considered as an inert. Following this reasoning, the reactions included in the kinetic model are as shown in Figure 3.2.

The introduction of these kinetics in Aspen is described below, based on the schemes presented in this figure and discussed in more detail in Section 1.3.1. These are referred to as Powerlaw models or Langmuir-Hinshelwood-Hougen-Watson (LHHW) kinetic, as appropriate. The former is an empirical adjustment suitable for unidirectional chemical reactions whose kinetics are free of the effect of the catalyst. For a simple reaction as

$$A + B \overset{k}{\rightarrow} C + D \qquad \textit{Eq. (3.1)}$$

the reaction rate is defined as:

$$-\frac{dC_A}{dt} = (-r_A) = kC_A^m C_B^n \qquad \textit{Eq. (3.2)}$$

where k is the kinetic constant defined by the Arrhenius equation as:

$$k = Ae^{(-\frac{Ea}{RT})} \qquad \textit{Eq. (3.3)}$$

The remaining terms are defined in the glossary Section for clarity. In contrast, LHHW kinetics are usually appropriate for describing kinetics in heterogeneous catalytic systems where the totality of the species can be absorbed into the active centres of the catalyst, the reactions are reversible, and the process is controlled by the chemical reaction, as in *Eq. (3.4)*. In the case described in this thesis, the catalyst is homogeneous, and the reactions are unidirectional, so the LHHW kinetic model is used to introduce the effect of the catalyst on the reaction rate as described hereafter.

$$A + B \overset{k_f k_r}{\longleftrightarrow} C + D \qquad \textit{Eq. (3.4)}$$

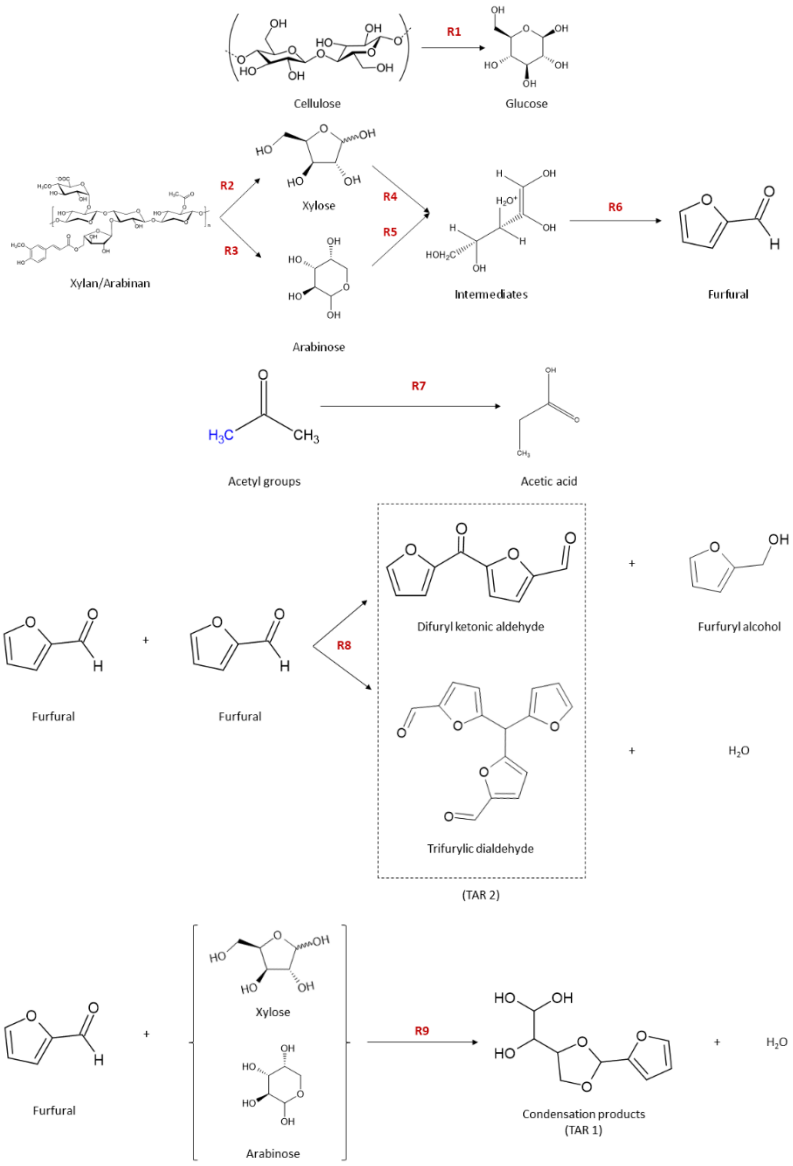

Figure 3.2. Set of reactions included in the kinetic model of Aspen Plus.

This is achieved by utilising the mathematical formulation of the equation in Aspen. The equation is generally expressed as:

$$r = \frac{(kinetic\ factor)(driving\ force)}{(adsorption\ term)} \qquad \textit{Eq. (3.5)}$$

Where:

$$kinetic\ factor = k^{*}e^{-\frac{Ea}{R}\left(\frac{1}{T}\right)} \qquad \textit{Eq. (3.6)}$$

$$dirving\ force = k_f \prod_{i=1}^{N} C_{A,B}^{\alpha_{A,B}} - k_r \prod_{j=1}^{N} C_{C,D}^{\beta_{C,D}} \qquad \textit{Eq. (3.7)}$$

$$adsorption\ term = \sum_{i=1}^{M} K_i \left(\prod_{j=1}^{N} C_j^{v_j} \right)^{m} \qquad \textit{Eq. (3.8)}$$

To fit these expressions to the case study, the reaction is defined as irreversible by setting the inverse equilibrium constant in the driving force to 0. These constants are defined in Aspen as the sum of several coefficients, as shown in *Eq. (3.9)*:

$$ln\left(k_{f-r}\right) = A + \frac{B}{T} + C \cdot \ln(T) + DT \qquad \textit{Eq. (3.9)}$$

Therefore, the following modifications are made for the inverse constant:

$$B = C = D = 0 \qquad \textit{Eq. (3.10)}$$

$$k_r = e^{A} \ \therefore A = -10^{30} \qquad \textit{Eq. (3.11)}$$

Thus, the reverse reaction is virtually zero. Conversely, for the direct constant all these coefficients are simply defined as 0, so that:

$$A = B = C = D = 0 \qquad \textit{Eq. (3.12)}$$

$$\ln\left(k_f\right) = 0 \ \therefore k_f = 1 \qquad \textit{Eq. (3.13)}$$

Finally, the adsorption term is used as a mathematical proxy to account for the influence of the homogeneous catalyst. Depending on the adsorption mechanism (*Eq. (3.14)*), multiple coefficients can be defined for each species in the reaction environment. These coefficients are assigned to represent the power each species in *Eq. (3.14)* are raised to.

$$Ads = \{1 + K_A[A] + K_B[B] + K_C[C] + K_D[D]\}^n \qquad \textit{Eq. (3.14)}$$

In this case, the coefficient n is assigned a negative value so that it moves to the numerator, multiplying the forward reaction constant and the kinetic factor. Thus, the final expression defined from the LHHW formulation is:

$$r = \frac{\left(k^* e^{-\frac{Ea}{R}\cdot\left(\frac{1}{T}\right)}\right)\cdot\left(k_f[A][B]\right)}{(\{1 + K_A[A] + K_B[B] + K_C[C] + K_D[D]\}^{-n})} \qquad \textit{Eq. (3.15)}$$

Table 3.2 summarises the kinetic expression and constants used for the simulation of the reaction mechanism shown in Figure 3.2.

Table 3.2. Kinetic expressions and constants.

Reaction no.	Mathematical expression	Kinetic constants	Ref.
1	$(-r_C) = \mathrm{k}C_C$ $\mathrm{k} = \left[(2{,}71 * 10^{19}) * C_{H_2SO_4}^{2,74}\right] * e^{\left(-\frac{Ea}{RT}\right)}$	$E_a = 189.5\frac{kJ}{mol}$	[98]
2,3	$(-r_{X,A}) = \mathrm{k}C_{X,A}$ $k = \left[\left(7{,}64 - \frac{3{,}68}{C_{H_2SO_4}}\right) * 10^{20}\right] * e^{\left(-\frac{Ea}{RT}\right)}$	$E_a = 171.5\frac{kJ}{mol}$	[98]
4,5	$(-r_{x,a}) = \frac{k'_{x,a}C_{x,a}}{C_{H_2SO_4}^{-2}} + \frac{k''_{x,a}C_{x,a}}{C_{H_2SO_4}^{-1}}$ $k'_{x,a} = 2{,}314 * 10^{12} * e^{\left(-\frac{Ea\frac{kJ}{mol}}{RT}\right)}$ $k''_{x,a} = 3{,}443 * 10^{13} * e^{\left(-\frac{Ea\frac{kJ}{mol}}{RT}\right)}$	$E_a = 128.7\frac{kJ}{mol}$ $E_a = 133.8\frac{kJ}{mol}$	[99]
6	$(-r_I) = \frac{k'_I C_I}{C_{H_2SO_4}^{-1}} + k''_I C_I$ $k'_I = 4{,}624 * 10^{15} * e^{\left(-\frac{Ea\frac{kJ}{mol}}{RT}\right)}$ $k''_I = 15{,}643 * e^{\left(-\frac{Ea\frac{kJ}{mol}}{RT}\right)}$	$E_a = 140.4\frac{kJ}{mol}$ $E_a = 31.6\frac{kJ}{mol}$	[99]
7	$(-r_{\mathrm{Ac}}) = \frac{k_1 C_{Ac}}{C_{H_2SO_4}^{-1,18}}$ $k_1 = 1{,}21 * 10^8 * e^{\left(-\frac{Ea\frac{kJ}{mol}}{RT}\right)}$	$E_a = 31.6\frac{kJ}{mol}$	[99]
8	$k = 0.000125$ [a]		[93]
9	$k = 0.000648$ [a]		[93]

a. Zero-order reaction kinetics

3.1.4. Simulation of the organosolv fractionation plant

As detailed in the objectives of this thesis (see OBJECTIVES), the conventional furfural production processes are compared with an alternative technology seeking to improve their sustainability. The process is based on the fractionation of biomass with gamma-valerolactone due to the properties of this solvent, as detailed in Section 1.2.2.II. The simulation of the process is presented in Chapter III and was conducted as part of a public-private venture in the context of a European project. As detailed in Section 6.1, the data used in the generation of the simulations were provided by project partners (CSIC). Additionally, the construction of the flowsheet in Aspen was carried out by the Process Design Center (PDC). The role of this work was to produce an initial design and to adapt the final concept to ensure comparability with the models presented in Chapter II. As a result, the details disclosed in this thesis are limited. However, this section summarizes the main definitions, limitations, and assumptions adopted.

The process of defining compounds for the organosolv process was performed in a similar way than for the conventional furfural systems, with a few exceptions. The reactors rely on experimental yields rather than kinetics, resulting in cellulose and lignin being obtained only as process outputs rather than inputs. Conversely, the reactions are defined based on the direct degradation of the compound 'biomass', which yields a different set of products depending on the process unit evaluated. In Aspen, this 'biomass' is defined as an unconventional solid based on its proximate analysis. This approach is a scientific method used to determine the approximate amounts of substances in a material. Aspen's evaluation is based on the biomass moisture content (wt.%), fixed carbon, volatile matter, and ashes proportion. The consequences of defining biomass in terms of its components or as a non-conventional solid are reflected in the way Aspen considers the effects of matter and energy transport. In this instance, the biomass is fed directly into the fractionation reactor. As this reactor is based on experimental yields, these effects can be ruled out.

Cellulose is defined in the same way as described above (Table 3.1), while lignin is considered within the soluble streams. This is because the process uses GVL as a solvent, which allows the dissolution of this polymer under the operating conditions (see Section 1.2.2.II). To represent their interaction properly, the trans-sinapyl alcohol compound is used as it is one of the most repeated monomers in the lignin structure. For the same reasons, hemicellulose is only considered in the solubilised phase and is represented by

B-D-xylopyranose, due to the high proportion of this C5 sugar in its structure. Ash and tars are assumed to be distributed between the two phases (solid and soluble) according to available experimental data.

The thermodynamic model used is again the NRTL. Although the Redlich-Kwong EOS was not consistently applied throughout the plant, it was considered in certain process units when necessary.

3.2. Life Cycle Assessment tools

The LCA cases were run using Brigthway (BW). BW is an open-source Python library, which works as a modular framework for life cycle analysis [101]. The tool is designed in blocks, allowing for customization of the workflow to meet specific needs and making it easy to expand and adapt the framework for different LCA applications. The software enables the performance of life cycle analyses that consider both spatial and temporal dimensions, as well as the assessment of uncertainty and sensitivity in LCA results in a simple and flexible manner. It features a graphical interface based on Python and Jupyter notebooks, although this has been simplified with the introduction of the Activity Browser application. The Activity Browser is a graphical interface that facilitates interaction with BW. The software permits the utilization of parameters, scenarios (including potential inventory databases from Premise [69]), and uncertainties. Additionally, it incorporates a module (Graph Explorer) that enables the visualization of inventories, simplifying their comprehension and interaction. BW was operated through the Activity Browser (AB) interface [102]. AB is an open-source tool that builds on the BW structure as a convenient graphical user interface (GUI).

The data for modelling the background system is retrieved from the V3.9 version of the Ecoinvent database. The APOS (at the point of substitution) model was selected. This approach was preferred over the cut-off version. The difference between the two is that in the cut-off version, recyclable materials are excluded from the system and are not allocated to any product. The environmental impacts are only calculated for the final products, taking the waste as a non-polluting input. In the APOS model, waste is allocated to by-products with economic value. This perspective distributes the impacts of products from recycling processes across all outputs so that the entire supply chain can be considered without "cutting off" at any "zero impact" points. In the same line, unless otherwise stated the processes introduced from Ecoinvent as inputs are considered as systems and not as unitary processes.

The methodology used for calculation is Environmental Footprint 3.1 (EF3.1). The use of this methodology aligns with the objectives of this doctoral thesis, which aims to produce results relevant to the European context. The EF3.1 was developed jointly by the European Commission and the EF Technical Advisory Board [103]. It outlines indicators and characterisation factors that have been agreed upon over almost a decade, based on existing

methodologies and through its application in several pilot projects covering different productive sectors.

Furthermore, Chapter III presents part of the results using the ReCiPe 2016 v1.03 methodology. The rationale for this approach is the convenience of this methodology for studying the trade-offs between objective functions of different natures. The EF3.1 methodology only considers impacts at the midpoint level, so it is discarded at this point as it would imply the comparison of the cost function against 16 impact indicators. Conversely, in the ReCiPe methodology, the environmental functions are observed at the end of the impact pathway to evaluate their influence on a set of protected areas (AoPs). Consequently, the environmental indicators are aggregated into three categories, significantly simplifying the analysis. Moreover, the ReCiPe 2016 is a procedure with broad scientific support, as demonstrated in Chapter I.

The uncertainty of all LCA results is quantified, taking into account variations in the technosphere inputs (industrial and human interactions), and the elementary flows with the biosphere (emissions and environmental removals). These variations are represented by lognormal probability distributions, characterized using the Pedigree matrix. Monte Carlo sampling is used to propagate these variations through the LCA model, thereby generating a probability distribution for each LCA result that describes its uncertainty.

3.3. Supply chain optimisation problem

For the supply chain optimisation problem presented in Chapter III, the GAMS (General Algebraic Modelling System) suite was used. GAMS is a mathematical modelling program that is commonly used to solve large-volume optimisation problems. It integrates linear and non-linear solvers that can be applied in a modular way. In this work, version 45.7 of GAMS Studio was employed, which is compatible with the Windows operating system (OS). This software is commonly used to model biomass supply chains, taking into account factors such as location, distribution, capacity, facility technology, and material flow design.

The problem was solved using the CPLEX solver. This solving method is commonly used for linear programming (LP) problems, which are common in decision making and planning. CPLEX implements optimisation methods based on simplex algorithms. Simplex algorithms are used to maximize or minimize a linear objective function subject to linear constraints. The algorithm starts with a basic feasible solution and iteratively improves it until an optimum is reached. This is done by exploring the vertices of the feasible solution space, moving between the corners of the polyhedron defined by the constraints. Following, a simplified example of an LP problem is solved to show how this tool works:

Let's consider a hypothetical company that produces two products, A and B, using three available machines. Each machine has a daily production capacity for both products. The profits per unit of product are:

Product A: Profit of $10 per unit
Product B: Profit of $15 per unit

The daily machine capacities are as follows:

Machine 1: 8 units of product (either A or B)
Machine 2: 10 units of product (either A or B)
Machine 3: 12 units of product (either A or B)

The aim is to maximise the total profit of the company while taking into account the capacity constraints of the machines. The decision variables are:

x(A): Quantity of product A produced
x(B): Quantity of product B produced

The objective function is defined as:

$$Z = 10x(A) + 15x(B)$$

Finally, the problem constrains would be defined as:

$$x(A) + x(B) \leq 8 \quad \text{for machine 1}$$
$$x(A) + x(B) \leq 10 \quad \text{for machine 2}$$
$$x(A) + x(B) \leq 12 \quad \text{for machine 3}$$
$$x(A), x(B) \geq 0$$

To solve this model in GAMS, first the intervening variables are declared, including the objective function that is to be maximised:

```
Variables
x_A
x_B
Z;
```

The capacity restrictions of the machines are defined in the equations MC1 to MC3. Then, the objective function (Z) is defined as the sum of the benefit of producing each product.

```
Equations
MC1
MC2
MC3;

MC1..   x_A + x_B =L= 8;
MC2..   x_A + x_B =L= 10;
MC3..   x_A + x_B =L= 12;

Z =E= 10 * x_A + 15 * x_B;
```

The problem is solved using the linear programming (LP) method by calling the solver (CPLEX) and executing the Solve command.

```
optionLP = CPLEX
Model MachineProduction /all/;
Solve MachineProduction using LP maximizing Z;
```

In addition, the Epsilon-constraint method was applied to study the trade-offs between different functions. The Epsilon-constrain method is based on the idea of transforming the multi-objective problem into several single-objective problems by introducing additional constraints. When there are different conflicting objectives, this method seeks to find a set of solutions that are not only feasible but also represent a balance between them. For example, in supply chain planning, objectives such as minimising costs and reducing carbon emissions may be considered. Let's suppose the optimisation these two objective functions: $f_1(x)$, $f_2(x)$, where (x) represents the vector of decision variables. For each objective $(f_i(x))$, an additional constraint is introduced in the original problem: $(f_i(x)) \leq \varepsilon)$. Where ε is a small value representing a

threshold for the objective *($f_i(x)$)* that is modified at specific intervals. The single-objective problem is solved for each objective *($f_i(x)$)* with the corresponding constraint. By varying the values of ε, a series of solutions are obtained that represent different trade-offs between the objectives. These solutions form a Pareto curve (also known as a Pareto front), which shows the non-dominated solutions, where one objective cannot be improved without worsening another. Depending on the decision-maker's preferences, a specific solution can be chosen from the Pareto curve. For example, if cost is considered more important, a lower-cost solution would be selected, even if it implies a slight increase in carbon emissions.

RESULTS AND DISCUSSION

CHAPTER I:
LIFE CYCLE ASSESSMENT APPLIED TO BIO-BASED PLATFORM MOLECULES - CRITICAL REVIEW OF METHODOLOGICAL PRACTICES

Fossil resources are one of the principal drivers of the global economy. Both energy and bulk commodities derived from petroleum are indivisible from our current way of life. Still, an already settled conscience of the damages inflicted by its unbridled consumption is forcing a paradigm shift. The environmental concerns resulting from their extraction and use, the depletion of fossil resources, the energy independence, and the climate change effects are perceived as especially urgent.

As stated before, the solution necessarily involves the transition to renewable and sustainable carbon sources, such as the lignocellulosic biomass. In 2018, 507 biorefineries in Europe were already producing biochemicals [64]. Bio-based platform molecules are a set of compounds identified as key intermediates for biorefineries development. Although this constitutes a promising scenario, these incumbent technologies are hampered by intrinsic difficulties such as the decentralized collection of raw materials or the fluctuations in their quantity and quality [104].

In this sense, life cycle assessment (LCA) is a fundamental tool to identify hotspots and ensure environmental improvements of the new bioresources-based processes as compared to their conventional fossil-based counterparts. As a measure of its importance, the environmental performance of novel bioprocesses has been extensively reviewed [105 - 111]. Even though the number of LCAs published on biomass-derived chemicals has rapidly

grown, comparison between them is still limited due to the heterogeneous methodological choices applied. This is also acknowledged in the case of bio-based plastics by other authors [112, 113], who greatly discussed how LCA is applied to this particular field. Additionally, Montazeri et al. [114] analysed the conclusions of 86 life cycle case studies on the main priority biochemicals to compare their impact on energy and greenhouse gas emissions.

The present chapter aims to cover two objectives. In a first step, an evaluation of how LCA is customarily applied to biomass-derived chemicals is presented. This first target aims at finding the main discrepancies between analogous studies. Next, the major findings in this stage are critically examined to derive recommendations based on consensus practices which might help to mitigate methodological divergences. In short, the main purpose of this chapter is to determine the key methodological choices that restrict the comparison between studies and try to find common ground around the best practices identified to converge underpinning decisions as much as possible. That will set the basis for the analysis in the rest of the work.

I.1. Literature review

Literature searching was conducted following a methodological procedure to ensure completeness and appropriateness of the retrieved data. Two databases were employed, namely Scopus and Google Scholar. In both cases, the same arrays of terms were defined, which are summarized in Table I.1.

Table I.1. Terms used for literature search. The Boolean function OR was introduced for items in the same columns, while function AND was introduced to separate items in different columns.

Col-1 (NAME)	Col-2 (TOPIC)	Col-3 (FIELD)
Molecule	Bio-	Assessment
		Life Cycle
Molecule Synonym 1		Environment-
		Eco-
		Sustainab-
Molecule Synonym 2		Green
		Footprint

All considered, 64 publications were deemed for the analysis. The selection of the molecules evaluated is justified in the following section.

I.2. Selection of the bio-based platform chemicals

The choice of the evaluated molecules was performed as described hereafter. First, a broad screening was carried out based on the report on global trends for bio-based building blocks published by the nova-Institute [115]. From this list, only molecules receiving the higher attraction from research community were considered for further analysis. The differentiation is based on two criteria, namely the number of publications in which the selected bio-derived chemical is mentioned and the expected industrial relevance for each one of them. For the first condition, the Col-1 and Col-2 arrays in Table I.1 were used. That contributed to distinguishing between oft-cited (e.g.: lactic acid, 3,241 documents) and scarcely cited (e.g.: caprolactam, 49 documents) molecules. The latter were then excluded from the analysis. For the second requirement the projections discussed by Bozell and Petersen in [74]. were considered. Thus, only the most relevant bio-based platform molecules were evaluated, as the data used in these studies is expected to be more accurate due to larger availability. A third cut-off criterion was applied to the remaining molecules in the list, introducing the terms in Col-3 of Table I.1**¡Error! No se encuentra el origen de la referencia.** to exclude molecules with a low number of published LCA studies, since its inclusion would not add any statistically significant information to the chapter. Additionally, ethanol is excluded from the analysis, since the profuse number of studies about its production would constitute a separate work itself. Furthermore, five review papers about environmental considerations in the production of bioethanol are already available in existing literature [116 - 120], so its consideration might be redundant.

All considered, eight molecules were chosen for the analysis. These include four acids: lactic, succinic, levulinic, and adipic acid; three furanics: furfural, 5-hydroxymethylfurfural, and 2,5-furandicarboxylic acid; and ethylene.

I.3. LCA Meta-analysis

The LCA meta-analysis has been performed through six critical aspects: the definition of the initial conditions (i.e., system boundaries and functional unit definition), the perspective followed (attributional or consequential), data gathering and management (i.e., inventory construction, data quality, and uncertainty), multifunctionality handling, impact assessment, and carbon flow considerations.

Table I.2. Complete list of reviewed LCA studies. C-Gt: Cradle-to-Gate, C-Gv: Cradle-to-Grave, Gt-Gt: Gate-to-Gate, MO: Multi-output, PAR: Parametric uncertainty, SCN: Scenario uncertainty, Q: Data quality. The rest of the abbreviations can be easily consulted in the corresponding sections.

Definition		**Primary**	**MO**	**LCIA** [c]		**Uncertainty**			**Ref.**
Bound	Persp.[a]	**data** [b]	**Handling**	Method	Focus	PAR	SCN	Q	
C-Gt	CLCA	X	SE	CED, IPCC, EI99 [d]	MP/EP		X		[121]
C-Gt	ALCA		SB, EA	ReCiPe	MP	X	X		[122]
C-Gt, C-Gv	ALCA			GREET	MP	X	X		[123]
C-Gt	ALCA, CLCA		SE, EA	EDP, ReCiPe	MP	X	X		[124]
C-Gt	ALCA		SB, EA	ReCiPe	MP		X		[125]
C-Gt	ALCA		EA	CML	MP		X		[126]
C-Gt	CLCA	X	SE, SD	ReCiPe	MP/EP	X	X		[127]
C-Gt	ALCA	X	SB, EA	IPCC, ReCiPe	MP		X		[128]
C-Gv	CLCA		SE	ReCiPe, SWB	MP/EP	X	X	X	[129]
C-Gt	CLCA	X	SE	Impact 2002+	EP	X	X		[130]
C-Gt	ALCA			TRACI	MP				[131]
C-Gt	ALCA		EA	ReCiPe	MP	X	X		[132]
C-Gv	CLCA	X	SE	ILCD	MP	X	X		[133]
C-Gt	ALCA		SB	IPCC	MP	X	X		[134]
C-Gt	ALCA	X	EA	ReCiPe	MP/EP	X	X		[135]
Gt-Gt	ALCA			GREET	MP	X	X		[136]
C-Gt	ALCA	X	SB, MA, EA	CED, IPCC	MP	X	X		[137]
C-Gv	ALCA			GREET	MP	X	X		[138]
C-Gt	ALCA	X	SB	ReCiPe	MP		X		[139]
C-Gt	ALCA			CED, IPCC, EI-99	MP/EP		X		[140]
C-Gt	ALCA	X	SB	IPCC	MP		X		[141]
C-Gt	ALCA	X		CED, IPCC	MP		X		[142]
C-Gt	ALCA			CED, CML	MP		X		[143]
C-Gt	ALCA	X	SB, MA, CE, EA	GREET	MP	X	X		[144]
C-Gt	ALCA		MA	-	MP	X	X		[145]
C-Gt	ALCA	X	EA	CML	MP	X	X		[146]
C-Gt	ALCA		MA	CED, IPCC	MP		X		[147]

Definition		Primary	MO	LCIA [c]		Uncertainty			Ref.
Bound	Persp.[a]	data [b]	Handling	Method	Focus	PAR	SCN	Q	
C-Gt C-Gv	ALCA		MA, EA	CML, IPCC, WSI, Impact 2002+	MP/EP	X	X		[148]
C-Gt	ALCA			IPCC	MP				[149]
C-Gt	ALCA	X		CML	MP				[150]
C-Gt	ALCA	X	EA	ReCiPe	MP				[151]
C-Gt	CLCA		SE	CML	MP				[152]
C-Gt	ALCA, CLCA	X	SE, MA, EA	ReCiPe	MP	X	X		[153]
C-Gt	ALCA			CML, IPCC, KWTIS	MP		X		[154]
C-Gt	ALCA	X		ReCiPe			X		[155]
C-Gv	CLCA		SE	CML, Impact 2002+	MP				[156]
C-Gt	ALCA				MP		X		[157]
C-Gt	ALCA			CML, IPCC, KWTIS [e]	MP		X		[158]
C-Gt	ALCA		EA	CML, AWARE, EI-99	MP	X	X		[159]
C-Gt	ALCA		MA	ReCiPe	MP	X			[160]
C-Gt	ALCA			ReCiPe	MP	X	X		[161]
C-Gt	ALCA	X		ReCiPe	MP		X		[162]
C-Gt	ALCA				MP				[163]
C-Gt	CLCA	X	SE	CML	MP	X	X		[164]
C-Gt	ALCA	X		CML	MP	X	X		[165]
C-Gt	ALCA	X		ReCiPe	MP/EP		X		[166]
C-Gt	ALCA		EA	ReCiPe	MP		X		[167]
C-Gv	ALCA	X		ReCiPe	MP	X	X		[168]
C-Gt	ALCA	X	EA, EnA	CED, GGP, ReCiPe	MP	X			[169]
C-Gt	ALCA		EA	ReCiPe	MP	X	X		[170]
C-Gt	ALCA	X		ReCiPe	MP				[171]
C-Gt	ALCA		MA	ReCiPe, Impact 2002+	MP/EP	X	X		[172]
C-Gt, C-Gv	ALCA		EA		MP		X		[173]
C-Gt	ALCA		EA		MP				[174]

Definition		Primary data [b]	MO Handling	LCIA [c]		Uncertainty			Ref.
Bound	Persp.[a]			Method	Focus	PAR	SCN	Q	
C-Gt	ALCA		SB, EA, EnA	CML	MP		X		[175]
C-Gt	ALCA		MA		MP				[176]
C-Gt	CLCA		SE	ReCiPe	MP/EP				[177]
C-Gt	ALCA			CML	MP				[178]
C-Gt	ALCA	X			MP				[179]
C-Gt	ALCA	X	EA	CED, CML	MP	X	X		[180]
C-Gt	CLCA	X	SE	IPCC, TRACI	MP	X	X		[181]
C-Gt	ALCA	X		CED, IPCC	MP				[182]
C-Gt	ALCA		MA	ReCiPe	MP	X			[183]
C-Gt	ALCA		MA	ReCiPe	MP	X			[184]

[a] Concepts in italics represent information adapted to the definitions used within this work (rather than specified by the authors). [b] Data obtained from simulations based on literature data have been considered as a secondary source. [c] The information on indicators has been excluded from the table for reasons of simplicity, as it is too long and redundant. [d] Ecoindicator-99. [e] As described in Khoo et al. [154].

I.3.1. Definition of initial conditions

The basis for any comparison between two LCA studies is the function(s) it provides, and the reference flow chosen as the basis for calculations. The aim of biorefineries is usually to deliver several valuable outputs from a single (and complex) input [185]. It is noteworthy that the difference between reference flow and functional unit is not always clear, and in many cases, the last is omitted. That can imply errors when determining the conditions required to fulfill the function(s) provided by the system. In this sense, the attributional or consequential perspective followed, as well as the method used to solve the multifunctionality, play a decisive role, as discussed later.

As for the system boundaries, 86% of the studies reported a cradle-to-gate scope (Figure I.1). That is coherent considering that the reviewed molecules are intermediate products that can follow multiple downstream pathways. Furthermore, most of these molecules are drop-in chemicals, so that effects occurring after the factory gate can be considered to be the same to those observed for analogue molecules obtained from non-biomass resources [186, 187].

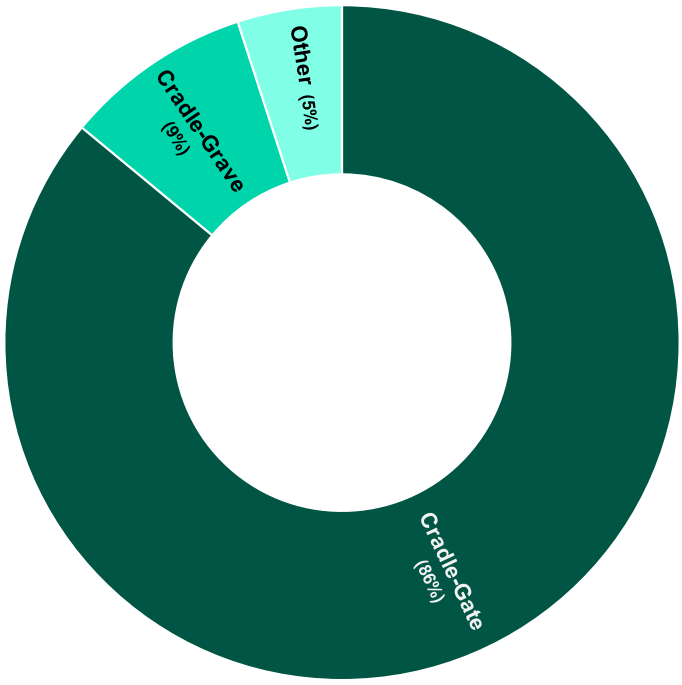

Figure I.1. System boundaries reported in the analysed LCA studies. The category "Other" include "gate-to-gate", and "gate-to-grave" scopes, as defined by the authors.

However, the scarcity of data could be slightly alleviated by including information related to well-stablished technologies for petrochemical counterparts' production, as it would serve as a benchmark reference. Additionally, carbon fate has a profound effect on the results, so that including end-of-life (EoL) scenarios could provide further insights about product system behavior [188].

Cradle-to-grave boundaries are covered most notably in the case of succinic (21%) and lactic acids (19%). That is in line with the state-of-the-art regarding the technologies to produce the main commodities derived from them: polybutylene succinate (PBS) [189] and poly(lactic acid) (PLA) [190].

I.3.2. Attributional vs Consequential perspective

The attributional approach (ALCA) is the most common way to perform LCA studies on bio-based platform molecules (Figure I.2). This type of analysis assesses the proportional share of the global impacts attributable to the function (product) under study and it is based on average data. As opposed to that, the consequential approach (CLCA) focuses on the changes implied by the use of the analyzed function (e.g., the production of bio-based FDCA would entail a decrease in the demand of fossil-based terephthalic acid), and thus it requires the use of marginal data.

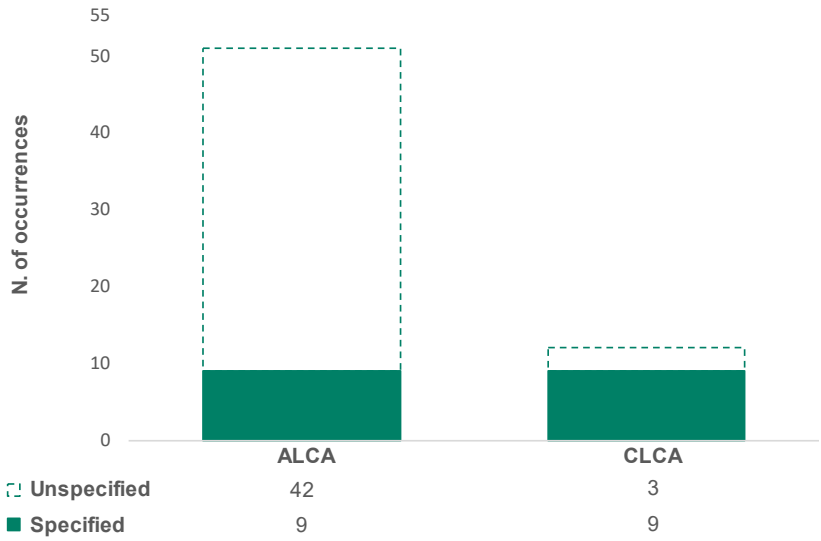

Figure I.2. LCAs with attributional (ALCA) and consequential (CLCA) focus. Filled portion of the bar represent the studies that specify the perspective followed, while hollow portion of the bar indicate the studies that do not mention it.

It is noteworthy that most of ALCA studies are unspecified (i.e., authors do not mention they are following the attributional approach). In fact, more than 80% of the case studies do not provide that information, probably because this is the most usual approach. In contrast, despite CLCA is less frequent, this type of analysis is indicated in the vast majority of the cases when used. There might be different reasons for explaining the difference. In the first place, attributional LCA is easier to conduct: the availability of average data, the more intuitive analysis, and avoiding the need for competing processes data, makes it reachable to a wider number of practitioners. On the contrary, dealing with external processes in the consequential approach also involves expanding the boundaries to consider the implications related to the functions provided by the system. That itself is a complex task and it is frequently confused with assigning the impacts to the main function by substitution, typical of the attributional perspective. Finally, since ALCA is the prevalent way of analysis, related publications have a broader context to rely on when following this approach. Bearing all that in mind, it is foreseeable that most practitioners prefer the attributional analysis, both for simplicity (more reported) and because it requires a shallower knowledge of the methodology and product system (mostly unspecified), and therefore is less time-consuming.

The data availability seems to restrict the application of CLCA on the other hand. Thus, from the total twelve consequential analysis reported, six allude to lactic acid and four to succinic acid, which are produced by more mature technologies.

I.3.3. Multifunctionality handling

Multifunctionality is expected to be solved mostly by allocation of the impacts between the different by-products. Indeed, allocation based on the economic value of system outputs is the most common method within the analyzed studies (21 occurrences). Figure I.3 depicts the aggregation of methodologies in three levels following the recommendations of the ISO 14044:2006 [191] and the International Life Cycle Data system Handbook (ILCD) [192]. Thus, level one (LV-1) considers studies in which impact allocation is avoided, level two (LV-2) includes approaches which allocate impacts based on physical relations, and level three (LV-3) comprises those works allocating the impacts based on non-physical relationships. That considered, it is possible to discern two overall findings. First, multifunctionality is addressed in a very heterogeneous way, and the only practice that garners more consensus than the others seem to be the economic allocation. Second, the recommended hierarchy for solving these systems does

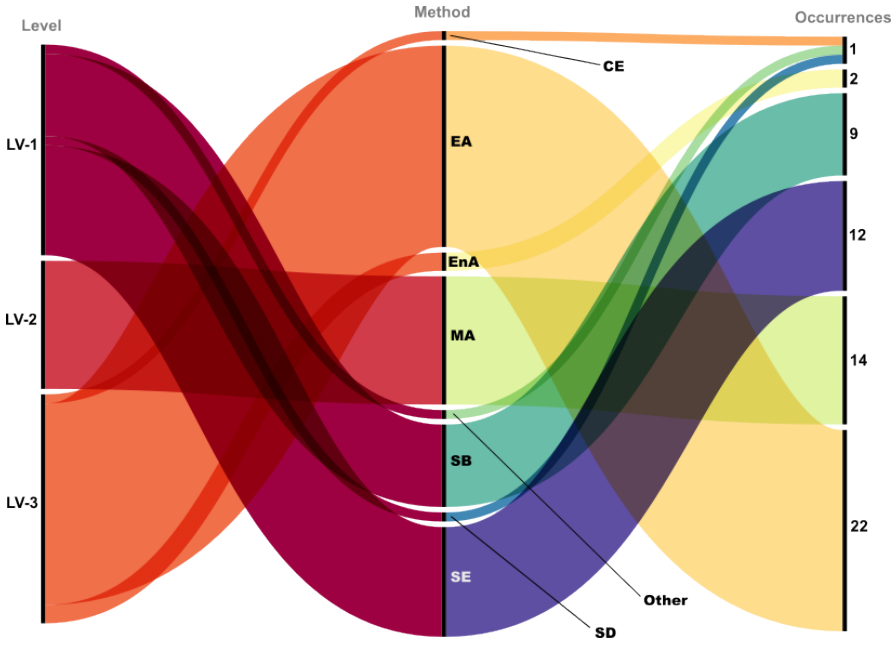

Figure I.3. Method used for multifunctionality handling. Level classification: LV-1: avoid allocation; LV-2: allocation based on physical relations; LV-3: allocation based on non-physical relations. Method classification: LV-1 (SB: Substitution | SE: System expansion | SD: Subdivision | Other); LV-2 (MA: Mass allocation); LV-3 (EA: Economic allocation | EnA: Energy allocation | CE: Carbon efficiency allocation).

not match the real practice, being LV-3 methods approaches the most reported.

One plausible cause for this trend might be the intelligibility of the results. Allocating the impacts among the different by-products relying on practical parameters (i.e., mass or economic value) is more intuitive than considering external systems to subtract their effects or subdivide a process attending to complex interactions. As an example, differences between substitution and system expansion are usually fuzzy, and the first is frequently reported as the expansion of the system boundaries. To account for this, the present work relies on the definition provided by Heijungs et al. in [193], where authors claim that more efforts in the differentiation between these two concepts should have been included in the second amendment (2020) of the ISO 14044:2006 [194]. Accordingly, expansion is considered when system boundaries are broadened to provide an integrated function containing the different products yielded. Conversely, substitution implies the isolation of the functional unit, deducting the burdens avoided by the co-generated products.

Results in Figure I.3. are shown adapted to this definition, aiming to homogenize the analysis.

Mass allocation is less reported than expected as compared to economic allocation, and it is relegated to steadier systems (e.g., cultivation and harvesting in the case of agricultural raw materials) to consider upstream effects. Although economic value is regarded by some authors as a more reliable way to account for predictable trends in an economic-driven context [126], fluctuations in the value chain might introduce significant errors. Therefore, this type of allocation should not be applied unless justified Nevertheless, accurately ascribing the effects of both the economic and physical systems is virtually impossible in attributional modeling, unless mass and revenue balances are proportional [195].

I.3.4. Data collection, quality, and uncertainty

Uncertainty is a critical aspect when approaching an LCA study. There are various sources of uncertainty[196, 197], although one of the most widely accepted classifications is that defined by Huijbregts et al. [198], which differentiates three sources: parametric, scenario and model. The first refers to the low representativeness or absence of data, the second is related to normative choices, and the third to the characterization methodology employed.

In the case of the studies included in this review, although a good number of them evaluated the parametric uncertainty, most cases approached uncertainty through scenario analysis. Thus, we focus on the methods to deal with these specific sources of variability, leaving aside model uncertainties. Reporting parametric uncertainty is not as straightforward as scenario building and comparison. Therefore, several methods have been developed. According to Mahmood et al. [199], some valid approaches are the pedigree matrix, sensitivity analyses, and sampling, analytical, and statistical methods. All these approaches are shown in Figure I.4, except for statistical methods since none were found.

A brief introduction to these methodologies is given below to facilitate the discussion. Concerning parametric uncertainty, two factors are relevant to its study. First, a variability is assigned to inputs and then it is propagated through all calculations to evaluate its effect on the outputs. Assuming that most of the uncertainty comes from the stochastic nature of the system, the most common approach is to assign a probabilistic distribution of the initial parameters. For this purpose, the pedigree matrix [200] defines five qualitative

indicators (i.e., reliability, completeness, and temporal, technological and geographical representativeness) which are assigned a value that is used to generate a lognormal distribution. A simplified approach, also widely used, is to assign an arbitrary normal, uniform, or triangular distribution based on scientific evidence or expert judgment. That is the basis for analytical models, while sampling models involve defining specific functions based on individual measurements of each input parameter. Alternatively, local sensitivity analyses allow determining which parameters lead to larger deviations in the results if they are modified. These are also known as perturbation analyses and are conventionally used for the identification of critical parameters (i.e., those that would explain most of the parametric uncertainty). These analyses are also often used *per se* to provide model sensitivity ranges. That is similar to scenario studies, where outputs are compared when varying inputs or methodological decisions (e.g., type of allocation, functional unit, etc.).

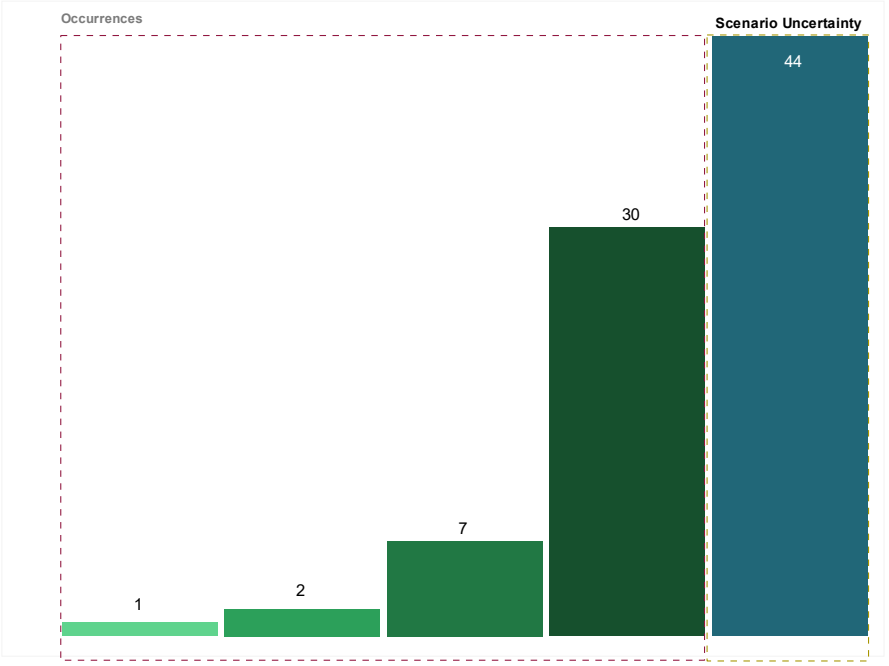

Figure I.4. Methods used for the evaluation of parametric (red-dotted box) and scenario (yellow-dotted box) uncertainty. The methods for assessing parametric uncertainty are further divided into the pedigree matrix, sensitivity analysis, and analytical and sampling methods.

Looking at Figure I.4, one consideration is necessary. Most of the investigated studies refer to methodologies for uncertainty propagation, rather than the definition of uncertainty on the input parameters. Bearing this in mind, and the classification defined by Mahmood et al. [199], models for uncertainty

propagation such as Monte Carlo or Latin Hypercube are considered sampling methods, while some others such as the use of Taylor series, are classified as analytical methods.

The difference between the use of sensitivity and scenario analysis and the rest of the methodologies is notorious, as evidenced in Figure I.4. The reason underlying this difference is clear: these formulas are more straightforward, and their interpretation is simpler. Additionally, in the case of scenario analysis, its more frequent use can be related to its usefulness for purposes beyond the study of uncertainty, such as the comparison of different operating configurations or the location of a production plant. In a context marked by the low maturity of the considered technologies, this type of analysis is clarifying as it provides a range of possible outcomes. On the other hand, perturbation analyses reliably identify the parameters whose uncertainty may lead to results that are farther from reality. Thus, they should be accompanied by the study of parametric errors in a greater number of cases than those shown in Figure I.4. For this purpose, the most repeated methodology is the propagation of uncertainty by Monte Carlo analysis. Six of the seven cases of sampling methods in Figure I.4 refer to this approach, while the remaining one is a Latin Hypercube analysis [136]. On the other hand, the only manuscript using an analytical method refers to an evaluation using the Taylor series [172]. All this is in line with the tools integrated into the most common LCA software, which frequently include modules for scenarios, sensitivity and Monte Carlo analyses.

Finally, it is noteworthy the scarce number of studies reporting the use of the pedigree matrix, only two, despite its implementation is easier than other methods when using widespread LCA utilities such as the SimaPro software and the Ecoinvent database, both of which are the most reported tools. Moreover, this contrasts with previous studies, as Thonemann et al.[201] identified the utilization of the pedigree matrix as the most extended method to assess data quality. Possibly the number could be higher, although this information was not always provided. Furthermore, from these two studies, only one of them reports data on quality indicators [129]. Overall, data quality receives little attention, and this is the only study that provides quantitative information. Again, in a context dominated by low TRL, data quality can be very influential over the results [202 - 205]. Most of the data reported for the foreground system is supported by secondary data. The main source of information is literature (including patents, book chapters, etc.), often in combination with the up-scale simulation of these secondary inputs. On the other hand, primary data usually rely on experimental work, although some

pilot and industrial scale data are available for succinic acid processes [137], [142]. In this context, the inclusion of data quality indicators might help to compensate for the lack of primary sources. In this regard, the method proposed by the European Commission [206] also makes use of temporal, geographical, and technology representativeness, as well as precision, to evaluate data quality and would perfectly meet this purpose.

I.3.5. Life cycle impact assessment

The life cycle impact assessment (LCIA) phase is subjected to multiple methodological divergences regarding the calculus method applied, the impact categories considered, and the indicators used for their quantification. In order to ascertain which are the most widespread options for LCIA in this complex analysis context, we have first outlook LCIA methods and stablished relationships with the reported categories and indicators. For the sake of clarity, categories are aggregated considering the framework adapted from the ILCD Handbook. This classification is performed to facilitate the comparison between works by overseeing the differences in the naming of some categories. As an example of the purpose of this analysis, consider indicators called "water consumption", "water depletion" and "water use". These are redefined as a single indicator called water use (WU). In this categorization, endpoint categories and areas of protection (AoPs) are disregarded. This simplification is accepted given that 98.5% of the reviewed studies consider the impact attribution based on a midpoint focus, while only 17% (i.e., 11 articles) provide further endpoint values.

Attending to the results in Figure I.5, the hierarchist perspective of the ReCiPe model [207] is the most used method to translate the results at the inventory level to actual impacts. The broad consensus around this model might arise from its long trajectory and the diversity of actors involved on its development, including academia, the private sector, and the public administration. That enables covering a great number of topics, and thus, some categories are studied almost exclusively with the ReCiPe (H), such as it is the case for the land use (LU). The CML 2001, developed by the Institute of Environmental Sciences of Leiden University [208], is the second most reported LCIA model. Other relevant models include Impact 2002+ [209], and TRACI [210].

The climate change category is not only the one most reported by the authors, but also the one with the greatest division of models for its calculation. As depicted in Figure I.6 at least eleven methodologies are identified for the

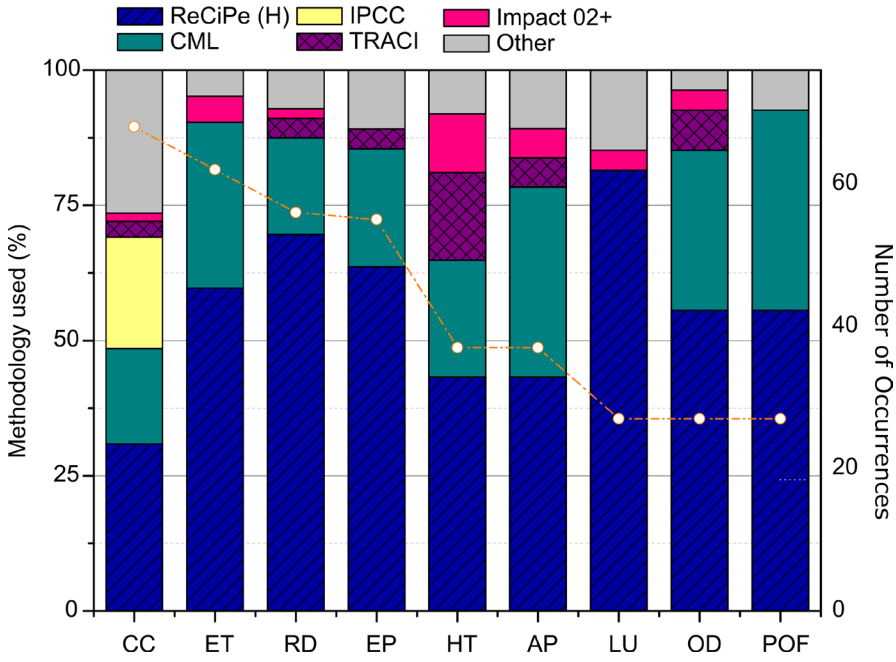

Figure I.5. LCIA methodologies reported for the most common impact categories. Bars filling color indicate the methodology used (%, left axis), while the orange dashed line represents the number of occurrences of each impact category (right axis). Categories displayed are CC: Climate Change; ET: Ecotoxicity; RD: Resources Depletion; EP: Eutrophication; HT: Human Toxicity; AP: Acidification Potential; LU: Land Use; OD: Ozone Depletion; POF: Photochemical Oxidants Formation.

calculation of the global warming potential (GWP, main indicator for climate change effects). In addition to the previous ones, the method developed by the Intergovernmental Panel on Climate Change (IPCC) has a prominent use in the estimate of the climate change, and most of the considered works rely on the fifth assessment report (AR5) published by the Panel [211], given the time range of the reviewed studies. Even though, since then (2013), a refinement report for the estimate of greenhouse gas inventories was launched in 2019 [212], and the contribution of working group I (WG1) of the sixth report is available since 2021 [213]. This method is based on the concepts thoroughly provided by the WG1 in chapter 8 of the AR5. Given the large scientific authority of this publication, other models follow an almost identical approach to define critical aspects such as the impact pathway, the considered substances, or the characterization factors. In this way, all of them lead to closer results when calculating the GPW indicator as compared to other impact categories. The time horizon is a more intricate question. Further discussion considering these features within the reported LCIA models across the board

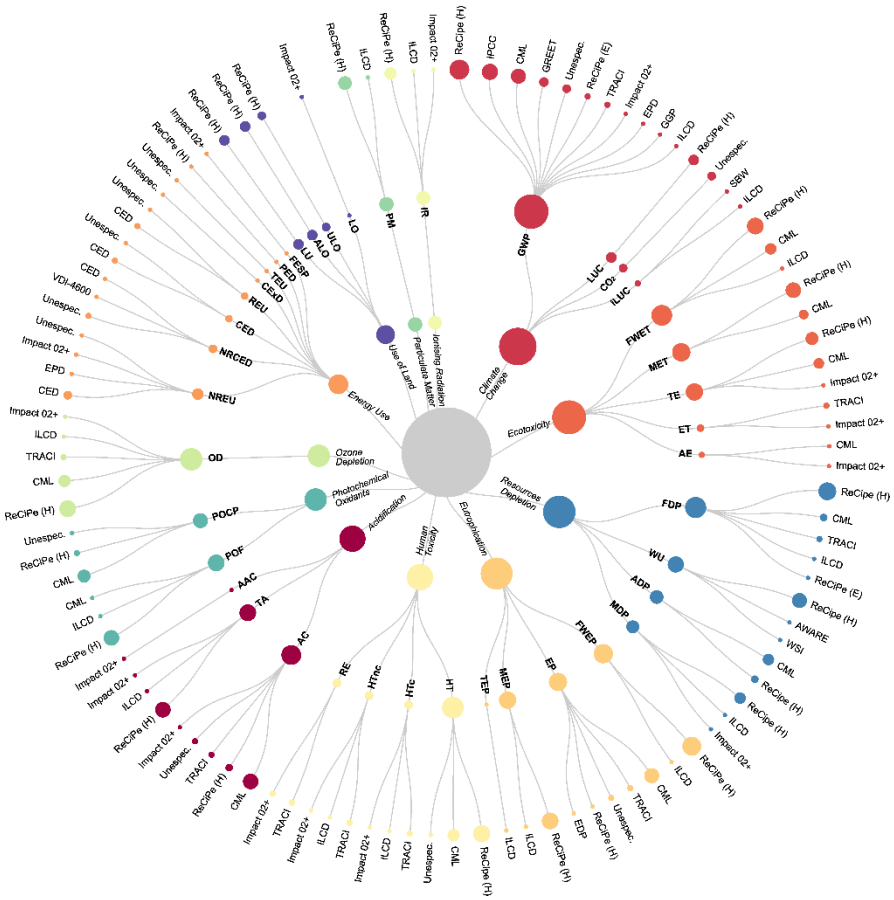

Figure I.6. Information is described from internal circumference outwards. First circumference: Environmental categories. Second circumference: indicators reported to quantify the environmental categories. Third circumference: LCIA methods to assign values to the indicators. Size of the coloured circles relates to the number of occurrences. For clarity, abbreviations in the figure are compiled in the abbreviations section.

would enrich the conclusions, but the version of the methodology is not usually reported, so that essential details are unavailable.

Regarding the frequency in the use of indicators, for some of them scarce references have been found (e.g., cancer and non-cancer effects, ionizing radiation, or particulate matter formation), and some are moderately reported (e.g., fossil depletion potential, freshwater ecotoxicity, or human toxicity). Within this point, it is remarkable that despite agricultural or forestry biomass being the raw materials for many bio-platform chemicals, indicators related to biodiversity or soil quality are barely reported. In the case of biodiversity, this is probably due to the lack of available methods for considering the main

drivers of biodiversity cost [214, 215]. On his part, soil indicators are usually related to land occupation and/or land transformation but not specifically to the determination of properties affecting its quality. Only GWP is thoroughly investigated, being considered in 93% of the studies. Furthermore, up to 10% of the published works rely solely upon this indicator (carbon footprint studies). This is a consequence of several coincidental factors. In the first place, scientific community is steeply devoted to understanding, alleviating, adapting, and communicating the climate change effects. Therefore, the physical basis and its implications are better understood, allowing for an accurate definition of the cause-and-effect chain. As a result, the amount of available and specific data is larger as compared to other categories and indicators (e.g., regionalized data, disaggregated inventories, etc.). Besides, as in the case of the ALCA vs CLCA section, a larger number of preceding studies including GWP as impact category are accessible, which might encourage new practitioners to undertake similar approaches. Finally, climate change is no longer a scientific-only concern but a socially relevant motif. As such, it is perceived as a crucial aspect above others.

Still, underlying any conclusions on one indicator might entail unfair outcomes as well as biased conclusions. In line with that, if the Environmental Footprint is considered as a reference, the communication of sixteen midpoint indicators is recommended. However, almost half of the reviewed studies reported four or fewer indicators (≤25%) to substantiate their findings. Furthermore, their inclusion or exclusion is rarely justified.

I.3.6. Carbon fate

Among the particularities on the inclusion of climate change impacts in LCA works applied to biogenic products, time horizon considerations, biogenic carbon accounting (BCA), and the effects of direct and indirect land-use changes (dLUC and iLUC) have been the focus of extensive debate.

Figure I.7 provides an overall picture of the application of these features in the considered publications. Regarding the relation between time horizon and biogenic carbon, two scenarios are defined: carbon neutral (CN) and carbon storage (CS) scenario. Carbon neutral scenario assumes a lifespan for the evaluated product shorter than the time horizon envisaged for the study, so that carbon absorbed during biomass growth is released into the atmosphere within the temporal boundaries of the analysis. On the other hand, assumption for carbon storage scenario is just the opposite. Consequently, carbon remains absorbed in the product and it is deducted from the emissions inventory.

Most authors do not specify how biogenic emissions are handled in the considered studies, as evidenced in Figure I.7. Thus, it is expected that the most probable situation in all these cases is that a neutral scenario is considered. That can be presumed since the deduction of biogenic emissions, if practiced, is foreseeable to be communicated within the methodology of the study. According to Wiloso et al. [216], although many studies assume a neutral scenario, this might conduct to misleading results, since many particularities, such as the form of the emissions or the soil carbon stocks are disregarded. In the same sense, Liu et al. [217] demonstrated that neutral scenario is limited on its predictions due to complex interactions, such as the required time for crop rotation (or biomass growth rate) as compared to the product lifespan. The sensitivity regarding the time considered for CO_2 uptake during biomass growth is also ratified by Garcia et al. in [218] by analyzing the implications of five existing allocation methods at the EoL stage and six BCA protocols in a multi-output wood-based cascade system. Also, long time lags between carbon uptake and emission are identified by Liptow et al.[219] as a determining factor that can disfavor routes based on slow-growing biomass.

A different approach to solve temporary issues in the accounting of carbon flows is the application of a dynamic assessment [220]. The dynamic GWP consideration is based on the integration of the results from the variation over time of both the inventory inputs and the characterization factors. In this way, it tries to overcome the temporal inconsistencies resulting from the conventional analysis. In this sense, in 2010 Levasseur et al. [221] proposed a dynamic expression of the GWP indicator. That definition has been recently updated by Ventura [222] to overcome the weaknesses derived from the difference in the definition of the time horizon of the impact and the time during which this impact is observed. Temporal reconciliation of these two parameters ensures that all flows are considered for quantification during the analysis. Although this approach helps to alleviate the drawbacks of a single point, steady state assessment, no dynamic assessments were found within the reviewed LCAs, probably because the difficulties on its application.

Carbon release behavior is more easily appreciated in cradle-to-grave studies since the evaluation of different EoL options would yield a range of results. In the case of the platform molecules, as shown in Figure I.1, cradle-to-gate boundaries are dominant. To solve that particularity in which the time frame needs to be set in a less tangible way, Pawelzik et al. [223], evaluated different protocols for carbon counting by comparing both scopes. Most fair results were achieved using the European Commission´s Lead Market Initiative

protocol [224], which advocates for biogenic carbon deduction in cradle-to-gate studies.

The assumptions necessary for the application of any methodology require an in-depth knowledge of both the protocol to be used and the process itself. As an example, in [133] Albizzati et al. provide a detailed discussion before allocating different factors to account for short- and long-term biogenic CO_2. Similarly, Liptow et al. separately reported biogenic CO_2 considering the peculiarities of their system [173]. Conversely, up to 34 studies did not specify the scenario assumed for biogenic CO_2 flows nor the effects regarding land use changes.

Figure I.7. Counting carbon fluxes depending on the defined scenario (inner circumference), the scope of the study (intermediate circumference), and consideration of dLUC and iLUC (outer circumference).

The impact that this last aspect can have on the results makes it indispensable for robust conclusions, as suggested by Tonini et al. [225]. The consideration of the effects derived from direct and indirect land use changes can turn around the conclusions in comparative studies concerning bio- and fossil-based routes, which is a critical aspect when novel bio-based transformation technologies are being evaluated. Moreover, this analysis can be decisive when comparing different raw materials. For example, the implications of using primary resources (crops) versus secondary resources (residues) are worth comparing. In the first case, utilization of dedicated crops usually implies further land use to compensate for their original use, thus inducing indirect changes. In the case of using residues, there are different possible scenarios to be considered, depending on their present use. If these are currently used e.g. for animal feed manufacture or soil amendments, again the reduced availability of these resources will lead to additional production (thus generating an indirect land use change). However, if their current use is non-productive (e.g. stubble burning), a previously non-existent waste valorization will occur, which is expected to have distinctly positive consequences.

I.4. Discussion and recommendations

Establishing a framework to normalize the application of LCA to these context-specific cases is out of the scope of this review since the lack of flexibility might incur in a desultory analysis. Instead, we try to compare consensus methodologies with actual practice, aiming to narrow the gap within a plausible margin. In other words, this thesis aims to converge methodological decisions around models that better represent this specific reality, making easier a broader comparison between studies.

To do so, this work focuses on looking for common features in the selected studies. Thus, three aspects are found to be ubiquitous among the reviewed assessments: cradle-to-gate scope (platform molecules), low TRL technologies (biomass-based novel developments), and multioutput systems (technologies based on biorefinery schemes). Insights on these three different aspects of the evaluated LCA studies are disclosed next.

I.4.1. Scope of the studies

As for the scope of the analyses, one of the main limitations in this regard, is the exclusion of use and end-of-life phases. Nevertheless, one fundamental objective of novel processes is to overcome the lack of environmental sustainability of conventional refinery technologies. Bearing that in mind, downstream effects could be disregarded since drop-in chemicals

would lead to identical impacts. However, there is one key aspect that cannot be overlooked: the accounting of carbon flows. This is a pivotal difference between bio and conventional products, and thus it should be addressed critically. In this sense, recommendation derived by Pawelzik et al. in [223] seems the most accurate choice up-to-date. This recommendation proposes considering the deduction of biogenic emissions in cradle-to-gate studies where the product lifespan does not exceed the time frame of the study, as described in the European Commission´s Lead Market Initiative protocol [224].

Also concerning the topic of carbon flows accounting, although not usually considered, emissions arising from land-use changes are also a determining factor. How to address this issue is an ongoing debate, since its application is subject to uncertainty [226, 227]. Even so, not considering the effects of land use change would lead to biased results. Biophysical (or deterministic) models generate more consensus. Among existing models, the framework developed by Schmidt et al. [228] has a prominent unifying character since its applicable to all regions in the world, considers intensification, and fits both from an attributional and consequential perspective. In any case, this is an evolving issue and therefore it would be wrong to fix a single way of approaching it. Therefore, the main recommendation at this point must be to avoid ignoring both direct and indirect effects derived from changes in land use, as well as to provide the greatest possible transparency and justification when communicating the results.

I.4.2. Low TRL technologies

Regarding the maturity of the technology, the studies included within the scope of this review present a generalized prospective nature. Many authors have previously made efforts to build models adapted to this context [84, 87, 117 - 119]. Prospective LCA studies are characterized by their application to technologies with low technological maturity, and much of their inputs are based on projections. Therefore, this type of analysis requires a great effort to ensure data quality and to reduce and correctly communicate uncertainty. Nevertheless, the effort is well deserved, as the conclusions of prospective LCA are very useful for process design based on life cycle thinking, and thus, its use is becoming a general practice in recent years.

The key aspects identified in these works are well reflected in [84] by structuring the main challenges of prospective analysis in three blocks: comparability, data, and uncertainty. In this review we have focused on how to address uncertainty and data handling. In this context, scarcity of data and the

complexities of up-scaling experimental results are two of the major sources of uncertainty. This can be partially overcome by coupling LCA studies with process design, for generating scenarios and the iterative optimization of the new technological developments from an environmental perspective [68, 232 - 236].

Although this serves to alleviate the unpredictability of scaling-up, only the measurement of data quality and uncertainty can improve the robustness of the analysis. The assessment of data quality can help improving two things both decision-making and interstudy comparison. On the one hand, it provides an idea of the extent to which a study enables decision-making based on its results. If the quality of the data is acceptable, this decision will be more endorsed than if it is not, whereas if this parameter is unknown, the decision will be taken "blindly". On the other hand, it provides a more appropriate framework for inter-study comparison. In this way, a comparison between studies with good data quality will be more justified. Among the existing methodologies for data quality assessment, that described within the Environmental Footprint method [206] is intuitive, easy to implement, and comprehensive. We therefore suggest its application, although we emphasize that the most important thing is the calculation of this factor regardless of the model.

As seen in Section 4.3.4, most studies include scenario analysis, and approximately 40% of them include sensitivity analysis, while the remaining assessments of parametric and model uncertainty are largely ignored. In this context, the analysis of different scenarios, taking into account different projections and giving flexibility to the models, is very positive and is in line with sound practice. Some critical aspects to be evaluated in this type of analysis might be the electricity and heat mix, the geographical scope, or the raw materials considered. On the other hand, parametric uncertainty is underrepresented. Although sensitivity analyses are of great interest, in our opinion it is a step that should be completed with the uncertainty analysis of the critical parameters to get solid conclusions for decision-making. To this end, the simplest way is by using the most consolidated tools in practice. Thus, the calculation of the uncertainty of the input parameters can be easily performed through the pedigree matrix [200], or the assignment of probabilistic distributions based on analytical methods (assumption of normal, uniform or triangular distributions according to expert criteria). For the propagation of this uncertainty throughout the calculations, Monte Carlo analysis generates reliable dispersions, and its application is straightforward since it is integrated into the main LCA software. On this basis, if we look at

the approaches proposed by Mahmood et al. [199], our recommendation would be, in a context so subject to variability, to follow the intermediate (Monte Carlo sampling + local sensitivity analysis) or advanced (advanced sampling + global sensitivity analysis) approaches, while studying different scenarios for parameters more subject to fluctuations.

I.4.3. Multifunctionality handling

Multifunctionality consideration is highly variable in the selected investigations. This is not only expected but beneficial since homogeneity in the criteria may work against the general interest. We have therefore attempted to define an appropriate hierarchy to guide decision-making rather than to unify the possible models. On the one hand, consequential analysis can cover a wider scope while avoiding problems in defining system boundaries. The latter is key in a projected environment, where a large number of elements are only assumptions. However, the low availability of marginal data makes it less applicable. In addition, basing the analysis on potential consequences may imply taking responsibility for actions outside the system. This would be an obstacle when communicating with stakeholders, although it is in any case preferable to circumvent impacts. On the other hand, attributional analysis is much more widespread and easier to apply. Also, the wide availability of data can often make it return more accurate results (at least for the time being). In this sense, in our view, a plausible scheme for resolving the multifunctionality of these processes could be the following: at the top of the hierarchy the approach from the consequential perspective should be considered. If the scarcity of data made it unfeasible or unrepresentative, the system would be represented following an attributional approach applying the substitution methodology where necessary. If none of these models is suitable, a subdivision of the system as much as possible, and the application of a distribution of impacts based on mass ratios, as recommended by the standard (i.e., prioritizing physical relationships over others), should be favored.

This sequence conforms, in our view, to what is described in ISO 14044, although it goes a little further in the hierarchy to fit this particular context.

I.4.4. Other aspects

As for the impact calculation methodology, it is beyond the scope of this study to propose any of them for the evaluation of the data. This is because it is not intended to restrict the flexibility of the practice, and certain methodologies are more adapted to some specific contexts. This is the case of

TRACI in the United States or LIME (Life-cycle Impact assessment Method based on Endpoint modelling) in Japan [237]. However, we do intend to identify the key aspects that allow us to expand the comparative framework at this point. First, the characterization factors may vary significantly within the same model depending on whether global or regionalized data are considered. This has a decisive influence on the results, so it is important to specify this information in detail, which is not always the case. If two studies provide regionalized data in two different locations, the results may be comparable because they provide accurate data from two different locations. However, if the provided data are unspecific, the comparison is restricted because the level at which they are described is unknown. On the other hand, in terms of the used methodology or the provided (midpoint) indicators, although we defend flexibility, we do consider it interesting to include data calculated based on standardized models beyond those used for the analysis. In other words, although a detailed review of the results is made concerning a specific model and indicators, it would be beneficial to include the results obtained when analyzing the inventory with consensus methodologies such as the Environmental Footprint. If all the indicators recommended by this standard are also included, it provides an extra point of support to sustain the comparison with other studies.

Finally, it is noteworthy that this comparison is only possible if two studies refer to an identical functional unit and the reference flow of both is in the same units. This fact cannot be modified as it must support the objective of each study in the most appropriate way. However, as seen in Section 4.3.1, most LCAs refer to a reference flux based on the mass of the main product at the outlet of the system. Considering this trend, this would not be an obstacle in most cases.

I.5. Final remarks

The objective of this review is to orient methodological decision-making towards the same direction, adapted to the context of biomass derived chemicals. In this way, the aim is both to adequately represent this particular reality and to increase comparability between studies.

Through the meta-analysis of the selected LCA studies, three broadly prevalent aspects were identified: cradle-to-gate scope (intermediate products), prospective analysis (technologies under development), and multifunctional processes (biorefineries). Although the practice of LCA must remain flexible, having references to guide methodological decisions toward a more accurate

representation of this context is undoubtedly beneficial. In the case of bioproducts, we find certain bottlenecks around the three aspects mentioned above that make it difficult to choose the most appropriate assessment practices. Some general conclusions about these three aspects are detailed below.

Regarding the scope of the studies, reconciling the temporal scope of the study with the correct allocation of biogenic carbon fluxes is the aspect that requires the most discussion. The application of methodologies such as those proposed in this work, or the analysis of scenarios to fill this gap, are essential for the consistency of the results. Also, the inclusion of indicators related to changes in land use will lead to more reliable conclusions once they are consolidated in standard practice.

Concerning the multifunctionality of processes, the degree of complexity of inputs and outputs is not restricted to the manufacturing stage, but also affects the value and supply chains of the process. Modelling this large number of flows and interactions fairly is a challenging task. The consequential perspective seems a more correct approach to capture all elements of this intricate system, although the scarcity of marginal data currently available in databases makes it unfeasible in many cases. It is to be hoped that over time, if efforts are devoted to it, the amount of such information will become more accessible. In our opinion, this would lead to a substantial improvement in the representation of multifunctional systems.

Likewise, the technologies that are now being discussed as future developments will materialize. At that time, the availability of reliable primary data will increase, allowing for more accurate analyses. Until then, careful scaling of system inputs and outputs, as well as the communication of the uncertainty of the results, is the only reality to which we can adhere.

With this in mind, future work should be directed towards increasing rigor and producing more accurate and transparent data. It is necessary not only to give a faithful approximation of reality but to provide information on how representative a model is. In addition, the number of environmental categories and mechanisms included in the studies should not disregard any information that could lead to burden shifting. This implies the development of indicators still in the pipeline, such as effects on biodiversity. The area of bioproducts is particularly sensitive to this indicator due to the significant changes in land use. Therefore, it is of great interest advancing in the definition of criteria and the formulation of representative characterization factors. A major research effort is therefore required in this regard. Similarly, progress in

integrating the other pillars of sustainability is essential. While cost analysis (LCC) has a high degree of maturity, the evaluation of social indicators is currently undergoing strong development. There must be a common effort by the community of LCA practitioners to implement these methodologies. All recommendations in this paper apply only to the depicted context and should be framed under the umbrella of higher standards. Methodologies such as the Environmental Footprint provide a skeleton from which further actions can be subscribed.

CHAPTER II:
SIMULATION, OPTIMISATION, AND LIFE CYCLE ASSESSMENT OF INDUSTRIAL PROCESSES FOR FURFURAL PRODUCTION AS A CRITICAL BENCHMARK FOR BIOREFINERIES

The true relevance of the bio-based monomers mentioned in Chapter I lies in their market penetration. The outlook for most bio-based compounds is for increased demand in the coming years. Among these chemicals, furfural has recently gained significant traction, supported by its main drivers, most notably the production of furfuryl alcohol. Its current market volume is around USD 550 million per year and is expected to grow at a compound annual growth rate of 6.5% from 2023 to 2030 [78, 87]. One of the main attractions of this compound is that it serves as a platform for the production of a wide range of chemicals with high market acceptance, such as maleic anhydride, levulinic acid or the aforementioned furfuryl alcohol, among others (see Section 1.3 for more details).

This chapter aims to accurately capture and represent the state of the art of furfural production technologies at a commercial level. From the overview presented in Section 1.3.3, the Quaker Oats and Chinese Batch processes are selected, assuming that these are the most suitable for benchmarking against future developments. Given the paucity of data in the literature, these processes will be rigorously simulated in Aspen Plus within the most commonly reported operating ranges to obtain reliable and exhaustive input and output inventories. Finally, these inventories will be used as a source for the life cycle analysis of these technologies, thus providing a baseline

environmental profile for this chemical that is currently unexplored (or poorly explored) in the literature and databases.

II.1. Rigorous simulation of benchmark technologies

The Quaker Oats Process (QOP) and the Chinese Batch Process (CBP) were selected as reference technologies based on the most recent published market data [78, 87]. A comprehensive inventory of these processes allows a detailed analysis of the environmental impacts associated with furfural production. That provides a solid basis for comparison with future developments. In the absence of absolute references, such as those provided by global assessment methods, comparative studies provide particularly useful information for direct application. Despite the market importance of this product and the problems associated with the use of acid and steam, there is no detailed reference in the literature on the inputs and outputs of its production processes and their impacts. This chapter aims to fill this gap.

Both the Quaker Oats and Chinese Batch plants are modelled at a capacity of 20 ktonne/y of furfural production, with an annual operating time of 8000 hours. This capacity is chosen because it is considered to be an average production, based on the output of some of the major producers [81]. In addition, the purity of the furfural obtained is set at 99%, as a commercially representative average.

The following subsections detail the rigorous simulation of both processes using Aspen Plus software (see Section 3.1).

II.1.1. Quaker Oats Process

The process flow diagram of the QOP is shown in Figure II.1. The process diagram illustrates the details described in Section 1.3.3. The process begins with the introduction of a dilute acid solution, which is subsequently preheated and mixed with the biomass in the MIX-102. The slurry is then fed into the R-101 reactor, where the mixture is heated by the injection of medium-pressure steam. Concurrently, the steam serves to entrain the furfural formed. This stream is partially condensed in a secondary steam generator. Once the furfural-rich stream has undergone complete condensation, it is subjected to a double distillation, as illustrated in area A-300. The first column is operated aided by a stripping steam stream to facilitate the separation of the furfural azeotrope. The second column is employed to dehydrate the diluted furfural to a purity of 99 wt.%.

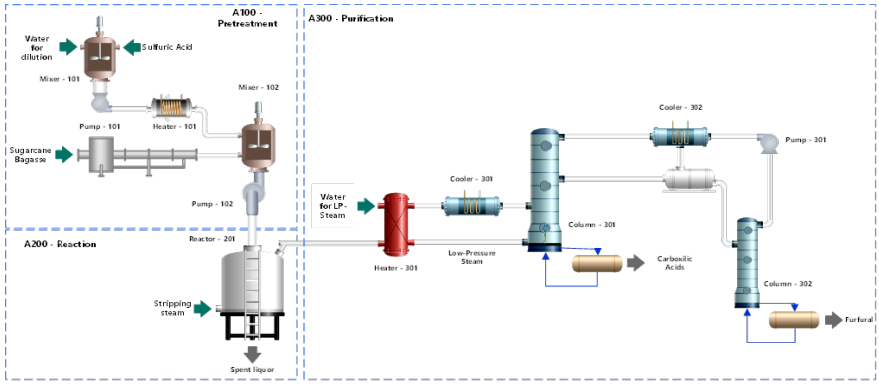

Figure II.1. Quaker Oats process flow diagram.

Central Romana is currently the largest company using this technology. This firm operates in the Dominican Republic, where it makes use of excess sugarcane bagasse (SCB) in the nearby region to feed its production plant. Therefore, this work takes this reference to define the raw material used. Table II.1 shows the composition of the SCB selected. This composition was estimated from average values published in the Phyllis database [238]. According to the same reference, an 8% moisture is considered. The presence of acetyl and formyl groups is calculated as detailed in Section 1.3.1. As opposed to other feedstocks, SCB is not methylated at any position, so formation of methanol does not take place.

Table II.1. Composition of the sugarcane bagasse used as QOP feedstock.

Component	Mass fraction
Cellulose	0.39
Xylan	0.35
Arabinan	0.05
Lignin	0.09
Ash	0.08
Acetyl groups	0.04
Formyl groups	$4 \cdot 10^{-4}$

The process is shown below by sections (A100 to A300). For each of these sections, the Aspen flowsheet is shown, and the process specifics are detailed.

I. Pretreatment

Figure II.2 shows the input of catalyst (diluted sulphuric acid) and solid biomass (SCB) with 8% moisture. The mineral catalyst is pumped from a storage tank and pre-heated before contact with the biomass. The biomass is then fed to the inlet of the plant by a screw conveyor. This contact raises the

temperature of the sludge formed and facilitates the digestion of the biomass. The mass ratio of sulfuric acid to dry biomass is 0.022, according to [75]. In addition, the initial dilution of the acid must result in an H_2SO_4/water ratio of 0.06 (wt. %), also considering the moisture content of the biomass. For producing 20 ktonne/y of furfural at 99% purity, the dry biomass input must be 16803.8 kg/h, based on Aspen calculations. Therefore, the water content provided by this feed will be 1344.3 tonne/hour and the amount of sulphuric acid introduced will be 377.4 tonne/h. This acid will in turn be diluted in 4515.5 tonne/h of water. All of it will result in an inlet stream to the reactor with 73% solids and a composition identical to that shown in Table II.1, where 25% of the total weight is water and approximately 1.6% is sulphuric acid.

Figure II.2 depicts the process diagram of this section, as designed in Aspen. The numerical values displayed on the labels, from bottom to top, represent the following parameters: mass flow rate (kg/h), pressure (bar), and temperature (°C).

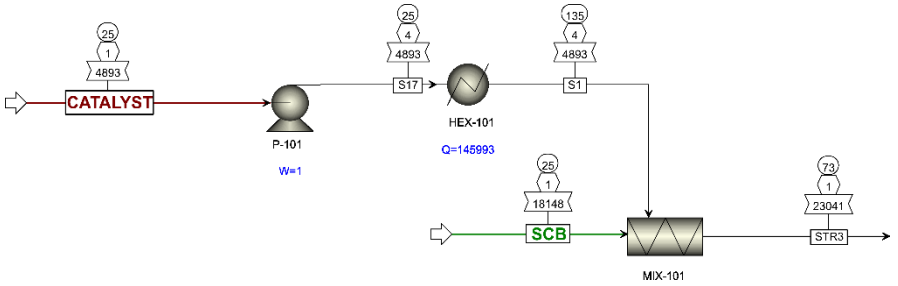

Figure II.2. Flowsheeting of pretreatment section of Quaker Oats process.

The P-101 pump provides a discharge pressure of 3.5 bar, resulting in an operating power consumption of 1.09 kW. It operates as a centrifugal pump with no inefficiencies. The S17 flow is forced through the HEX-101 heat exchanger. This is a "shortcut" unit designed to provide the maximum allowable temperature for the fluid without going into the gas phase, as the purpose is spraying it on the biomass to increase contact. The calculated outlet temperature is 135°C, for which it consumes 1.19 tonne/h of medium-pressure steam (MPS). The screw works only as a mixer, and its electrical consumption is considered negligible.

II. Reaction

The STR3 (Figure II.2) stream is introduced into the R-101 reactor. The reactor is designed using the kinetics described in Section 3.1.3. These kinetics are implemented in the RCSTR module of Aspen Plus. Each batch is

contacted with medium-pressure steam for a residence time of 4 hours. This steam partially condenses to maintain the desired temperature while continuously drawing the azeotrope formed by the furfural and water at the top of the reactor. After the reaction is complete, the tank is emptied from the bottom, resulting in the spent stream. The liquid occupies 0.75 of the total volume, allowing the vapour in the reactor to reach a residence time of 13 seconds.

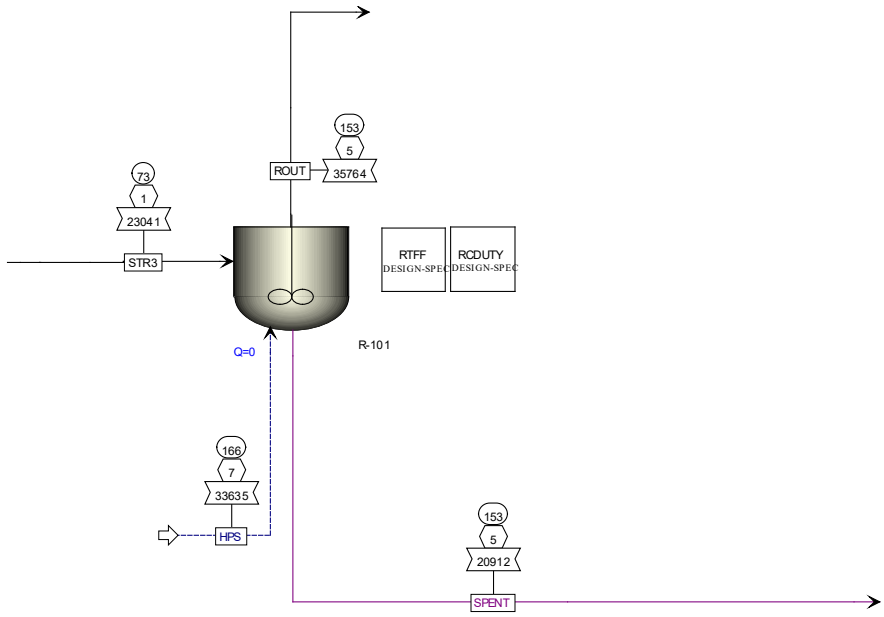

Figure II.3. Flowsheeting of reaction section of Quaker Oats process.

The amount of vapour added and its conditions are calculated based on two design specifications, namely "RTFF" and "RCDUTY". Both aim to achieve the objectives set for this vapour, i.e. entraining the formed furfural and reaching the desired temperature. The "RTFF" specification seeks to obtain the appropriate amount of furfural through the ROUT stream. According to Section 1.3.3, this amount is around 50% of the theoretical maximum due to limitations caused by steam condensation heating. The stoichiometric maximum is 72%. Therefore, the design target for the furfural mass flow rate is defined by multiplying the pentosan input (xylan and arabinan) by 0.72 (theoretical maximum) and by 0.523 (operational maximum). To achieve this objective, the manipulated variable is the mass flow rate of steam injected, which is varied in a wide range. On the other hand, the pressure and temperature conditions of the steam are determined by the "RCDUTY"

design specification. The objective is to achieve a reactor temperature of 153°C, which is accomplished by manipulating the pressure of the injected steam. Additionally, the vapour stream is defined through pressure and vapour fraction (V_{frac} = 1) values. This way, the model itself selects the temperature, making the stream completely defined. Moreover, in the reactor, the pressure is set at 5.1 bar [75], while the duty is set to 0. This enforces providing all heating power from the steam stream, avoiding the use of auxiliaries or jacketing.

III. Purification

The purification process involves a double distillation with a neutraliser and a decanter in between. From the decanter, part of the process stream is recirculated to the first column. As the purification train is considerably larger than the other sections, it is represented in sub-groups, along with its explanation in the text.

A unique aspect of this process is that the first column is operated by replacing the reboiler with a steam stream, which is used as a stripping and heating agent, similar to the reactor. The high temperature of the reactor product stream is used to generate low-pressure steam in a secondary generator (HEX-102 + CMP-101, see Figure II.4), as it must be condensed before entering the distillation tower. The amount of steam required is calculated using the "WMFRSSG" design specification. This specification makes use of a 0.99 distillate to feed ratio for the furfural in the C-101 column show in Figure II.5. To reach this ratio, the water inlet in the "CWATER" stream is varied. Depending on the mass flow rate of water, the amount of stripping steam generated is adjusted to entrain the required quantity of furfural in the column. The HEX-102 heat exchanger is designed to increase the water temperature to 125°C at atmospheric pressure, resulting in partial condensation of the product stream to a vapour fraction of 0.69. The generated water vapour is forced through an isentropic compressor before injection at the bottom of the first column. The CMP-101 compressor is designed to raise the pressure of the vapour stream so that it maintains the vapour fraction at 1, despite the temperature increase. This is consistent with the typical conditions of low-pressure steam. The product stream totally condenses in the CND-101, requiring a cooling water consumption of 295 tonne/h. To reduce this consumption, a recirculation system is employed for this auxiliary stream. The design of this system is discussed later in this section. Passing through this equipment results in a pressure drop of 0.3 bar, leaving the feed stream to the distillation column with conditions of 144°C and 4.2 bar.

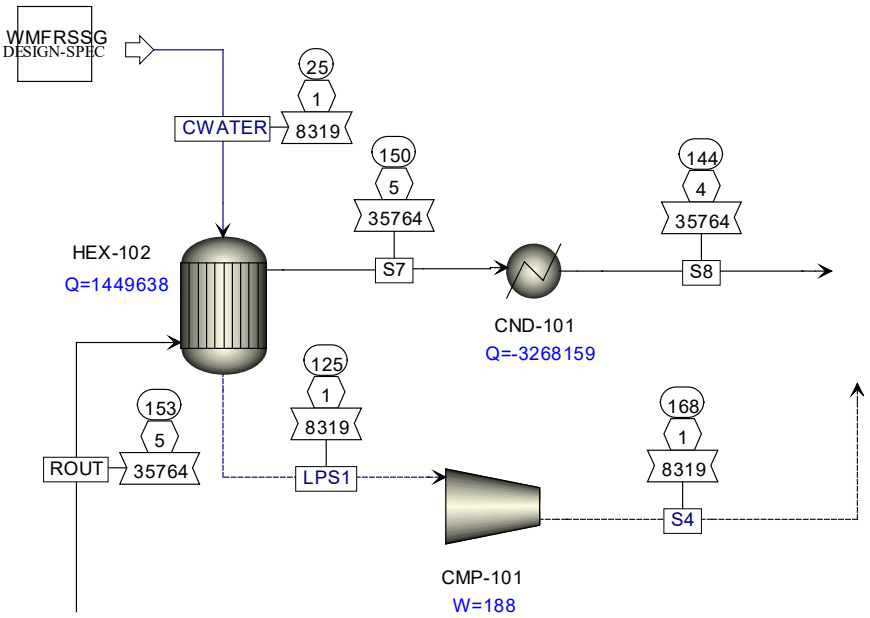

Figure II.4. Condensation of the product stream prior to introduction into the first distillation column with secondary steam generator.

The stream S8 is fed to the C-101 column to separate the furfural-water azeotrope (top) from the heavy fraction consisting mainly of carboxylic acids (bottom). The scheme is provided in Figure II.5. Aspen's equilibrium "RadFrac" module is used to implement this column using the azeotropic convergence method. The column consists of 30 stages and operates with an external condenser and a stripping vapour as a heating agent, as previously discussed. The carboxylic acid stream is continuously withdrawn from the bottom ("CARBOX" stream) and directed to the water treatment section. The mass fraction of acetic acid obtained in this stream is 1.2%, which falls within the expected range discussed in 1.3.3.I, but is too low to justify its recovery. The light fraction ("S11" stream) carries water and furfural in a ratio of approximately 70:30 (see Figure III.3), along with some impurities (mainly acetic acid entrained). The DEC-101 decanter aims to transfer these impurities to the water and recirculate them back to the C-101 column. To achieve this, the fraction is completely condensed in the CND-102, which operates at atmospheric pressure and a temperature close to that of the azeotrope to facilitate phase separation. The aqueous phase is pumped back to the top of COL-101, while the organic phase undergoes a second round of distillation.

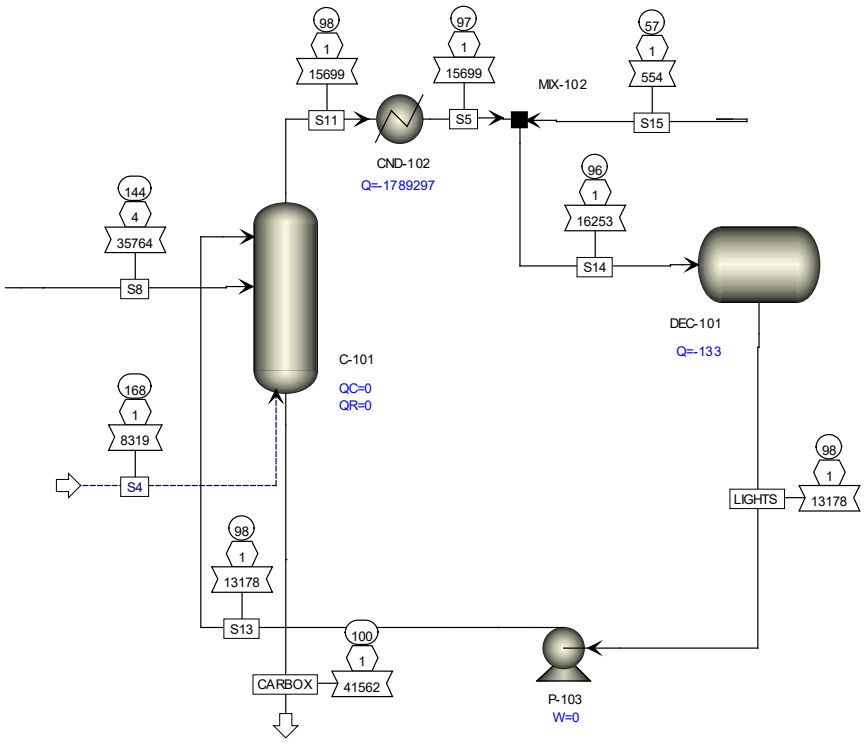

Figure II.5. First furfural distillation column with bottom separation of carboxylic acids and recycling of the aqueous phase from the decanter.

Before entering the second distillation column, the acid residues existing in the organic phase coming from decanter DEC-101 (stream HEAVY in Figure II.6) are neutralised in a reaction with sodium carbonate. The amount of carbonate required is added to the model using a calculator, taking into account the stoichiometry for the conversion of acetic acid to sodium acetate, water and carbon dioxide as follows:

$$CH_3COOH + Na_2CO_3 \rightarrow 2CH_3COONa + H_2O + CO_2$$

This calculator imports the acid concentration value and exports the intervening carbonate, acetate, and water concentration variables. The CO_2 produced is not considered at this point but is taken into account for life cycle assessment (LCA) calculations assuming controlled venting. Additionally, sodium acetate is precipitated in the same tank. This is simulated by adding a separator. Although the separator is located at the outlet, it works as a single unit with the neutraliser.

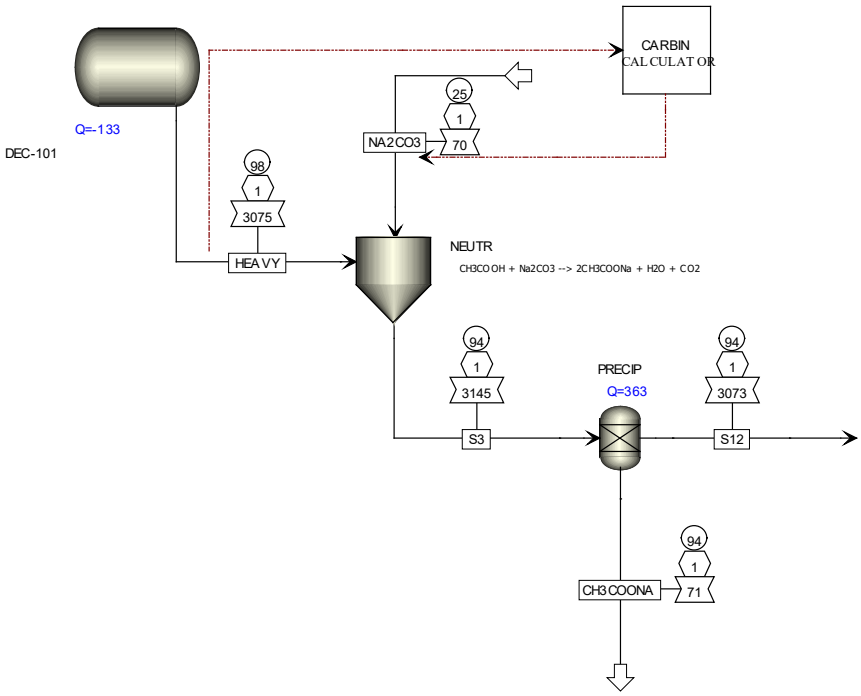

Figure II.6. Neutralisation of the acid residues in the organic phase with precipitation of the sodium acetate formed.

Finally, the neutralised stream (S12) is fed to a second column where the furfural is dehydrated to a purity of 99 wt.% (Figure II.7). Again, the "RadFrac" model available in Aspen Plus employs azeotropic convergence but now to break the furfural-water azeotrope. The temperature profile in the tower ranges from 58°C at the top to 92.5°C at the reboiler, occurring over 8 equilibrium stages. The primary difference with de C-101 unit is that it operates under pressures below the atmospheric (0.2 bar) to prevent undesired condensation and resinification reactions of the dehydrated furfural. To achieve the desired purity, the distillate to feed ratio is adjusted to obtain a relation of 0.45. Minimizing column size is desirable. Fewer equilibrium stages reduce size and cost, but complicate separation, necessitating increased reboiler heat input. Bearing this in mind, the number of stages was chosen by studying the variation in the number of plates versus the heat duty in the reboiler. The smallest possible setting was selected before the point where the reboiler consumption spikes, assuming it is the most cost-effective configuration. After purification, the furfural (stream FURFURAL) is stored in tanks under vacuum

pressure, while the water is pumped back to the decanter DEC-101 (Figure II.5) after condensation (CND-103).

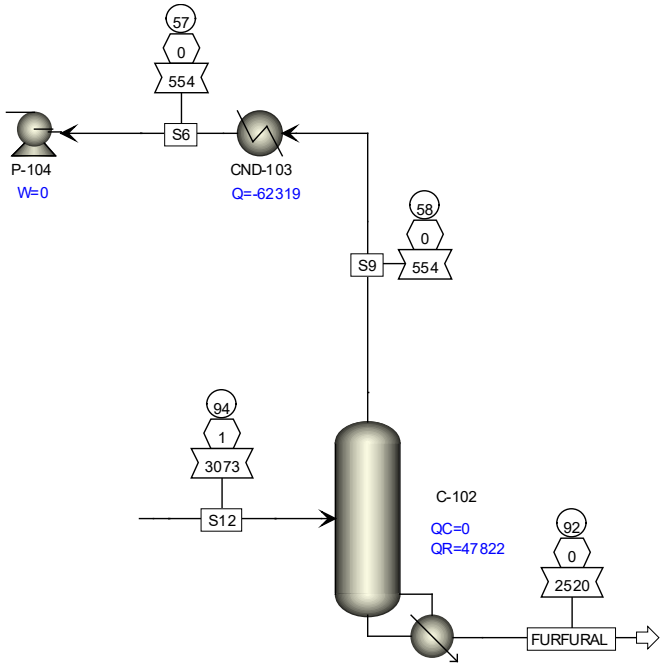

Figure II.7. Dehydration of the furfural in the second distillation column and pumping the water back to the decanter.

Finally, residual effluents from the plant undergo treatment before being discharged into natural watercourses. The waste flows mainly originate from the spent liquor of the R-101 reactor (stream SPENT) and the bottom of the COL-101 column (stream CARBOX in Figure II.8). The exhausted material from the reactor contains a significant amount of unreacted solids, primarily cellulose, lignin, ash and tars. This represents approximately 55% by weight of solids in this effluent. This is essentially a wet solid. The most common practice is controlled landfilling. If the amount of solids is lower, they are commonly separated by filtration. The solid fraction is then buried, and the liquid fraction is treated by anaerobic digestion. In this case, the spent stream is mixed with the CARBOX stream from the C-101 to reduce the percentage of solids to 18 wt.% (3% molar). The resulting mixture is then fed into an anaerobic digester for treatment to obtain biogas. This stream is primarily composed of water and cellulose, with smaller amounts of other polymers, sugars, and acids. The Aspen simulation module used for this treatment is an "RStoic", which includes decomposition reactions of the mixture's various

compounds into methane and carbon dioxide. The following reactions are considered:

$C_6H_{12}O_6$ (Glucose) → $3CH_4 + 3CO_2$
$C_5H_{10}O_5$ (Xylose) → $2.5CH_4 + 2.5CO_2$
$C_5H_{10}O_5$ (Arabinose) → $2.5CH_4 + 2.5CO_2$
CH_3COOH (Acetic acid) → $CH_4 + CO_2$
$(C_{12}H_{20}O_{10})n$ (Cellulose) + H_2O → $3CH_4 + 3CO_2$
$C_5H_8O_4$ (Xylan) + H_2O → $2.5CH_4 + 2.5CO_2$
$C_5H_8O_4$ (Arabinan) + H_2O → $2.5CH_4 + 2.5CO_2$

Both acetic acid (in the liquid phase) and unreacted acetyl groups present in the solid biomass (in the solid phase) are replicated by CH_3COOH. The calculations of this stage are used as a reference for the definition of the unit process of anaerobic digestion with biogas recovery in the LCA.

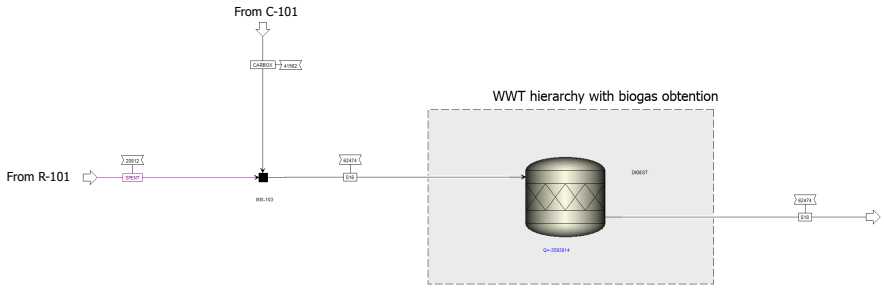

Figure II.8. Collection of reactor waste streams and azeotropic column for anaerobic digestion prior to disposal.

Table II.2 summarises the inputs and outputs of the QOP, including materials, wastes and utilities consumed. All flows are referenced to one tonne of furfural, which will be the functional unit used in Section 5.2.

Table II.2. Input/output table of the QOP. Flows normalised to 1 tonne of furfural.

Name	Process	Value	Unit/tonne furfural
Inputs			
Materials	TO		
Biomass (dry)	MIX-101	6.7	tonne
Moisture		1.3	tonne
Dil. water	MIX-101	1.8	tonne
H_2SO_4	MIX-101	0.15	tonne
Stripping steam	R-101	33.6	tonne
2nd steam gen.	HEX-102	3.3	tonne
Na_2CO_3	NEUTR	6	kg
Utilities	TO		
Electricity	P-101	0.4	kW
	P-102	0.7	kW
	P-103	0.01	kW
	K-101	74.8	kW
MPS	HEX-101	0.4	tonne
LPS	C-102	0.33	tonne
Cooling Water [a]	COND-101	117.7	tonne
	COND-102	129.73	tonne
	COND-103	44.52	tonne
Outputs			
Materials	FROM		
Furfural	C-102	1	tonne
CO_2	NEUTR	1	kg
CH_3COONa	NEUTR	9.3	kg
Solids	R-101	4.6	tonne
Waste water	R-101	3.8	tonne
Waste water	C-101	16.6	tonne

[a] *The input for the LCA calculations consider only 3% of this utility, assuming the regeneration of the remaining water.*

II.1.2. Chinese Batch Process

The production process for furfural in China presents similarities with the one described in the previous section, with some notable differences. One such difference is the reactor configuration: the QOP uses refractory bricks, while the CBP uses 50 mm thick mild steel walls (see 1.3.3). Additionally, the primary companies that implement this technology are based in China. In the regions where this process is carried out, there is a large production of maize. Therefore, there is a synergistic relationship with the agricultural industry as corn cobs, a residue from the maize production, are used. Alternatively, they can be used as animal feed, but at a much lower cost. Another significant divergence at the operational level is the configuration of the first distillation tower. In this case, the CBP utilises the product vapours at the reactor outlet to exchange heat in the column boiler, significantly reducing the auxiliary steam consumption required to achieve the necessary reflux ratios (Figure II.9).

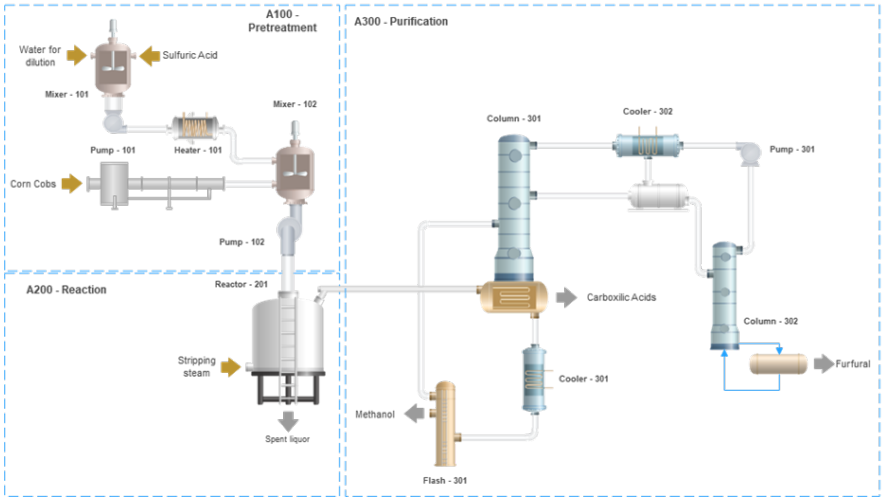

Figure II.9. Chinese Batch process flow diagram.

The median composition of corn cobs was obtained from samples collected in the Phyllis database [238]. Samples #979 to #2791 were specifically used to determine the average composition of cellulose, hemicellulose, lignin, and ash. The difference between arabinans and xylans was determined from [77], with the former comprising 12% of the hemicellulose and the remainder being xylans. Furthermore, the hemicellulose was found to be acetylated at the C3 position by 24%, at the C2 position by 12%, and at both positions by 6%. Additionally, 3% of the acetyl groups present were accounted for by formyl groups [75]. The moisture content of biomass is 8%, according to the same

references. The composition of the corn cobs stream at the inlet of the process is shown in Table II.3.

Table II.3. Composition of the corn cobs used as CBP feedstock.

Component	Mass fraction
Cellulose	0.39
Xylan	0.24
Arabinan	0.03
Lignin	0.14
Ash	0.03
Acetyl groups	0.03
Formyl groups	$3 \cdot 10^{-4}$

Both plants operate under the same assumptions, i.e. they produce 20 ktonne/y of 99% pure furfural, with an operating time of 8000 h/y. Each section of the process is discussed below, with a particular focus on those that differ from the QOP.

I. Pretreatment

The pretreatment configuration is similar to the QOP, but the amounts of catalyst and dilution water vary significantly according to literature. The ratio of protons H_2SO_4 per kilogram of dry biomass remains constant at 2.25 wt.%. However, owing to the lower amount of pentosans present in corn cobs, almost 500 kg/h of sulphuric acid is required for the hydrolysis of 2,250 kg/h of dry biomass. As per [75], the ratio of sulfuric acid to initial dilution water is reduced notably to 0.015. Therefore, the amount of dilution water in the initial mixture is slightly higher than 28 tonne/h.

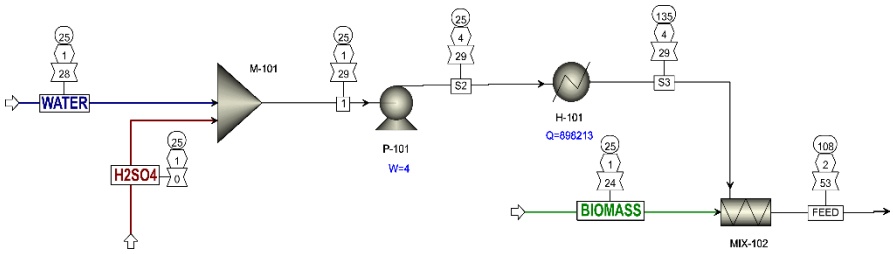

Figure II.10. Flowsheeting of the pretreatment section of CBP. The mass flow rate in the labels is presented per tonne/h.

The process involves contacting a mixture of catalyst and water with the biomass in the form of a spray along a screw conveyor. This preheats the mixture to 108°C before introducing it into the reactor. The P-101 pump has a discharge pressure of 3.5 bar, and the HEX-101 exchanger raises the temperature of the diluted catalyst to the maximum allowable without phase

change. Due to the high water content, the consumption increases to 3.6 kW at the pump, and 6.6 tonne/h of steam at the exchanger.

II. Reaction

The reaction conditions were designed using the same procedure as described in the previous section for the QOP (Figure II.11). The liquid phase occupies 75% of the volume and it has a residence time of 4 hours. Furthermore, the vapour is continuously removed by the PRODUCT stream, with a residence time of 13 seconds. The literature does not specify the reaction temperature in this case. However, given the similarity of both processes, it is expected to operate under analogous conditions. To establish the optimal reaction temperature, a sensitivity analysis was conducted within a range of ±25%. Consequently, the optimal temperature was determined to be 160°C, and the same design specifications were applied as for the QOP reactor. The necessary amount of medium-pressure steam for heating and stripping was calculated to be 63.8 tonne/h. The mass flow rate of the steam should ideally be between 17 and 25.5 tonne/h, according to literature data. However, this amount was not reproducible under the evaluated operating conditions. The calculated volume in this case is 283.5 m^3, which would require the installation of 24 reactors. This number of reactors is not unreasonable for this type of plant [81].

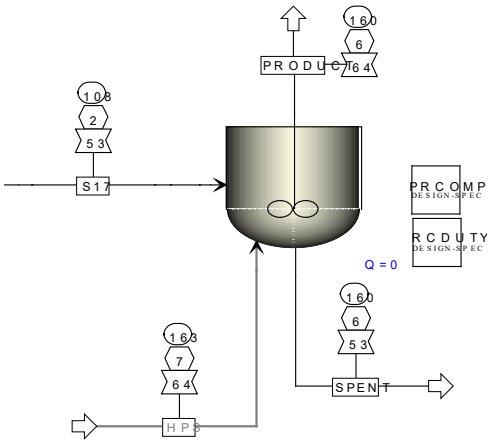

Figure II.11. Reaction section of the Chinese Batch Process.

One particular aspect of this process is that the use of maize results in the production of methanol as a by-product. This methanol is removed from the top of the reactor along with the rest of the product stream and then purged in a flash unit due to its low boiling point compared to the azeotrope furfural

water. The kinetics for the obtention of methanol from biomass under the evaluated conditions were not found in the literature. As an alternative solution, the theoretical ratio of furfural to methanol in the product was used, as suggested in [88]. According to Win, 16.5 Kg of methanol per 100 Kg of furfural would be obtained using corn cobs as feed. This was simulated by introducing a calculator at the reactor outlet, as shown in Figure II.12. This calculator imports the furfural mass flow rate value in the product stream and multiplies it by a factor of 0.1625 to export a variable that will be the methanol flow rate introduced into the gas phase (through the MIX-103 mixer).

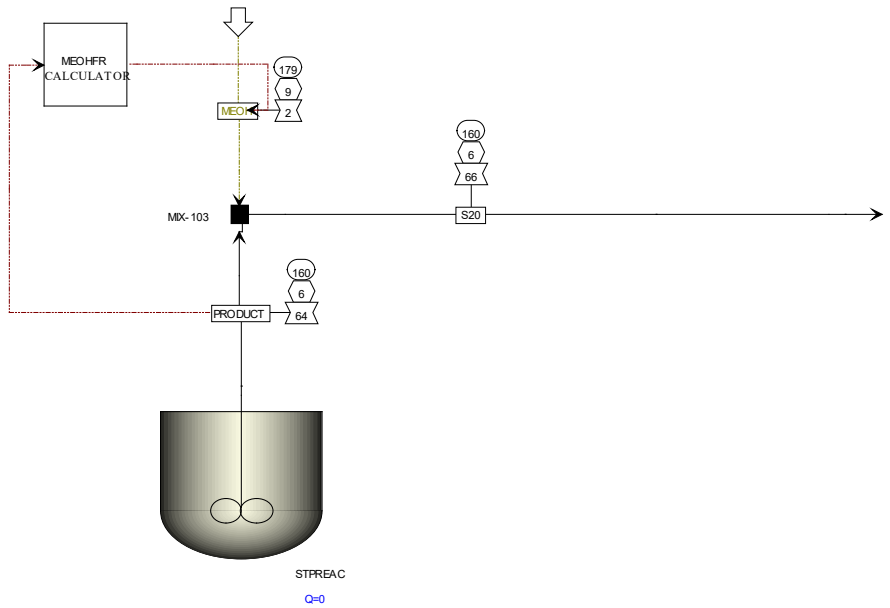

Figure II.12. Methanol calculator as a by-product in the CBP at the reactor outlet.

III. Purification

Before entering the first distillation tower, the product stream (S20) undergoes partial condensation in the reboiler of the column C-101 (Figure II.13). In Aspen, this is simulated by combining a heat exchanger and a flash unit, which function as two steps of the same process. In Figure II.13 this is represented inside the grey box. The bottom of the flash unit (S11) is a pseudo stream representing the column output, while the vapour phase (S9) corresponds to the fraction recirculated to the column. To simulate this, a pseudo-flow is introduced to export the heat duty in the reboiler (output from the REBCAL calculator). This demand then passes through the heat exchanger, where it contacts the reactor product stream (S20) which partially

condenses. Afterwards, this stream still has a vapour fraction of 0.75, so it is passed through a second exchanger for full condensing. The stream is passed through a flash unit (SEP block) to separate the methanol (LBOIL stream) before distillation. A methanol recovery of 100% is considered in this unit.

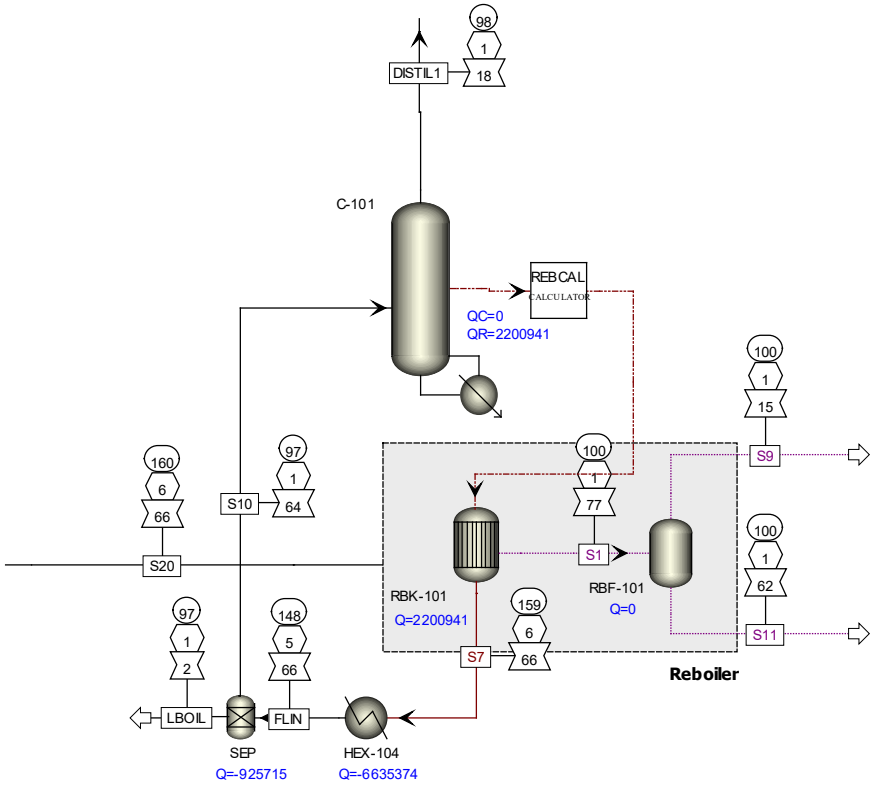

Figure II.13. CBP reactor outlet condensation before distillation in COL-101.

The process of double distillation is used to purify furfural in a similar way to QOP (Figure II.14). The initial column comprises a 30-plate tower that is designed to achieve a >99% molar recovery of the incoming furfural from the S10 stream. To achieve this, a design specification is used to vary the distillate rate, resulting in a molar flow of 805 Kmol/h. The product (stream DISTIL1) is condensed and mixed with the water from the second column (stream S12) before being decanted. The decanter recirculates the aqueous phase (stream LIGHT) to the C-101, while the organic phase (90% furfural, stream HEAVY) is neutralised and dehydrated. The C-102 column is designed and optimised in the same way as in the previous case, achieving a tower with only 5 equilibrium stages. The output of furfural is 2.5 tonne/h with a purity of 99% (stream FURFURAL).

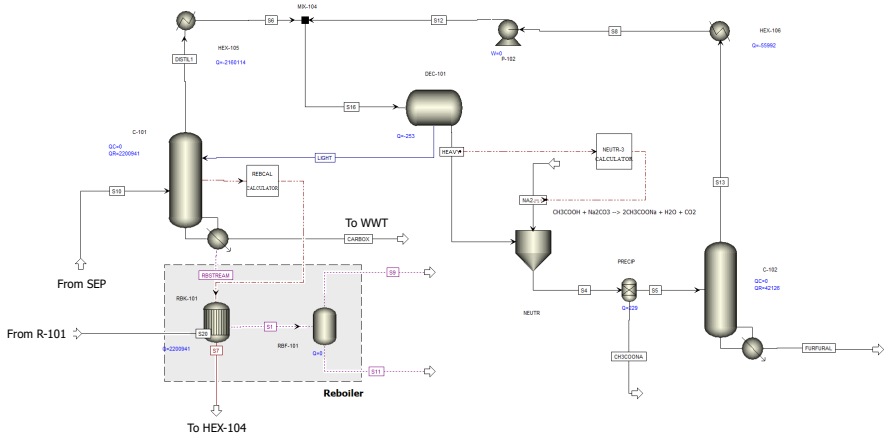

Figure II.14. Double distillation sequence for furfural purification in the CBP.

Finally, the anaerobic digestion of the residual flows coming from the reactor (stream SPENT) and the bottom of the first distillation column (stream CARBOX) follows the same principles as the QOP (Figure II.15).

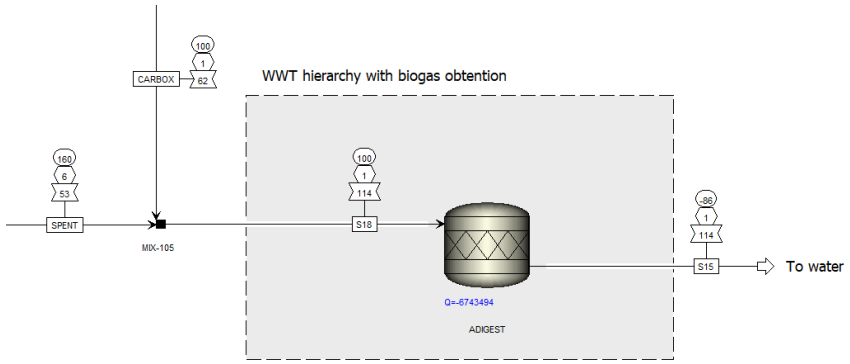

Figure II.15. Wastewater treatment section by anaerobic digestion of reactor and distillation effluents in the CBP.

Table II.4 summarises the inputs and outputs of the CBP, including materials, wastes and utilities consumed. All flows are referenced to one tonne of furfural, which will be the functional unit used in Section 5.2.

Table II.4. Input/output table of the CBP. Flows normalised to 1 tonne of furfural.

Name	Process	Value	Unit/tonne furfural
Inputs			
Materials	TO		
Biomass (dry)	MIX-101	8.5	tonne
Moisture		0.68	tonne
Dil. water	MIX-101	11.2	tonne
H_2SO_4	MIX-101	0.19	tonne
Stripping steam	R-101	63.8	tonne
Na_2CO_3	NEUTR	6	kg
Utilities	TO		
Electricity	P-101	1.4	kW
	P-102	0.01	kW
MPS	HEX-101	2.6	tonne
LPS	C-101	6.04	tonne
	C-102	0.12	
Cooling Water [a]	HEX-104	1910.2	tonne
	HEX-105	622	tonne
	HEX-106	16.1	tonne
Outputs			
Materials	FROM		
Furfural	C-102	1	tonne
Methanol		0.16	tonne
CO_2	NEUTR	0.7	kg
CH_3COONa	NEUTR	9.3	kg
Solids	R-101	5.8	tonne
Waste water	R-101	15.2	tonne
Waste water	C-101	24.7	tonne

[a] *The input for the LCA calculations consider only 3% of this utility, assuming the regeneration of the remaining water.*

II.2. Life Cycle Assessment of benchmark technologies

Once the simulations were completed and optimized, the inputs and outputs obtained were used as inventories for the environmental analysis. The methodological choices are described below following the main steps of LCA.

I. Goal and scope

The functional unit is defined as the production of 1 tonne of furfural with a purity of 99% at the factory gate. The study uses an attributional approach to perform a hotspot analysis of the Quaker Oats and Chinese batch processes for furfural production.

The system boundaries extend from the cultivation of raw materials to the delivery of furfural at the factory gate. All background processes in the first level of the production chain are allocated based on mass ratios with other products. For the remaining by-products in the foreground system, also mass allocation was applied to address multifunctionality for system coherence. System boundaries are schematically shown in Figure II.16.

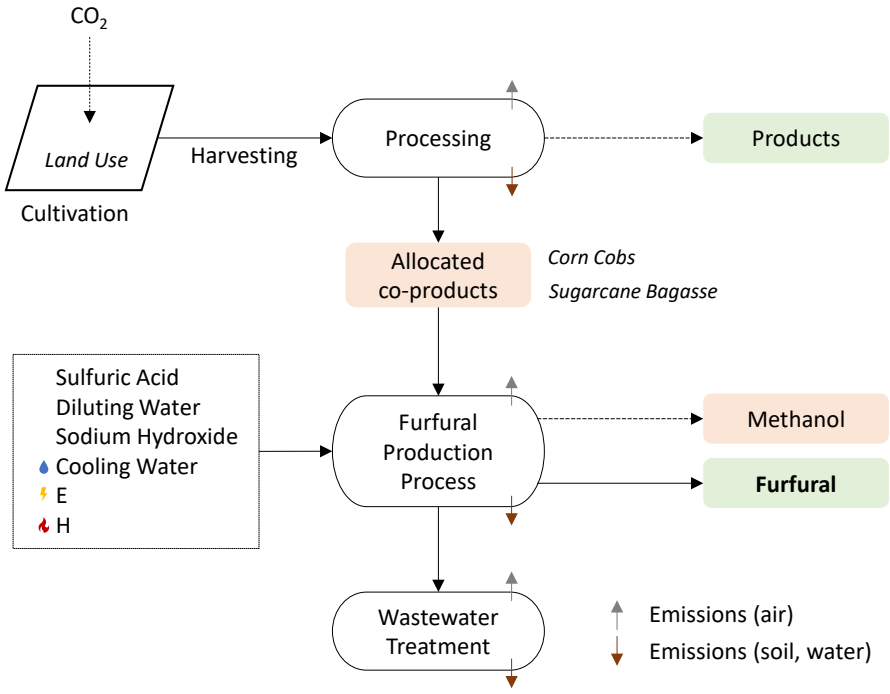

Figure II.16. System boundaries for the studied processes.

The geographical scope of the study is designed to match both technologies to their expected locations. The Quaker-Oats process is located in the Dominican Republic, while data from China are used for the Chinese technology. In both systems, biogenic carbon is assumed to be retained in the furfural during the time horizon of the study. This assumption is based on the reasons detailed in Chapter I.

II. Life Cycle Inventory

The study aims to evaluate the cradle-to-gate effects of all unit processes in the foreground system while also considering the complete life cycle of immediately related background processes. The APOS (At the Point Of Substitution) version of the Ecoinvent (v3.9) database was used for this purpose. Table II.2 and Table II.4 summarise the inventories used to model QOP and CBP respectively. In cases where the information was not in the database, data bridging was performed by adapting the most similar datasets as a proxy.

III. Life Cycle Impact Assessment

The methodology used to translate the inventory into environmental impacts was the Environmental Footprint 3.1, as implemented in Ecoinvent. The Activity Browser interface for Brightway was employed for calculations (see Section 3.2). In this study, effects were assessed at the midpoint level and all indicators described in the method were reviewed. Following a contribution analysis, only a subset of these indicators is presented in the main discussion, while the remaining midpoint results are shown but not further commented. The selected indicators include acidification (AC), climate change (CC), freshwater ecotoxicity (FWET), marine eutrophication (MEP), terrestrial eutrophication (TEP), human toxicity non-carcinogenic effects (HTnc), particulate matter (PM), photochemical ozone formation (POF) and fossil depletion (FD). The contribution analysis results are displayed in Figure II.17.

A hotspot analysis was carried out to identify the most significant process contributors to each environmental category. The impact assessment was carried out taking into account the uncertainty of the inputs. This uncertainty is considered as a probability distribution of the input data, which is propagated through LCA calculations by Monte Carlo sampling. The result is a probability distribution of the output data, which constitutes a more transparent way of interpreting LCA outcomes. Variability of both the technosphere and biosphere exchanges is considered.

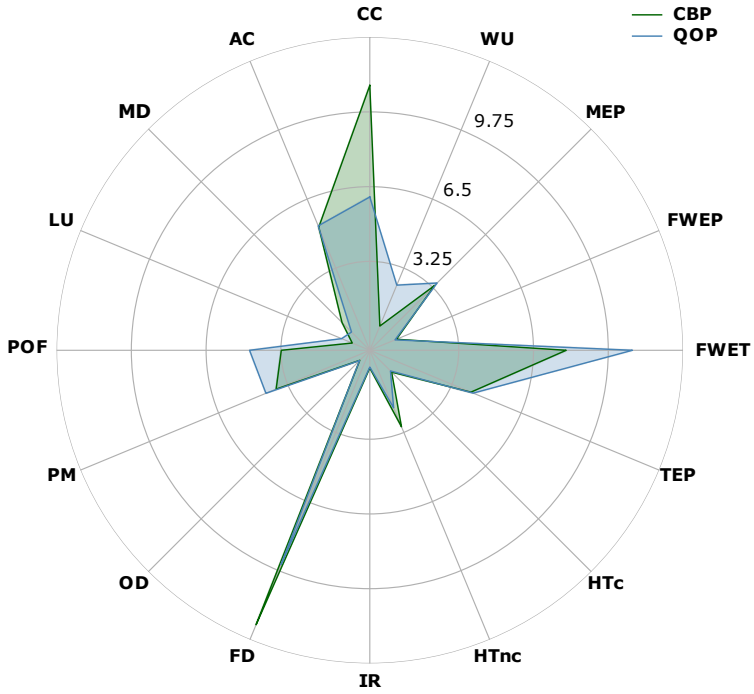

Figure II.17. Contribution analysis results (in person equivalents ·10^{-6}) for the QOP and CBP processes using the EF3.1 methodology.

IV. Assumptions and limitations

In the Dominican Republic, heat is mainly produced from fossil fuels (>88% of the total share). Most natural gas (NG) and light fuel oil (LFO) imports come from the United States, while coal imports come mainly from Brazil. In China, coal is the main source of thermal energy, with bituminous coal being the most abundant and commonly used. The heating steam production is modelled using average data and adapted to these two specific mixes. These mixes shares are displayed in Table II.5.

Table II.5. Energy mixes considered for China and Dominican Republic.

	CN Energy mix [239]	**DO Energy mix** [240]
Natural Gas	13%	15%
Hard Coal	64%	15.5%
Heavy Fuel Oil	23%	
Light Fuel Oil		58%
Biomass		11.5%

Both processes result in two main waste streams: one at the reactor outlet (consisting of solids with a relatively low moisture content) and the other at the bottom of the first column (containing acetic and other carboxylic acids).

In this study, it is assumed that both streams are mixed and subsequently sent to anaerobic digestion. The quantity of biogas generated is calculated by the methodology outlined in the previous section. This quantity acts as a reference flow for retrieving the wastewater treatment process from the database in LCA calculations.

II.2.1. LCA results

A summary of all the midpoint indicators calculated for QOP can be found in Table II.6. The table illustrates the impacts, disaggregated by environmental category and plant section, according to the division depicted in Figure II.1. The pretreatment section involves the heating of the dilute acid and the pumping of the wet biomass into the reactor. The reaction section is supplied with steam for heating and stripping purposes. Furthermore, all materials (biomass, sulphuric acid and dilution water) are considered to enter at this point for results breakdown. These materials are considered in the reaction section rather since it is where they are utilised. Conversely, in the pre-treatment only electricity and heat are consumed to condition the mixture. The secondary steam generator (2nd steam gen.) refers to the heat recovery equipment described in Figure II.4. The purification section comprises the distillation columns, the decanter and the neutraliser shown in Figure II.5 toFigure II.7.

Table II.6. Midpoint results summary for the QOP.

	Pretreatment	**Reaction**	**2nd steam gen.**	**Purification**	**WWT**
AC	0.56	19.35	0.47	0.28	0.30
GWP100	145.42	4522.10	65.33	59.33	113.96
FWET	684.28	26664.48	456.55	750.35	175.89
ADPf	1748.81	54736.51	824.51	720.08	1299.38
FWEP	1.29E-02	4.12E-01	6.96E-03	1.09E-02	2.38E-02
MEP	0.09	4.09	0.07	0.05	0.06
TEP	0.89	36.03	0.74	0.47	0.65
HTc	4.62E-08	1.48E-06	2.30E-08	2.77E-08	3.12E-08
HTnc	8.13E-07	2.68E-05	3.42E-07	6.20E-07	7.91E-07
IR	0.62	20.17	0.23	1.90	6.75
LU	207.38	19528.34	81.20	124.72	379.03
ADPm	4.76E-05	2.03E-03	6.72E-05	4.20E-04	3.51E-04
ODP	1.79E-06	5.68E-05	1.43E-06	8.27E-06	1.63E-06
PMF	8.86E-06	2.89E-04	2.82E-06	3.66E-06	2.57E-06
POF	0.37	12.18	0.26	0.17	0.25
WU	16.39	536.10	8.25	25.50	16.63

The list of the names and the units of the indicators in Table II.6 and Table II.7 can be found in the glossary of terms and abbreviations.

Most impacts on all environmental categories assessed are attributable to steam generation. The principal reason is the considerable quantity of this utility consumed throughout the process. In particular, the reactor heating and stripping is responsible for the most harmful effects in this plant. Consequently, the impacts on almost all the environmental categories are one or two orders of magnitude higher than those observed in the other sections shown in Figure II.1.

On the other hand, midpoint indicators calculated for the CBP are summarised in Table II.7. As previously stated, CBP is based on QOP, and therefore both processes are analogous. Therefore, the sections depicted in Table II.7 are identical to those in Table II.6, except for the secondary steam generator due to the configuration of the CBP (Figure II.9). However, key differences lie in the type of biomass used, the configuration of the initial distillation column, and the volume of dilution water introduced at the inlet.

Table II.7. Midpoint results summary for the CBP.

	Pretreatment	Reaction	Purification	WWT
AC	8.98	93.86	21.06	0.87
GWP100	1202.08	11669.13	2812.59	330.22
FWET	3088.04	31777.69	9596.55	509.65
ADPf	10956.33	106352.67	25717.68	3765.06
FWEP	0.29	2.84	0.69	0.07
MEP	1.02	11.82	2.40	0.18
TEP	10.63	125.68	24.93	1.89
HTc	6.57E-07	6.49E-06	1.56E-06	9.03E-08
HTnc	8.61E-06	9.08E-05	2.10E-05	2.29E-06
IR	9.41	93.63	24.30	19.55
LU	1511.19	26266.40	3620.43	1098.27
ADPm	2.42E-04	4.05E-03	1.63E-03	1.02E-03
ODP	6.73E-06	6.79E-05	2.94E-05	4.72E-06
PMF	1.29E-04	1.29E-03	3.02E-04	7.46E-06
POF	3.61	35.58	8.46	0.73
WU	46.93	1371.64	159.63	48.20

The main source of impact in the CBP is again the generation of stripping steam for the reactor. The consumption of this steam is higher in the CBP for two main reasons. First, the larger amount of water at the inlet to dilute the H_2SO_4 makes the size of the equipment increase, so the heating steam input rises accordingly. Second, the quantity of arabinoxylans in the corn cobs is lower than in the Sugar Cane Bagasse (SCB), as indicated by the data in Table II.3 and Table II.1. Thus, using the same kinetic model under similar operation conditions, more resources are required to produce the same functional unit.

The effects on each environmental compartment and the reasons for them are discussed in detail below. The objective of this chapter is not to compare the two processes but rather to describe their environmental profile. Nevertheless, the figures presented in this section illustrate the outcome of both processes in parallel to illustrate these differences. Here, the uncertainty of the output is included and commented on to provide further insight into both processes.

I. Acidification

Steam production is responsible for almost all acidification effects caused by both processes (Table II.6 and Table II.7). In particular, the combustion of coal and light fuel oil (LFO) represents a significant source of sulphur dioxide (SO_2) emissions to the atmosphere (Figure II.18). In the QOP, LFO accounts for 57.5% of the energy mix and is responsible for 30% of the acidification effects. On the other hand, despite representing only 15.5% of the energy mix, coal accounts for 43% of the impact. This provides insight into the consequences of the release of sulphur from this fossil resource. In fact, acidification is significantly promoted in the CBP due to the higher consumption of heating steam and the use of coal to generate it. In this case, the SO_2 emitted during coal burning is responsible for 65-70% of the total SO_2 emissions of the plant.

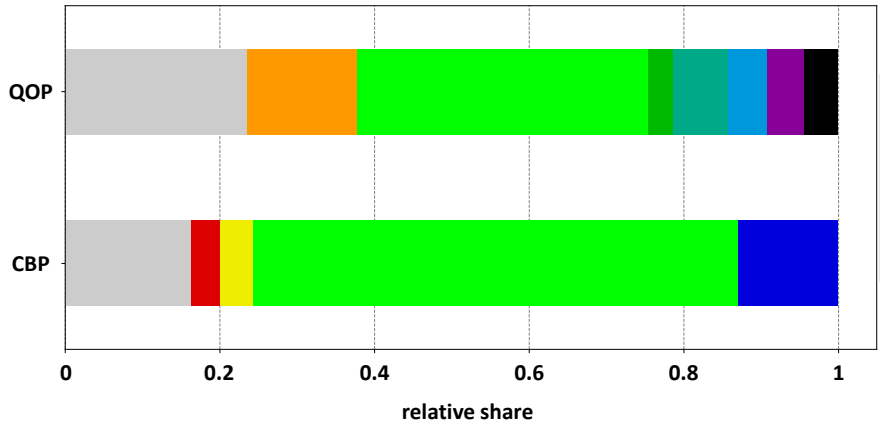

Figure II.18. Relative share of the impacts of QOP and CBP on acidification. (●) Rest, (●) Heat from light fuel oil, (●) Corn production, (●) Heat from coke, (●) Heat from hard coal, (●) Electricity from hard coal, (●) Electricity from oil, (●) Transport of petroleum, (●) Light fuel oil production, (●) Sugarcane production, (●) Heat from natural gas.

The utilisation of SCB also has implications due to ammonia emissions during the production of sugarcane, although to a lesser extent. On the other hand, corn cobs utilisation has a very low effect on the acidification produced

by the CBP. The environmental impacts of electricity use in the QOP arise from the operation of the compressor for secondary steam production. This electricity is generated mainly by LFO combustion, according to the DO electricity mix. Accordingly, most of the impact is associated to SO_2 emissions during its valorisation. It is noteworthy that the utilisation of sulphuric acid does not result in a discernible enhancement in acidification in either of the processes. The neutralisation of effluent streams prior to discharge is a design consideration, as this is assumed to be the most likely configuration. However, it should be noted that this is not necessarily the layout applied in all current plants, as noted in [75].

The values displayed in Figure II.19 represent the median of the probabilistic distribution of the outputs. The distribution is based on a lognormal variation of the input data, as captured by the Ecoinvent pedigree matrix. Consequently, the median data is slightly shifted to the right concerning the point reported in both processes without uncertainty. The mean values are closer to this point.

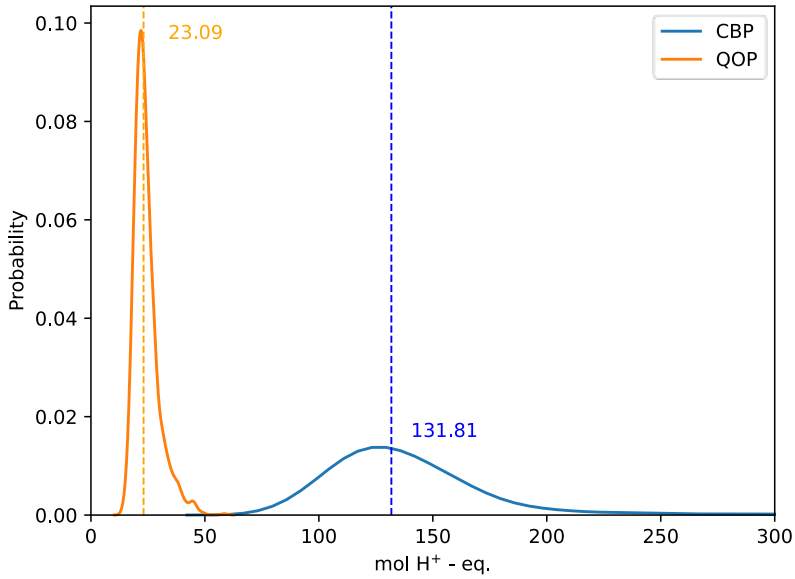

Figure II.19. Probabilistic distribution of the impacts of QOP and CBP on acidification.

The results of the CBP are subject to greater uncertainty. Most of the observed variability in these data can be attributed to exchanges with the biosphere. The effect of SO_2 emitted during the combustion of coal is to increase the concentration of SO_2 in natural environments, which causes acidification problems at the midpoint level. The accumulation is estimated

based on a sulphur balance, which is associated with lower levels of reliability and completeness than in the case of other elements. As coal consumption is higher in the CBP, the distribution of the results exhibits a wider range.

II. Climate Change

Once more, most of the impact is associated with steam consumption in the reactor (Figure II.20). In the QOP, the combustion of fossil fuels results in CO_2 emissions (>3500 kg CO_2 - eq./tonne furfural) that are significantly higher than the amount of CO_2 that is absorbed during the growth of sugarcane (274 kg CO_2 - eq./tonne furfural). Similarly, the role of CO_2 absorbed by the maize in the CBP (320 kg per tonne of furfural) is negligible in comparison to the emissions (>13,500 kg CO_2 per tonne of furfural). Consequently, in both processes biogenic carbon plays a relatively minor role, given the undue steam consumption of the reactor. The utilisation of agricultural wastes serves to significantly mitigate the effects on land occupation (Table II.6 and Table II.7), which is a common issue in bioprocesses due to the use of extensive farming areas. In this case, this increase is marginal, yet the carbon sequestered is considerably lower. The explanation in both cases is the allocation of CO_2 absorbed by the primary agricultural products. Bagasse is a by-product of the production of cane sugar, while cobs are a by-product of maize production. Therefore, the carbon absorption attributed to them is smaller.

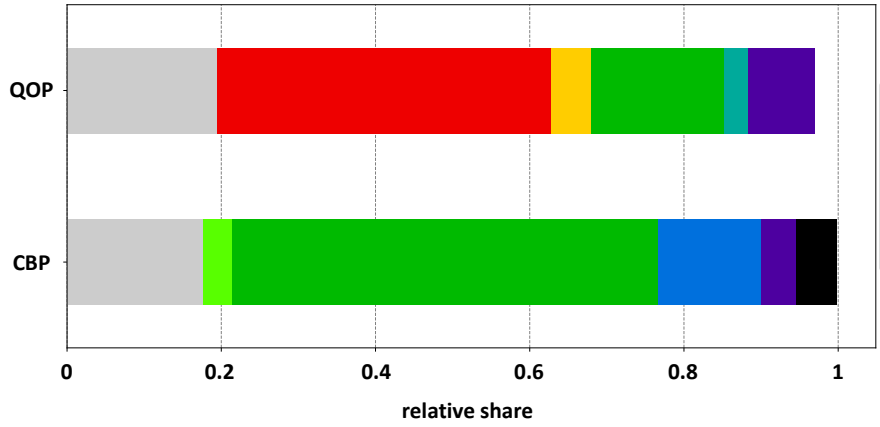

Figure II.20. Relative share of the impacts of QOP and CBP on climate change. (●) Rest, (●) Heat from light fuel oil, (●) Heat from coke, (●) Natural gas venting, (●) Heat from hard coal, (●) Electricity from oil, (●) Heat from heavy fuel oil, (●) Heat from natural gas, (●) Hard coal mine.

The sum of the relative impacts in Figure II.20 does not equal unity for the QOP due to the CO_2 absorbed by the herbaceous crops used as fuel

for steam generation. The amount of carbon dioxide absorbed by this material amounts to 1840 kg CO_2 - eq. per tonne of furfural, which far exceeds the contribution of biomass used as feedstock.

Direct carbon dioxide emissions (characterisation factor = 1) account for a significant proportion of the impact in this category, exceeding 90%. The majority of these emissions are attributable to the combustion of LFO in the QOP, and hard coal in the CBP. As the steam consumption is slightly more than twice as high in the first case, and the Chinese energy mix is heavily reliant on coal, the global warming caused by CBP is approximately three times higher than in the case of QOP (Figure II.21).

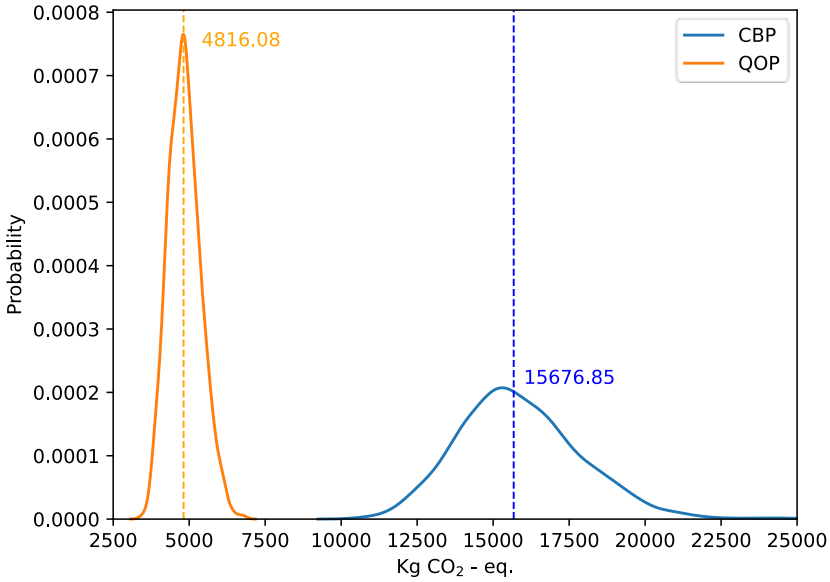

Figure II.21. Probabilistic distribution of the impacts of QOP and CBP on global warming potential.

Apart from combustion, methane venting during LFO and natural gas (NG) production exerts a somewhat significant influence on this category in the QOP, while the combustion of heavy fuel oil (HFO) gets almost 14% of the equivalent CO_2 emissions in the CBP. Carbon dioxide emitted in the neutraliser accounts for <5% of the impact on the purification train of both processes and is negligible in the overall calculations.

III. Freshwater ecotoxicity

The ecotoxicity in freshwater ecosystems is primarily influenced by two key processes related to the stripping vapour consumption. First, the discharge of aromatic hydrocarbons during the extraction of crude oil. Overall,

the use of LFO accounts for a 64% of the impact on this category in the case of QOP, and 37% in the case of CBP (Figure II.22). On the other hand, coal mining results in a significant discharge of chlorides to water, accounting for approximately 42% in the CBP. It is worth noting that the process of water discharge during the extraction of oil and gas has the greatest impact on this impact category. China's energy mix comprises less than 30% of these resources, in comparison to more than 70% in the Dominican Republic. Nevertheless, the consequences of water contamination in this process are similar to those of coal mining (60% of China's energy share).

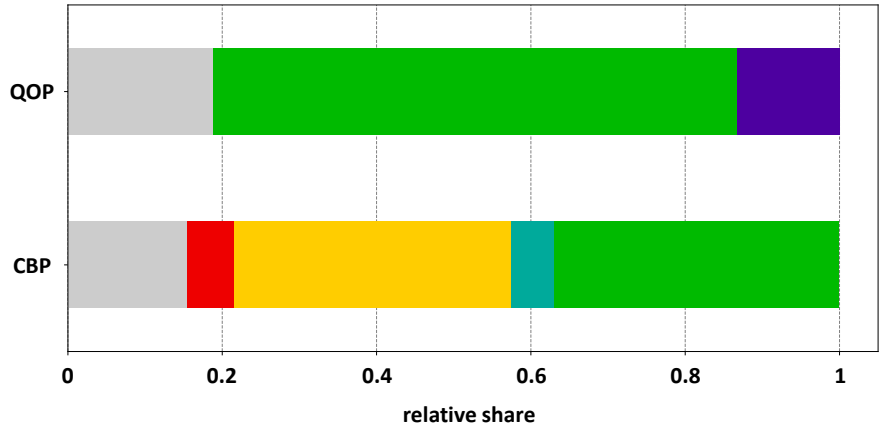

Figure II.22. Relative share of the impacts of QOP and CBP on freshwater ecotoxicity. (●) Rest, (●) Heat from hard coal, (●) Hard coal mine, (●) Water discharge from petroleum/natural gas extraction, (●) Deionised water production, (●) Sugarcane production.

The use of pesticides during SCB cultivation has a severe implication in the QOP. In particular, the use of fipronil accounts for 19% of the impact on this impact category, despite the use of residual bagasse in the processing of this feedstock. Interestingly, water emissions of this compound at the inventory level are three orders of magnitude below for the cultivation of maize, resulting in a negligible impact despite the higher biomass consumption by the CBP.

It is notable that the production of deionised water in CBP exhibits visible toxicity effects, comparable to those produced by coal combustion. The reason is that the quantity of cooling water required to fully condense the stream entering the C-101 column (Figure II.14) is considerably large (Table II.4), resulting in a notable emission of chlorides during its production. This is attributed to the mass flow rate of the product stream, as discussed in 5.2.1. This flow rate also influences the design of the first column, which requires a larger size and a higher energy consumption. Moreover, it is infeasible to

operate with a stripping vapour in place of the reboiler as is in the QOP, since steam requirements would be excessively high due to the column dimensions. Furthermore, the steam injection would also result in the dilution of the furfural below the azeotropic point (see 3.1.2). Consequently, it would be necessary to increase the reflux ratio from the decanter to enhance the water separation at the bottom of the column.

Uncertainty results for this environmental category have been omitted due to the high dispersion of results. This variability makes the probability of any result too low to make the visualisation of the data interesting. Instead, a global sensitivity analysis (GSA) was carried out to identify the parameters that most influence the uncertainty of each process. In both cases, the emission of hydrocarbons and chlorides to freshwaters introduces high variability in the model at the level of interaction with the biosphere. In other words, a minor deviation of these flows results in a considerable modification in the LCA outcomes, since the toxicity effects are based on less robust estimates than desirable. In particular, the geographical, technological and temporal correlation values in the Pedigree matrix are high (>3), implying a relatively low reliability. Given the characterisation factor of both flows for FWET and their large emissions due to steam consumption, the distribution of results is singularly wide.

IV. Abiotic depletion potential: fossil fuels

The consumption of fossil fuels is considerable in both processes, although it is higher in CBP due to the heating requirements of the pre-treatment, reactor and first distillation column. As anticipated, the greatest consumption is observed in the reactor in the two cases. This consumption is also proportional to the energy mix of the Dominican Republic and China. The relative share figure is omitted for this impact category, as it basically shows the energy mix utilised in each country. Even though it provides insights into the production chain of each fuel, it does not significantly enhance the comprehension of the processes.

In the Chinese case, the use of coal has a less pronounced impact than in the Dominican case, given that it is a more abundant resource. However, the introduction of coal into the model represents a considerable increase in uncertainty. The values in the Pedigree matrix used to ascertain the deviation of the calculations yield the worst possible values. This means the data is old and technological representativity cannot be assured. This results in a wide distribution of the results (Figure II.23). Furthermore, the incorporation of biomass and renewable energy sources into the DO energy mix serves to

mitigate the consumption of fossil fuels. This is not achieved by including nuclear power in China.

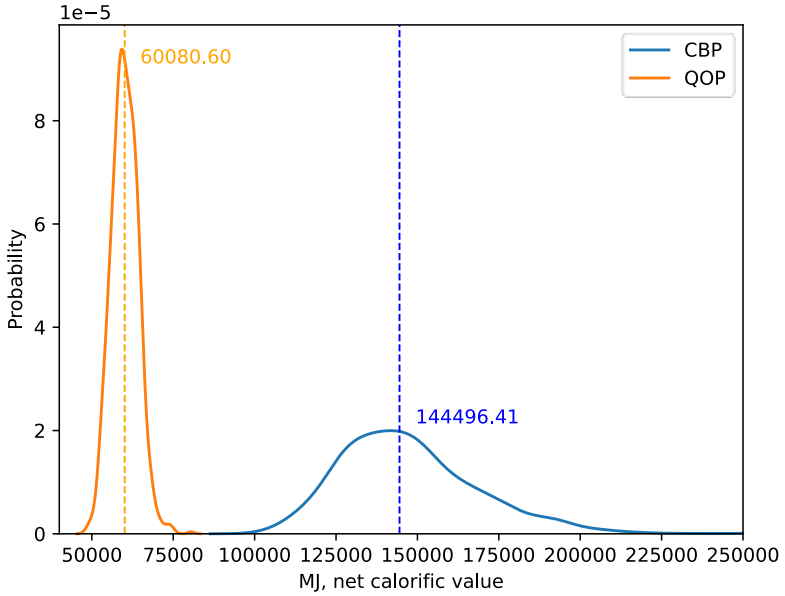

Figure II.23. Probabilistic distribution of the impacts of QOP and CBP on fossils consumption.

V. Marine eutrophication potential

The effects of eutrophication in marine environments are typically the result of the entrainment of nutrients into these environments. In this context, the results observed in Figure II.24 are consistent with the release of nitrates during biomass production and nitrogen oxides (NO_x) during coal and LFO combustion. In comparison, the quantity of NO_x generated during the combustion of hard coal is considerably larger. Coal contains nitrogen as part of its organic structure. During combustion, this nitrogen is released and reacts with oxygen to form NO_x [241]. Oil typically has a lower nitrogen content than coal, which results in less fuel nitrogen available to form nitrogen oxides. Moreover, at high temperatures, nitrogen and oxygen in the air can react to form NO_x. The combustion temperature of oil is generally lower, which reduces the formation of thermal NO_x.

It is noteworthy that the utilisation of corn or bagasse exhibits a comparable impact, despite the nature of the crops and geographical locations under consideration. The production of 1.8 kg of nitrogen equivalent per tonne of furfural is observed in the case of corn, while 1.2 kg is observed in the case of SCB. This discrepancy is primarily attributable to the biomass consumption

in each process. The observed differences in Figure II.24 can be attributed to the fact that the impacts are normalised to unity. Given the considerable role of coal in the Chinese process, the relative effect of biomass decreases proportionally. Interestingly, the production of heat from biomass, despite its relatively minor contribution to the energy mix, accounts for a notable 6% of the MEP in the QOP, due to both nitrate and NO_x emissions during cultivation and combustion respectively.

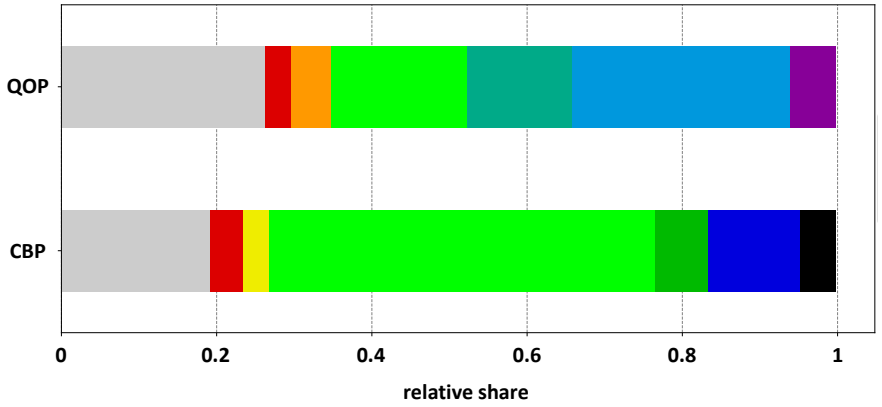

Figure II.24. Relative share of the impacts of QOP and CBP on marine eutrophication. (●) Rest, (●) Electricity from hard coal, (●) Heat from coke, (●) Electricity from oil, (●) Heat from hard coal, (●) Heat from light fuel oil, (●) Sugarcane production, (●) Heat from heavy fuel oil, (●) Corn production, (●) Transport of petroleum, (●) Treatment of spoil in hard coal mining.

Essentially, the differences observed in Figure II.25 can be attributed to the higher heating steam consumption in the QOP process. As illustrated in Table II.6 and Table II.7, the reactor represents the largest hotspot in both processes. As previously noted, the wastewater composition considered for the LCA calculations is only partially representative. This constitutes a limitation of the study that should be addressed in future work to test the effects of treating an effluent with the actual chemical and biological oxygen demand levels. This effect has been considered in the uncertainty calculations, resulting in wider distributions due to the influence of this parameter on eutrophication.

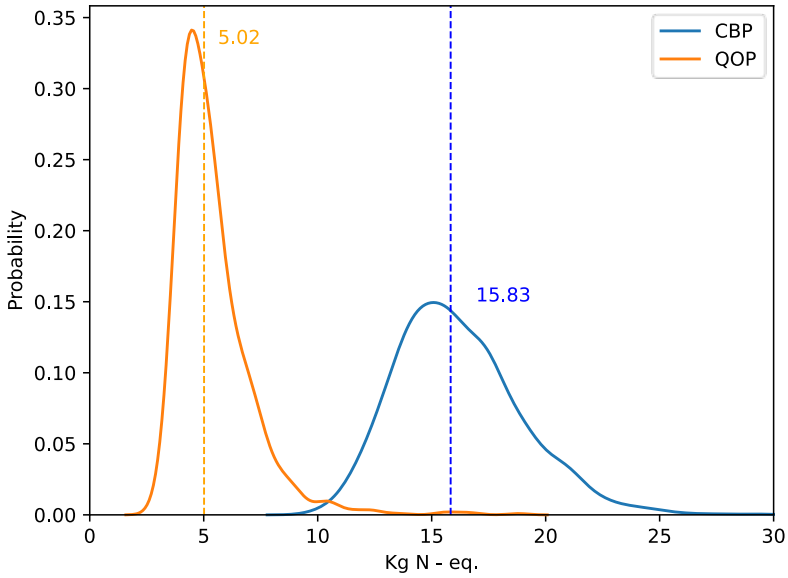

Figure II.25. Probabilistic distribution of the impacts of QOP and CBP on marine eutrophication potential.

VI. Terrestrial eutrophication potential

In this instance, the impact is quantified in terms of moles of nitrogen equivalent, rather than in mass, which partially accounts for the discrepancy between the two results. More importantly, the observed impact pathways for measuring TEP and MEP in the EF3.1 methodology are very similar, although they exhibit a slight divergence in focus. In the case of marine eutrophication, this process can lead to an uncontrolled proliferation of phytoplanktonic organisms and macrophytic plants, which can disrupt the passage of light to lower levels, decrease dissolved oxygen and affect water quality. On the other hand, terrestrial eutrophication refers to the excessive accumulation of nutrients in soils, which can alter the balance of terrestrial ecosystems and affect biodiversity. In this case, the accumulation of nitrogen equivalent in soils is somewhat higher than in marine environments (where it arrives by deposition or runoff). Therefore, the results over this category are somewhat higher than the multiplication of the MEP results by the molar mass of nitrogen. The distribution of impacts by sub-process is identical to that shown in Figure II.24 and Figure II.25 and therefore omitted to avoid redundancy.

VII. Human toxicity, non-cancer effects

Once more, most of the adverse effects on human health (non-carcinogenic effects) associated with the process are attributable to the

consumption of steam in the reactor (Table II.6 and Table II.7). The impact of fossil fuels is associated with the leaching of heavy metals. Coal naturally contains a variety of elements, including heavy metals like arsenic, lead, and mercury. During combustion, volatile toxic elements are released from the coal and a significant part of these elements gets adsorbed on the ash particles at cooler zones of the furnace [242]. Heavy metals and other toxic elements in coal ash can leach into groundwater and surface water bodies. This water pollution poses risks to human health through bioaccumulation in the food chain [243]. The LFO case is analogous. Naturally present metals can be found in the post-combustion ashes. If the ash is landfilled without proper treatment, it can pollute ground and surface water through leaching and runoff, leading again to human toxicity related effects [244].

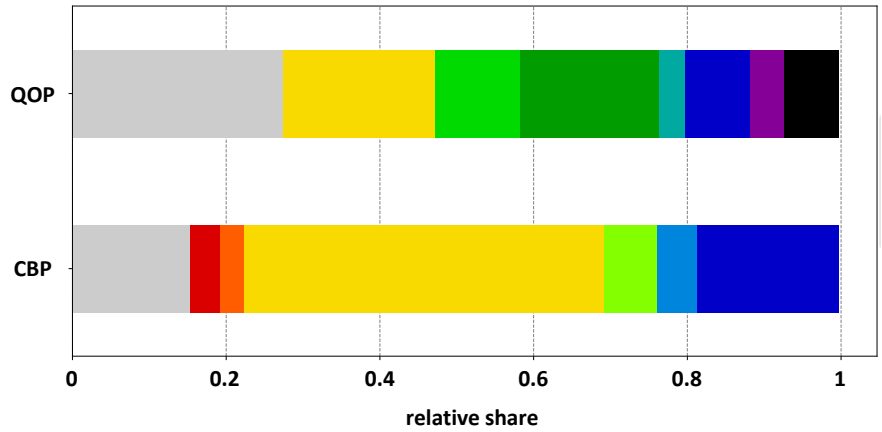

Figure II.26. Relative share of the impacts of QOP and CBP on human non-cancer toxicity. (●) Rest, (●) Hard coal production, (●) Heat from coke, (●) Heat from hard coal, (●) Heat from light fuel oil, (●) Heat from straw, (●) Heat from heavy fuel oil, (●) Smelting of copper, (●) Corn production, (●) Landfill of hard coal ash, (●) Treatment of water discharge from petroleum/ natural gas extraction, (●) Landfarming of wood ash.

The combustion of straw, understood as a mixture of different herbaceous fuels, also poses a risk to human health. This fuel, present in the Dominican Republic's energy mix, can contain trace amounts of cadmium and mercury [245]. During combustion, volatile toxic elements like cadmium and different mercury species are absorbed on the ash particles [246]. The toxic effects derive from leaching of the absorbed compounds.

In this instance, the results of the Monte Carlo sampling are open to misinterpretation due to the proximity of the impact value to zero and the introduction of negative flows. In the Ecoinvent database, waste treatment activities must produce a product. In the case of wastewater treatment, this

product is the wastewater. In reality, this flow would operate as an input, so to maintain the mass balance, this product is given a negative sign. At the same time, the lognormal distributions of input parameters, taken by default in Ecoinvent, do not have negative values. The rationale is that lognormal distribution is a probability function of a random variable whose logarithm is normally distributed. Because the natural logarithm is undefined for negative numbers and zero, a lognormal distribution can only take positive values. If a negative flow is subjected to Monte Carlo sampling, it does not consider negative values (because it cannot) but 'negative supply chains' (because of waste modelling). In other words, all values within the lognormal distribution of the variable will be negative without affecting the calculation. However, when propagating this uncertainty, the results from this flow will subtract the rest of the values. Consequently, if the outcome is close to zero, overall negative results may be observed, leading to the assumption that there is a positive impact on the category under study. For this reason, the results of uncertainty are omitted in this case.

VIII. Particulate matter formation

The highest number of particles is emitted in both processes during the combustion of fuels. Incomplete combustion and fly ashes lead to the formation of particulate matter. Accordingly, the production of steam exerts a significant influence. Given the nature of the resources employed, there are two sources with a higher incidence, namely coal and biomass combustion (Figure II.27). In the QOP, the biomass utilised for energy production has been modelled as residual straw since it is the most likely source in a refinery utilising sugarcane bagasse. Burning this biomass is associated with the emission of a high amount of particulate matter with a diameter of less than 2.5 microns (PM2.5) [247]. This process emits 1.2 kg of PM2.5 per tonne of furfural. Of this, 33% is attributable to straw burning. Coal additionally contains different impurities such as sulphur. Upon combustion, the sulphur might be released into the air. According to the results, part of the impact is related to sulphur dioxide (SO_2) emissions during coal combustion. In the case of the CBP, SO_2 emissions account for 30% of the disease incidences caused. Since the energy consumed by QOP is larger, the number of disease incidences caused by particle emissions is also higher (Figure II.28).

Electricity has a high impact on particle formation, as illustrated in Figure II.27. Interestingly, this electricity does not refer to electricity consumed directly by any of the processes. In that case, its relative contribution would be higher in the QOP due to the operation of the compressor (see Figure II.4).

Conversely, this electricity is used in coal mining processes (machinery operation, ore processing, ventilation systems, etc.). Since both processes consume large amounts of energy, and this energy is partly generated from coal (Table II.6 and Table II.7), a significant amount of coal is required to supply the extraction processes of the fuel itself.

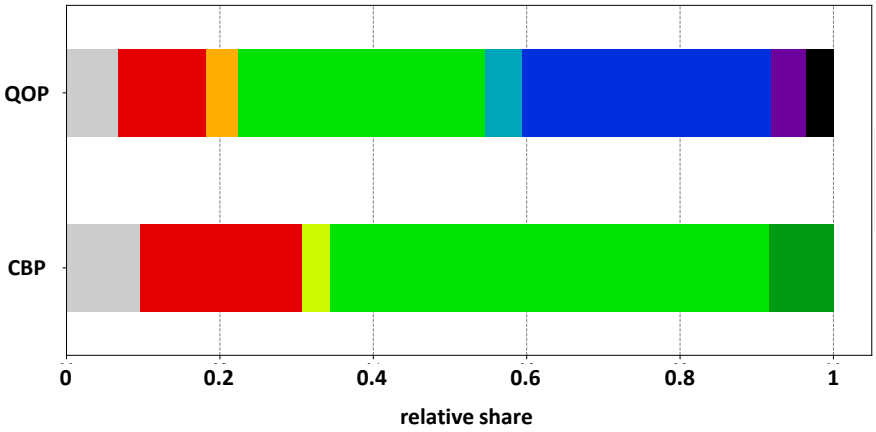

Figure II.27. Relative share of the impacts of QOP and CBP in the formation of particulate matter. (●) Rest, (●) Electricity from hard coal, (●) Electricity from oil, (●) Heat from coke, (●) Heat from hard coal, (●) Heat from light fuel oil, (●) Heat from straw, (●) Heat from heavy fuel oil, (●) Light fuel oil production, (●) Sugarcane production.

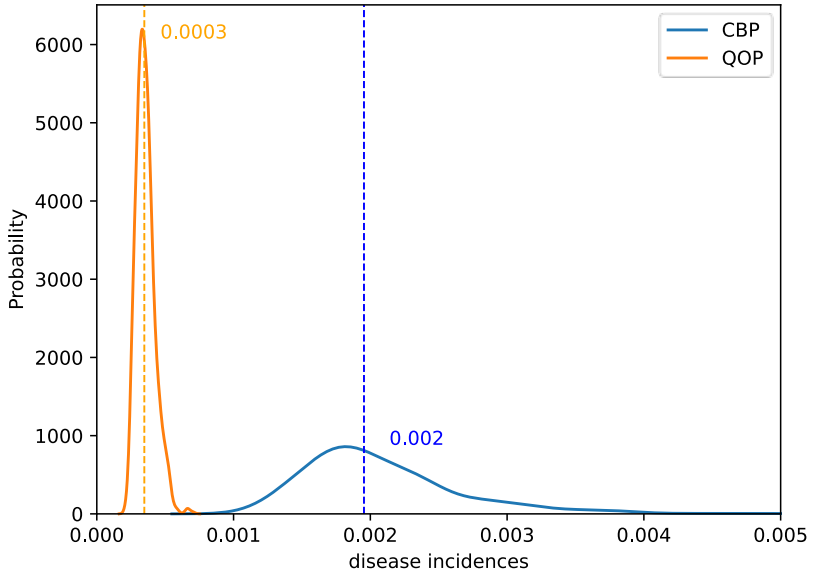

Figure II.28. Probabilistic distribution of the impacts of QOP and CBP on particulate matter formation.

The difference in impact between the two processes can be attributed to the higher energy consumption in the CBP. Most of the impact is related to coal combustion. Consequently, the dispersion of the results in Figure II.28 is associated to the uncertainty in the amount of PM2.5 produced in the coal-fired furnaces. As no primary data are available, the dataset relies on estimates. Hence, the correlation values in the Pedigree matrix are high (>4), yielding a wider distribution.

IX. Photochemical ozone formation

During the combustion of both coal and LFO, a significant amount of nitrogen oxides is emitted as discussed in the section. NO_x can react with other chemicals in the atmosphere to produce severe environmental effects such as smog or increased greenhouse effects. In the QOP, this compound accounts for 54% of the oxidants emitted. In the CBP, this figure increases by over 60%, primarily due to higher coal consumption.

The impact of natural gas venting on the QOP is noteworthy. Natural gas is often vented during petroleum extraction for several reasons. It can be an unwanted byproduct with no immediate use or market, or the infrastructure to capture and process it may be lacking or too costly. Venting can also serve as a safety measure to prevent pressure build-up in reservoirs and equipment. The emissions of natural gas directly into the atmosphere contribute to photochemical oxidant formation by reacting with other chemicals. This is a characteristic effect of volatile organic compounds, which can form ground-level ozone in the presence of sunlight.

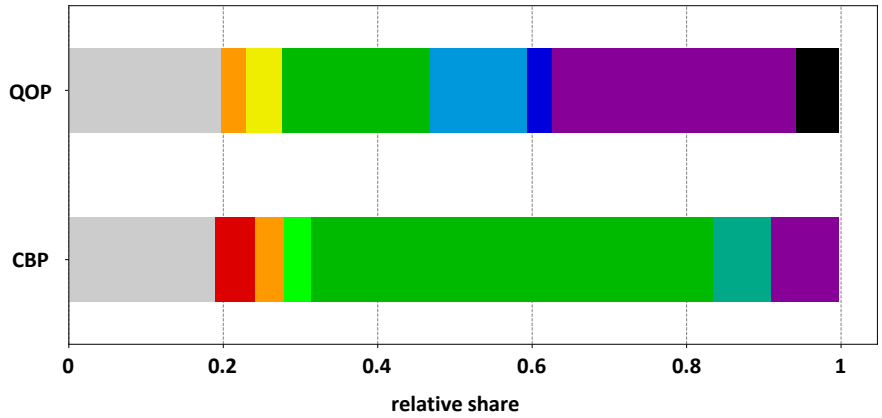

Figure II.29. Relative share of the impacts of QOP and CBP in the formation of photochemical oxidants. (●) Rest, (●) Coking, (●) Electricity from hard coal, (●) Electricity from oil, (●) Heat from coke, (●) Heat from hard coal, (●) Heat from light fuel oil, (●) Light fuel oil production, (●) Natural gas venting, (●) Heat from heavy fuel oil, (●) Transport of petroleum.

The main difference between the two processes (Figure II.30) pertains to the higher energy consumption observed in the pre-treatment, reaction, and purification units (Table II.6 and Table II.7). Moreover, the incorporation of biomass into the Dominican Republic's energy mix has a beneficial impact on this category. Although biomass contains nitrogen, which is transformed into NO_x during combustion, the amount emitted is significantly lower compared to other fuels. Overall, it constitutes less than 2% of the impact.

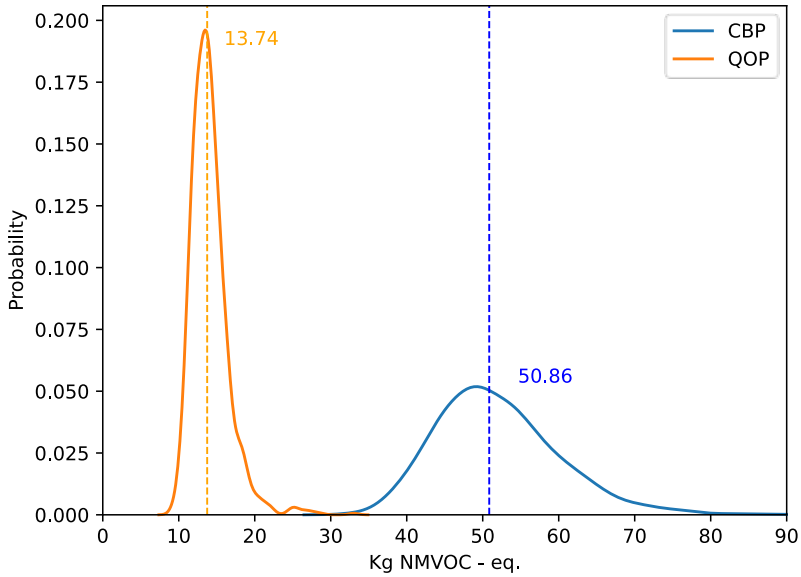

Figure II.30. Probabilistic distribution of the impacts of QOP and CBP on photochemical oxidants formation.

II.3. Final remarks

Furfural production processes are considered harmful to the environment for two reasons. Their high energy consumption and their use of large quantities of acid [82]. The discharge of acidic wastes into the environment can be a significant environmental concern, particularly given the lack of robust environmental legislation in the past. This has led to numerous companies failing to treat their effluents before discharging them. Nevertheless, this is unexpected to be the case in the future. In contrast, the issue of acid use presents a far more challenging problem to address. As previously outlined in Section 1.3.3, the presence of large quantities of acid in the reactor forces to change the usual configuration for preventing corrosion, which in turn limits the effectiveness of heating. Despite the high dilution of sulphuric acid, jacketed heating is unfeasible due to the reinforced reactor walls, imposed to counteract premature wear. This necessitates the injection of steam directly into the reactor to elevate the temperature of the mixture through the latent heat released by the condensing fluid. This approach is highly inefficient, as it implies a significant dilution of the mixture, which increases the size of all process units and forces the use of vast quantities of steam. This is undoubtedly the most critical point identified in the environmental profiling of the QOP and CBP. Consequently, this represents the most pertinent aspect for enhancing furfural production in future technological developments.

The latter serves to address one of the limitations of the simulation detailed at the beginning of this chapter. This limitation is that the design of the column internals was not carried out. In practice, the absence of a condenser in the column is compensated for by a narrowing of the upper plates, as illustrated in Figure 1.19. In light of the aforementioned results, it can be concluded that the critical point of both processes is the reactor. In other words, enhancing the column design would not result in a significant divergence of the conclusions, particularly in the QOP.

Some processes, such as Suprayield (see Section 1.3.3), propose ingenious solutions to this problem, which make it possible to achieve yields of 100% of the theoretical maximum. It is anticipated that steam consumption will be reduced in this instance, as the process does not involve continuous injection. In contrast, the reactor is pressurised on a single occasion, and the product is released into the gas phase in a controlled manner. The process was significantly scaled up in the late 2000s. An initial pilot plant was built in South Africa and subsequently scaled to commercial size by the Proserpine Cooperative Sugar Mill in Queensland, Australia (2009). However, to the best

of our knowledge, the furfural line in this plant is either not used or has a negligible commercial impact.

Other potential solutions involve modifying the solvent used. This may entail a reduction in the quantity of sulphuric acid utilised in the reactor, or its utilisation as a co-solvent with other compounds that mitigate corrosion-related issues. This case is presented in Chapter III of this doctoral thesis, in which gamma-valerolactone is employed as the principal solvent.

It has been observed that the generation of heating steam is the most significant factor influencing both processes. The generation of this energy vector is strongly dependent on the combustion of fossil fuels. These are the dominant energy sources in the two geographical areas under consideration, where the majority of the furfural exported to Europe is produced. The production and combustion of coal (China) and light fuel oil (Dominican Republic) have a profound impact on all the impact categories evaluated. In the current European Union, only a few countries produce furfural on a commercial scale: Austria, Slovenia and Italy (Table 1.4). The majority of production is displaced to circumvent the aforementioned impacts within their territory. Nevertheless, its consumption is already high and expected to increase (see Section 1.3.2), thus this impact is not eliminated but simply externalised, in addition to the impacts of transport. Should new technological developments reach Europe, it is anticipated that the energy mix used will improve in the coming decades by the objectives of the European Green Deal, as detailed in Section 1.1.2. This chapter demonstrates the pivotal role of energy decarbonisation in the sustainability of these processes.

In addition to the reactor, purification represents a crucial aspect of the CBP process. The rationale for this is analogous to that of the other units: the incorporation of more water to dilute the catalyst necessitates a larger equipment size. In the reactor, the larger the size, the greater the diffusion and mixing problems that must be overcome. Consequently, the quantity of steam required for heating is also increased. Additionally, corn cobs exhibit a lower pentosan content than sugarcane bagasse (Table II.3 and Table II.1). Therefore, to achieve the same functional unit, it is necessary to operate the process for a longer time, increasing energy consumption. The combination of these two factors renders separation in the first distillation column more costly. In addition, the configuration that optimises heat transfer in this column might be less efficient in the case of CBP. The QOP employs a secondary steam generator through which the reaction effluent is circulated. This process involves partial condensation, whereby this stream cedes its latent heat to a

water inlet to vaporize it. The resulting steam is then compressed and used as a stripping and heating agent in the column (Figure II.4). In the CBP, the gas-phase reactor product exchanges heat directly within the reboiler of the same column (Figure II.13). As illustrated in Table II.4, the energy savings are lower in the second model. However, it is not possible to ascertain whether this increase in consumption is related to the layout of the processing units. It is likely that the observed increase in consumption is solely attributable to the dilution and biomass effects. Consequently, it would be advisable to study both configurations in future technological developments.

This configuration is, however, mandatory in the CBP. The stripping steam, given the mass flowing upwards and downwards the column, is unable to raise the temperature of the mixture to the desired value. Moreover, even with the configuration in use, this column requires a significant additional supply of medium-pressure steam to operate (Table II.4). Furthermore, the injection of stripping steam would result in a further dilution of the mixture. This would result in the furfural at the top of the distillation column being below the azeotropic point (Figure III.3). Consequently, to achieve the desired performance, it would be necessary to recirculate a larger proportion of the aqueous stream from the decanter back to the column.

It has been demonstrated that the quantity of initial dilution water is of paramount importance, beyond the acid strength influence. Both processes are modelled using the same kinetics (see Section 3.1.3), the same compounds (in different ratios), and the same reactions. Furthermore, the kinetics account for protons present in the medium as a result of the dissociation of sulfuric acid. Finally, the ratio of H^+ to dry biomass at the inlet is maintained at a constant level in both models. In essence, the sole differentiating factor is the degree of acid dilution. A comparison of the data from the literature [75] with that from the CBP and QOP indicates that the acid used in the QOP is four times more concentrated than in the CBP. This is one of the most crucial aspects identified, as it severely penalises the environmental performance of the Chinese batch process. Therefore, it is a key insight for future developments.

As previously stated, the utilisation of different types of biomass has significant implications on the furfural yield, as the process is constrained by the presence of pentosans in the feedstock. The overall yield of both technologies is low, with a significant proportion of the biomass consumed being discarded as waste. In addition, this waste is acidic in nature, which implies the need to treat it before disposal, increasing the economic cost. In

turn, environmental impacts might significantly increase if the treatment is avoided. If a starting biomass with 30 wt% of arabinoxylans is assumed, stoichiometry indicates that the theoretical maximum furfural that can be obtained is 72%, which equates to 21.6% of the starting biomass. Due to operational limitations, the theoretical yield is constrained to a maximum of approximately 50%. This implies that, in the optimal scenario, only 10% of the biomass can be utilised, with the remaining 90% being discarded. This severely constrains the processes and directly contravenes the intended sustainable development objectives. The aforementioned Suprayield process has the capacity to significantly enhance furfural yield, potentially reaching 100% of the theoretical maximum. Nevertheless, even with this considerable enhancement, 80% of the raw material would be discarded. The technological concept proposed in Chapter III of this thesis has the potential to overcome this limitation.

The utilisation of agricultural or forestry residues instead of biomass confers several advantages. One of the key benefits of this approach is that it does not compete with food products, which is one of the reasons why this work focuses on lignocellulosic refineries (see Section 1.2). Additionally, utilising waste materials represents a means of reintroducing them into the production chain, thereby supporting the circular bioeconomy (see 1.1.2.I). Moreover, the findings of this study indicate that land use is significantly reduced. This has implications for a lower CO_2 release due to land use changes, which is of particular interest in agricultural plantations, as they tend to cover large areas. This impact is typically associated with bioprocesses, and it can be reduced with this solution. On the other hand, the distribution of impacts with the rest of the co-products from which this "residue" is obtained also takes most of the benefits from CO_2 sequestration during biomass growth. The database model employed (APOS) allocates a portion of the credits for absorbed CO_2 to the SCB or corn cobs in each case. Nevertheless, it is justifiable to utilise alternative models, such as the cut-off model, where the residue is introduced at no environmental cost. This would result in the produced furfural not receiving any credit for biogenic carbon, regardless of the observed time frame. In this study, the influence of biogenic carbon sequestration has been considered, although it is negligible in comparison with the CO_2 emitted by steam consumption.

One distinction between the two processes is that in CBP, a methanol stream is recovered as a by-product. The credits that the process receives for methanol production are indistinguishable in the overall impacts. This compound represents an output of less than 2% of the biomass used. To rule

out the potential impact of methodological choices, a sensitivity analysis was conducted using the substitution method. A comparison of the two methods reveals that the results are almost identical, as this compound plays a minor role in the overall system. A further iteration of this operation was conducted in both processes to investigate the potential impact of acetic acid recovery in the first column. Even in the absence of further purification of acetic acid, the outcome remains largely unaffected by its inclusion as a by-product. In the case of CBP, the recovery is equivalent to 1.2 wt% of the output at the bottom of the first column, while in QOP it is 0.6 wt%. Once more, in comparison to the input biomass, this output is insignificant, and therefore its effects are similarly inconsequential.

The impact of in-plant wastewater treatment may vary depending on the indicator under consideration. The introduction of pollutants into the process is partially mitigated by the treatment of the effluent before its discharge into the environment. Nevertheless, in this study, an anaerobic digestion process analogous to the conventional municipal water treatment process has been considered. A more rigorous modelling of this process would likely result in a slightly lower benefit, due to the high acidity of the wastewater. Furthermore, the solid fraction is typically filtered and neutralised prior to disposal in a controlled landfill. This would result in increased impacts on land use and energy consumption due to the necessity of additional processes for sludge handling and transport. It is therefore necessary to exercise caution when interpreting these results and to further develop these calculations in future work.

A further method for reducing the uncertainty in these data would be to replace inputs from literature with inputs from industries. In this thesis, all ranges obtained from literature sources have been subjected to a sensitivity analysis in a simulation environment. The rationale behind this approach is the assumption that the more optimal the operating point is, the more representative of reality it will be. However, the available data are somewhat generic and may not be representative of the latest developments in this industry, despite the reactor being quite constrained for the reasons previously stated. The availability of anonymised data from a range of companies would help to significantly improve the reliability of the results reported in this chapter.

CHAPTER III:
LIFE CYCLE ASSESSMENT AND SUPPLY CHAIN OPTIMISATION OF A NOVEL PROCESS FOR FURFURAL PRODUCTION.

Chapter II describes processes that generate a significant amount of waste compared to the amount of products produced. This is mainly because only the C5 sugar fraction contained in the hemicellulose is utilised, while both cellulose and lignin are partially degraded, resulting in a inefficient utilisation. The introduction of the circular bioeconomy (1.1.2.I) and biorefineries (1.2.1) has made this approach increasingly unattractive. Using all the plant inputs is essential for optimising resource consumption and minimising waste.

This section examines the effects of furfural production using an organosolv process based on gamma-valerolactone (GVL). Section 1.2.2.II provides an overview of the benefits of this process, including the ability to operate under a wider range of conditions while keeping all products solubilised in the reaction medium. Furthermore, even under high pressure and temperature conditions, the structure and properties of these products remain largely unchanged. This makes purification easier and enables the recovery of commercial-grade cellulose and lignin along with the furfural. This Chapter presents the process in detail, including data on its design in Aspen. The techno-economic and environmental evaluations of the process are then discussed, comparing the LCA data with the conventional processes previously described. Finally, the feasibility of installing a fractionation plant in Spain to produce furfural using this new technology is evaluated by using a multicriteria approach. Additionally, the optimal configuration of the supply chain of the plant was assessed attending to economic and environmental criteria.

III.1. Background and process design

The plant considered as a case study in this chapter is based on the process described by Alonso et al. [63]. This technology has generated significant interest, leading to the constitution of a public-private consortium (FRACTION project, funded by Bio Based Industries Joint Undertaking) to test it at a TRL (technology readiness level) below 5. The presented data are the result of experimental tests carried out by the different partners involved (Spanish National Research Council, CSIC) and scaled up by the company Process Design Center (PDC) [248] and Rey Juan Carlos University (URJC).

Figure III.1 shows the Process Flow Diagram (PFD) of the plant being studied. The scheme is relatively intricate, and therefore the following provides an overview of the plant's operational sequence. The purpose of the plant is to separate the three fractions of biomass with a high purity. In this way, their recovery is carried out separately, maximising the use of the biomass. The feedstock used is eucalyptus. The initial composition of the eucalyptus is presented in Table III.1, as reported by the CSIC. The moisture content measured is 6.33 wt%.

Table III.1. Composition of the Eucalyptus globulus used as a raw material for the fractionation plant. Source: CSIC.

Component	wt% on dry basis
Glucan (C6, cellulose)	44.53%
Galactan (C6, hemicellulose)	2.00%
Mannan (C6, hemicellulose)	0.91%
Xylan (C5, hemicellulose)	16.49%
Arabinan (C5, hemicellulose)	0.68%
Acetic Acid	5.43%
Extractives	0.43%
Lignin	26.80%
Ash	0.44%

The biomass is fed directly into the reactor (R1-A + R1-B), while the GVL, water and sulphuric acid streams are mixed and preheated in the mixer M1 and the heater E1, respectively. The GVL:H_2O mass ratio is 70:30, with the addition of a mass of water equal to the mass of biomass entering through stream S7. This is possible due to the solubility of GVL in water at any concentration. This also allows the wet wood chips to be introduced into the reactor, thus avoiding the previous drying process. The acid (H_2SO_4) concentration is 0.1M. The reaction is carried out at a low temperature (130˚C) and pressure (3 bar) for 1 hour. At this point the cellulose, hemicellulose and

lignin fractions are isolated. The cellulose remains as a solid and is continuously separated at the outlet using a decanter centrifugal filter (F1). Due to high solids loading, the outlet is resuspended with a solution of recovered GVL and then subjected to a second filtration process (F2), after which the cellulose is countercurrent-washed (W1-W4) to recover the entrained GVL. The moisture content of the cellulose following the second filtration is 60%. The solvent at the outlet of this filter is collected (M8) with the remaining solvent recovered downstream and sent to a flash tank (EV6). Here, the excess water is evaporated, and the GVL is returned to the process head. The GVL is relatively expensive (circa 2500 €/tonne). Consequently, the plant has been designed and optimised for its recovery, with a rate of over 99% in the final plant concept.

On the other hand, the liquid fraction at the outlet of F1 is resuspended in water. Lignin is highly soluble in GVL, which enables the fractionation reactor to operate at high solids loadings. Thus, lignin is simply recovered by adding water, which is used as an antisolvent to allow its precipitation (water/GVL mass ratio = 8). Water is added to the mixture in M4 and lignin precipitates in vessel V1 at 50˚C, after which it is recovered at >99% purity in decanter F5. The recovered lignin is subjected to backwashing (W5-W6) to recover the impregnated GVL, which is subsequently transferred to the recovery unit REC1. The remaining fraction, rich in C5 sugars, is dehydrated in the multi-effect evaporator (MEE) system to remove the excess water resulting from lignin precipitation. Lignin precipitation involves the additional feeding of water in quantities ranging between 450 and 500 tonne/h. This entails an increase in the equipment size and energy consumption. The maximum allowable temperature of this evaporator is 100˚C. The resulting vapour is rich in GVL and is therefore recovered and sent to the REC1 section.

The selection of the MEE as the equipment to concentrate the C5-rich stream is related to the GVL-water equilibrium. At the exit of the precipitator, the concentration of GVL in water is slightly higher than 10 wt.%. Therefore, it is in a region very close to the pinch between the two phases (Figure III.2). Separation at this point makes the operation very difficult, which can result in a significant increase in energy and economic costs. The configuration comprises the partial evaporation of the mixture in contact with a heating vapour in a first effect (EV1). The liquid fraction is then conveyed to a second effect, where the pressure is slightly lower and the stream is again vaporised, this time in contact with the vapour resulting from the head of the first effect. This process is repeated successively, maintaining the vacuum in the final evaporator (EV4), after which the product is completely condensed (E4).

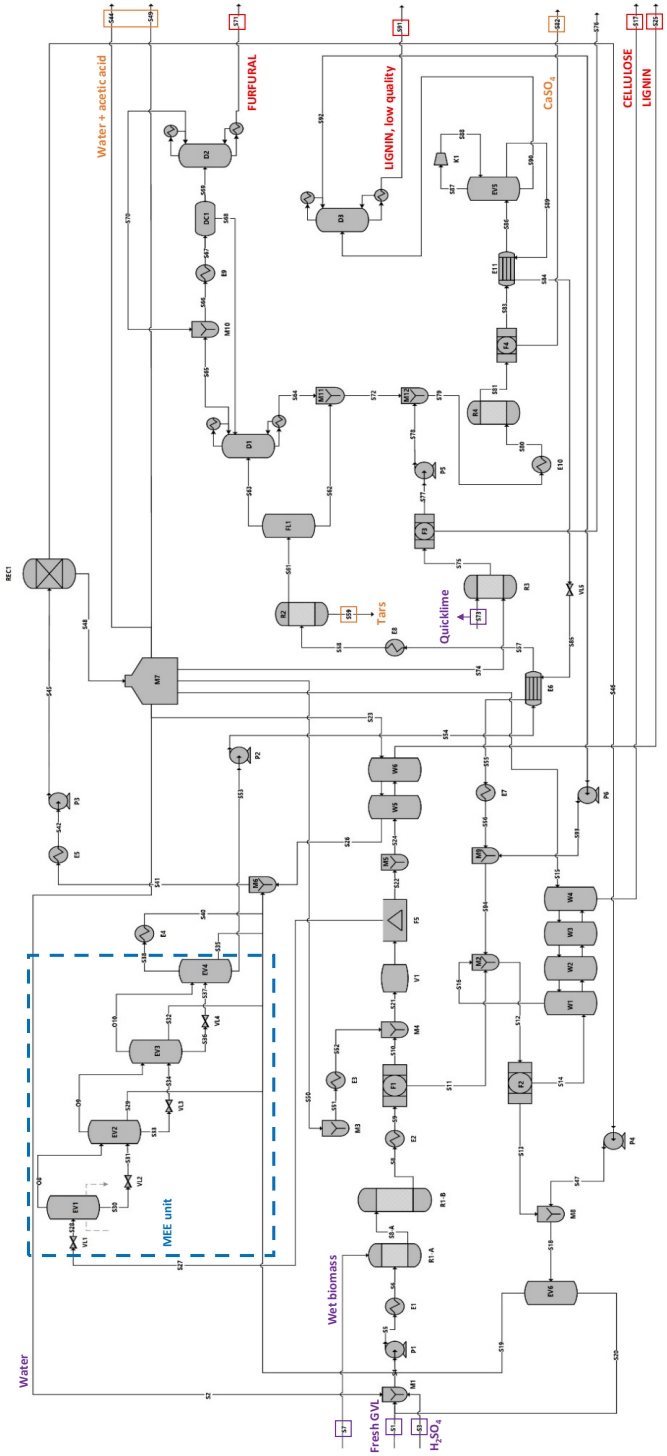

Figure III.1. PFD of the organosolv fractionation plant.

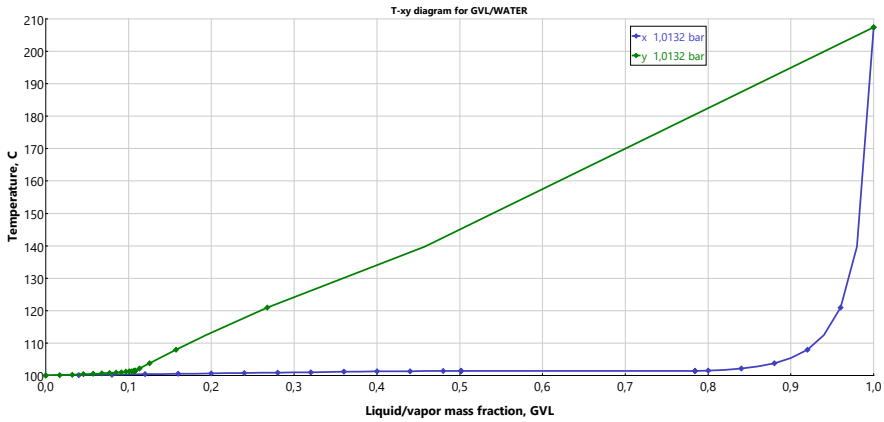

Figure III.2. T-xy diagram for GVL/water mixture at P = 1 atm. Predicted by Aspen Plus using NRTL model (see 3.1).

The concentration of sugars is increased from ~1% to over 10% by weight, resulting in a GVL:H_2O mass ratio of 4:1 to reach optimal conditions for furfural obtention. This C5-rich stream is conditioned to meet the operating conditions in reactor R2, which are 21 bar and 225°C. Under these conditions, the conversion reaches 100%, with a yield of 72% to furfural, i.e. the theoretical maximum (see Section 1.3.1). The remaining xyloses and arabinose (28%) are converted to degradation compounds (humins), which remain dissolved in the mixture due to the presence of GVL. The C6 sugars present are 75% converted to HMF (5-hydroxymethyl furfural), humins and levulinic and formic acids under the reaction conditions. This is because the reaction conditions are more severe than in conventional processes, where cellulose is only partially degraded to glucose, with the other products of the reaction cascade being much less abundant. These conditions can be achieved without the corrosion problems due to the presence of GVL. The fractionation reactor receives a significantly more dilute sulphuric acid input than in the conventional process, due to the high flow rate of GVL and water, which prevents this problem from occurring. Furthermore, the residence time within the reactor is only 30 seconds. While the performances considered in the furfural reactor do not account for diffusional effects at the reactor scale-up and other deviations, the yields are based on scientific evidence demonstrated by CSIC.

The outlet stream of the furfural reactor is depressurised (FL1) to 1.2 bar before introduction into the first distillation column (D1) to enhance the separation efficiency. In essence, the purification process is carried out analogous to conventional cases (see 1.3.3), although the presence of GVL

introduces some specific conditions that are explained below. The concentration of furfural at the reactor outlet is 6 wt% with respect to GVL, water and heavy compounds. However, the concentration of furfural in water is 22 wt%. The problem is that furfural forms an azeotrope with water at a mass concentration of 33% (Figure III.3). Consequently, if the concentration is below this value, the furfural cannot be further concentrated relative to water by distillation. It is therefore necessary to increase the concentration at the head of the column to 33 wt% for a molar recovery above 99.5% furfural. In essence, this requires removing approximately 50% of the water entering the distillation column.

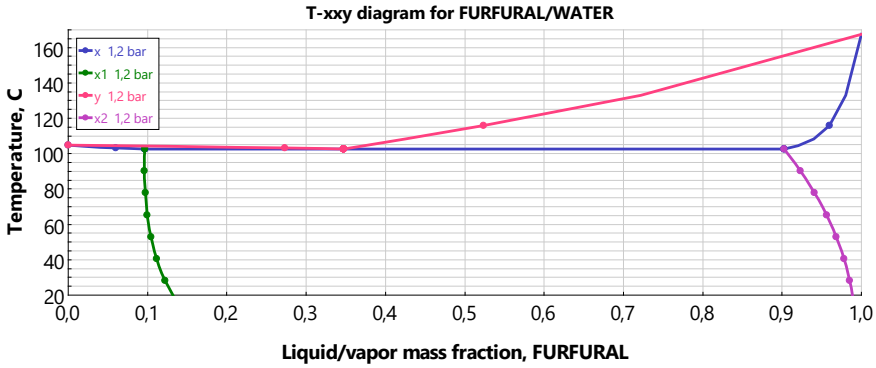

Figure III.3 T-xxy diagram for furfural / water mixture at 1.2 bar (D1 operating pressure). Predicted by Aspen Plus using NRTL model (see 3.1).

An additional objective of having a considerable flow of condensed water in a downward direction is to create a liquid phase stream within the column that entrains the GVL ascending vapour. Mass transfer phenomena cause the GVL in the gas phase to enrich the recirculated water in which it is soluble at any concentration. The recovery of the solvent is of paramount importance to the economic viability of this process, as discussed below. Consequently, an additional requirement of this column is the separation of as much GVL as possible. To enhance this recovery, the internal reflux ratio is increased to a factor of eight. This implies that for every mole of distillate, eight moles of condensate are recirculated to the column. The greater the downward flow of water, the more GVL is entrained. This results in a 99.5 mol% GVL recovery at the bottom of the column (Figure III.4). However, it significantly increases the energy consumption well above the business-as-usual processes. The rest of the fractionation steps operate as in state-of-the-art technologies (see 1.3.3).

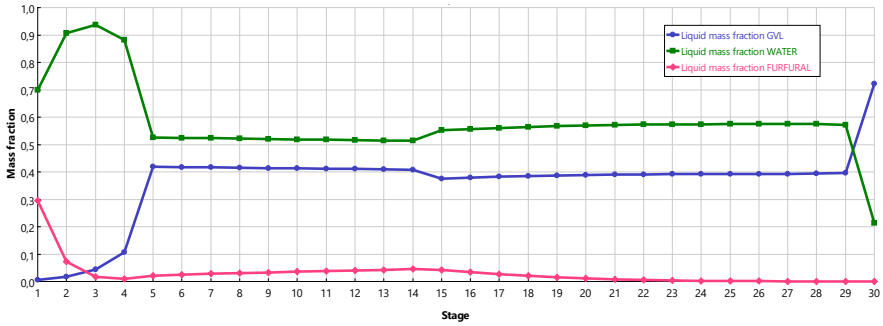

Figure III.4. Composition profile of furfural distillation column (D1). Predicted by Aspen Plus using NRTL model (see 3.1).

The bottom streams of FL1 and D1 are mixed and contacted with calcium oxide to neutralise the remaining sulphuric acid (H_2SO_4). This sulphuric present in the mixture must be neutralised before concentrating the GVL in subsequent stages. Otherwise, the H_2SO_4 would also increase its concentration, resulting in corrosion problems. The input to the neutraliser is quicklime milled, which is contacted with water at the inlet to form $Ca(OH)_2$ with a 97% molar yield (R3). The unreacted quicklime is discharged into the F5 filter, while the $Ca(OH)_2$ is sent to the M12 mixer. The entire mixture is then conditioned, and neutralisation occurs in tank R4. The calcium sulphates produced are removed in a centrifugal filter (F4), while the resulting stream is fed to a mechanical vapour recompression-type evaporator (MVR, EV5). This equipment recompresses the exhaust vapour to increase its pressure and temperature. The steam is reintroduced into the EV5 so that it is used as heating steam, significantly reducing energy costs. In this evaporator, 94% of the GVL contained in the S86 stream is recovered and sent back to the M2 mixer used to resuspend the cellulose after filtration in the F1 unit. The remaining fraction is fed to the distillation column D3, resulting in a nearly pure GVL stream per head that is recirculated upstream. The bottom stream contains mainly lignin with a lower purity. This lignin is valuable depending on the intended application, and thus it is recovered separately.

The GVL recovery unit (REC1) is designed to extract as much GVL as possible from the multi-effect evaporator (MEE) vapour outlet. The vapours from the MEE are enriched in GVL (approximately 36 tonne/h), which, due to its price, needs to be recycled back into the process. However, this GVL is highly diluted (approximately 6-7 wt%). This unit is in the process of being patented by PDC, so further details are omitted. In the same line, for reasons of know-how sensitive to the plant concept, details about sizing and certain specific configurations are also not provided. However, all calculations

for the economic balance and LCA consider the inputs and outputs from this unit.

III.2. Techno-economic evaluation

The economic balance of the process is derived from the data provided by PDC. In this thesis, the balance sheet is used to estimate the minimum selling price of the cellulose, which is essential information for Section 6.4. The principal findings and underlying assumptions of the cost estimation are presented below, although the specifics of this balance are beyond the scope of this work.

The capacity of the plant is 25 tonnes per hour of dry biomass, with an operating time of 8000 hours per year. On this basis, costs are calculated considering equipment sizing, to which items are subsequently added as described in [249]. First, direct and indirect costs are calculated for each process unit. Indirect costs include concepts such as insurance, equipment transport, taxes or engineering contracts. To all of these costs, 15% is added for equipment not considered, such as pumps or conveyors. To this total, 30% is added for contingencies and 3% for fees. The contingency figure is that high due to the novelty of the design and the absence of any industrial-scale testing, which increases the associated risk. Furthermore, the costs are augmented by an additional 3% for the purchase of the land for the plant, 5% for the site development, 4% for the construction of auxiliary buildings (control rooms, warehouses, etc.) and 50% for off-site facilities. These facilities include the generation of utilities and everything associated with them (cooling towers, water or fuel storage, electrical substations, etc.), additional equipment (furniture, fire extinguishers, etc.), and packaging and distribution costs.

Finally, to this amount is added the additional cost per start-up (2%) due to lower productivity and higher financing needs. A further 15% is added for working capital, which includes items such as exceptional invoices or advance payments. This ultimately results in a capital investment as illustrated in Table III.2.

The main product is cellulose. Consequently, the strategy for achieving cost compensation is to establish an estimated selling price for furfural and lignin, based on conventional market rates. With these prices in place, the costs of the plant's inputs, and the fixed costs detailed in Table III.2, can be balanced to determine a minimum selling price of cellulose that ensures net profit.

Table III.2. Capital Investment (CAPEX) of a fractionation plant at a capacity of 25 tonne/h of dry eucalyptus chips.

Concept	Unit	Value
Heat exchangers	K€	15755
Process vessels		20677
Pressure equipment		2087
Drives		165
Separators		8804
Mixers		981
Unlisted equipment		7271
Total	M€	55.7
Contingency	K€	16722
Engineering		4144
Construction		4144
Automation + control systems		3315
Contractor's Fee		1672
Total	M€	85.7
Land cost	K€	1653
Site development		2756
Auxiliary buildings		2205
Off-site facilities		27557
Total	M€	119.9
Startup expenses	K€	2398
Working capital		17986
Total investment (CAPEX)	**M€**	**140.3**

Table III.3 presents the inputs and outputs of the plant, along with the market price of the former and the selling price of the latter. These values are multiplied by the mass flow rate of each compound to obtain the cost/benefit of each total stream.

Table III.3. Utilities, raw materials, and co-products material flows and cost/benefit estimations. MPS: medium-pressure steam; HPS: high-pressure steam; C-Water: cooling water; WWT: wastewater treatment; lignin, lq: low-quality lignin.

Input	Duty	Unit	Price	Unit	M€/y
Utilities					
MPS	157.98	ton/h	18.74	€/ton	23.69
HPS	77.46		14		8.96
C-Water	7205.05		0.06		3.46
Electricity	0.48	MW	200	€/MWh	0.76
WWT	22.13	ton/h	15	€/ton	2.66
Total					39.53
Raw Materials					
GVL	579.2	Kg/h	2500	€/ton	11.58
H_2SO_4	980		40		0.31
Eucalyptus	25000		40		6.50
Quicklime	573.25		250		1.15
GVL recovery					3.30
Total					22.84
Co-products					
Lignin	4604	Kg/h	425	€/ton	15.65
Lignin, lq	2037		127.5		2.08
Furfural	1707		1450		19.80
Total					37.53

The most critical costs arise from the high consumption of medium-pressure steam in various units: MEE, MVR, D1 column and E1 heater. On the other hand, GVL represents half of the raw material consumption costs, although the plant only supplies 0.7 wt.% as fresh solvent.

Table III.4 is constructed from these data. The minimum selling price of the cellulose is estimated for a given production rate (calculated in Aspen at 10.60 tonne/h). With the average cost of conventional cellulose at around €900/tonne, the potential reduction would be around €246/tonne, i.e. a 27% deduction.

Table III.4. Annual manufacturing expenses and calculated minimum selling price (MSC) of cellulose.

	Unit	Price
Direct expenses		
Raw materials	M€	22.8
Co-products & waste streams	M€	-37.5
Operating labour	M€	1.9
Supervisory	M€	0.3
Utilities	M€	39.5
Maintenance and repairs	M€	9.6
Operating supplies	M€	1.4
Laboratory charges	M€	0.3
Patents and royalties	M€	0.9
Total	M€	39.2
Indirect expenses		
Overhead, packaging & storage	M€	3.5
Local taxes	M€	2.4
Insurance	M€	1.2
Total	M€	7.1
General expenses		
Administrative costs	M€	0.9
Research and development	M€	4.7
Total	M€	5.6
Depreciation	M€	4
Total annual costs	M€	55.9
Plant capacity	kton/y	85.5
MSC Cellulose	**€/ton**	**654.12**

III.3. LCA of the fractionation process

The life cycle analysis of the process was conducted by the methodology described in 3.2. The information in that section is further elaborated below. For this purpose, all model choices, assumptions and limitations are discussed following the usual life cycle analysis framework.

I. Definition of objectives, scope and system boundaries

The objective of the study is twofold. Firstly, to identify each hotspot, in order to ascertain the causes and potential solutions. Secondly, to compare the impact over each environmental category against the conventional process to determine whether there has been an improvement or a deterioration. The functional unit is defined as the delivery at the factory gate of 1 tonne of furfural at 99% purity. The scope is defined as cradle-to-gate. All processes related to the plant are modelled as part of the foreground system, while all inputs supplied to the plant are included as part of the background system. The Ecoinvent v3.9 database was employed for this purpose. The APOS (at the point of substitution) version was used to ensure that the entire value chain of the auxiliary elements was captured in the study.

II. Life Cycle Inventory

The input/output inventory is summarised in Table III.3. As previously stated, most of the data utilised for the construction of the inventory is derived from primary sources (data provided by CSIC). However, there are exceptions to this, such as the areas of the plant designated for conditioning and purification (e.g. conditioning of the mixture, or distillation of furfural). In these cases, the data was sourced from the available literature, which was used as a starting point for the development of the plant concept to the configuration shown in the previous section and depicted in Figure III.1. This model was adapted as part of this work to ensure comparability with the simulations discussed in Chapter II. The adaptation primarily involved the convergence in the definition of compounds, the thermodynamic model, and binary interactions. This was validated by analysing the equilibrium diagrams of the critical components of the system (water, furfural, GVL, carboxylic acids, and sulphuric acid), to ensure that the model assumptions did not result in modifications to the input/output inventory calculated.

Although fresh GVL is introduced to the plant due to losses and purges, the income needed is significantly low as compared to the total GVL

consumed by the plant (99.3 wt.% recycled). Thus, the impact of this makeup can be considered negligible by applying a simple cut-off in inputs by mass.

The approach followed in this study is attributional. This requires the definition of system boundaries and the allocation of impacts between the different outputs of the plant. Any decision in this regard leads to a potentially significant variation of the results. Therefore, the allocation of plant impacts has been modelled following the recommendations described in Chapter I of this thesis. The method of subdividing the system has been selected according to the aforementioned hierarchy. This subdivision has been carried out in two parts. Firstly, the process units attributable to each of the products have been identified to be able to isolate their inputs and outputs. The result of this treatment is shown in Figure III.5. The diagram is divided into 10 blocks, plus one block not shown for the inclusion of the plant's wastewater treatment. The specifics of these blocks are outlined below, except those pertaining to furfural production, which are detailed separately. The process units common to all three products are denoted by the letter S (for 'Shared'). Similarly, the equipment attributable to each product is named according to the initial letter of the product (i.e. C stands for cellulose, L for lignin, F for furfural, and LF for shared blocks between lignin and furfural).

- **S1**: mixture and conditioning of the solvent (GVL, water, and sulfuric acid). Only the consumption related to conditioning is included here: electricity for pumping, and steam consumption for preheating the mixture. Solvent inputs are considered at the point of use, i.e. the reactor.
- **S2**: fractionation reactor, including the input of the solvent and the biomass.
- **S3**: this section concerns the recovery of GVL. It includes the REC1 retriever, whose data is currently protected. It also includes all units used for GVL recovery in other areas of the plant, such as after the second cellulose centrifugation or the treatment of the FL1 flash and the first furfural distillation (D1) bottom streams.
- **S4**: wastewater treatment unit (outside the battery limits of the plant).
- **C**: second cellulose filter and subsequent backwashing. The first filter is considered common equipment (S2) as it is used to separate the three components.

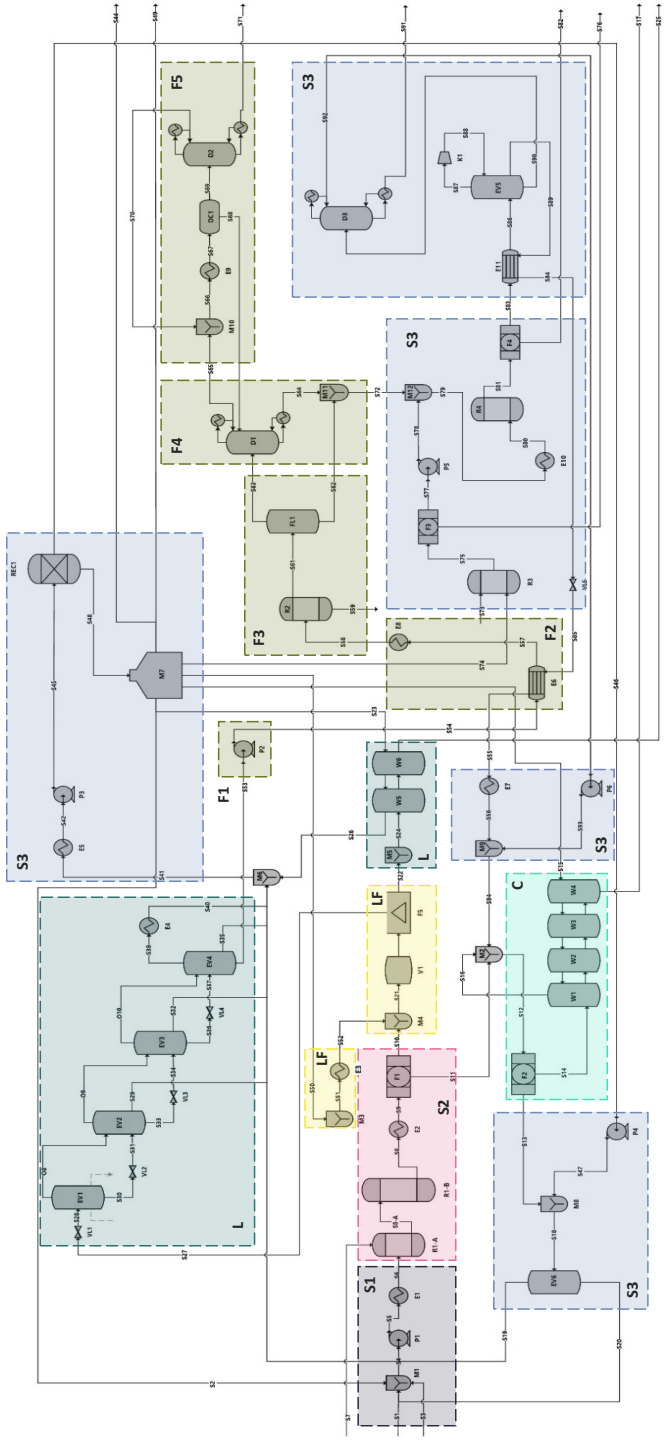

Figure III.5. Fractionation plant PFD subdivided for LCA calculations.

- **LF**: equipment common to the treatment of the lignin and hemicellulose fraction.
- **L**: the section assigned to lignin includes washing and subsequent evaporation of the added water for precipitation. In fact, the fraction that is concentrated in the MEE unit is the hemicellulose fraction. The rationale for attributing this evaporation to lignin is that, in reality, all the water that is evaporated is added solely to obtain lignin. If lignin was not to be recovered, the stream exiting the F1 centrifuge could be conditioned directly for entry into the furfural production reactor (R2) without the necessity of further concentrating the sugars.

Hereafter, all blocks displayed in green are associated with furfural and are attributed to this product. The objective of their segregation is to disaggregate the impacts of its production for identification of the critical areas.

- **F1**: pumping and preheating of the C5 sugars-rich stream.
- **F2**: furfural reactor.
- **F3**: first distillation column.
- **F4**: second distillation column. The impacts of the two distillation towers are considered separately, given the significant differences in utility consumption between the two.

In the case of the common areas, a subdivision based on input rather than output was applied. This decision was taken to ensure a fair distribution of impacts across all units. The absence of any weighting implies a penalty for products with the lowest output, here considered as by-products, which is not representative of the mass and economic balances (0.33 allocation factor for each product). At the other extreme, the distribution based on mass allocation greatly favours these products, unrealistically distorting the material balances (e.g.: 0.07 allocation factor to furfural). Conversely, basing the distribution on economic weights is not particularly rigorous given the inherent uncertainties in the commercial price of lignin, as well as being inconsistent with the material balances (see Chapter I). Therefore, the alternative of distributing the weights according to biomass composition was chosen. It is assumed that only the cellulosic fraction of the biomass input is used for cellulose production, the lignin fraction for lignin production, and the hemicellulose fraction for furfural production. Therefore, taking into account the composition of eucalyptus in Table III.1, 50% of the impacts on the common units would be attributed to cellulose, 20% to furfural, and 30% to lignin. This would be tantamount to

considering three reactors instead of one, which would entail a subdivision of the system in accordance with that applied in the rest of the plant.

III. Life Cycle Impact Assessment

The calculation methodology employed is the Environmental Footprint 3.1 at the midpoint level. To account for the effect of biogenic carbon emissions and emissions due to land use change, these are reported separately. The observed time scope is 100 years for the indicators considering the carbon flows. Consequently, the data provided as a baseline assumes that this carbon remains sequestered in the products during this time. The Chinese batch process (CBP) is selected for benchmarking given its higher global market penetration (82% of revenue share, as detailed in Chapter II).

The average energy mix in Europe is represented in Table III.5. These data have been extracted from the Ecoinvent database. The energy mix for China utilised in the construction of the CBP is available in Table II.5.

Table III.5. Average energy mix considered for heat production in Europe (RER).

	RER energy mix
Natural Gas	60%
Coke	0.5%
Hard Coal	9%
Heavy Fuel Oil	7%
Light Fuel Oil	7%
Propane	2%
Refinery gases	11%
Coal tar	0.5%
Wood chips	1%
Electricity	2%

IV. Interpretation, limitations, and assumptions

The data used to build the models representing the fractionation plant are derived from experimentation. Scaling is conducted to obtain inventories comparable to industrial processes assuming a linear relation, which may result in deviations from reality (e.g., unconsidered material transport effects, heat losses, etc.). This is addressed by considering the uncertainty of both the foreground and background systems. For the inputs in the foreground system, a lognormal distribution based on the Pedigree matrix was considered. To propagate this uncertainty through the calculations, a Monte Carlo sampling was conducted, whereby data was varied at the level of the technosphere, biosphere, and model characterisation factors.

III.3.1. LCA results

Figure III.6 shows the results of the evaluation of each process section for all indicators at midpoint level. In view of this figure, it becomes apparent that the majority of the impacts originate from the first distillation column within the furfural purification train (F3). This is expected based on the explanations in Sections III and 6.2. There are only two categories for which this operation does not present the most significant impacts, global warming potential due to land use, and land use itself. Consequently, both are closely related to biomass consumption. Additionally, the impacts related to the recovery of GVL (S3) also stand out from the other plant sections, followed by the conditioning of the inlet stream to the fractionation reactor. The remaining operations have a significantly lower impact in comparison. The high impact on the three named sections is a consequence of the high heating steam requirements, as will be seen throughout the discussion.

The study objectives include the identification of hotspots and the comparison of the conventional process. Accordingly, the discussion will focus on the impact categories most affected by CBP, as identified in Chapter II (Figure II.17), to ascertain the main differences. The discussion includes or excludes certain indicators depending on their relevance to the conclusions drawn. Consequently, indicators such as land use are discussed in detail, whereas aspects such as terrestrial eutrophication or human toxicity effects are relegated. In any case, all indicators of lesser relevance are assessed together at the end of the section.

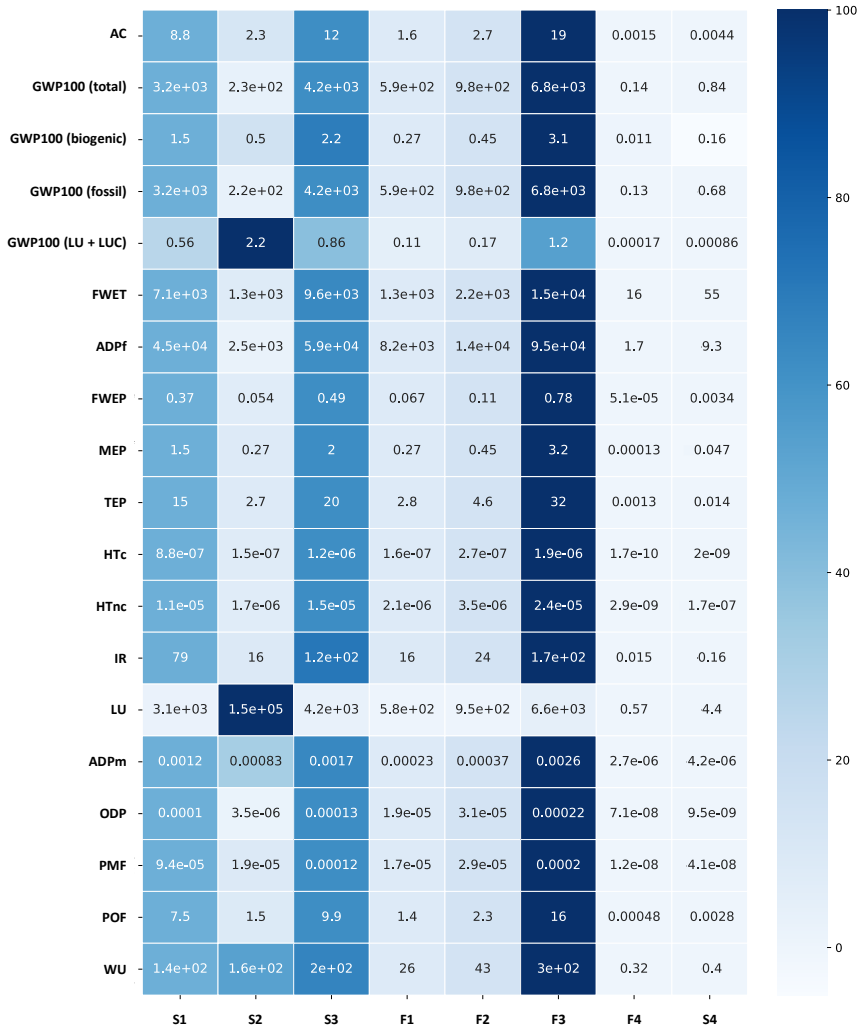

Figure III.6. Overview of the impacts of each section of the fractionation process. AC: Acidification, (mol H^+ eq.); GWP100: Global Warming Potential (kg CO_2 eq.); FWET: Freshwater Ecotoxicity (CTUe); ADPF: Abiotic Depletion Potential, fossil (MJ); FWEP: Freshwater Eutrophication (kg P eq.); MEP: Marine Eutrophication (kg N eq.); TEP: Terrestrial Eutrophication (mol N eq.); HTc: Human Toxicity, cancer effects (CTUh); HTnc: Human Toxicity, non-cancer effects (CTUh); IR: Ionising Radiation (kBq U235 eq.); LU: Land Use (dimensionless); ADPm: Abiotic Depletion Potential, minerals/metals (kg Sb eq.); ODP: Ozone Depletion Potential (kg CFC-11 eq.); PMF: Particulate Matter Formation (disease incidences); POF: Photochemical Ozone Formation (kg NMVOC eq.); WU: Water Use, deprivation (m^3 world eq.).

I. Acidification

Most acidification is attributed to the combustion of fuels with elevated sulphur content. Sulphur contained in coal and oil is released into the atmosphere as sulphur dioxide (SO_2). SO_2 reacts with the water in the atmosphere to form sulphuric acid, promoting acidification effects. Similarly, the emission of nitrogen oxides (NO_x) associated with coal and oil use derives from the formation of nitric acid, which is responsible for nearly 20% of the impact observed in both processes (Figure III.7).

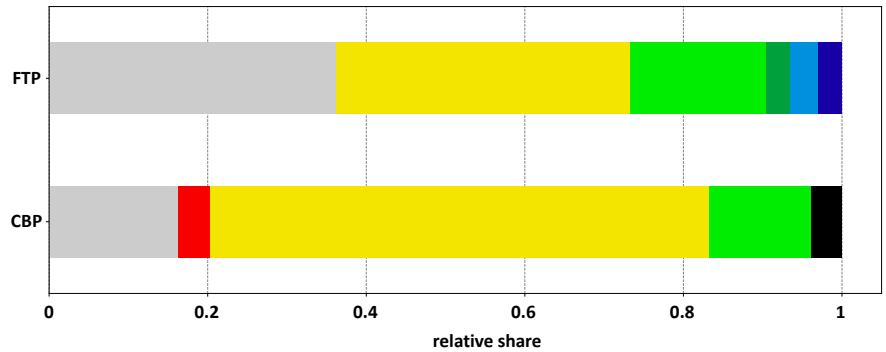

Figure III.7. Relative share of impacts over acidification in FTP and CBP. (●) Rest, (●) Hard coal mine operation and preparation, (●) Heat from hard coal, (●) Heat from heavy fuel oil, (●) Heat from light fuel oil, (●) Heat from natural gas, (●) Natural gas venting at petroleum/natural gas production, (●) Refinery gas combustion at furnace.

Sulphuric acid consumption has a relatively minor impact on the environment in terms of direct effects. As previously demonstrated (see 5.3), corrosion effects force heating the reactor by steam injection in the CBP. In the FTP, the presence of GVL in the medium allows jacket heating, thereby reducing energy consumption to a significant extent (Table II.4 and Table III.3). As most acidification is attributable to the combustion of coal and LFO, the enhanced efficiency of the reactor significantly reduces the impact at this point. H^+ equivalent emissions are reduced from 94 to 3, also as a consequence of the lower proportion of these fuels in the European fuel mix. Conversely, the energy consumption of the first distillation column (D1, Figure III.1) increases from 6 to 22.4 tonne/tonne furfural in the FTP. Consequently, the acidification effects of distillation in both processes are almost identical (Figure III.6 and Table II.7), even though coal and LFO are 56% lower in the European mix.

Overall, FTP significantly improves furfural production in terms of acidification, reducing the current impact by up to 38%, as shown in Figure III.8. As previously stated in Chapter II, the distribution of data observed in

the CBP is mostly attributable to the utilisation of coal. The technology employed exhibits considerable uncertainty in the Chinese energy mix at various stages of its production chain. Consequently, elevated coal consumption results in a heightened uncertainty in the outcomes of this process.

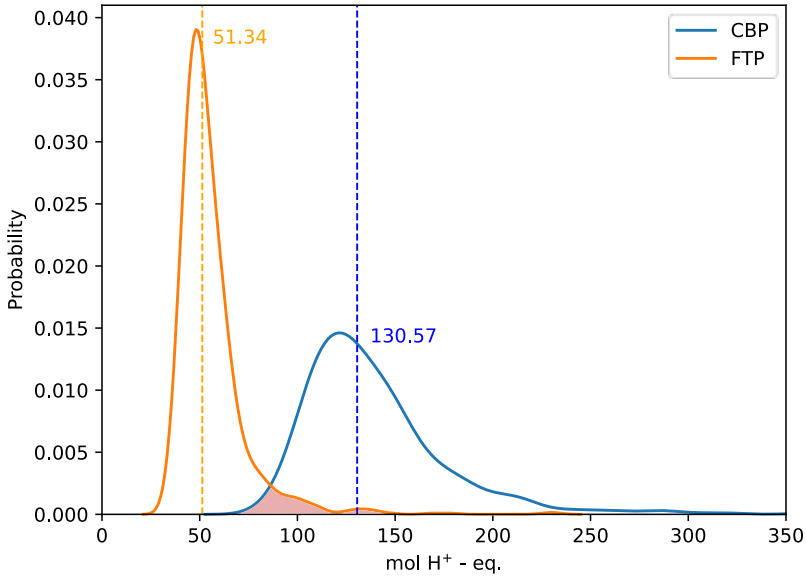

Figure III.8. Probabilistic distribution of the impacts of FTP and CBP on acidification.

II. Climate Change

The effects on climate change are described using the characterisation factors, substances and impact pathways described in the latest report of the Intergovernmental Panel on Climate Change (IPCC) [2]. According to this methodology, the radiative forcing induced in the atmosphere derives mainly from energy production. Given that the European energy mix is heavily reliant on the consumption of natural gas, the most significant impact is related to its combustion (Figure III.9). Emissions are primarily attributable to the energy consumption of producing heating steam. The highest consumption is associated with the first furfural distillation column (D1), which requires 22.5 tonnes of high-pressure steam per tonne of furfural produced.

The quantity of emitted carbon is not affected by considerations of biogenic sources, as the amount is negligible in comparison to fossil CO_2 (Figure III.6). In the case of the conventional processes reviewed in Chapter II, the use of residues resulted in a penalty for CO_2 absorption. In this instance, despite the utilisation of a dedicated forest crop, carbon sequestration is not a

viable means of offsetting the emissions associated with energy consumption. In turn, land occupation is five times higher than for the CBP.

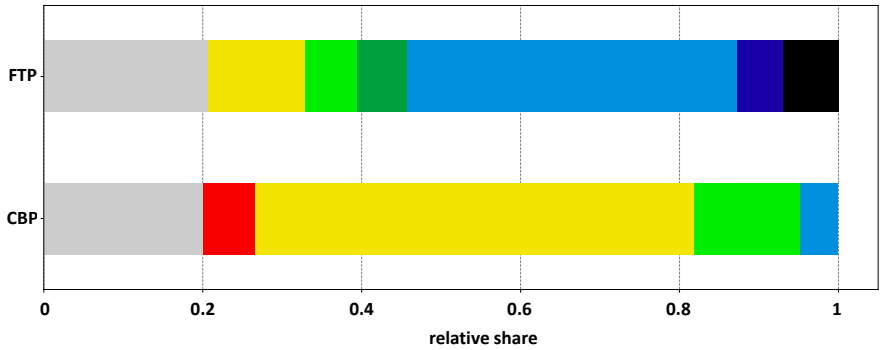

Figure III.9. Relative share of impacts over climate change in FTP and CBP. (●) Rest, (●) Hard coal mine operation and preparation, (●) Heat from hard coal, (●) Heat from heavy fuel oil, (●) Heat from light fuel oil, (●) Heat from natural gas, (●) Natural gas venting at petroleum/natural gas production; (●) Refinery gas combustion at furnace.

Overall, the impact of FTP on climate change is greater than that of CBP (Figure III.10). There are two critical points. First, distillation in FTP leads to 2.5 times higher emissions than the conventional process, due to the GVL recovery requirements. On the other hand, FTP achieves a reduction of more than half of the emissions caused by reactor heating. The emissions avoided and exceeded in each case are close to balance. Given the inherent uncertainties associated with both processes, the probability that the FTP would emit an equal or lesser amount of CO_2 equivalent is very high, as can be inferred from the overlapping in Figure III.10. The discrepancy between these values and those presented in Figure III.6 and Table II.7 is attributed to the fact that the depicted median represents the most probable result within the distribution of potential outcomes, taking into account the uncertainty inherent in the data. This result is typically observed to be slightly shifted to the right, due to the assumption of a lognormal distribution of the inputs.

In any case, although the consumption in the FTP is significantly higher, how the vapour is produced is of crucial importance in determining the emissions. In China, the majority of this mix is derived from coal combustion, while in Europe it is predominantly derived from natural gas. Therefore, it must be noted that the conventional process would be favoured when using the same energy mix. In other words, regional considerations should not mask the operational observations, and FTP has a significantly higher consumption rate of energy.

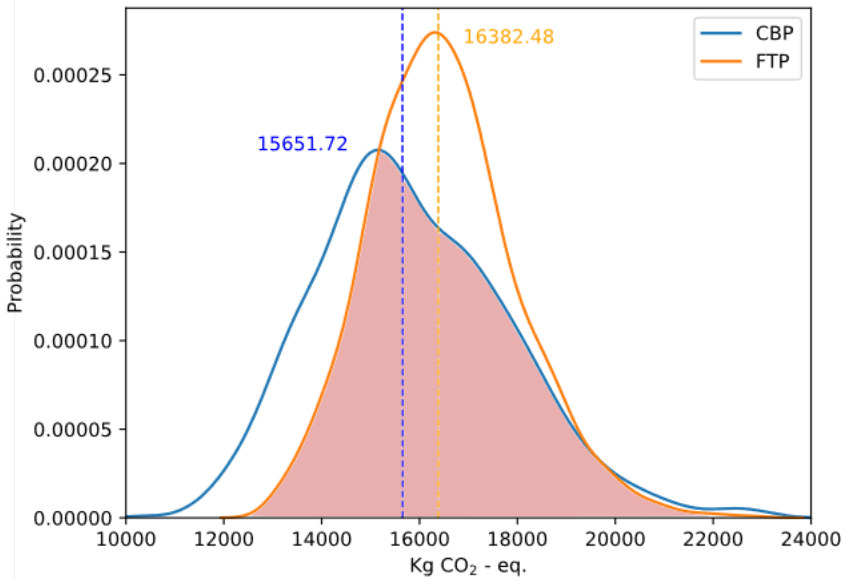

Figure III.10. Probabilistic distribution of the impacts of FTP and CBP on global warming potential.

III. Freshwater Ecotoxicity

The largest impacts on the freshwater toxicity category (FWET) are attributable to the discharge of chlorinated compounds into natural watercourses. High levels of chlorides can harm aquatic life, upsetting the balance of an ecosystem and affecting biodiversity [250]. Most emissions of chlorides are related to oil consumption. While the composition of energy mix in Europe is not heavily based on oil derivatives, refinery gas, light fuel oil, and heavy fuel oil significantly contribute to this category. Oil extraction involves the use of large bodies of water. Water can be either naturally present in geological formations or previously injected to enhance oil extraction by water or steam flooding. Additionally, water from neighbouring formations may also contribute to the produced water that surfaces [251]. These waters dissolve the salts in oil and gas formations, leading to high concentrations of sodium and chloride. Upon extraction, water is partially discharged into the natural environment. These water losses during oil extraction are responsible for nearly 70% of the impact in this category (Figure III.11).

The impact of sodium hypochlorite production is related to the natural gas regasification process. At the time the dataset was created, Europe was receiving a significant supply of liquefied natural gas from Russia. During the regasification process, heat exchangers utilise natural waters as utility. Sodium hypochlorite is frequently employed as a biocide to prevent the proliferation

of organisms which can cause fouling within the heat exchanger. Contact with water results in the loss of some of the hypochlorite, which has the potential to cause ecotoxic effects.

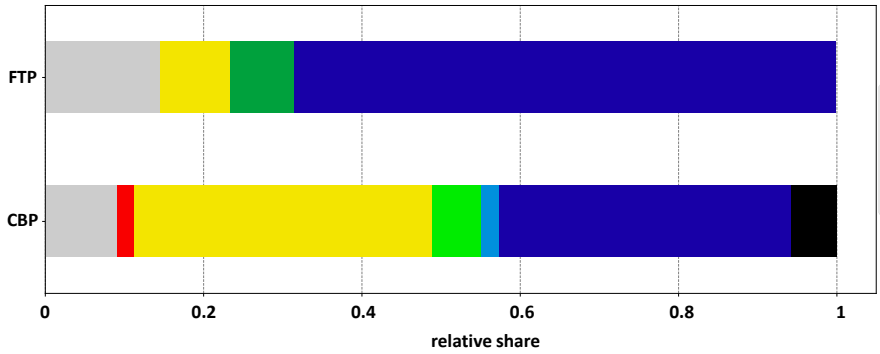

Figure III.11. Relative share of impacts over freshwater ecotoxicity in FTP and CBP. (●) Rest, (●) Blasting, (●) Hard coal mine operation and preparation, (●) Sodium hypochlorite production, (●) Treatment of water discharge from petroleum extraction, onshore, (●) Heat from hard coal, (●) Corn production, (●) Water production, deionised.

The CTUe (Comparative Toxic Unit for Ecosystems) is the unit employed in freshwater ecotoxicity measurements. It represents the estimated Potentially Affected Fraction of species (PAF) integrated over time and volume, per unit mass of a chemical emitted. This provides an estimate of the fraction of species that could potentially be affected. A discrepancy of over 9000 CTUe is observed between the FTP and CBP, indicating that for every kilogram of a specific chemical emitted (principally chlorides), the CBP could potentially affect a significantly larger proportion of species. The main reason is again the energy mix since coal extraction is additionally associated with a significant emission of chlorides.

CBP results have a wider uncertainty (Figure III.12). A global sensitivity analysis (GSA) was conducted to identify the flows that contribute most to this variability. The analysis revealed that the uncertainty in these data is mainly related to emissions of chlorinated compounds during coal extraction. Furthermore, the consumption of pesticides (fipronil) for maize cultivation also has a notable effect on the distribution of the calculated impact.

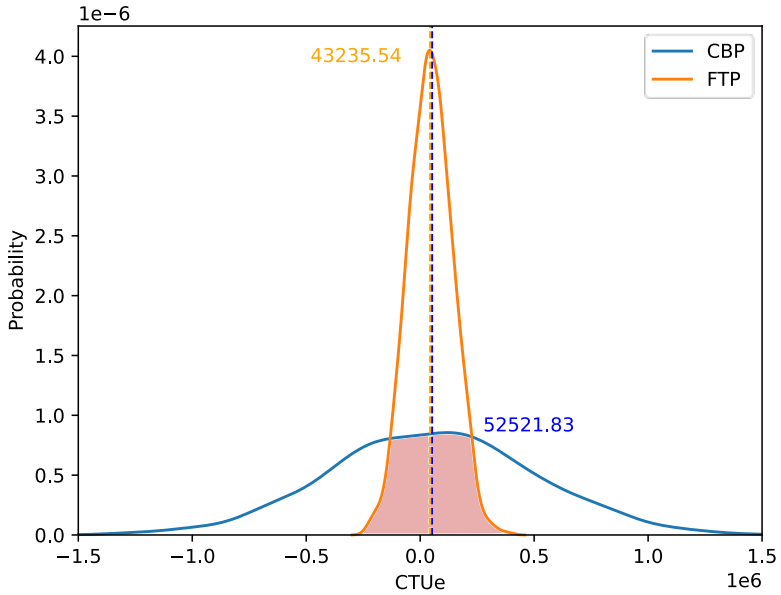

Figure III.12. Probabilistic distribution of the impacts of FTP and CBP on freshwater ecotoxicity.

IV. Abiotic Depletion Potential, fossil consumption

Fossil resources consumption is driven by the same effects as climate change, so relative contributions in Figure III.13 arise from similar sources. The total amount of fuel used is greater in the FTP (Table III.3 and Table II.4). However, the impact on climate change is attenuated (Figure III.10) due to the type of energy used in China, which results in significantly higher greenhouse gas (GHG) emissions. This discrepancy is highlighted in Figure III.14. Uranium consumption relates to the presence of nuclear power within the European mix.

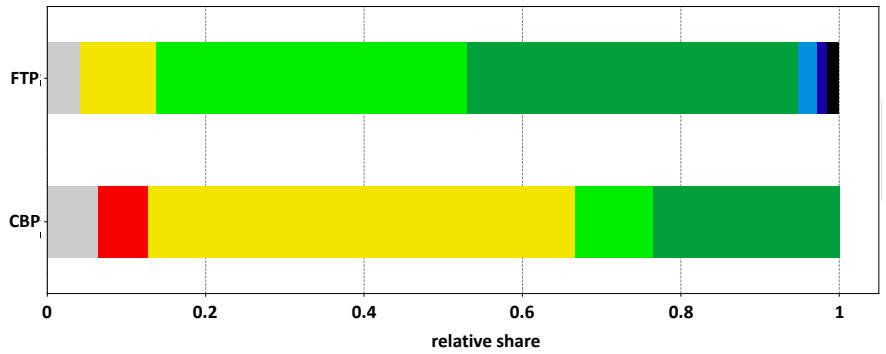

Figure III.13. Relative share of impacts over fossil depletion in FTP and CBP. (●) Rest, (●) Hard coal mine preparation, (●) Hard coal mine operation, (●) Petroleum/gas production, offshore; (●) Petroleum/gas production, onshore; (●) Sweet gas, burned in turbine; (●) Treatment of waste sweet gas, from gas turbine; (●) Uranium mine operation.

Given that the focus is on the consumption of resources rather than the effects of emissions, the variability associated with the exchanges of elementary flows is not as significant. The extraction of a resource is more easily quantifiable than the effects on any environmental compartment of using that resource. Consequently, the distribution shown in Figure III.14 is fairly similar for both processes. As the fuel consumptions are very different, the two trends have little overlap.

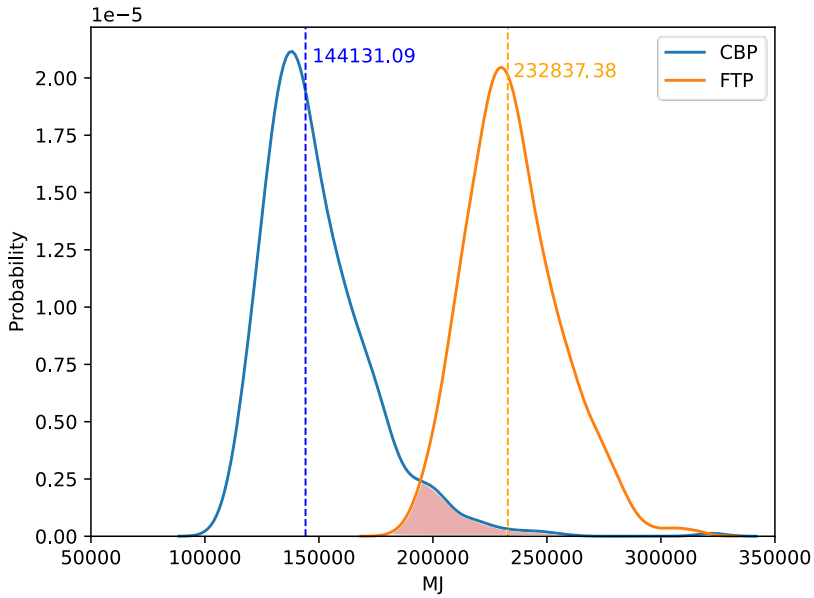

Figure III.14. Probabilistic distribution of the impacts of FTP and CBP on fossils depletion.

V. Marine eutrophication

A comprehensive analysis of NO_x production from coal and oil is presented in Section 5.2.1.V. While these sources do not represent the largest proportion of the European energy mix, the emissions of nitrogen oxides (NO_x) to the atmosphere during the consumption of oil and coal have a significant impact on eutrophication in marine environments, as illustrated in Figure III.15. More than 95% of the marine eutrophication effects relate to the use of fossil fuels to produce heating steam in the FTP. The CBP has a greater impact because the extraction of coal in large quantities leads to the increased emission of NO_x into the atmosphere (Figure III.16). Additionally, the use of corn derives in the discharge of nitrates into freshwater bodies, which eventually reach marine environments. The use of a forest species such as eucalyptus does not entail such a problem, as fertilisation needs are very limited in comparison.

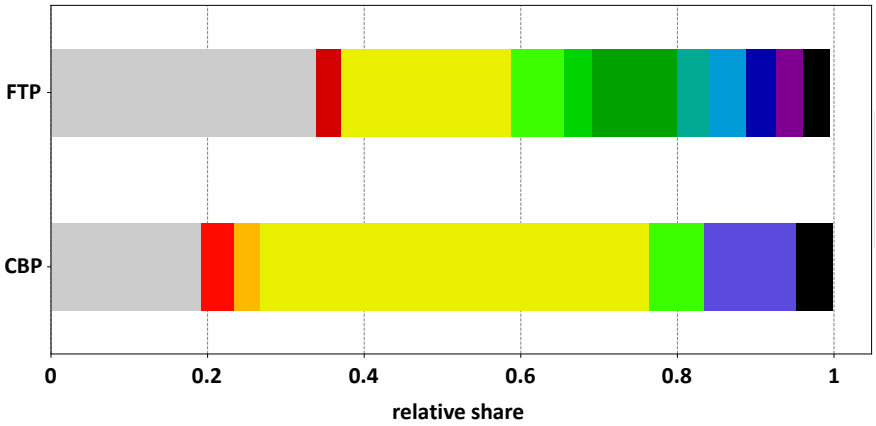

Figure III.15. Relative share of impacts over marine eutrophication in FTP and CBP. (●) Rest, (●) Electricity from hard coal, (●) Heat from coke, (●) Diesel, burned in building machine, (●) Heat from hard coal, (●) Heat from heavy fuel oil, (●) Heat from light fuel oil, (●) Heat from natural gas, (●) Natural gas, burned in turbine, (●) Refinery gas, burned in turbine, (●) Sea transportation of liquefied natural gas, (●) Corn production, (●) Sea transportation of petroleum, (●) Landfilling, of spoil from hard coal mining.

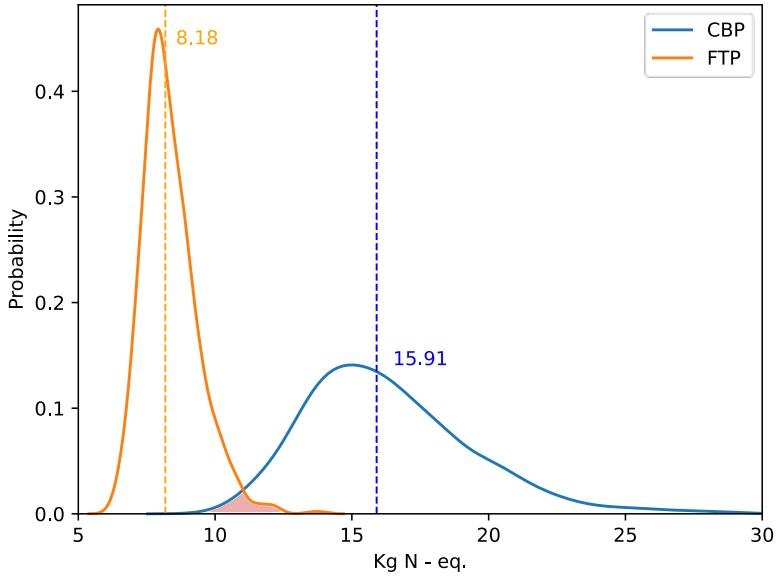

Figure III.16. Probabilistic distribution of the impacts of FTP and CBP on marine eutrophication.

At the inventory level, 15 kilograms of NO_x are emitted into the atmosphere at the FTP for the 29 kilograms emitted at the CBP. These emissions are responsible for more than 90% of eutrophication in marine environments. This aligns with the median values of both distributions shown

in Figure III.16, where the amount of nitrogen equivalent in the CBP is approximately twice as high.

VI. Land use

As expected, most of the land occupation is attributable to the utilisation of biomass. The eucalyptus at the entrance of the plant is modelled in the LCA in two parts. Firstly, forestry practices associated with wood chip production are taken into account using average European data. This involves work such as thinning, felling, amendments, harvesting, transport, etc. The impacts observed in Figure III.17 are directly attributable to these forestry practices. Secondly, in order to adapt the dataset to the real input, the growth of *Eucalyptus globulus* is considered, as it is the most abundant species. A carbon balance is carried out as follows: the carbon to CO_2 ratio is obtained by dividing the molar mass of both elements, from which a factor of 0.27 is obtained. The average carbon content of the eucalyptus is then calculated from data from the Phyllis database [238]. Finally, the carbon content is multiplied by the CO_2/C ratio to obtain the value of tonnes of CO_2 fixed by the eucalyptus during its growth. This value is 137.5 kg CO_2/tonne eucalyptus. The offset of the CO_2 absorbed during the eucalyptus growth is negligible, as discussed in III.3.1.II.

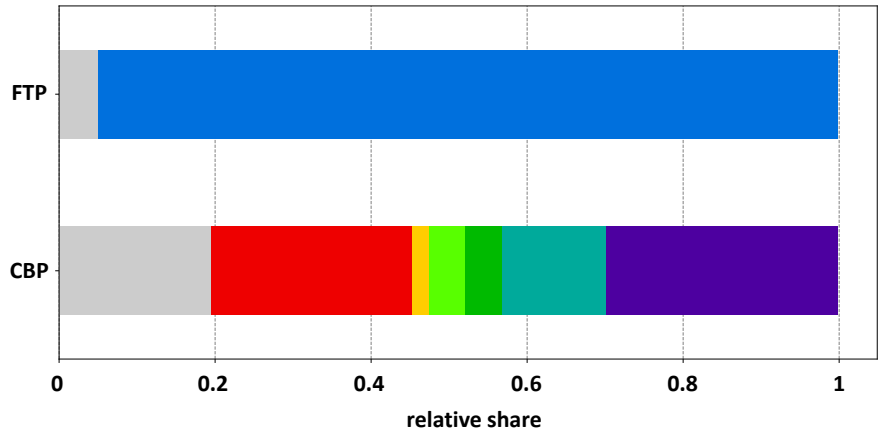

Figure III.17. Relative share of impacts over marine eutrophication in FTP and CBP. (●) Rest, (●) Wood chips, (●) Hard coal mine operation, (●) Manure for fertilization, (●) Hard coal mine infrastructure, (●) Petroleum onshore field infrastructure, (●) Sawlog and veneer log, hardwood, (●) Corn production.

When compared to the impact of the conventional process, the impacts of FTP are substantially higher. Forests typically exhibit a larger biomass density per hectare than most agricultural crops due to the vertical structure of forests. It is estimated that more than half of the global forest loss

is due to the conversion of forest into cropland. Consequently, agricultural crops occupy a greater land area than forests. However, the allocation of impacts at the plant inlet (in the CBP, cobs are allocated with a 0.1 factor based on mass) significantly reduces the land occupied by maize crops. The land requirement for facilities is considerably lower., although the conventional process, coal mining also has a substantial impact.

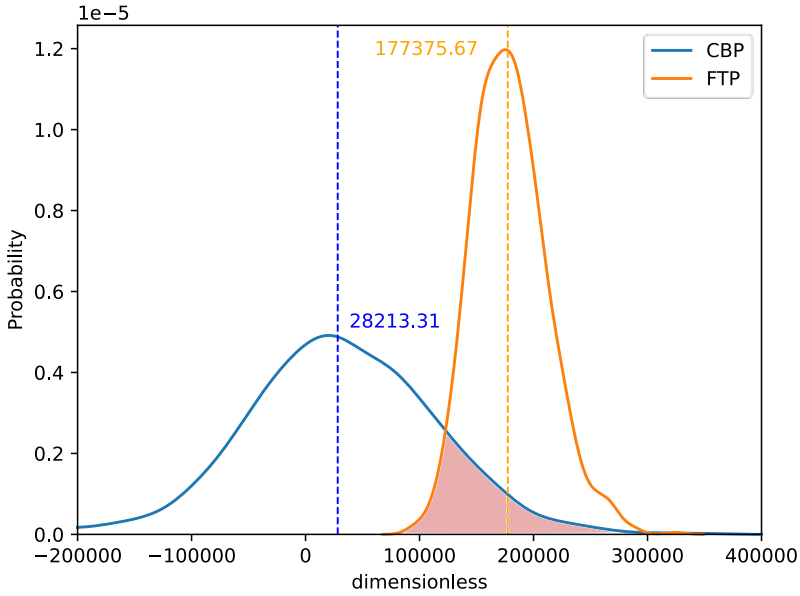

Figure III.18. Probabilistic distribution of the impacts of FTP and CBP on land use.

VII. Particulate matter formation

As previously discussed in 5.2.1.VIII, the combustion of coal and LFO for steam generation represents the primary source of emissions of particulate matter smaller than 2.5 microns (PM2.5). At FTP, despite using less coal and LFO, burning these fuels accounts for almost 80% of the particulate matter emissions (Figure III.19). As illustrated in Figure III.6, most of these particles are emitted to fulfil the requirements of the distillation column (D1, Figure III.1), followed by the GVL recovery units (S3, Figure III.5), and to a lesser extent the pre-treatment (S1, Figure III.5).

It is noteworthy that electricity generation is also contingent on fuel combustion downstream. In Figure III.19, (●) illustrates the generation of electricity from coal, which accounts for approximately 3% of the impact. It is noteworthy that the production of sulphuric acid results in a relatively small quantity of SO_2 emissions. These emissions represent 2% of the disease

incidences caused by the emission of particulate matter in the process. Although this is a very low amount, with a more decarbonised energy mix, this contribution would be more visible in Figure III.19.

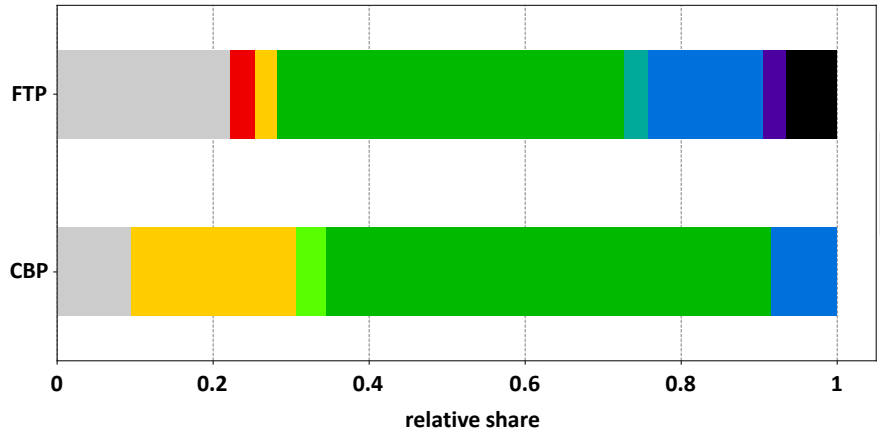

Figure III.19. Relative share of impacts over fossil depletion in FTP and CBP. (●) Rest, (●) Electricity from hard coal, (●) Diesel, burned in building machine, (●) Heat from coke, (●) Heat from hard coal, (●) Heat from wood chips, (●) Heat from heavy fuel oil, (●) Refinery gas production, (●) Refinery gas, burned in furnace.

It is also remarkable that the biomass consumed contributes to this category at two levels. On the one hand, the combustion of biomass to produce heating steam results in the production of fly ash. These account for approximately 3% of the impact. Furthermore, the consumption of eucalyptus as a feedstock accounts for approximately 1.5% of the impact. Nevertheless, this contribution is attributed to emissions from the trucks used for the transportation of harvested biomass from the harvesting areas to the plants for treatment.

The effects of these emissions are measured in "disease incidences". This means that the potential impact of a process is quantified in terms of the number of disease incidences it could potentially cause. This is based on the understanding that particulate matter can have significant health impacts, including respiratory diseases. Figure III.20 shows that CBP can potentially cause 0.001 more incidences than FTP. This means that for each tonne of furfural produced, there is a potential to cause 0.001 more instances of disease due to the particulate matter emissions. The largest uncertainty in the data in the CBP is related to the use of coal for the reasons discussed in previous sections.

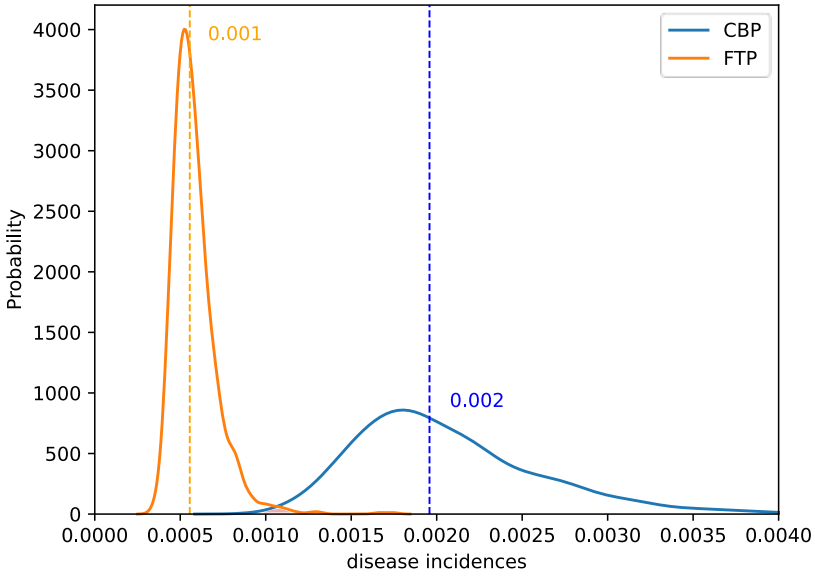

Figure III.20. Probabilistic distribution of the impacts of FTP and CBP on particulate matter emissions.

VIII. Photochemical oxidants formation

The quantification of oxidant emissions is measured in terms of volatile organic compounds other than methane (kg of NMVOC equivalents). Throughout the production phase of the natural gas utilized for heating, a fraction of the gas is liberated into the atmosphere through venting (see 5.2.1.IX). This release constitutes the principal effect on this environmental category (Figure III.21). NO_x liberated upon consumption of other fossil fuels also account for a significant proportion of the impact, with coal being the major source.

As for the blasting and coking processes observed in the CBP, a short explanation is provided hereafter. In the context of mining or construction, blasting is the process of using explosives to break down rock or other hard materials. On the other hand, coking is a procedure where coal is heated in an oxygen-free environment to produce a high-carbon substance called coke, which is used as fuel in various industries. Both the blasting and coking processes involve conditions of high temperature that can release gases such as NO_x and SO_2. These substances, when they interact with oxygen in the air, can form oxidants, contributing to this category as shown in Figure III.21.

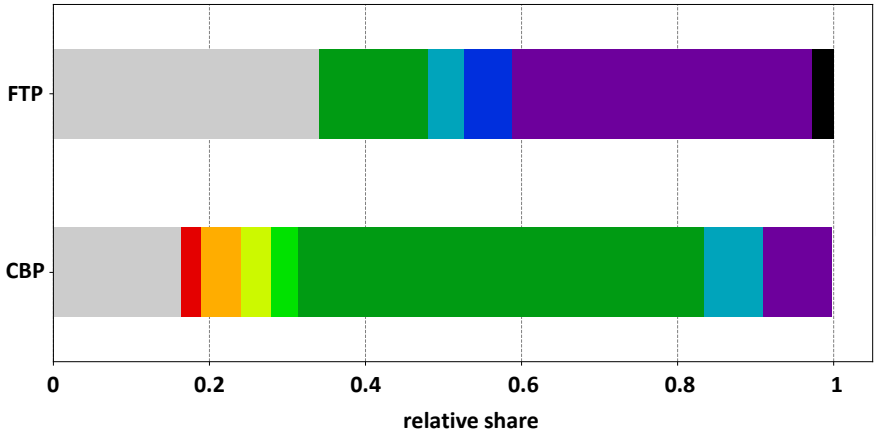

Figure III.21. Relative share of impacts over photochemical oxidants formation in FTP and CBP. (●) Rest, (●) Blasting, (●) Coking, (●) Electricity from hard coal, (●) Heat from coke, (●) Heat from hard coal, (●) Heat from heavy fuel oil; (●) Heat from natural gas, (●) Natural gas venting, from petroleum/natural gas extraction, (●) Refinery gas, burned in furnace.

For the conventional process, this impact is more pronounced due to the elevated nitrogen oxides and sulphur dioxide emissions, which are related to coal extraction and combustion (Figure III.22).

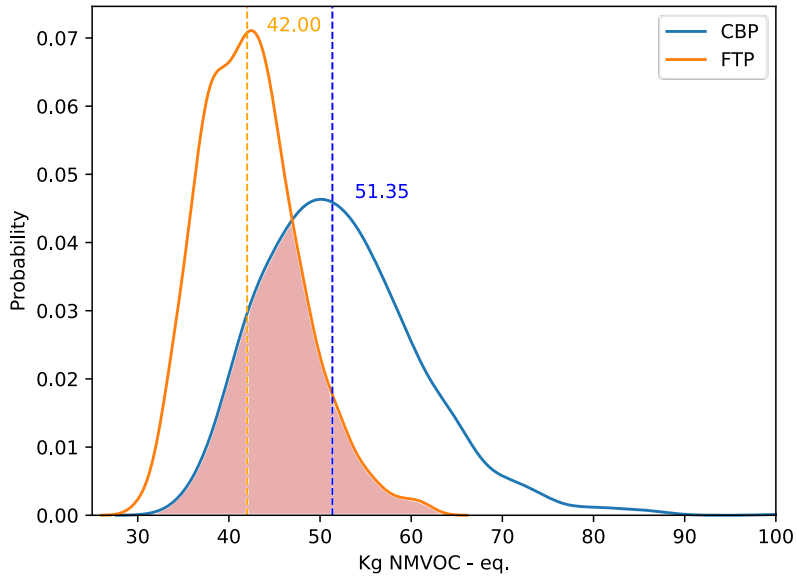

Figure III.22. Probabilistic distribution of the impacts of FTP and CBP on photochemical oxidants formation.

The high energy consumption and the influence of natural gas venting, result in a very close correlation between the two results. Consequently, the

overlapping of both trends renders it challenging to assert the decrease in this impact through the implantation of FTP.

IX. Other categories

A comprehensive review has been conducted on the most significant impact categories linked to furfural production via FTP. An exhaustive comparison has been made with the globally dominant Chinese batch process. This section compares other environmental categories from the EF3.1 methodology, which exert a minor influence on the overall impacts of the fractionation process. This structure is intended to avoid redundancies, provide a thorough overview of the studied environmental compartments, and ensure no important information is left out. Finally, a summary of the impact score on all the environmental categories assessed for both processes is provided (Figure III.23).

- Eutrophication effects

Eutrophication is a process that occurs when a water body receives an excessive input of nutrients, mainly nitrogen (N) and phosphorus (P), which can trigger a series of adverse effects on the ecosystem. In relative terms, hard coal use is responsible for just over 56% of the FTP impact on this category, due to phosphate emissions to groundwater and wet deposited NO_x. In this case, the spoils from the mining of coal have a moderate impact on eutrophication in freshwater. Furthermore, a minimal proportion of the European electricity mix is generated by burning this fossil. Phosphate and nitrogen oxides emissions from these mines contribute approximately 20.5% of this amount. Given the high level of dependency on coal extraction, the impact is higher in the case of the conventional Chinese process (Figure III.6 and Table II.7). As for terrestrial eutrophication, nitrogen oxide emissions account for more than 95% of the impacts. The mechanism is analogous to that explained in III.3.1.V and 5.2.1.VI.

- Human toxicity effects

The carcinogenic and non-carcinogenic effects on human health are relatively low. The contribution analysis shown for CBP in Chapter II demonstrated that these effects were negligible compared to the other categories assessed. In the case of FTP, these effects are slightly below. They are mainly related to the emission of metals (lead, arsenic, and mercury) and teratogenic compounds (formaldehyde, benzopyrene) during cocking, combustion of natural gas and coal, and the treatment of waste during energy production. Of these substances, only formaldehyde is emitted to a significant

extent (approximately 72 grams per tonne of furfural). The rest are emitted in much smaller quantities, by several orders of magnitude. The impact on both categories is measured in human toxicity units (CTUh). For FTP and CBP, the values are almost zero. When compared to the conventional process, FTP presents a slight improvement, although the effects on human health remain negligible. The FTP results in carcinogenic effects measured at $4.49 \cdot 10^{-6}$ CTUh and non-carcinogenic effects at $5.75 \cdot 10^{-5}$ CTUh. In contrast, the CBP process shows slightly higher values, with carcinogenic effects at $8.62 \cdot 10^{-6}$ CTUh and non-carcinogenic effects at 0.0001 CTUh.

- Ionising radiation

The generation of heating steam implies a moderate to low consumption of electricity. As the geographical scope considered for heat generation in the plant is Europe, the electricity mix considered in this process is weighted between the different EU-28 countries. Among the most widespread sources, France makes a notable contribution in terms of electricity from nuclear plants. Although the contribution of nuclear power to furfural production in Europe is negligible on a global scale, it accounts for almost 100% of the impact of ionising radiation. This impact comes mainly (circa 50%) from the treatment of tailings, as a by-product from uranium milling. Other significant contributors include the reprocessing of nuclear fuel and reactor operations. Ionising radiation is measured in kBq U235-eq. The main contributors to this measurement are the emissions of radon-222 (280.6 kBq U235-eq) and carbon-14 (129.3 kBq U235-eq), both of which are highly unstable. Their instability leads to high levels of radioactive decay, resulting in a high characterisation factor for this impact category.

As compared to CBP, the presence of nuclear power leads to a fourfold increase in the impacts. It is, however, expected that this would be modified by the use of a more specific energy mix, such as the burning of excess biomass in the plant. Moreover, the consumption of the K1 compressor in the MVR unit (Figure III.1) results in a 5.5-fold increase in electricity consumption compared to the CBP. Overall, the GVL recovery section contributes 3.65% of the total impact due to electricity consumption. Nevertheless, this net consumption is relatively insignificant compared to the net duty during steam generation, which is again the critical point.

- Abiotic depletion potential, minerals and metals

The consumption of minerals and metals in the FTP results in the depletion of 0.0069 kilograms of antimony equivalent per tonne of furfural.

The largest impact is observed in tellurium (Te) depletion, although the flow of this material from the biosphere is $7.43 \cdot 10^{-5}$ kg per tonne of furfural. Consequently, the impact results from a high characterisation factor determined by the limited global Te reserves, which are estimated at 31,000 metric tonnes [252]. This Te is utilised in the anodes for electrolytic copper refining [253]. In the background of the observed model, copper is employed for the production of electricity for the process and the generation of heating steam. The second input is the largest contributor to tellurium consumption, mainly due to the consumption of natural gas and propane. The conventional process is less dependent on these sources, resulting in a lower consumption of copper, which consequently has a reduced impact on this category. Other metals such as silver or gold are also consumed in the production system, but in smaller quantities compared to copper.

- Ozone Depletion Potential

The CFC-11 equivalent emissions resulting from the FTP process are notably higher than those generated by the conventional process. However, in absolute terms, these emissions remain insignificant. Specifically, slightly over 0.0005 kg of this substance is emitted per functional unit. Remarkably, more than 95% of these emissions consist of methane emissions occurring at various levels deep within the natural gas supply chain. This particular source significantly influences the overall impact within this category, thereby accounting for the observed differences between the two processes.

- Water Use

Water consumption is assessed based on the volume that is diverted from reaching the end-user due to its alternative used in the evaluated process. Predominantly, this water, quantified in cubic meters, is utilized at three critical points of the process. Initially, the electricity necessary for generating the steam utilized by the process is derived from the European energy mix. Within this mix, the role of hydropower is substantial. The Alpine region, known as a water-rich environment, is the primary contributor to this source. However, the complex orography of this region presents challenges for water recovery and storage, thereby creating competition with human consumption needs. On the other hand, the manufacture of sulfuric acid exerts a considerable influence on this category. This is attributed to the fact that its production integrates a range of technologies across Europe. Considering these technologies results in substantial direct and indirect water consumption, the latter through electricity usage. Collectively, these factors lead to sulphur accounting for nearly 12% of the water consumed by the process. In comparison to the conventional

process, the impacts are reduced by up to 44%. This is primarily due to the higher water consumption in maize production relative to the cultivation of woody species such as eucalyptus, which has a significantly higher density as a raw material, i.e. more weight in exchange for occupying less area due to its greater height and density. Furthermore, coal mining also contributes significantly to water consumption.

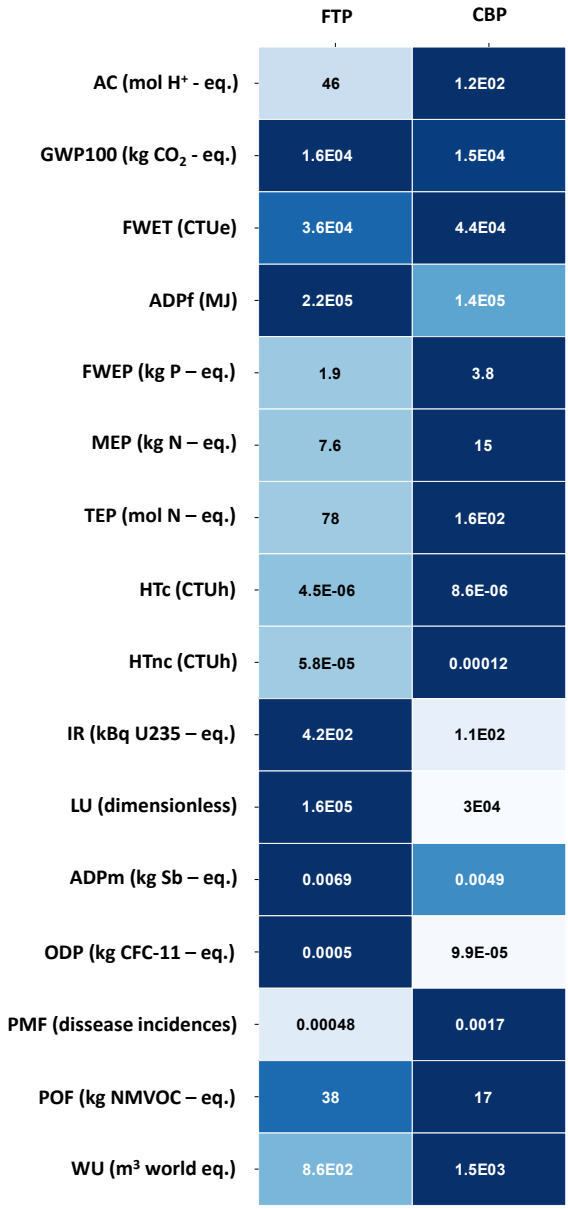

Figure III.23. Impact summary FTP vs CBP.

III.3.2. LCA remarks

In essence, the proposed method has the potential to lessen the environmental impacts in 10 out of the 16 evaluated categories, when compared to the traditional process (Figure III.23). Chapter II elaborates on why 9 out of these 16 categories were significantly harnessed by the Chinese Batch Process. These categories are represented in the Figure II.17.

The proposed technology (FTP) could potentially reduce the impact on seven out of these nine critical categories, marking a 78% improvement in absolute terms. However, there are two categories, namely climate change effects and fossils consumption, where the FTP could have a negative impact compared to the current scenario. These two categories are closely related, since the more fossil resources are utilised, the more carbon is released into the atmosphere. Given the uncertainties in calculating the results of the CBP on climate change effects, it is likely that the proposed method would yield similar or better results. This is primarily because, even though the proposed method consumes more energy, it sources this power from cleaner alternatives, since the European mix is assumed. Still, the consumption of fossil resources remains higher for the FTP, irrespective of the mix considered. The highest consumption occurs in the reboiler of the first distillation column in the furfural purification train (D1, Figure III.1), and the GVL recovery units (S3 sections, Figure III.5).

In particular, the greatest energy requirement of the plant occurs at the REC1 unit for solvent recovery. The environmental cost associated with furfural in this unit is somewhat lower as this is a common process for all three products (cellulose, lignin and furfural), and therefore the impact is allocated in accordance with the principles set out in Section 6.3. This subdivision provides a fair representation of the competitive advantage of FTP due to the higher utilisation of the biomass consumed compared to the conventional process. In CBP, only approximately 10% of the corn cobs utilised are converted into furfural, with the remainder of the biomass being discarded as waste. In the case of FTP, more than 75% of the biomass is transformed into valuable products. In addition, the high heat duty in the distillation column is attributed to the need of maximising the recovery of the GVL. A reduction in the recovery rate would compromise the economic viability of the process, according to the prices shown in Table III.3. Consequently, the economic and environmental objectives of the plant are in conflict.

The current plant design operates at the economic optimum, with no consideration of environmental impacts. In the first design phase, this

configuration has been chosen as it is a first-of-its-kind concept. In other words, the objective is to minimise economic risks in scaling up to favour the market penetration. With this configuration, the environmental impacts of the plant are as high as possible. Further sensitivity analysis is provided at the end of Section 6.4.4, in which the economic and environmental costs of the three products at the exit of FTP are compared with those of conventional products. Future work on the design of the fractionation plant will involve the study of the trade-offs between the economic and environmental functions, aiming at operating within an environmentally safe space and an economically attractive conditions.

In terms of land use, the utilisation of biomass derived from dedicated crops has a far greater impact than the utilisation of agricultural residues. As illustrated in Figure III.23, the land occupation is approximately one order of magnitude greater than that of CBP. Furthermore, the CO_2 absorbed by eucalyptus during its growth is insufficient to offset the emissions generated in the rest of the process. Consequently, residual biomass should be explored in future work.

In conclusion, the production of furfural by the proposed fractionation process described in Section 6.1 represents a clear potential for environmental improvement over the conventional predominant process (Table 1.4). The energy consumption for solvent recovery is very large, representing the main drawback of the process. Additionally, the land occupation associated with the use of biomass represents a second critical point of concern. The plant produces three distinct products, namely furfural, cellulose, and lignin. Consequently, biomass utilization is approximately 75% by weight, so the impact associated with each product is minimised.

The environmental and economic performance of the entire plant, i.e. including sections not related to furfural production, is discussed in Section III.4. This is intended to elucidate the effects of the remaining products and compare them with appropriate benchmarks, thus enabling the feasibility of building and operating a fractionation plant in Spain to be examined.

III.4. Supply chain optimization problem

III.4.1. Problem statement

In this chapter section, the optimization of the supply chain for producing marketable cellulose, furfural, and lignin from eucalyptus in Spain is considered. The objective is to address the following challenges within a three-echelon supply chain:

- to minimize total costs, including those associated with feedstock cultivation, processing, transformation to chemical products, and transportation between nodes;
- and to reduce environmental impacts. To that matter, the ReCiPe2016 methodology is used to focus on environmental endpoints.

Furthermore, for a better interpretation of the results, it is intended to compare the proposed supply chain with a Business-As-Usual (BAU) scenario, evaluating both environmental and economic improvements. The model developed in this work only considers variable costs, excluding fixed costs in transport and plant operation (CAPEX). The key decisions to be made include:

- determining the optimal configuration of processing plants for plant capacity, number, and location;
- identifying suitable locations for feedstock cultivation for farming site, location and capacity;
- and optimizing the movement of biomass and intermediate products for material flows between nodes, including transport means.

Figure III.24 shows the topology of the problem. The products are intended to fulfil the demand in the European markets. The focus is on three eucalyptus species: *Eucalyptus globulus, Eucalyptus nitens,* and *Eucalyptus camadulensis*. Data from the Spanish Fourth National Forestry Inventory (NFI) is used to account for the abundance of these species while accounting for their current uses [254]. Currently applied economic activities are subtracted from the total abundance of each species. Thus, there is no need to further constrain the upper limit defined by this value.

On the other hand, the demand values for the three target products were obtained from trade data in Observatory of Economic Complexity (OEC) database. The demand approximation was calculated as the difference between imports and exports of each product, including only those countries with net imports. This simplification is valid under the assumption that regions with more exports than imports would be able to satisfy their demand internally.

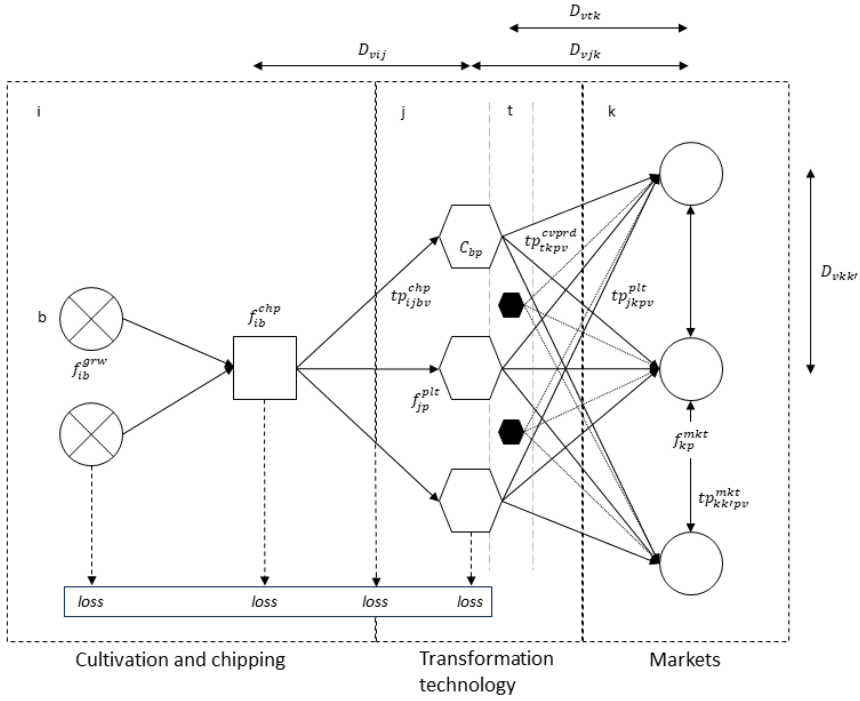

Figure III.24. Supply chain structure for the provision of furfural, cellulose and lignin from Eucalyptus in Spain.

The geographical scope encompasses European markets, including EU-27, European Free Trade Association (EFTA), and Schengen countries. The purpose of this scope is to cover the European territory and adjacent regions with the highest effective trade flows. The model's resolution involves using a slightly different mesh in each echelon. This allows for the collection of raw material abundance data at the provincial level, based on NFI data. Additionally, potential processing plants are considered at the Autonomous Community level for logistical reasons. Finally, the demand is met at the country level. This approach is partly due to the available information and partly because the target decisions are at a strategic rather than operational level.

According to this regional distribution, the Spanish electricity mix is considered for the operation of the fractionation plants. However, due to the lack of specific data, the production of heating steam in the plant is modelled from European average data.

The distance matrix is calculated for each vehicle. For road transport, distances were obtained from Google Maps, assuming the shortest route between capital cities. In the case of rail transport, the distance is assumed to be 20% shorter than for road transport, due to the less tortuous nature of the route [71]. For maritime transport, the tool ports.com was used to calculate the distance between the main ports of each country.

6.4.2. Mathematical formulation

For clarity, parameters are shown in capital letters, while variables appear in lowercase. All the terminology can be consulted in the glossary.

I. Mass balances

The types of biomasses considered are differentiated in set b. The site's (i) maximum capacity to produce biomass b is defined as an upper bound ($\bar{F}_{ib}$). The biomass feeding the supply chain (f_{ib}^{grw}) is constrained by that upper limit as shown in Equation (III.1):

$$f_{ib}^{grw} \leq \bar{F}_{ib}^{bms} \quad \forall i \in I, b \in B \qquad \textit{Eq. (III.1)}$$

Losses of biomass are accounted throughout the supply chain steps. During cultivation stage, a 3% (wt) loss is considered ($LOSS_{ib}^{hrv}$) while the rest of it undergoes chipping (f_{ib}^{hrv}):

$$f_{ib}^{hrv} = f_{ib}^{grw}\left(1 - LOSS_{b}^{hrv}\right) \quad \forall i \in I, b \in B \qquad \textit{Eq. (III.2)}$$

Lost biomass is expected to decay over time, thus leading to the release of the carbon embodied within it (em_{ib}^{lshrv}):

$$em_{ib}^{lshrv} = f_{ib}^{grw} \cdot LOSS_{b}^{hrv} \cdot CC_{ib} \cdot \frac{M^{CO2}}{M^{C}} \quad \forall i \in I, b \in B \qquad \textit{Eq. (III.3)}$$

Where CC_{ib} is the carbon content of the lost biomass b, and $\frac{M^{CO2}}{M^{C}}$ is the ratio between the molecular weights of carbon and carbon dioxide. That allows the translation of the carbon content of the plant to the carbon dioxide emitted during oxidation.

Chipping process is carried onsite. A loss of 5% ($LOSS_{b}^{chp}$) is assumed during this stage as a result of managing practices, constraining the number of chips to be transported (f_{ib}^{chp}). Again, emissions from the decayed biomass (em_{ib}^{lschp}) are accounted in Equation (III.5).

$$f_{ib}^{chp} = f_{ib}^{hrv}\left(1 - LOSS_b^{chp}\right) \quad \forall i \in I, b \in B \qquad \textit{Eq. (III.4)}$$

$$em_{ib}^{lschp} = f_{ib}^{hrv} \cdot LOSS_b^{chp} \cdot CC_{ib} \cdot \frac{M^{CO2}}{M^C} \quad \forall i \in I, b \in B \qquad \textit{Eq. (III.5)}$$

These chips are then conveyed to transformation plants either by lorry, train, or ship. The different types of vehicles are captured in set v.

$$f_{ib}^{chp} = \sum_{v \in V} \sum_{j \in J} tp_{ijbv}^{chp} \quad \forall\, i \in I, b \in B \qquad \textit{Eq. (III.6)}$$

Some routes are not allowed to prevent incoherent transportation routes (e.g.: ship transportation by land):

$$tp_{ijbv}^{chp} = 0 \quad \forall\, b \in B, (i,j,v) \in FR_{i,j,v} \qquad \textit{Eq. (III.7)}$$

Additionally, a 5% loss is considered during transportation ($LOSS^{tp}$). Thus, the amount of chips available at transformation plants ($f_{j,b}^{chpav}$) is expressed as follows:

$$f_{j,b}^{chpav} = \left(1 - LOSS^{tp}\right) \sum_{i \in I} \sum_{v \in V} tp_{ijbv}^{chp} \quad \forall\, j \in J, b \in B \qquad \textit{Eq. (III.8)}$$

$$em_{ijb}^{lstp} = \sum_{v \in V} tp_{ijbv}^{chp} \cdot LOSS^{tp} \cdot CC_{ib} \cdot \frac{M^{CO2}}{M^C} \qquad \textit{Eq. (III.9)}$$
$$\forall\, i \in I, j \in J, b \in B$$

Capacity constraint at plants j must be achieved by defining the parameter CAP_{jb}^{plt}, which accounts for the maximum capacity of the plant j to receive an input of biomass b from the chipping stage. Chips are lumped considering all types of biomasses as shown in Equation (III.10), so maximum capacity is applied as a total.

$$f_j^{chpt} = \sum_{b \in B} f_{j,b}^{chpav} \quad \forall\, j \in J \qquad \textit{Eq. (III.10)}$$

$$f_j^{chpt} \leq CAP_j^{plt} \cdot BAU_j \quad \forall\, j \in J \qquad \textit{Eq. (III.11)}$$

A binary decision variable (BAU_j) is also defined. This variable allows the activation of as many plants as necessary to analyse their impact. The number of plants in operation is defined by the scalar OPPLANTS, as shown in Equation (III.12):

$$\sum_{j \in J} BAU_j \leq OPPLANTS \quad \forall j \in J \qquad \textit{Eq. (III.12)}$$

Product distribution exiting the transformation plants is obtained as the multiplication of the biomass b available as a factory input by the yield to each output p represented in matrix ($CV_{b,p}$):

$$f_{jp}^{plt} = \sum_{b \in B} f_{j,b}^{chpav} \cdot CV_{b,p} \quad \forall j \in J, p \in P \qquad \textit{Eq. (III.13)}$$

The products are finally sent to their respective markets to satisfy the demand in each country. All the products obtained at the factory gate (j) are transported to markets k, as in Eq. (III.14). Distances are calculated in the same way than shown above, although no losses are considered in this step.

$$f_{jp}^{plt} = \sum_{k \in K} \sum_{v \in V} tp_{jkpv}^{prd} \quad \forall j \in J, p \in P \qquad \textit{Eq. (III.14)}$$

Again, only certain routes are allowed to avoid inconsistencies. Eq. (III.16) represents the flow of products p arriving to markets k from plants j.

$$tp_{jkpv}^{prd} = 0 \quad \forall p \in P, (j,k,v) \in FR_{j,k,v} \qquad \textit{Eq. (III.15)}$$

$$f_{kp}^{pmkt} = \sum_{j \in J} \sum_{v \in V} tp_{jkpv}^{prd} \quad \forall k \in K, p \in P \qquad \textit{Eq. (III.16)}$$

Finally, demand is defined by the parameter DD_{kp}^{mkt}, which stands for the demand of each product p in each market k. This demand can be either satisfied by products from plants j (f_{kp}^{pmkt}), or by conventional technologies (f_{kp}^{cvmkt}). Conventional sites t are integrated within the set T and depend on the capacity of these sites to produce each product p ($\bar{F}_{tp}^{cnv}$).

$$\bar{F}_{tp}^{cnv} \geq f_{t,p}^{cvprd} \quad \forall p \in P, t \in T \qquad \textit{Eq. (III.17)}$$

$$f_{tp}^{cvprd} = \sum_{k \in K} \sum_{v \in V} tp_{tkpv}^{cvprd} \quad \forall t \in T, p \in P \qquad \textit{Eq. (III.18)}$$

$$tp_{tkpv}^{cvprd} = 0 \quad \forall (t,k,p,v) \in FR_{t,k,p,v} \qquad \textit{Eq. (III.19)}$$

$$f_{tp}^{cvmkt} = \sum_{k \in K} \sum_{v \in V} tp_{tkpv}^{cvprd} \quad \forall t \in T, p \in P \qquad \textit{Eq. (III.20)}$$

$$f_{kp}^{pmkt} + f_{kp}^{cvmkt} \geq DD_{kp}^{mkt} \quad \forall k \in K, p \in P \qquad \textit{Eq. (III.21)}$$

II. Life cycle costs

Costs are calculated from the unitary cost of each activity. The total cost of the modelled SC includes the growth, harvest, collection and chipping of the biomass, its transportation to production plants, the biomass transformation to products at plants, and the cost of transportation to the final markets from the different production sites.

Biomass cost (co_{ib}^{bms}), [€·y^{-1}]. Price of the biomass is supposed to have already internalised all the costs upstream (seedling, growing, harvesting, etc.). Thus, the cost of purchase is equal to the cost per ton multiplied by the tons acquired.

$$co_{ib}^{bms} = f_{ib}^{hrv} \cdot UC_b^{hrv} \quad \forall i \in I, b \in B \qquad \textit{Eq. (III.22)}$$

Chipping cost (co_{ib}^{chp}), [€·y^{-1}]. Cost of chipping is calculated multiplying the amount of produced chips (f_{ib}^{chp}) by the unitary cost of producing them (UC^{chp}) (i.e.: chipping, collecting, and bundling).

$$co_{ib}^{chp} = f_{ib}^{chp} \cdot UC^{chp} \quad \forall i \in I, b \in B \qquad \textit{Eq. (III.23)}$$

Transport of chips to plants (co_{ijb}^{itp}), [€·y^{-1}]. Transport depends on the distance travelled, the technology used for transportation, and the variable costs, which include costs for fuel, repair, tire, lubrication, and labour. Different locations have different fuel or labour rates [255]. Fixed costs are excluded from the analysis since no temporal considerations are taken into account. Additionally, each transport technology will have different costs, so the total cost will be the sum of all of them.

$$co_{ijbv}^{itp} = \sum_{v \in V} (UC_v^{tp} \cdot D_{vij}^{i})\, tp_{ijbv}^{chp} \quad \forall\, i \in I, j \in J, b \in B \qquad \textit{Eq. (III.24)}$$

Where UC_v^{tp} is the unitary cost in tkm of the use of each vehicle v and D_{vij} is the distance matrix between sites i and j in kilometres.

Transformation plant costs (co_j^{plt}), [€·y^{-1}]. The costs of the plant are derived from the sum of its operating costs (OPEX). OPEX is a function of utilities, raw materials, main product and co-products, waste streams and others like operating labour, supervision, maintenance, royalties, taxes, administrative costs, or deprecation among others. Since it is related to the amount of biomass treated. Thus, costs are referred to ton of chip processed. CAPEX is excluded at this point since temporal dimension is disregarded.

$$co_j^{plt} = \sum_{b \in B} OPEX^{plt} \cdot f_{jb}^{chpav} \quad \forall j \in J \qquad \textit{Eq. (III.25)}$$

The cost is only defined for the production sites (j) and not for each product (p) since it depends linearly on the amount of the biomass treated. The mass relations between the inlet and the outlets remains constant, as show in Eq. (III.13). OPEX excludes the cost of biomass purchasing (Eq. (III.22)) and product selling (Eq. (III.30)) to avoid double counting.

At this point in the supply chain, conventional products are also manufactured and purchased, as displayed in Figure III.24 and Eq. (III.17). This means that the model is free to choose between conventional and alternative sources to meet the demand of products (p) in the markets (k). Transport costs are detailed below.

Transport of products from plants j to markets k. The same explanation for the transportation of chips applies to this connection.

$$co_{jkpv}^{jtp} = \sum_{v \in V} \left(UC_v^{tp} \cdot D_{vjk}^{j} \right) tp_{jkpv}^{plt} \qquad \textit{Eq. (III.26)}$$
$$\forall j \in J, k \in K, p \in P$$

Transport of products from conventional sites t to markets k:

$$co_{tkpv}^{ttp} = \sum_{v \in V} (UC_v^{tp} \cdot D_{vtk}^{t})\, tp_{tkpv}^{cvprd} \qquad \textit{Eq. (III.27)}$$
$$\forall t \in T, k \in K, p \in P$$

Cost of purchasing conventional products. Purchasing cost of these products is assumed to reflect upstream processing as internalised costs (UC_p^{cvprd}).

$$co_{pk}^{cvmkt} = f_{kp}^{cvmkt} \cdot UC_p^{cvprd} \quad \forall k \in K, p \in P \qquad \textit{Eq. (III.28)}$$

Cost of selling products from transforming plants j in markets k. This is represented as a negative cost since it effectively represents a sell (i.e., a benefit).

$$co_{pk}^{pmkt} = f_{kp}^{pmkt} \cdot UC_p^{prd} \quad \forall k \in K, p \in P \qquad \textit{Eq. (III.29)}$$

III. Environmental life cycle assessment

Environmental impacts were assessed for each step in the supply chain using an attributional approach. The supply chain is distributed over five echelons including transport stages, so the functional unit varies at each level.

Therefore, the impacts of each biomass/product flow were calculated per unit mass. This value was stored as an impact vector and multiplied by the reference flow in each case. This vector contains the scores of each stage over three environmental endpoints: ecosystem quality, natural resources, and human health. These endpoints are retrieved from the Ecoinvent database (v3.9.1) accessed via Activity Browser. The scope of the life cycle analysis (LCA) is cradle-to-gate as the target products are always production intermediates.

Biomass growth, harvesting and chipping (ei_{be}^{hrv}), [imact·y^{-1}]. All forestry practices are considered at this point (site preparation, planting, tending, young growth tending, clearing, thinning, and harvesting operations including the processing of wood fuel to chips, bundles and chopped wood) over one rotation period. Additionally, CO_2 uptake during biomass growth is also considered as a negative input from biosphere.

$$ei_{ibe}^{chp} = f_{ib}^{chp} \cdot IMP_{be}^{chp} \quad \forall i \in I, b \in B, e \in E \qquad \textit{Eq. (III.30)}$$

Transport of chips to transformation plants (ei_{ijbve}^{tp}), [imact·y^{-1}]. Impact vector (IMP_{ve}^{tp}) is expressed per tkm. Results depend on the distance (D_{vij}^{i}), the amount of chips transported (tp_{ijbv}^{chp}) and a correction factor (CFD_{v}^{chp}). Here, the impact vector is defined as dependent of v, thus representing a different value for each transportation mean.

$$ei_{ijbve}^{itp} = \sum_{v \in V} D_{vij}^{i} \cdot CFD_{v}^{chp} \cdot tp_{ijbv}^{chp} \cdot IMP_{ve}^{tp} \qquad \textit{Eq. (III.31)}$$
$$\forall\, i \in I, j \in J, b \in B, e \in E$$

The correction factor (CFD_{v}^{chp}) accounts for the relation between the density of the biomass and the capacity of the transportation technology. It relates the capacity of the transportation mean (maximum carry load/volume of the transport) to the density of the biomass. For lorry-based transport we assume a volume of 70 m^3 and a maximum carry load of 22.7 t, from which the capacity can be calculated (324 kg/m^3). For the chips, a correction factor of 1.25 is applied. It is considered to acknowledge emissions deriving from not fully loaded trucks. For trains and ships CFD_{v}^{chp} is set to 1.

Biomass losses at collection sites (ei_{ibe}^{iloss}), [imact·y^{-1}]. Environmental impacts related to the emissions derived from the oxidation of biomass losses at sites i can be defined as:

$$ei_{ibe}^{iloss} = \left(em_{ib}^{lschp} + em_{ib}^{lshrv}\right) \cdot IMP_{ibe}^{iloss} \quad \forall i \in I, b \in B, e \in E \qquad \textit{Eq. (III.32)}$$

Biomass losses at plant sites (ei_{ijbe}^{jloss}), [imact·y^{-1}]. Similarly, environmental impacts related to the emissions derived from the oxidation of biomass losses while transportation to plants j can be defined as:

$$ei_{ijbe}^{jloss} = em_{jb}^{lstp} \cdot IMP_{jbe}^{jloss} \quad \forall b \in B, j \in J, e \in E \qquad \textit{Eq. (III.33)}$$

Transformation plant impacts (ei_{je}^{plt}), [imact·y^{-1}]. The environmental impacts resulting from the operation of the plant are calculated based on the products obtained. The multi-functionality of the system is solved by subdividing the processes that give rise to each product at the factory level, while the inputs and outputs of the common equipment are partitioned based on the biomass composition as explained in 6.3.I. The impact vector is then calculated over a functional unit referenced to each product, as shown in Eq. (III.34). This results in a virtual expansion of the system, enabling comparison with conventional production.

All activities providing an input to the foreground system of the plant modelling are captured and aggregated in the Activity Browser to retrieve the impact vector IMP_{pe}^{plt} [impact·t^{-1}].

$$ei_{je}^{plt} = \sum_{p \in P} IMP_{pe}^{plt} \cdot f_{jb}^{chpav} \quad \forall j \in J, e \in E \qquad \textit{Eq. (III.34)}$$

Now again, two transport pathways are evaluated: from plants j to demand sites k, and from conventional sites t to markets k. The impact derived from all these routes is modelled as detailed below. Inefficiencies for the imperfect filling of the vehicles are disregarded at this point.

Transport to demand sites from plants j (ei_{jkpve}^{tp}), [imact·y^{-1}]. Same approach as for the transport of chips to transformation plants. The correction factor is excluded in this step.

$$ei_{jkpve}^{jtp} = \sum_{v \in V} D_{vjk}^{j} \cdot tp_{jkpv}^{prd} \cdot IMP_{ve}^{tp} \quad \forall j \in J, k \in K, p \in P, e \in E \qquad \textit{Eq. (III.35)}$$

Transport to demand sites k from conventional sites t (ei_{tkpve}^{tp}), [imact·y^{-1}].

$$ei_{tkpve}^{ttp} = \sum_{v \in V} D_{vtk}^{t} \cdot tp_{tkpv}^{cvprd} \cdot IMP_{ve}^{tp} \quad \forall\, t \in T, k \in K, p \in P, e \in E \qquad \textit{Eq. (III.36)}$$

Impact of purchasing conventional products (ei_{pke}^{cvmkt}), [imact·y^{-1}]. At this point, impacts derived from the production of conventional products (IMP_{pe}^{cvprd}) are also added to the model. Although conventional products are produced in different places, average inventories are considered.

$$ei_{pke}^{cvmkt} = f_{kp}^{cvmkt} \cdot IMP_{pe}^{cvprd} \quad \forall\, k \in K, p \in P, e \in E \qquad \textit{Eq. (III.37)}$$

IV. Objective functions

The model aims to minimise costs throughout the supply chain while considering three environmental indicators at the endpoint level: ecosystem quality, human health, and natural resources. To achieve this, the following objective functions are defined.

Economic function:

$$\begin{aligned} co = \sum_{i}\sum_{b}(co_{ib}^{bms} + co_{ib}^{chp}) + \sum_{b}\sum_{i}\sum_{j}\sum_{v} co_{ijbv}^{itp} \\ + \sum_{j} co_{jp}^{plt} + \sum_{p}\sum_{j}\sum_{k}\sum_{v} co_{jkpv}^{jtp} \\ + \sum_{p}\sum_{t}\sum_{k}\sum_{v} co_{tkpv}^{ttp} \\ + \sum_{k}\sum_{p}(co_{pk}^{cvmkt} + co_{pk}^{pmkt}) \end{aligned} \qquad \textit{Eq. (III.38)}$$

Environmental objective functions:

$$ei_{EQ} = \sum_{i}\sum_{b}(ei_{ib}^{hrv} + ei_{ib}^{iloss}) + \sum_{i}\sum_{j}\sum_{b} ei_{ijb}^{jloss} + \sum_{i}\sum_{b}\sum_{j}\sum_{v} ei_{ijvb}^{itp} + \sum_{j} ei_{j}^{plt} + \sum_{j}\sum_{p}\sum_{k}\sum_{v} ei_{jkvp}^{jtp} + \sum_{t}\sum_{p}\sum_{k}\sum_{v} ei_{tkvp}^{ttp} + \sum_{p}\sum_{k} ei_{p,k}^{cvmkt} \quad \textit{Eq. (III.39)}$$

$$ei_{HH} = \sum_{i}\sum_{b}(ei_{ib}^{hrv} + ei_{ib}^{iloss}) + \sum_{i}\sum_{j}\sum_{b} ei_{ijb}^{jloss} + \sum_{i}\sum_{b}\sum_{j}\sum_{v} ei_{ijvb}^{itp} + \sum_{j} ei_{j}^{plt} + \sum_{j}\sum_{p}\sum_{k}\sum_{v} ei_{jkvp}^{jtp} + \sum_{t}\sum_{p}\sum_{k}\sum_{v} ei_{tkvp}^{ttp} + \sum_{p}\sum_{k} ei_{p,k}^{cvmkt} \quad \textit{Eq. (III.40)}$$

$$ei_{NR} = \sum_{i}\sum_{b}(ei_{ib}^{hrv} + ei_{ib}^{iloss}) + \sum_{i}\sum_{j}\sum_{b} ei_{ijb}^{jloss} + \sum_{i}\sum_{b}\sum_{j}\sum_{v} ei_{ijvb}^{itp} + \sum_{j} ei_{j}^{plt} + \sum_{j}\sum_{p}\sum_{k}\sum_{v} ei_{jkvp}^{jtp} + \sum_{t}\sum_{p}\sum_{k}\sum_{v} ei_{tkvp}^{ttp} + \sum_{p}\sum_{k} ei_{p,k}^{cvmkt} \quad \textit{Eq. (III.41)}$$

III.4.2. Model solution

Model L2CHEM is calculated for various sets of ε-values, resulting in a distinct optimal solution for each set. These solutions jointly define the Pareto frontier, which describes the trade-off between multiple objectives (i.e., an objective can be improved by necessarily worsening at least another). Using this methodology, the problem of simultaneously optimizing the total cost and the three endpoint ReCiPe2016 indicators is addressed. The case at hand involves solving a single optimization problem with four objectives, which necessitates three independent sets of ε-values. For this case, a sampling space is generated, defined by the maximum and minimum values of the cost functions, spaced at equal intervals. The model L2CHEM (Lignocellulose To Chemicals) is defined as follows:

Model L2CHEM;

Min{co, ei_{HH}, ei_{NR}, ei_{EQ}};

s.t. Eqs. III.1 – III.37;

To solve the multi-objective linear programming (MIP) optimization problem, the CPLEX solver is employed within the GAMS suite.

III.4.3. Supply chain optimization results

The model is solved using GAMS software version 45.7 on an Intel Core i5-10210U 1.6GHz chip. At each iteration of the Pareto solution, the model features 70,205 equations containing 82,741 continuous variables and 15 discrete variables.

The results analysis is divided into two phases. Firstly, the model selects the optimal location of active plants, their capacity, the biomass type and collection sites preferred, and the flows between nodes by each transportation mean. These selections are made by minimising each of the objective functions individually. In the text, first, the cost minimisation (III.4.4.I) is shown, followed by the minimisation of each of the environmental functions (III.4.4.II and III.4.4.III). Secondly, the best number and plants is assessed by disregarding the constraint on the number of active plants (Eq. (III.12)). These results are presented in Section III.4.4.IV.

Depending on the minimised objective function, the model returns a specific solution for the stated objectives. Figure III.25 shows the calculated values for each minimisation pass. Each scenario represents the minimisation of one of the target variables separately. In the cost minimisation

scenario (min_CO), the overall costs of covering the annual demand for furfural, cellulose and lignin are minimised. The same occurs for the min_EQ, min_HH, and min_NR scenarios, where the environmental functions of Ecosystem Quality, Human Health, and Natural Resources are respectively minimised. It is crucial to highlight that the model aggregates the cost and environmental impact values for all three products and all markets. Consequently, when seeking to reduce e.g. costs, the model selects the least expensive option to meet the demand for the three products, including purchasing the products from conventional plants. Furthermore, the results are presented annualised. In other words, the cost and environmental impact of supplying all products from any available source to all markets over the course of a year is calculated.

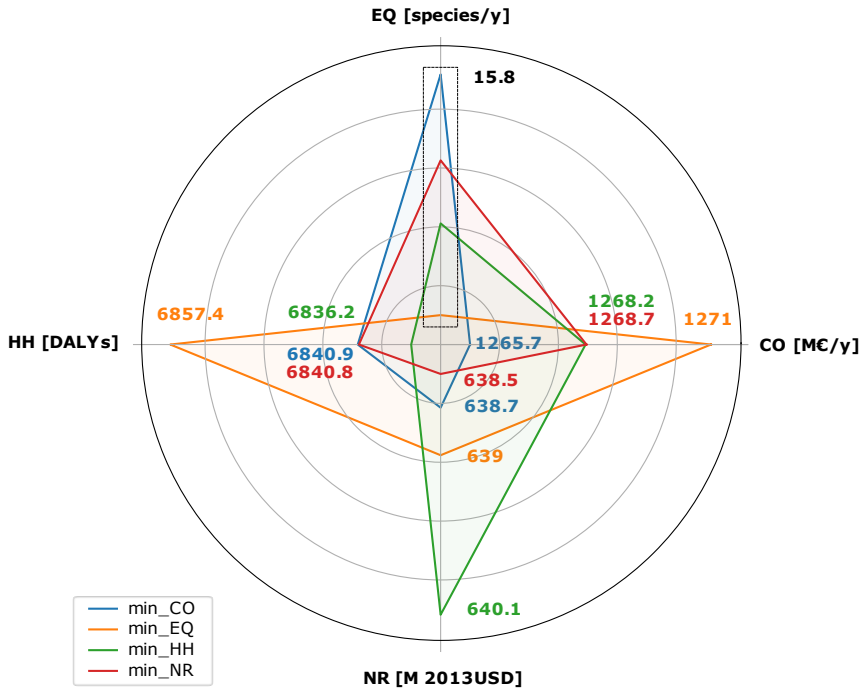

Figure III.25. Values obtained for the four objective functions when minimizing each individually.

I. Minimisation of costs

First, the insights from the cost minimisation scenario (min_CO) are discussed. In each of the four scenario solutions, the plant operates at its peak capacity of 200ktonne/y. This results in identical operational expenses (OPEX) across all scenarios. The model generally prefers the use of *Eucalyptus globulus*, except in the scenario that aims to minimize human health impacts (min_HH).

This preference is due to the higher cellulose yield from this species, which is a result of its composition. Cellulose is the primary product of the fractionation plant, accounting for 56 wt.% of the product distribution, and thus provides the highest economic benefit (26.2 €/tonne of input biomass). On the other hand, the combined environmental impact of the three products is greater than that of conventional products in terms of ecosystem quality (EQ) and natural resources (NR). Therefore, in the min_EQ and min_NR scenarios, the model also favours *E. globulus* although due to its location rather than its economic benefit, in order to reduce transport impacts. Since the eucalyptus species is the same in all three scenarios (min_CO, min_EQ, min_HH), the prices before chipping are identical.

In min_HH scenario, *E. camadulensis* is prioritized, since it has the highest yield of furfural, which has approximately 25% lower effects on human health than conventional furfural. This means that it is the only scenario in which the biomass price is slightly different. Conversely, the chipping cost per tonne is consistent for all types of biomass, leading to no variation between scenarios. Furthermore, since the type of biomass and the capacity of the plants are the same, the distribution of products at the factory gate is identical in all the cases studied.

Overall, the main cost reduction observed across all scenarios compared to business as usual (BAU) can be attributed to the fact that the production of cellulose, lignin, and furfural has an equivalent or lower cost for all three products (Table III.3). In addition, the rest of cost savings in the min_CO scenario occur at two points in the supply chain (see Table III.6). Firstly, transportation from the harvesting areas to the plants is the shortest among all the scenarios evaluated. All the biomass used is collected in the region of Asturias, where the plant is also located. This results in a reduction of up to 96% of transportation needs compared to the min_HH scenario, which yields the higher costs at this point. Figure III.26 illustrates the network of connections between the harvesting areas and fractionation plants for the four model solutions. The min_NR scenario is the only additional solution with comparable costs to those obtained in the min_CO.

The second significant savings point in the supply chain is the transportation of products to demand areas. The model selects fewer markets than other solutions to minimize transport costs at the point of sale. Given that rail transport is the most cost-effective mode per tonne-kilometre, and cellulose is the most common and least expensive product, all cellulose produced is transported by train to Madrid, Spain, to partially meet its demand.

This strategy maximizes the benefits from this fraction. For lignin and furfural, they are shipped to the nearest markets as other European capitals are farther away by land. Despite the slightly higher cost per tonne-kilometre, the shorter sea distance compensates for it. All lignin produced is shipped to the Netherlands, along with some of the furfural. The remaining furfural is shipped to nearby countries, such as Ireland (Dublin, with 100% demand coverage) and Belgium (Antwerp). The remaining supply is sourced from conventional plants.

Table III.6. Costs and environmental impacts breakdown over the supply chain for each scenario.

	min_CO [M€/y]	**min_EQ [species/y]**	**min_HH [DALYs]**	**min_NR [MUSD2013/y]**
HRV	7.202	0.918	20.515	1.204
CHP	2.443			
ITP	0.178	0.028	1.553	0.046
OP	52.570	2.609	885.638	119.015
JTP	1.500	0.035	6.607	0.377
PMKT	-67.218			
TTP	53.871	0.453	242.722	6.286
CVMKT	1215.114	11.826	5679.195	511.565
Total	1265.66	15.84	6836.23	638.49
Total_BAU	1472.17	14.44	6960.89	571.35

II. Minimisation of environmental impacts

The impact on ecosystem quality is highly constrained. The difference between the minimum (min_EQ) and maximum impacts on EQ, achieved by the min_CO scenario, for this aggregated indicator is only 0.0042 species per year, which is less than 0.03%. This variation virtually means that this indicator remains unchanged (Figure III.25). The effects on EQ produced by each of FTP products are superior to conventional ones. Thus, the model reaches its optimum by supplying 100% of products from conventional sources. To ensure the study of the effect of the use of a fractionation plant on global impacts, a minimum plant capacity is enforced.

Looking at the FTP supply chain (excluding the impacts from conventional sources), most of the burden is attributed to the operation of the fractionation plant. Again, the model prioritizes the use of *E. globulus* as cellulose has the lowest impact on EQ among the three products. However, its impact on EQ is 25% superior to that from conventional cellulose. In addition, lignin and furfural increase the impact on biodiversity (loss of species per year) by 70% and 89% respectively, compared to the BAU case. The reasons for this are discussed in greater detail in III.4.4.III Section. Bearing all in mind, the impact variation on the EQ category is marginal and mainly depends on the

proportion of demand met from conventional sources and fractionation plants, as the model prefers the BAU case regardless of the configuration.

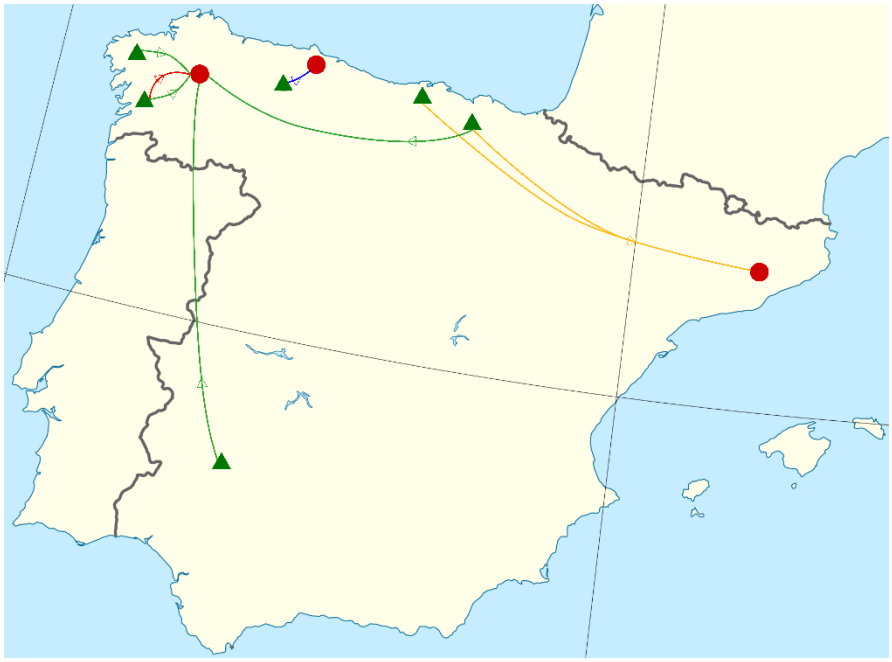

Figure III.26. Collection sites and fractionation plants network for: a) min_CO scenario (blue line), b) min_EQ scenario (yellow line), c) min_HH scenario (green line), d) min_NR scenario (red line). Red dots represent the fractionation plants in each scenario, and green triangles stand for biomass collection sites.

The same applies when optimizing the "natural resources" function (min_NR scenario). In this case, the environmental impact of lignin production is lower than that of phenol production, which is utilised for benchmarking of lignin. This comparison is justified by two arguments. Firstly, lignin does not currently have an established market, therefore its penetration cannot affect the market for "conventional lignin". Moreover, this polymer is anticipated to serve as a direct substitute for phenol in the manufacture of resins and other phenolic compounds due to its composition [254, 255]. Despite the high consumption of heating steam, and therefore of fuels for its generation, the impact of its fossil counterpart is reduced by 5%. On the other hand, the production of cellulose increases the impact by around 18%, and furfural by around 33% due to the consumption in the recovery of GVL. Consequently, the combined impact of the three products results in the systematic underperformance of conventional products. Therefore, the model is largely constrained and chooses the use of zero FTP plants as the preferred option.

Again, everything other than transport remains unchanged as the model has no other degree of freedom.

The only feasible reduction in environmental impact at the endpoint level is to minimize damage to human health, since furfural and lignin have a lower impact on this indicator compared to their conventional counterparts (impact reduction of 5% and 32% respectively). The model selects *Eucalyptus nitens* and *camadulensis* as the primary sources of biomass in this scenario because it favors the production of furfural, thus reducing the impact compared to the benchmark technology. Consequently, the model minimizes this impact primarily by decreasing the use of conventional technologies, where furfural produced in the fractionation plant displaces that from conventional sources. The plant is optimally located in Galicia and is fed by regions where *nitens* grows in greater abundance, such as Coruña, Lugo, and the Basque Country. Additionally, Eucalyptus camadulensis from Extremadura is also used (Figure III.26).

In summary, it is only feasible to enhance cost efficiency while simultaneously reducing impacts on human health. Human health impacts are quantified in terms of Disability Adjusted Life Years (DALYs), a comprehensive metric that encapsulates the overall disease burden. It is expressed as the number of years lost due to illness, disability, or premature death. The current configuration of the Fractionation Process (FTP) has the potential to decrease these years by 125 annually. The endpoints of the ReCiPe2016 methodology delineate the level of impact on different protection areas. It is not objective to compare these values directly, as further aggregation into a single score introduces larger uncertainties. However, the trade-off would involve reducing the 125 years of disease-free life in exchange for an increase in the number of extinct species per year by 1.4 and the extraction of natural resources by 68.71 million dollars per year, according to values shown in Table III.6. On the other hand, the total costs associated with meeting the demand for the three products under consideration in Europe could be reduced by 203.9 million euros annually with the operation of a single production facility.

III. Effect of environmental impacts aggregation

In this section, the ReCiPe2016 methodology has been employed, as EF3.1 does not have the necessary characterisation factors to aggregate impact categories at the endpoint level. This methodology utilizes similar indicators, and a substantial proportion of them are calculated using either the same methodology or other comparable ones. This means that comparable impact

pathways, emitted or consumed substances, and characterisation factors are considered.

Figure III.27 provides a visual representation of how the midpoints are categorized in the protection areas evaluated in this study. This matrix is used to identify and discuss the critical areas, or 'hotspots', of cellulose, lignin, and furfural production at the midpoint level.

Table III.7 summarises all midpoint level impacts of the three products from the FTP and conventional processes. A summary of the long name of each indicator its units is provided in the GLOSSARY OF TERMS AND ABBREVIATIONS, to avoid overloading the table caption.

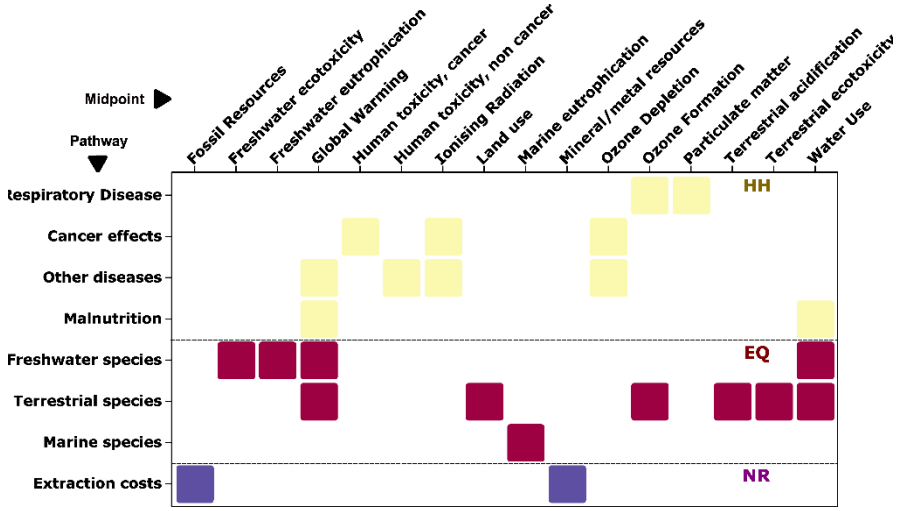

Figure III.27. Impact categories covered by the ReCiPe2016 methodology and their aggregation into areas of protection. Y axis shows the impact pathway for translating each midpoint category in X axis into each endpoint category. HH: human health; EQ: ecosystem quality; NR: natural resources.

- Human health midpoint categories

The production of lignin and furfural significantly reduces the impact on nearly all human health-related categories compared to the business as usual (BAU) approach (Table III.7). Only the indicators of climate change and ionising radiation are exceeded in both cases. Lignin also has a slightly higher impact on ozone depletion, although this is very low in absolute terms. In all cases, the impacts are mainly derived from the heating steam requirement. As previously observed, the main driver of increased steam consumption is the high recovery of GVL. Considering the allocation methodology described in Section III.3, cellulose assumes 50% of the associated impacts in the common

plant areas where this GVL is recovered. However, the impact of cellulose is consistently lower than that of the other two products. This is due to the high associated impact of lignin caused by the multi-effect evaporator (MEE) unit, and the D1 furfural distillation column (Figure III.5).

The reason why cellulose from FTP is less environmentally attractive than conventional one, is that current production of the latter is neat. The cellulose selected from the Ecoinvent database (v3.9.1, APOS) is the production of cellulose fibre from waste paper. This process results in a lower quality fibre than the FTP product, with applications as insulation in buildings. Although this inventory is used as a proxy, the functional unit is not completely comparable and favours the conventional process.

Table III.7. Midpoint impacts of FTP and conventional product per ton of each product.

	Cellulose		**Lignin**		**Furfural**	
	Conv	**FTP**	**Phenol**	**FTP**	**Conv**	**FTP**
TAP	1.20	3.90	9.57	9.69	77.24	31.33
GWP100	469.86	1897.48	3542.21	4142.62	13748.77	16777.31
FETP	33.65	13.61	95.01	47.27	130.31	109.02
METP	42.74	20.05	123.83	66.62	187.05	161.33
TETP	2453.81	3207.01	8495.89	8115.36	15332.16	25183.42
FFP	86.49	561.10	1963.49	1203.70	2823.43	5011.70
FEP	0.12	0.22	0.69	0.54	3.31	1.86
MEP	0.05	0.03	0.05	0.07	0.73	0.24
HTPc	20.62	38.14	135.22	107.56	339.52	317.47
HTPnc	419.72	428.71	1932.91	1292.02	5607.91	3602.18
IRP	14.41	48.64	81.58	117.60	77.05	384.27
LOP	122.05	565.81	33.18	560.50	311.03	1510.92
SOP	46.21	6.37	15.89	55.89	18.50	49.10
ODPinfinite	1.61E-04	2.44E-04	3.74E-04	7.59E-04	3.34E-03	2.02E-03
PMFP	0.60	1.35	4.44	3.45	27.16	10.98
HOFP	1.12	2.49	7.56	5.47	29.45	20.95
EOPF	1.16	2.72	8.38	5.93	30.24	22.88
WCP	5.01	3.32	45.24	21.81	33.98	20.02

In any case, the optimisation model compares the sum of the impacts and costs of the three products. The model is unable to send fewer products to the demand areas, nor can the fractionation plants change their product distribution for a given biomass. Therefore, the minimisation performed is equivalent to comparing the sum of cellulose, lignin and furfural of FTP with conventional processes. Consequently, in the context of human health impacts, the reduction in the impacts of furfural and lignin offsets the increased impacts on cellulose in comparison to recycled paper fibre.

- Ecosystem quality midpoint categories

The aggregate midpoint impacts on ecosystem quality are visibly dominated by several aspects. The first of these is land occupation (LO). LO effects are by far the most important pressure on this Area of Protection (AoP), as previously identified for furfural production (6.3.1.VI). Compared to conventional products, the space occupied by Eucalyptus (assuming dedicated cultivation) is much larger. This leads to a 4-5 times higher impact for cellulose and furfural, and almost 17 times higher for lignin. The latter case is considerably more pronounced since its conventional counterpart is of fossil origin, which results in a significantly lower impact on this category compared to biomass utilization. The remaining categories under this AoP are once again driven by steam generation. In particular, the presence of hard coal in the energy mix significantly affects almost all categories (acidification, ecotoxicity, eutrophication). The data considered for this mix represent a European average. This is logical when compared with the most likely conventional processes, as the model will prioritise the use of European sources for the BAU scenario for proximity reasons. However, not all demand in the BAU scenario is met from European sources, which would probably result in a greater penalty for the impacts in this scenario than in the current model.

Similarly, if average data is superseded with a more representative mix, the FTP's demand for heating steam is likely to be less dependent on coal or nuclear sources, depending on its final location. Replacing these sources by burning surplus biomass at the plant is not a clear alternative in this case. If waste biomass is employed, this source would only have a marginal increase in land occupation, which is the main impact on EQ. However, the availability of waste with sufficient calorific value to cover the plant's medium and high-pressure steam needs is a complex task. In summary, the reduction of impacts on this AoP involves a reduction in land use by biomass, which implies a transition to the use of residues or the implementation of sustainable forestry practices that minimise the impact on biodiversity in eucalyptus plantations. Again, such practices are not considered with the average data used.

- Natural resources midpoint categories

The consumption of natural resources is characterised by the depletion of fossil fuels, minerals and metals. As these resources become scarcer, their characterisation factor increases. In the case of fossil fuel consumption, furfural significantly worsens the BAU scenario (see Figure III.14) for the reasons discussed in the previous section. The case of cellulose is similar, although more pronounced due to the lower consumption in the conventional

process. Consequently, the consumption of fossil fuels is around 6.5 times higher. Lignin exhibits an improvement concerning fossil phenol, despite the high steam consumption in the MEE unit. This is to be expected, given that phenol is produced from cumene in the Hock process. Cumene, is previously manufactured with a yield of 95% from the alkylation of benzene and propane, which explains the higher consumption of fossil resources. Concerning the depletion of metals and minerals, the only product that improves the BAU is cellulose. In this case, the conventional process from waste paper utilises magnesium sulphates in the process, which has a significant consumption of this element and thus significantly penalises the process. Consequently, FTP improves cellulose production by up to seven times in this category. However, lignin and furfural show a worse performance. In the case of lignin, the production of deionised water has the greatest impact. Given that this consumption is extremely high in the precipitation process (Table III.3), the impact is up to 3.5 times higher than for phenol. The production of deionised water utilises magnesium oxide and sodium chloride, which accounts for more than 80% of the environmental impact. However, the improvement in the use of fossil fuels is more pronounced, resulting in a reduction in the overall impact on this AoP in the case of lignin. However, as previously stated, the objective is to minimise the sum of the three products. Consequently, the NR category benefits most from the use of conventional sources.

IV. Multi-objective optimization

Considering these factors, the only two objectives that can potentially be improved simultaneously are costs and human health effects, as depicted in Figure III.28. Given the problem's topology, the model aims to optimize transport flows, capacity, and the number and location of the plants. If a single objective is minimized and only one plant is allowed to operate, the solution remains the same regardless of the relaxation of the epsilon value (see 6.4.3). As a result, the number of plants is not constrained for the purpose of constructing this curve. Consequently, the model selects a larger number of fractionation plants as the economic optimum is approached (moving from left to right in Figure III.28). The Business As Usual (BAU) scenario is closer to the environmental optimum (HH), although it falls within the region of sub-optimal solutions. In practical terms, this implies that both functions can be minimized simultaneously using the proposed supply chain.

The second point on the curve is identified as the only instance where two of the objective functions can be minimized simultaneously. Under these conditions, the values of the objective functions are as shown in Table III.8.

These values indicate that the impacts on human health can be minimally reduced, which would significantly impair other environmental functions. In other words, the current configuration of the process allows for only a limited improvement in economic terms, which in turn compromises the environmental objectives.

Table III.8. Values of the objective functions when costs and human health impacts are optimised.

	CO [M€/y]	EQ [species/y]	HH [DALYs]	NR [MUSD2013/y]
Value	1414.8	17.18	6821.7	629
% from BAU	-24%	+26%	-2%	+21%

Should any other point on the curve be chosen, there would be a substantial improvement in costs, particularly for the initial four points on the curve. Conversely, the three target functions would deteriorate significantly due to increased energy consumption and land occupation, as outlined in Section III.4.4.III. Given the current configuration, the evaluation of trade-offs is considerably constrained. Within the existing technological framework, it would be essential to examine the energy savings resulting from a reduction in the recovery of GVL, against the cost increase associated with the procurement of additional fresh solvent. Furthermore, replacing eucalyptus from dedicated cultivation with forestry or agricultural residues could potentially address the issues arising from land use.

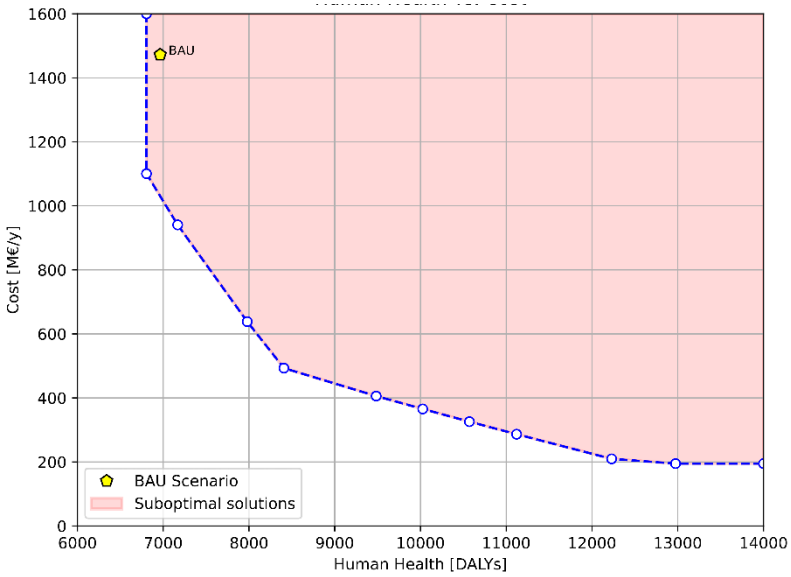

Figure III.28. Pareto front of optimal solutions in the simultaneous optimization of costs and human health effects.

However, according to the results, the distribution map of this scenario would look as shown in Figure III.29. In this case, two fractionation plants operate, one in Asturias and the other in the Basque Country. The Asturias plant would be entirely supplied with eucalyptus from the same region, while the Basque Country plant would receive this feedstock from the Basque Country itself and Cantabria. Most of the transportation would be conducted by sea, due to its comparatively lower cost and environmental impact. The use of road transport by lorry is a disregarded option for the transportation of goods over long distances. Hence, only railroad transportation is considered.

Figure III.29. Map of the biomass and product flows under the optimal scenario for current process configuration. Green triangles: biomass collection sites. Red circles: fractionation plants, Black lines: transportation routes of raw biomass by train, Blue lines: transportation routes of products by ship, Brwon lines: transportation routes of products by train.

III.4.4. Supply chain problem remarks

In conclusion, the fractionation process has the potential to significantly enhance the conventional process in terms of cost. Nevertheless, the process fails to enhance the impact on natural resource consumption due to the high energy consumption involved, and it also has a detrimental effect on ecosystem quality due to the high land occupation.

- GVL recovery implications

This high requirement stems from the fact that the plant is optimised for maximum recovery of gamma-valerolactone (GVL), its primary solvent. The high price of gamma-valerolactone (GVL), as indicated in Table III.3, is a significant factor in this context. Given that this technology represents a novel approach, it is deemed prudent to operate at an economic optimum to mitigate market risk and facilitate implementation. However, it should be noted that environmental impacts have not been factored into this plant configuration. As a result, the trade-off between maximizing GVL recovery (for minimum cost) and introducing more fresh GVL (for minimum impact) has not been evaluated. A thorough examination of the supply chain reveals that the annualized costs associated with meeting the demand for the three products can be reduced by up to 206.5 million euros per year. This suggests a significant opportunity to increase the selling price of cellulose by forgoing the recovery of a certain percentage of the GVL, thereby mitigating the impacts associated with steam generation.

The environmental impacts of fresh gamma-valerolactone are considered negligible compared to those of recovered GVL, considering the mass flows of each at the plant inlet. However, an approximation is made for the global warming potential (GWP) indicator to conduct a cursory sensitivity analysis. This indicator is chosen as it is representative, given its influence on the deterioration of the ecosystem quality area of protection, its correlation with fossil consumption, and its significant impact on both conventional and alternative processes for furfural production. Although GVL is a solvent with an optimistic prospect, it is currently not produced on a commercial scale, leading to a scarcity of reliable inventories in industry or literature. Consequently, a simulation of the production process from cellulose was carried out. This simulation was based on data provided by the CSIC (for the conversion of cellulose to levulinic acid) and bibliographic data (for the conversion of levulinic to GVL).

The production process is schematically represented in Figure III.30. It involves the hydrolysis of a 15 wt.% aqueous cellulose solution (CELL stream) to glucose in the presence of 0.15M H_2SO_4 at 170°C. The glucose is then cyclodehydrated to levulinic acid, with an overall yield of 48%. This reaction takes place at R-1 reactor. In a subsequent step, levulinic acid is hydrogenated to GVL via 4-hydroxypentanoic acid (4HPA) as a reaction intermediate, following the reaction represented in Figure 1.7. This reaction occurs at 127°C, under a pressure of 45 bar, in the presence of a heterogeneous ruthenium catalyst supported on carbon. Hydrogen is compressed in the COM-1 and COM-2 compressors, and the reaction takes place in the tubular reactor units R2-A and R2-B. The GVL exiting the second reactor is purified from 4HPA in a flash separator (FLASH) and recovered under conditions suitable for injection into the fractionation reactor (PRODUCT stream). The hydrogen is recovered by the flash tank head and recirculated to the process (H2-REC stream). The feed to this plant is assumed to be a biomass stream with a mass flow rate of 2500 kg/h of cellulose, a value estimated based on the yields of both reactions to provide the plant with the required GVL makeup. Interestingly, this stream could be obtained from biomass rejects at the inlet of the plant, or from lower-quality cellulose from the outlet of the centrifugal filter F1 depicted in Figure III.1.

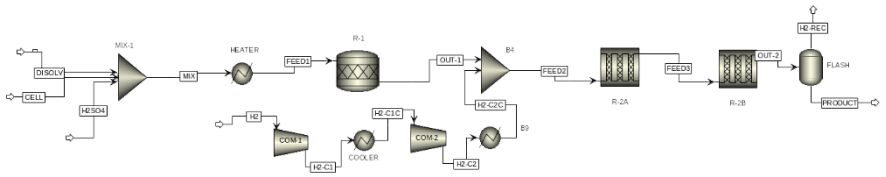

Figure III.30. Flowsheeting of the fresh GVL production plant.

The price for commercial GVL is estimated at €2500/tonne, compared to €11.5/tonne of plant-recovered GVL, according to data shown in Table III.3. This implies that for every tonne that is not recovered, the cost increases by €2,488.5. As a result, up to 10.4 tonne/h of GVL could be unrecovered without the process becoming unprofitable, considering the benefits observed in Table III.8. Concurrently, the recovery of GVL is estimated to produce an impact of 1,210 kg CO_2 eq./tonne GVL recovered, while 1,019.4 kg CO_2 eq. are emitted per tonne of fresh GVL. Therefore, for every tonne not recovered, equivalent emissions would be reduced by 190.6 kg CO_2 eq./tonne GVL. This means that by operating within the profitability margin, CO_2 equivalent emissions could be reduced by 1981.9 kg CO_2 eq./h, resulting in a savings of 15.86 million tonnes of CO_2 equivalent emitted per year.

While this reduction is insufficient to improve the emissions associated with the current supply chain of cellulose, lignin, and furfural, it does bring the process significantly closer to the BAU scenario. It is important to note that, even if the entire process does not reach the current scenario, furfural production via FTP will improve CBP production in terms of CO_2-eq. emissions.

In addition to this, two further effects must be considered. Firstly, it is to be expected that the price of GVL will decrease over time. This solvent has not yet received the same level of attention as other solvents, and its commercial development is not yet very mature. As it becomes more widely used in this and other processes, its cost is likely to fall. Similarly, the production of solvent from biomass input rejects, or lower quality cellulose after the first filtration (F1, Figure III.1), has only been investigated through a cursory analysis. As more research is conducted, it is expected that both costs and impacts will decrease in this plant. In any case, both factors indicate that the need for solvent recovery in the process will tend to drop, through the minimisation of the impacts and costs associated with in-plant GVL production or the purchase of cheaper GVL. This allows the boundaries of the sensitivity analysis to be pushed. That is, while maintaining the price of the products, to obtain higher profitability.

- Other environmental performance remarks

Even without considering the reduction in emissions, if the midpoint impacts shown in Table III.7 are annualised, i.e. multiplied by their annual demand, FTP outperforms conventional production for 11 of the 18 indicators in the ReCiPe2016 methodology, as illustrated in Table III.9. This implies that the process is subject to penalisation as a result of the aggregation of these indicators. In other words, considering each AoP studied, there is a higher indicator that results in the FTP products performing less favourably at the endpoint level. For instance, impacts at the ecosystem quality endpoint exceed conventional ones due to the disproportionate land occupation by eucalyptus compared to corn cobs. Yet, disaggregating these values reveals an improvement that is otherwise masked.

The energy mix used in the production process is currently generic to Europe. As the process evolves, it will be possible to model this mix with greater accuracy. It is likely that the process will rely less on sources such as coal, which, despite its relatively low presence, has a significant impact, as shown in Section III.3.1. Improvements are expected not only with regionalisation but also over time. The EU's climate targets, as described in

Section 1.1.2 force the decarbonisation of the economy in all member states, as well as greater independence from fossil resources. This will have a significant impact on almost all categories assessed.

- Final remark

Summarizing, the fractionation process holds significant potential to surpass conventional methods of cellulose, lignin, and furfural production. However, the primary economic and environmental constraint is the utilisation of gamma-valerolactone as solvent, followed by the use of a dedicated forest crop as a feedstock. The use of fresh GVL incurs a high cost, and its recovery within the plant also has a substantial impact. However, as GVL utilisation becomes more widespread, its price is expected to decrease. Furthermore, the in-plant production of GVL is currently in the conceptual stage. The development and optimisation of this process could lead to significant cost savings. Similarly, the substitution of eucalyptus for other types of residual feedstocks has the potential to significantly reduce the impact on land use, thereby improving ecosystem quality. If these issues are resolved, FTP has the potential to outperform conventional furfural, cellulose and lignin production processes.

Table III.9. Annualised impact score for FTP and conventional processes as the sum of the three studied product over each midpoint category. Values in (%) show the improvement (green) or detriment (red) of FTP respective to BAU. For complete names see the glossary of terms and abbreviations.

Midpoint indicator	Annualised FTP score		Annualised conventional score
TAP	1.06E+07	13%	9.37E+06
GWP100	4.77E+09	51%	3.17E+09
FETP	4.65E+07	51%	9.57E+07
METP	6.64E+07	47%	1.24E+08
TETP	8.78E+09	13%	7.80E+09
FFP	1.40E+09	8%	1.53E+09
TEP	5.91E+05	13%	6.82E+05
MEP	7.54E+04	19%	9.36E+04
HTPc	1.13E+08	4%	1.17E+08
HTPnc	1.33E+09	27%	1.82E+09
IRP	1.29E+08	18%	1.09E+08
LOP	8.48E+08	613%	1.19E+08
SOP	4.59E+07	3%	4.47E+07
ODPinfinite	7.72E+02	73%	4.47E+02
PMFP	3.73E+06	7%	4.02E+06
HOFP	6.25E+06	3%	6.43E+06
EOFP	6.80E+06	4%	7.06E+06
WCP	1.85E+07	50%	3.71E+07

III.5. Final remarks

Regarding the production of furfural, the fractionation process has the potential to reduce environmental impacts in 10 out of 16 evaluated categories compared to the Chinese batch process. Moreover, it could potentially lessen the impact on seven out of the nine categories identified as the most critically affected by current furfural production. However, it could have a negative impact on climate change effects, fossil consumption, and land use.

In the FTP, 75 wt.% of the incoming biomass is converted into products. This contrasts with the CBP, where only a maximum of 10% of the biomass is transformed into furfural, with the remainder being discarded. This efficient use of biomass in the FTP reduces the environmental impacts associated with each product. As the production of furfural, cellulose, and lignin in the FTP is inseparable, the environmental impact of these three products was analysed in comparison to their conventional counterparts.

Overall, the fractionation process presents two hotspots. The principal is the energy required for the recovery of the gamma-valerolactone, the main solvent used in the plant. The process is optimized for minimum GVL makeup due to its high price. As the technology is a first-of-its-kind concepts, it operates at an economic optimum to mitigate market risk and facilitate implementation. However, environmental impacts have not been factored into this configuration. Operating within the profitability margins, the GVL makeup could increase reaching savings of up to 15.86 million tonnes of CO_2 equivalent emitted per year.

Considering the supply chain of furfural, cellulose, and lignin produced by FTP, conventional processes are generally more environmentally friendly. However, the aggregation of environmental effects into endpoint indicators results in less favourable performance. A significant factor is the disproportionate land occupation by eucalyptus compared to conventional counterpart's utilised feedstock, leading to higher impacts at the ecosystem quality endpoint. Despite this, disaggregating these values uncovers hidden improvements, leading to a surpass of the conventional production in 11 out of 18 indicators according to the ReCiPe2016 methodology.

Additionally, the energy mix, currently generic to Europe, is expected to improve upon greater accuracy of the datasets, as it will likely rely less on sources such as coal or light fuel oil. This evolution, along with the impositions from EU's climate targets, will significantly contribute to decrease almost all assessed categories.

In summary, while the FTP shows promise, its successful implementation requires careful consideration of both economic and environmental factors. Future research should focus on evaluating different energy mixes and regions, exploring the use of different types of biomass, and considering social criteria. A comprehensive sensitivity analysis is crucial for connecting different aspects. First, determine the amount of GVL that may not be recovered within the profitability margin. This can be done by contrasting the increased economic impact of purchasing additional fresh GVL versus the reduction in the environmental impact of decreasing energy use in solvent recovery processes. Furthermore, an in-depth examination of on-site GVL production is required. This involves determining the optimal amount of fresh biomass or lower-purity cellulose that can be redirected for solvent production, taking into account both economic efficiency and environmental impact.

CONCLUSIONS AND FUTURE WORK

Throughout this doctoral thesis, several relevant conclusions have been drawn. These are detailed below in order of appearance in the main text.

I. LCA modelling choices

Firstly, regarding the methodological framework for conducting life cycle assessment (LCA) studies on platform biomolecules, several factors affecting the modelling choices were observed. The majority of the studies reviewed have a cradle-to-gate scope, as these molecules serve as the basis for synthesising a multitude of end products. This implies that a comprehensive end-of-life (EoL) study is not feasible in most cases. Consequently, these impacts are not considered, which hampers the comparison with their fossil counterparts. On the bright side, many of these molecules serve as direct replacements for conventional compounds, as they function as drop-ins. Consequently, downstream effects can be assumed to be analogous, except in cases where toxicity and/or biodegradability are involved. To compensate for the lack of EoL modelling, the inclusion of scenarios is a valuable addition. Another crucial aspect to consider is the accounting of carbon flows. In studies conducted on intermediate products, the fate of biogenic carbon is ignored, as the lifetime of the final product is unknown. In such instances, it is recommended that the sequestration of biogenic carbon in the biomolecule be considered. This approach more closely predicts the results against the carbon-

neutral scenario, where the absorbed CO_2 is released back into the atmosphere, resulting in a net zero balance.

Secondly, the majority of studies focus on incumbent technologies, which necessitates the use of secondary data or laboratory-scale procedures. Such data is more susceptible to uncertainty when it comes to assessing industrial-scale impacts, which may lead to erroneous conclusions when compared to mature technologies. A significant number of studies report the uncertainty of the foreground system through sensitivity studies and scenario analyses. However, a significant proportion of the observed variability in the data can be attributed to the probability distribution of the inputs, which is frequently overlooked. It is important to consider the uncertainty associated with the parameterisation of the foreground and background systems, as well as the model itself. Monte Carlo sampling (MC) is therefore proposed as a direct alternative due to its acceptance and integration with most commercial software. An appropriate and straightforward approach is to utilise the Pedigree matrix to assign a distribution to the inputs, which can then be propagated through the LCA calculations using MC. Additionally, the number of iterations can be assumed by almost any processor.

Finally, the majority of processes result in the generation of multiple outputs. The distribution of impacts between the different co-products is a complex task that requires careful consideration. Some uniformity is observed in the literature, although this is at odds with the standards. Most studies report an allocation based on the economic value of the products, or alternatively by their output mass flow rate. This should be replaced by alternatives that avoid allocation, as determined in ISO 14044. This work proposes the use of this hierarchy, with consequential analysis (CLCA) situated at the pinnacle. This modelling perspective is particularly beneficial in this context, as it avoids the aforementioned problem and the setting of system boundaries. However, the data available for CLCA is limited, and thus the system subdivision method is a sufficiently appropriate approach in its absence.

II. LCA of benchmark technologies

Regarding the benchmarks for furfural production, several key findings have been clarified and are summarised in the following paragraphs.

Furfural production processes pose environmental concerns due to high energy consumption and extensive acid use. While acid wastes are treatable, the H_2SO_4 induces secondary challenges. Specifically, it forces the increase of the reactor wall thickness to prevent corrosion, limiting heating

effectiveness. The need for direct steam injection into the reactor for temperature elevation leads to significant mixture dilution, dramatically increasing the steam usage as well as the size of process units downstream. This inefficiency is the most critical point in the environmental profiling of the processes, representing a key area for improvement in future furfural production developments.

Heating steam production is heavily reliant on fossil fuel combustion, which significantly influences furfural production processes. This is particularly prominent in China and the Dominican Republic, the major exporters of furfural to Europe. While furfural production is limited within the European Union to a few countries, consumption is elevated and expected to increase. That does not avoid the impact but externalises it. The European energy mix is expected to improve over the coming decades. Therefore, future technologies will likely rely on a more decarbonised heating production.

The quantity of initial dilution water is crucial in furfural production processes. The acid used in the QOP is four times more concentrated than in the CBP, significantly impacting the environmental performance of the Chinese batch process. Since the amount of input water is lower, the equipment size decreases accordingly, which results in a reduced energy consumption. This insight is vital for future developments in furfural production.

The heat transfer optimization in the first distillation column of the CBP is also modified as a consequence of the input water. The QOP uses a secondary steam generator for stripping in the first column, produced by partially condensing the reactor outlet. In contrast, the CBP exchanges heat directly within the reboiler of the same column. Energy requirements in the latter are larger due to the column size. The CBP configuration is mandatory due to the inability of the stripping steam to raise the mixture temperature to the desired level, and further diluting the furfural at the top of the distillation column below the azeotropic point.

The type of biomass used significantly affects furfural yield due to the process's dependency on pentosans in the feedstock. Both technologies have low overall yields, with a large portion of the biomass discarded as acidic waste, necessitating treatment before disposal. Assuming a 30 wt% pentosans content in the biomass, the best-case scenario imposes a maximum of 10% furfural yield, with the remaining 90% of the biomass directly discarded. This limitation contradicts the goals of sustainable development. Therefore, a much higher utilisation of biomass is mandatory.

Using agricultural or forestry residues instead of biomass offers several benefits, including a reduction in land use. This leads to lower CO_2 emissions from use changes, especially in large agricultural plantations. Since this impact is typically associated with bioprocesses, this must be considered as a plausible solution on top of energy crops. However, the distribution of impacts with other co-products derived from these residues also absorbs most benefits from CO_2 sequestration during biomass growth. In the studied processes, the low amount of CO_2 absorbed is insignificant in comparison to process emissions.

III. LCA and supply chain optimisation of the proposed technology of furfural production

The proposed process for furfural production has the potential to reduce environmental impacts in 10 out of 16 evaluated environmental categories. Furthermore, of the nine indicators most affected by the CBP, only global warming potential and fossil fuel consumption are worsened.

The reason is the higher energy consumption, despite sourcing power from cleaner alternatives. The primal hotspot relates to the GVL recovery in the process. The plant is designed to maximise solvent recovery due to its high price. This causes the economic and environmental objectives to go in opposite directions. In this first design, the plant operates at its economic optimum to minimise risk and facilitate market penetration. However, through a cursory sensitivity analysis, it was determined that the emission of almost two tonnes per hour of CO_2 equivalent could be avoided by operating within the profitability margin. A thorough sensitivity analysis is required in future work to determine the most beneficial trade-off between the two functions, including the possible in-plant production of GVL from biomass rejects or lower-quality cellulose.

The primary challenge in GVL recovery arises from the recovery unit and the initial furfural distillation column. The consumption in the distillation is markedly higher than in the conventional process for two reasons. Firstly, the lower energy integration is a consequence of the gas phase product not being forced through any recuperator to aid the reboiler. Secondly, to achieve the greatest possible GVL recovery, it is necessary to increase the reflux ratio. Consequently, the aqueous phase recirculated to the column flows downwards, thereby enriching the heavy fraction in the liquid phase. Therefore, this results in a significant increase in steam consumption in the reboiler. Reducing the energy consumption at these two points is critical for the viability of the process.

Upon examination of the performance of the three co-products, only cellulose underperforms conventional production. In contrast, lignin performs comparably to phenol. Global warming, ionising radiation, mineral consumption and land occupation are systematically increased by the fractionation process.

When looking at the supply chain effects on the demand for the three products across Europe, the assessed process has the potential to reduce the sum of annualised costs by up to 14%. This is in part due to the fact that the minimum selling price of cellulose fibre is approximately €250 per tonne cheaper than in the conventional production process. Additionally, transportation costs are significantly reduced due to the closer proximity between the points of production and demand. The optimal location for the fractionation plant in this scenario is Asturias. It is possible to obtain all the biomass required for a 200,000-tonne-per-year treatment plant within the same region.

From an environmental perspective, the fractionation process has the potential to diminish the impact on 11 of the 18 impact categories assessed. These impacts are then aggregated at the level of protection areas to reduce the number of target functions to minimise. With this aggregation, the observed information decreases, partly masking the identification of trade-offs with the economic function. Consequently, the model prioritises conventional outputs when attempting to reduce biodiversity damage and natural resource consumption. The damage to biodiversity is caused by increased greenhouse gas emissions, acidification effects, and land use. The initial two indicators are outweighed by the increased energy consumption resulting from GVL recovery. The third indicator pertains to the utilisation of eucalyptus from dedicated crops instead of biomass residues. Conversely, the fractionation process has a lower impact on human health than the conventional one. It is concluded that the implementation of this technology is contingent upon a reduction in heat demand for GVL recovery and the substitution of biomass-dedicated crops for biomass wastes.

REFERENCES

[1] V. Tulus, J. Pérez-Ramírez, and G. Guillén-Gosálbez, 'Planetary metrics for the absolute environmental sustainability assessment of chemicals', *Green Chemistry*, vol. 23, no. 24, pp. 9881–9893, 2021, doi: 10.1039/D1GC02623B.

[2] H. Lee and J. Romero, 'IPCC, 2023: Climate Change 2023: Synthesis Report. Contribution of Working Groups I, II and III to the Sixth Assessment Report of the Intergovernmental Panel on Climate Change', Geneva, Switzerland. doi: 10.59327/IPCC/AR6-9789291691647.

[3] World Health Organization, *Quantitative risk assessment of the effects of climate change on selected causes of death, 2030s and 2050s*. WHO, 2014. Accessed: Mar. 25, 2024. [Online]. Available: https://www.who.int/publications-detail-redirect/9789241507691

[4] A. Stips, D. Macias, C. Coughlan, E. Garcia-Gorriz, and X. S. Liang, 'On the causal structure between CO2 and global temperature', *Sci Rep*, vol. 6, no. 1, Art. no. 1, Feb. 2016, doi: 10.1038/srep21691.

[5] M. Höök and X. Tang, 'Depletion of fossil fuels and anthropogenic climate change—A review', *Energy Policy*, vol. 52, pp. 797–809, Jan. 2013, doi: 10.1016/j.enpol.2012.10.046.

[6] A. Nabera, I.-R. Istrate, A. José Martín, J. Pérez-Ramírez, and G. Guillén-Gosálbez, 'Energy crisis in Europe enhances the sustainability of green chemicals', *Green Chemistry*, 2023, doi: 10.1039/D3GC01053H.

[7] M. E. Kahn, K. Mohaddes, R. N. C. Ng, M. H. Pesaran, M. Raissi, and J.-C. Yang, *Long-Term Macroeconomic Effects of Climate Change: A Cross-Country Analysis*. in NBER working paper series, no. no. w26167. Cambridge, Mass: National Bureau of Economic Research, 2019.

[8] United Nations Framework Convention on Climate Change, 'Climate Change: Impacts, vulnerabilities and adaptation in developing countries', Bonn, Germany, 2007. [Online]. Available: https://unfccc.int/resource/docs/publications/impacts.pdf

[9] T. M. Lenton *et al.*, 'Climate tipping points — too risky to bet against', *Nature*, vol. 575, no. 7784, pp. 592–595, Nov. 2019, doi: 10.1038/d41586-019-03595-0.

[10] K. Richardson *et al.*, 'Earth beyond six of nine planetary boundaries', *Science Advances*, vol. 9, no. 37, p. eadh2458, Sep. 2023, doi: 10.1126/sciadv.adh2458.

[11] D. Gielen, F. Boshell, D. Saygin, M. D. Bazilian, N. Wagner, and R. Gorini, 'The role of renewable energy in the global energy transformation', *Energy Strategy Reviews*, vol. 24, pp. 38–50, Apr. 2019, doi: 10.1016/j.esr.2019.01.006.

[12] IEA, 'Power Systems in Transition', 2020. Accessed: Mar. 25, 2024. [Online]. Available: https://www.iea.org/reports/power-systems-in-transition

[13] *European Commission, A new Circular Economy Action Plan For a cleaner and more competitive Europe*. 2020. Accessed: Mar. 27, 2024. [Online]. Available:

https://eur-lex.europa.eu/legal-content/EN/TXT/?qid=1583933814386&uri=COM:2020:98:FIN

[14] D. Keegan, B. Kretschmer, B. Elbersen, and C. Panoutsou, 'Cascading use: a systematic approach to biomass beyond the energy sector', *Biofuels, Bioproducts and Biorefining*, vol. 7, no. 2, pp. 193–206, 2013, doi: https://doi.org/10.1002/bbb.1351.

[15] E. Commission, E. Directorate-General for Internal Market Industry, and SMEs, *Guidance on cascading use of biomass with selected good practice examples on woody biomass*. Publications Office, 2018. doi: doi/10.2873/68553.

[16] E. Commission *et al.*, *Bioeconomy strategy development in EU regions*. Publications Office of the European Union, 2022. doi: doi/10.2760/065902.

[17] L. Lange *et al.*, 'Developing a Sustainable and Circular Bio-Based Economy in EU: By Partnering Across Sectors, Upscaling and Using New Knowledge Faster, and For the Benefit of Climate, Environment & Biodiversity, and People & Business', *Front. Bioeng. Biotechnol.*, vol. 8, Jan. 2021, doi: 10.3389/fbioe.2020.619066.

[18] European Commission, 'Finance and the Green Deal'. Accessed: Mar. 26, 2024. [Online]. Available: https://commission.europa.eu/strategy-and-policy/priorities-2019-2024/european-green-deal/finance-and-green-deal_en

[19] European Commission, 'The European Green Deal'. Accessed: Mar. 26, 2024. [Online]. Available: https://commission.europa.eu/strategy-and-policy/priorities-2019-2024/european-green-deal_en

[20] 'The European Green Deal - European Commission'. Accessed: Mar. 26, 2024. [Online]. Available: https://commission.europa.eu/strategy-and-policy/priorities-2019-2024/story-von-der-leyen-commission/european-green-deal_en

[21] 'Inforegio - Financing the green transition: The European Green Deal Investment Plan and Just Transition Mechanism'. Accessed: Mar. 26, 2024. [Online]. Available: https://ec.europa.eu/regional_policy/en/newsroom/news/2020/01/14-01-2020-financing-the-green-transition-the-european-green-deal-investment-plan-and-just-transition-mechanism

[22] 'InvestEU Programme - European Union'. Accessed: Mar. 26, 2024. [Online]. Available: https://investeu.europa.eu/investeu-programme_en

[23] 'CBE JU: enabling the European Green Deal | Circular Bio-based Europe Joint Undertaking (CBE JU)'. Accessed: Mar. 26, 2024. [Online]. Available: https://www.cbe.europa.eu/news/cbe-ju-enabling-european-green-deal

[24] 'Open calls for proposals | Circular Bio-based Europe Joint Undertaking (CBE JU)'. Accessed: Mar. 28, 2024. [Online]. Available: https://www.cbe.europa.eu/open-calls-proposals

[25] IEA Bioenergy: T42, 'Biorefineries: adding value to the sustainable utilisation of biomass', IEA, Copenhagen, Denmark, 2009. Accessed: Nov. 21, 2023. [Online]. Available: https://www.ieabioenergy.com/wp-content/uploads/2013/10/Task-42-Booklet.pdf

[26] F. Cherubini, 'The biorefinery concept: Using biomass instead of oil for producing energy and chemicals', *Energy Conversion and Management*, vol. 51, no. 7, pp. 1412–1421, Jul. 2010, doi: 10.1016/j.enconman.2010.01.015.

[27] F. Gírio *et al.*, 'Biorefineries in the World', in *Biorefineries: Targeting Energy, High Value Products and Waste Valorisation*, M. Rabaçal, A. F. Ferreira, C. A. M. Silva, and M. Costa, Eds., in Lecture Notes in Energy, Cham: Springer International Publishing, 2017, pp. 227–281. doi: 10.1007/978-3-319-48288-0_9.

[28] L. Bhatia, R. K. Bachheti, V. K. Garlapati, and A. K. Chandel, 'Third-generation biorefineries: a sustainable platform for food, clean energy, and nutraceuticals production', *Biomass Conv. Bioref.*, vol. 12, no. 9, pp. 4215–4230, Sep. 2022, doi: 10.1007/s13399-020-00843-6.

[29] H. R. Ghatak, 'Biorefineries from the perspective of sustainability: Feedstocks, products, and processes', *Renewable and Sustainable Energy Reviews*, vol. 15, no. 8, pp. 4042–4052, Oct. 2011, doi: 10.1016/j.rser.2011.07.034.

[30] K. Wagemann and N. Tippkötter, Eds., *Biorefineries*, vol. 166. in Advances in Biochemical Engineering/Biotechnology, vol. 166. Cham: Springer International Publishing, 2019. doi: 10.1007/978-3-319-97119-3.

[31] International Finance Corporation, 'Converting Biomass to Energy: A Guide for Developers and Investors', Jun. 2017, doi: 10.1596/28305.

[32] J. Shankar Tumuluru, C. T Wright, R. D Boardman, N. A Yancey, and S. Sokhansanj, 'A review on biomass classification and composition, co-firing issues and pretreatment methods', presented at the 2011 Louisville, Kentucky, August 7-10, 2011, in ASABE Paper No. 1110458. St. Joseph, MI: ASABE, 2011. doi: 10.13031/2013.37191.

[33] V. Singh *et al.*, 'Advancement on Biomass Classification, Analytical Methods for Characterization, and Its Economic Importance', in *Bioenergy Research: Biomass Waste to Energy*, M. Srivastava, N. Srivastava, and R. Singh, Eds., in Clean Energy Production Technologies, Singapore: Springer, 2021, pp. 249–272. doi: 10.1007/978-981-16-1862-8_10.

[34] J. Arauzo, F. Bimbela, J. Ábrego, J. L. Sánchez, and A. Gonzalo, 'Introducción a las tecnologías de aprovechamiento de biomasa', *An introduction to biomass valorisation technologies*, Sep. 2014, Accessed: Dec. 08, 2023. [Online]. Available: https://digital.csic.es/handle/10261/108763

[35] P. Mäki-Arvela, T. Salmi, B. Holmbom, S. Willför, and D. Yu. Murzin, 'Synthesis of Sugars by Hydrolysis of Hemicelluloses- A Review', *Chem. Rev.*, vol. 111, no. 9, pp. 5638–5666, Sep. 2011, doi: 10.1021/cr2000042.

[36] M. Kaltschmitt, 'Biomass as Renewable Source of Energy, Possible Conversion Routes', in *Encyclopedia of Sustainability Science and Technology*,

R. A. Meyers, Ed., New York, NY: Springer New York, 2012, pp. 1198–1231. doi: 10.1007/978-1-4419-0851-3_244.

[37] S2Biom, 'Vision for 1 billion dry tonnes lignocellulosic biomass as a contribution to biobased economy by 2030 in Europe', Nov. 2016. Accessed: Jan. 04, 2024. [Online]. Available: https://s2biom.wenr.wur.nl/doc/D8.2_S2Biom_Vision_for_1_billion_tonnes_biomass_2030.pdf

[38] C.-H. Zhou, X. Xia, C.-X. Lin, D.-S. Tong, and J. Beltramini, 'Catalytic conversion of lignocellulosic biomass to fine chemicals and fuels', *Chem. Soc. Rev.*, vol. 40, no. 11, pp. 5588–5617, Oct. 2011, doi: 10.1039/C1CS15124J.

[39] N. Romano, 'Chapter 19 - Alternative and new sources of feedstuffs', in *Enzymes in Human and Animal Nutrition*, C. S. Nunes and V. Kumar, Eds., Academic Press, 2018, pp. 381–401. doi: https://doi.org/10.1016/B978-0-12-805419-2.00019-8.

[40] A. G. McDonald and L. A. Donaldson, 'Wood, Constituents of', in *Encyclopedia of Materials: Science and Technology*, K. H. J. Buschow, R. W. Cahn, M. C. Flemings, B. Ilschner, E. J. Kramer, S. Mahajan, and P. Veyssière, Eds., Oxford: Elsevier, 2001, pp. 9612–9615. doi: 10.1016/B0-08-043152-6/01739-3.

[41] E. Rudnik, '10 - Compostable Polymer Materials: Definitions, Structures, and Methods of Preparation', in *Handbook of Biopolymers and Biodegradable Plastics*, S. Ebnesajjad, Ed., in Plastics Design Library, Boston: William Andrew Publishing, 2013, pp. 189–211. doi: 10.1016/B978-1-4557-2834-3.00010-0.

[42] R. Sun, X. F. Sun, and J. Tomkinson, 'Hemicelluloses and Their Derivatives', in *Hemicelluloses: Science and Technology*, vol. 864, in ACS Symposium Series, no. 864, vol. 864, American Chemical Society, 2003, pp. 2–22. doi: 10.1021/bk-2004-0864.ch001.

[43] H. V. Scheller and P. Ulvskov, 'Hemicelluloses', *Annual Review of Plant Biology*, vol. 61, no. 1, pp. 263–289, 2010, doi: 10.1146/annurev-arplant-042809-112315.

[44] J. Rao, Z. Lv, G. Chen, and F. Peng, 'Hemicellulose: Structure, chemical modification, and application', *Progress in Polymer Science*, vol. 140, p. 101675, May 2023, doi: 10.1016/j.progpolymsci.2023.101675.

[45] M. Erfani Jazi *et al.*, 'Structure, chemistry and physicochemistry of lignin for material functionalization', *SN Appl. Sci.*, vol. 1, no. 9, p. 1094, Aug. 2019, doi: 10.1007/s42452-019-1126-8.

[46] S. Constant *et al.*, 'New insights into the structure and composition of technical lignins: a comparative characterisation study', *Green Chemistry*, vol. 18, no. 9, pp. 2651–2665, 2016, doi: 10.1039/C5GC03043A.

[47] X. Wang, Q. Tian, Q. Li, C. Liao, M. He, and F. Liu, 'Lignin characteristics in soil profiles in different plant communities in a subtropical mixed forest', *Journal of Plant Ecology*, vol. 11, no. 4, pp. 560–568, May 2018, doi: 10.1093/jpe/rtx028.

[48] C. G. Yoo, X. Meng, Y. Pu, and A. J. Ragauskas, 'The critical role of lignin in lignocellulosic biomass conversion and recent pretreatment strategies: A comprehensive review', *Bioresource Technology*, vol. 301, p. 122784, Apr. 2020, doi: 10.1016/j.biortech.2020.122784.

[49] A. A. Vaidya, K. D. Murton, D. A. Smith, and G. Dedual, 'A review on organosolv pretreatment of softwood with a focus on enzymatic hydrolysis of cellulose', *Biomass Conv. Bioref.*, vol. 12, no. 11, pp. 5427–5442, Nov. 2022, doi: 10.1007/s13399-022-02373-9.

[50] A. R. Mankar, A. Pandey, A. Modak, and K. K. Pant, 'Pretreatment of lignocellulosic biomass: A review on recent advances', *Bioresource Technology*, vol. 334, p. 125235, Aug. 2021, doi: 10.1016/j.biortech.2021.125235.

[51] J. Zheng and L. Rehmann, 'Extrusion pretreatment of lignocellulosic biomass: a review', *Int J Mol Sci*, vol. 15, no. 10, pp. 18967–18984, Oct. 2014, doi: 10.3390/ijms151018967.

[52] A. T. Hoang *et al.*, 'Insight into the recent advances of microwave pretreatment technologies for the conversion of lignocellulosic biomass into sustainable biofuel', *Chemosphere*, vol. 281, p. 130878, Oct. 2021, doi: 10.1016/j.chemosphere.2021.130878.

[53] M. J. Bussemaker and D. Zhang, 'Effect of Ultrasound on Lignocellulosic Biomass as a Pretreatment for Biorefinery and Biofuel Applications', *Ind. Eng. Chem. Res.*, vol. 52, no. 10, pp. 3563–3580, Mar. 2013, doi: 10.1021/ie3022785.

[54] I. Ziegler-Devin, L. Chrusciel, and N. Brosse, 'Steam Explosion Pretreatment of Lignocellulosic Biomass: A Mini-Review of Theorical and Experimental Approaches', *Frontiers in Chemistry*, vol. 9, 2021, https://doi.org/10.3389/fchem.2021.705358

[55] H. Alizadeh, F. Teymouri, T. I. Gilbert, and B. E. Dale, 'Pretreatment of switchgrass by ammonia fiber explosion (AFEX)', *Appl Biochem Biotechnol*, vol. 124, no. 1, pp. 1133–1141, Mar. 2005, doi: 10.1385/ABAB:124:1-3:1133.

[56] X. Zhuang *et al.*, 'Liquid hot water pretreatment of lignocellulosic biomass for bioethanol production accompanying with high valuable products', *Bioresource Technology*, vol. 199, pp. 68–75, Jan. 2016, doi: 10.1016/j.biortech.2015.08.051.

[57] J. C. Solarte-Toro, J. M. Romero-García, J. C. Martínez-Patiño, E. Ruiz-Ramos, E. Castro-Galiano, and C. A. Cardona-Alzate, 'Acid pretreatment of lignocellulosic biomass for energy vectors production: A review focused on operational conditions and techno-economic assessment for bioethanol production', *Renewable and Sustainable Energy Reviews*, vol. 107, pp. 587–601, Jun. 2019, doi: 10.1016/j.rser.2019.02.024.

[58] J. S. Kim, Y. Y. Lee, and T. H. Kim, 'A review on alkaline pretreatment technology for bioconversion of lignocellulosic biomass', *Bioresource Technology*, vol. 199, pp. 42–48, Jan. 2016, doi: 10.1016/j.biortech.2015.08.085.

[59] X. Zhao, K. Cheng, and D. Liu, 'Organosolv pretreatment of lignocellulosic biomass for enzymatic hydrolysis', *Appl Microbiol Biotechnol*, vol. 82, no. 5, pp. 815–827, Apr. 2009, doi: 10.1007/s00253-009-1883-1.

[60] D. M. Alonso, S. G. Wettstein, and J. A. Dumesic, 'Gamma-valerolactone, a sustainable platform molecule derived from lignocellulosic biomass', *Green Chem.*, vol. 15, no. 3, pp. 584–595, Feb. 2013, doi: 10.1039/C3GC37065H.

[61] D. Fegyverneki, L. Orha, G. Láng, and I. T. Horváth, 'Gamma-valerolactone-based solvents', *Tetrahedron*, vol. 66, no. 5, pp. 1078–1081, Jan. 2010, doi: 10.1016/j.tet.2009.11.013.

[62] J. S. Luterbacher *et al.*, 'Nonenzymatic Sugar Production from Biomass Using Biomass-Derived γ-Valerolactone', *Science*, vol. 343, no. 6168, pp. 277–280, Jan. 2014, doi: 10.1126/science.1246748.

[63] D. M. Alonso *et al.*, 'Increasing the revenue from lignocellulosic biomass: Maximizing feedstock utilization', *Science Advances*, vol. 3, no. 5, p. e1603301, 2017, doi: 10.1126/sciadv.1603301.

[64] C. Parisi, 'Biorefineries distribution in the EU', *JRC Publications Repository*, Oct. 2018, doi: 10.2760/126478.

[65] E. Commission, *Insights into the European market for bio-based chemicals – Analysis based on 10 key product categories*. Publications Office, 2019. doi: doi/10.2760/549564.

[66] E. Commission, *EU biorefinery outlook to 2030 – Studies on support to research and innovation policy in the area of bio-based products and services*. Publications Office, 2021. doi: doi/10.2777/103465.

[67] D. Yue, S. Pandya, and F. You, 'Integrating Hybrid Life Cycle Assessment with Multiobjective Optimization: A Modeling Framework', *Environ. Sci. Technol.*, vol. 50, no. 3, pp. 1501–1509, Feb. 2016, doi: 10.1021/acs.est.5b04279.

[68] I. Ioannou, S. C. D'Angelo, Á. Galán-Martín, C. Pozo, J. Pérez-Ramírez, and G. Guillén-Gosálbez, 'Process modelling and life cycle assessment coupled with experimental work to shape the future sustainable production of chemicals and fuels', *React. Chem. Eng.*, vol. 6, no. 7, pp. 1179–1194, 2021, doi: 10.1039/D0RE00451K.

[69] R. Sacchi, 'PRospective EnvironMental Impact asSEment (premise): A streamlined approach to producing databases for prospective life cycle assessment using integrated assessment models', *Renewable and Sustainable Energy Reviews*, p. 12, 2022.

[70] R. Calvo-Serrano, M. Guo, C. Pozo, Á. Galán-Martín, and G. Guillén-Gosálbez, 'Biomass Conversion into Fuels, Chemicals, or Electricity? A Network-Based Life Cycle Optimization Approach Applied to the European Union', *ACS Sustainable Chem. Eng.*, vol. 7, no. 12, pp. 10570–10582, Jun. 2019, doi: 10.1021/acssuschemeng.9b01115.

[71] V. Negri *et al.*, 'Life cycle optimization of BECCS supply chains in the European Union', *Applied Energy*, vol. 298, p. 117252, Sep. 2021, doi: 10.1016/j.apenergy.2021.117252.

[72] F. Lechtenberg, 'flechtenberg/pulpo'. Nov. 30, 2023. Accessed: Apr. 07, 2024. [Online]. Available: https://github.com/flechtenberg/pulpo

[73] T. Werpy and G. Petersen, 'Top Value Added Chemicals from Biomass: Volume I -- Results of Screening for Potential Candidates from Sugars and Synthesis Gas', DOE/GO-102004-1992, 15008859, Aug. 2004. doi: 10.2172/15008859.

[74] J. J. Bozell and G. R. Petersen, 'Technology development for the production of biobased products from biorefinery carbohydrates—the US Department of Energy's "Top 10" revisited', *Green Chem.*, vol. 12, no. 4, p. 539, 2010, doi: 10.1039/b922014c.

[75] Karl J. Zeitsch, *The chemistry and technology of furfural and its many by-products*, 13 vols. in Sugar Series, no. 13. Elsevier, 2000. [Online]. Available: https://www.sciencedirect.com/bookseries/sugar-series/vol/13/suppl/C

[76] J. W. Döbereiner, 'Ueber die medicinische und chemische Anwendung und die vortheilhafte Darstellung der Ameisensäure', *Annalen der Pharmacie*, vol. 3, no. 2, pp. 141–146, 1832, doi: https://doi.org/10.1002/jlac.18320030206.

[77] H. E. Hoydonckx, W. M. Van Rhijn, W. Van Rhijn, D. E. De Vos, and P. A. Jacobs, 'Furfural and Derivatives', in *Ullmann's Encyclopedia of Industrial Chemistry*, Wiley-VCH Verlag GmbH & Co. KGaA, Ed., Weinheim, Germany, 2007, doi: 10.1002/14356007.a12_119.pub2.

[78] 'Furfural Market Size, Share, Growth & Trends Report, 2030'. Accessed: Aug. 10, 2023. [Online]. Available: https://www.grandviewresearch.com/industry-analysis/furfural-market

[79] 'Furfural Market, Industry Size Growth Forecast Report, [Latest]', MarketsandMarkets. Accessed: Apr. 07, 2024. [Online]. Available: https://www.marketsandmarkets.com/Market-Reports/furfural-market-101056456.html

[80] *Furfural chemicals and biofuels from agriculture: a report for the Rural Industries Research and Development Corporation.* Barton, A.C.T.: Rural Industries Research and Development Corporation, 2006. [Online]. Available: http://www.rirdc.gov.au/reports/EFM/06-127.pdf

[81] K. J. Yong *et al.*, 'Furfural production from biomass residues: Current technologies, challenges and future prospects', *Biomass and Bioenergy*, vol. 161, p. 106458, Jun. 2022, doi: 10.1016/j.biombioe.2022.106458.

[82] M. Dashtban, A. Gilbert, and P. Fatehi, 'Production of furfural: overview and challenges', *Journal of Science & Technology for Forest Products and Processes*, vol. 2, no. 4, p. 11, 2012.

[83] 'Illovo Sugar Africa - Home'. Accessed: Apr. 07, 2024. [Online]. Available: https://www.illovosugarafrica.com/

[84] 'Tanin d.d. Sevnica'. Accessed: Apr. 07, 2024. [Online]. Available: http://www.tanin.si/
[85] 'Lenzing Group'. Accessed: Apr. 07, 2024. [Online]. Available: https://www.lenzing.com/sustainability/production/biorefinery
[86] 'Silvateam', Silvateam. Accessed: Apr. 07, 2024. [Online]. Available: https://www.silvateam.com/es/
[87] https://www.stratviewresearch.com, 'Furfural Market Share, Forecast, Trend & Growth | 2023-28', stratviewresearch.com. Accessed: Aug. 10, 2023. [Online]. Available: https://www.stratviewresearch.com/1097/furfural-market.html
[88] D. Tin Win, 'Furfural - Gold from garbage', *AU Journal of Technology*, vol. 8, no. 4, pp. 185–190, Apr. 2005.
[89] D. J. Hayes, S. Fitzpatrick, M. H. B. Hayes, and J. R. H. Ross, 'The Biofine Process– Production of Levulinic Acid, Furfural, and Formic Acid from Lignocellulosic Feedstocks', in *Biorefineries-Industrial Processes and Products*, B. Kamm, P. R. Gruber, and M. Kamm, Eds., Weinheim, Germany: Wiley-VCH Verlag GmbH, 2005, pp. 139–164. doi: 10.1002/9783527619849.ch7.
[90] G. Marcotullio, 'The chemistry and technology of furfural production in modern lignocellulose-feedstock biorefineries', 2011.
[91] W. de Jong and G. Marcotullio, 'Overview of Biorefineries based on Co-Production of Furfural, Existing Concepts and Novel Developments', *International Journal of Chemical Reactor Engineering*, vol. 8, no. 1, 2010. https://doi.org/10.2202/1542-6580.2174
[92] R. J. Wooley and V. Putsche, 'Development of an ASPEN PLUS physical property database for biofuels components', National Renewable Energy Lab. (NREL), Golden, CO (United States), NREL/TP-425-20685, Apr. 1996. doi: 10.2172/257362.
[93] I. Agirrezabal-Telleria, J. Requies, M. B. Güemez, and P. L. Arias, 'Furfural production from xylose + glucose feedings and simultaneous N_2-stripping', *Green Chem.*, vol. 14, no. 11, pp. 3132–3140, Oct. 2012, doi: 10.1039/C2GC36092F.
[94] L. C. Nhien, N. V. D. Long, and M. Lee, 'Design and optimization of the levulinic acid recovery process from lignocellulosic biomass', *Chemical Engineering Research and Design*, vol. 107, pp. 126–136, Mar. 2016, doi: 10.1016/j.cherd.2015.09.013.
[95] G. Contreras-Zarazúa *et al.*, 'Inherently Safer Design and Optimization of Intensified Separation Processes for Furfural Production', *Ind. Eng. Chem. Res.*, vol. 58, no. 15, pp. 6105–6120, Apr. 2019, doi: 10.1021/acs.iecr.8b03646.
[96] L. Fele and V. Grilc, 'Separation of Furfural from Ternary Mixtures', *J. Chem. Eng. Data*, vol. 48, no. 3, pp. 564–570, Mar. 2003, doi: 10.1021/je020117y.
[97] R. E. Davis *et al.*, 'Process Design and Economics for the Conversion of Lignocellulosic Biomass to Hydrocarbon Fuels and Coproducts: 2018

Biochemical Design Case Update; Biochemical Deconstruction and Conversion of Biomass to Fuels and Products via Integrated Biorefinery Pathways', National Renewable Energy Lab. (NREL), Golden, CO (United States), NREL/TP-5100-71949, Nov. 2018. doi: 10.2172/1483234.

[98] N. Bhandari, D. G. Macdonald, and N. N. Bakhshi, 'Kinetic studies of corn stover saccharification using sulphuric acid', *Biotechnology and Bioengineering*, vol. 26, no. 4, pp. 320–327, 1984, doi: https://doi.org/10.1002/bit.260260405.

[99] V. Krzelj, J. Ferreira Liberal, M. Papaioannou, J. van der Schaaf, and M. F. Neira d'Angelo, 'Kinetic Model of Xylose Dehydration for a Wide Range of Sulfuric Acid Concentrations', *Ind. Eng. Chem. Res.*, vol. 59, no. 26, pp. 11991–12003, Jul. 2020, doi: 10.1021/acs.iecr.0c01197.

[100] G. Garrote, H. Domínguez, and J. C. Parajó, 'Generation of xylose solutions from Eucalyptus globulus wood by autohydrolysis-posthydrolysis processes: posthydrolysis kinetics', *Bioresour Technol*, vol. 79, no. 2, pp. 155–164, Sep. 2001, doi: 10.1016/s0960-8524(01)00044-x.

[101] 'Brightway LCA Software Framework — Brightway documentation'. Accessed: Apr. 07, 2024. [Online]. Available: https://docs.brightway.dev/en/latest/index.html

[102] 'The Activity Browser — An open source LCA software building on top of the brightway framework', *Software Impacts*, vol. 3, p. 100012, Feb. 2020, doi: 10.1016/j.simpa.2019.100012.

[103] E. Commission *et al.*, *Updated characterisation and normalisation factors for the environmental footprint 3.1 method*. Publications Office of the European Union, 2023. doi: doi/10.2760/798894.

[104] S. S. Hassan, G. A. Williams, and A. K. Jaiswal, 'Lignocellulosic Biorefineries in Europe: Current State and Prospects', *Trends in Biotechnology*, vol. 37, no. 3, pp. 231–234, Mar. 2019, doi: 10.1016/j.tibtech.2018.07.002.

[105] M. R. Yates and C. Y. Barlow, 'Life cycle assessments of biodegradable, commercial biopolymers—A critical review', *Resources, Conservation and Recycling*, vol. 78, pp. 54–66, Sep. 2013, doi: 10.1016/j.resconrec.2013.06.010.

[106] R. Kajaste, 'Chemicals from biomass – managing greenhouse gas emissions in biorefinery production chains – a review', *Journal of Cleaner Production*, vol. 75, pp. 1–10, Jul. 2014, doi: 10.1016/j.jclepro.2014.03.070.

[107] T. A. Hottle, M. M. Bilec, and A. E. Landis, 'Biopolymer production and end of life comparisons using life cycle assessment', *Resources, Conservation and Recycling*, vol. 122, pp. 295–306, Jul. 2017, doi: 10.1016/j.resconrec.2017.03.002.

[108] G. Fiorentino, M. Ripa, and S. Ulgiati, 'Chemicals from biomass: technological *versus* environmental feasibility. A review', *Biofuels, Bioprod. Bioref.*, vol. 11, no. 1, pp. 195–214, Jan. 2017, doi: 10.1002/bbb.1729.

[109] S. Kakadellis and Z. M. Harris, 'Don't scrap the waste: The need for broader system boundaries in bioplastic food packaging life-cycle assessment – A critical review', *Journal of Cleaner Production*, vol. 274, p. 122831, Nov. 2020, doi: 10.1016/j.jclepro.2020.122831.

[110] N. Ryan and P. Yaseneva, 'A critical review of life cycle assessment studies of woody biomass conversion to sugars', *Phil. Trans. R. Soc. A.*, vol. 379, no. 2206, p. 20200335, Sep. 2021, doi: 10.1098/rsta.2020.0335.

[111] N. Escobar and N. Laibach, 'Sustainability check for bio-based technologies: A review of process-based and life cycle approaches', *Renewable and Sustainable Energy Reviews*, vol. 135, p. 110213, Jan. 2021, doi: 10.1016/j.rser.2020.110213.

[112] S. Spierling *et al.*, 'Bio-based plastics - A review of environmental, social and economic impact assessments', *Journal of Cleaner Production*, vol. 185, pp. 476–491, Jun. 2018, doi: 10.1016/j.jclepro.2018.03.014.

[113] S. Walker and R. Rothman, 'Life cycle assessment of bio-based and fossil-based plastic: A review', *Journal of Cleaner Production*, vol. 261, p. 121158, Jul. 2020, doi: 10.1016/j.jclepro.2020.121158.

[114] M. Montazeri, G. G. Zaimes, V. Khanna, and M. J. Eckelman, 'Meta-Analysis of Life Cycle Energy and Greenhouse Gas Emissions for Priority Biobased Chemicals', *ACS Sustainable Chem. Eng.*, vol. 4, no. 12, pp. 6443–6454, Dec. 2016, doi: 10.1021/acssuschemeng.6b01217.

[115] P. Skoczinski *et al.*, 'Bio-based Building Blocks and Polymers – Global Capacities, Production and Trends 2020 – 2025', Renewable Carbon, Jan. 2021. [Online]. Available: https://renewable-carbon.eu/publications/product/bio-based-building-blocks-and-polymers-global-capacities-production-and-trends-2020-2025/

[116] H. von Blottnitz and M. A. Curran, 'A review of assessments conducted on bioethanol as a transportation fuel from a net energy, greenhouse gas, and environmental life cycle perspective', *Journal of Cleaner Production*, vol. 15, no. 7, pp. 607–619, 2007, doi: https://doi.org/10.1016/j.jclepro.2006.03.002.

[117] A. Singh, D. Pant, N. E. Korres, A.-S. Nizami, S. Prasad, and J. D. Murphy, 'Key issues in life cycle assessment of ethanol production from lignocellulosic biomass: Challenges and perspectives', *Bioresource Technology*, vol. 101, no. 13, pp. 5003–5012, 2010, doi: https://doi.org/10.1016/j.biortech.2009.11.062.

[118] A. L. Borrion, M. C. McManus, and G. P. Hammond, 'Environmental life cycle assessment of lignocellulosic conversion to ethanol: A review', *Renewable and Sustainable Energy Reviews*, vol. 16, no. 7, pp. 4638–4650, 2012, doi: https://doi.org/10.1016/j.rser.2012.04.016.

[119] M. Morales, J. Quintero, R. Conejeros, and G. Aroca, 'Life cycle assessment of lignocellulosic bioethanol: Environmental impacts and energy balance', *Renewable and Sustainable Energy Reviews*, vol. 42, pp. 1349–1361, 2015, doi: https://doi.org/10.1016/j.rser.2014.10.097.

[120] K. Gerbrandt *et al.*, 'Life cycle assessment of lignocellulosic ethanol: a review of key factors and methods affecting calculated GHG emissions and energy use', *Current Opinion in Biotechnology*, vol. 38, pp. 63–70, 2016, doi: https://doi.org/10.1016/j.copbio.2015.12.021.

[121] M. Morales *et al.*, 'Environmental and economic assessment of lactic acid production from glycerol using cascade bio- and chemocatalysis', *Energy Environ. Sci.*, vol. 8, no. 2, pp. 558–567, 2015, doi: 10.1039/C4EE03352C.

[122] A. G. Daful, K. Haigh, P. Vaskan, and J. F. Görgens, 'Environmental impact assessment of lignocellulosic lactic acid production: Integrated with existing sugar mills', *Food and Bioproducts Processing*, vol. 99, pp. 58–70, Jul. 2016, doi: 10.1016/j.fbp.2016.04.005.

[123] F. K. Adom and J. B. Dunn, 'Life cycle analysis of corn-stover-derived polymer-grade l-lactic acid and ethyl lactate: greenhouse gas emissions and fossil energy consumption', *Biofuels, Bioprod. Bioref.*, vol. 11, no. 2, pp. 258–268, Mar. 2017, doi: 10.1002/bbb.1734.

[124] R. Parajuli, M. T. Knudsen, M. Birkved, S. N. Djomo, A. Corona, and T. Dalgaard, 'Environmental impacts of producing bioethanol and biobased lactic acid from standalone and integrated biorefineries using a consequential and an attributional life cycle assessment approach', *Science of The Total Environment*, vol. 598, pp. 497–512, Nov. 2017, doi: 10.1016/j.scitotenv.2017.04.087.

[125] A. Gezae Daful and J. F. Görgens, 'Techno-economic analysis and environmental impact assessment of lignocellulosic lactic acid production', *Chemical Engineering Science*, vol. 162, pp. 53–65, Apr. 2017, doi: 10.1016/j.ces.2016.12.054.

[126] M. A. Mandegari, S. Farzad, E. van Rensburg, and J. F. Görgens, 'Multi-criteria analysis of a biorefinery for co-production of lactic acid and ethanol from sugarcane lignocellulose', *Biofuels, Bioprod. Bioref.*, vol. 11, no. 6, pp. 971–990, Nov. 2017, doi: 10.1002/bbb.1801.

[127] R. Helmes *et al.*, 'Environmental Impacts of Experimental Production of Lactic Acid for Bioplastics from Ulva spp.', *Sustainability*, vol. 10, no. 7, p. 2462, Jul. 2018, doi: 10.3390/su10072462.

[128] S. Awiszus, K. Meissner, S. Reyer, and J. Müller, 'Environmental Assessment of a Bio-Refinery Concept Comprising Biogas Production, Lactic Acid Extraction and Plant Nutrient Recovery', *Sustainability*, vol. 11, no. 9, p. 2601, May 2019, doi: 10.3390/su11092601.

[129] Ó. Ögmundarson, S. Sukumara, A. Laurent, and P. Fantke, 'Environmental hotspots of lactic acid production systems', *GCB Bioenergy*, vol. 12, no. 1, pp. 19–38, Jan. 2020, doi: 10.1111/gcbb.12652.

[130] B. Khoshnevisan *et al.*, 'Environmental life cycle assessment of different biorefinery platforms valorizing municipal solid waste to bioenergy, microbial protein, lactic and succinic acid', *Renewable and Sustainable Energy Reviews*, vol. 117, p. 109493, Jan. 2020, doi: 10.1016/j.rser.2019.109493.

[131] Q. Fei *et al.*, 'Biological valorization of natural gas for the production of lactic acid: Techno-economic analysis and life cycle assessment',

Biochemical Engineering Journal, vol. 158, p. 107500, Jun. 2020, doi: 10.1016/j.bej.2020.107500.

[132] E. R. Pachón, P. Mandade, and E. Gnansounou, 'Conversion of vine shoots into bioethanol and chemicals: Prospective LCA of biorefinery concept', *Bioresource Technology*, vol. 303, p. 122946, May 2020, doi: 10.1016/j.biortech.2020.122946.

[133] P. F. Albizzati, D. Tonini, and T. F. Astrup, 'High-value products from food waste: An environmental and socio-economic assessment', *Science of The Total Environment*, vol. 755, p. 142466, Feb. 2021, doi: 10.1016/j.scitotenv.2020.142466.

[134] U. Lee, A. Bhatt, T. R. Hawkins, L. Tao, P. T. Benavides, and M. Wang, 'Life cycle analysis of renewable natural gas and lactic acid production from waste feedstocks', *Journal of Cleaner Production*, vol. 311, p. 127653, Aug. 2021, doi: 10.1016/j.jclepro.2021.127653.

[135] M. Munagala, Y. Shastri, K. Nalawade, K. Konde, and S. Patil, 'Life cycle and economic assessment of sugarcane bagasse valorization to lactic acid', *Waste Management*, vol. 126, pp. 52–64, May 2021, doi: 10.1016/j.wasman.2021.02.052.

[136] Y. Li *et al.*, 'Sustainable Lactic Acid Production from Lignocellulosic Biomass', *ACS Sustainable Chem. Eng.*, vol. 9, no. 3, pp. 1341–1351, Jan. 2021, doi: 10.1021/acssuschemeng.0c08055.

[137] B. Cok, I. Tsiropoulos, A. L. Roes, and M. K. Patel, 'Succinic acid production derived from carbohydrates: An energy and greenhouse gas assessment of a platform chemical toward a bio-based economy', *Biofuels, Bioprod. Bioref.*, vol. 8, no. 1, pp. 16–29, Jan. 2014, doi: 10.1002/bbb.1427.

[138] F. Adom, J. B. Dunn, J. Han, and N. Sather, 'Life-Cycle Fossil Energy Consumption and Greenhouse Gas Emissions of Bioderived Chemicals and Their Conventional Counterparts', *Environ. Sci. Technol.*, vol. 48, no. 24, pp. 14624–14631, Dec. 2014, doi: 10.1021/es503766e.

[139] E. Gnansounou and J. Kenthorai Raman, 'Life cycle assessment of algae biodiesel and its co-products', *Applied Energy*, vol. 161, pp. 300–308, Jan. 2016, doi: 10.1016/j.apenergy.2015.10.043.

[140] M. Morales *et al.*, 'Sustainability assessment of succinic acid production technologies from biomass using metabolic engineering', *Energy Environ. Sci.*, vol. 9, no. 9, pp. 2794–2805, 2016, doi: 10.1039/C6EE00634E.

[141] H. I. Moussa, A. Elkamel, and S. B. Young, 'Assessing energy performance of bio-based succinic acid production using LCA', *Journal of Cleaner Production*, vol. 139, pp. 761–769, Dec. 2016, doi: 10.1016/j.jclepro.2016.08.104.

[142] A. Zucaro, A. Forte, and A. Fierro, 'Greenhouse gas emissions and non-renewable energy use profiles of bio-based succinic acid from Arundo donax L. lignocellulosic feedstock', *Clean Techn Environ Policy*, vol. 19, no. 8, pp. 2129–2143, Oct. 2017, doi: 10.1007/s10098-017-1401-6.

[143] S. González-García, L. Argiz, P. Míguez, and B. Gullón, 'Exploring the production of bio-succinic acid from apple pomace using an

environmental approach', *Chemical Engineering Journal*, vol. 350, pp. 982–991, Oct. 2018, doi: 10.1016/j.cej.2018.06.052.

[144] H. Cai, J. Han, M. Wang, R. Davis, M. Biddy, and E. Tan, 'Life-cycle analysis of integrated biorefineries with co-production of biofuels and bio-based chemicals: co-product handling methods and implications', *Biofuels, Bioprod. Bioref.*, vol. 12, no. 5, pp. 815–833, Sep. 2018, doi: 10.1002/bbb.1893.

[145] B. Brunklaus, E. Rex, E. Carlsson, and J. Berlin, 'The future of Swedish food waste: An environmental assessment of existing and prospective valorization techniques', *Journal of Cleaner Production*, vol. 202, pp. 1–10, Nov. 2018, doi: 10.1016/j.jclepro.2018.07.240.

[146] A. Foulet, T. Bouchez, E. Desmond-Le Quéméner, L. Giard, L. Renvoisé, and L. Aissani, 'Eco-design of microbial electrochemical technologies for the production of waste-based succinic acid thanks to a life cycle assessment', *Journal of Cleaner Production*, vol. 225, pp. 1155–1168, Jul. 2019, doi: 10.1016/j.jclepro.2019.03.231.

[147] S. Gadkari, D. Kumar, Z. Qin, C. S. Ki Lin, and V. Kumar, 'Life cycle analysis of fermentative production of succinic acid from bread waste', *Waste Management*, vol. 126, pp. 861–871, May 2021, doi: 10.1016/j.wasman.2021.04.013.

[148] M. Nieder-Heitmann, K. F. Haigh, and J. F. Görgens, 'Life cycle assessment and multi-criteria analysis of sugarcane biorefinery scenarios: Finding a sustainable solution for the South African sugar industry', *Journal of Cleaner Production*, vol. 239, p. 118039, Dec. 2019, doi: 10.1016/j.jclepro.2019.118039.

[149] R. H. Hafyan, L. Bhullar, Z. A. Putra, M. R. Bilad, M. D. H. Wirzal, and N. A. H. M. Nordin, 'Sustainability assessment of levulinic acid and succinic acid production from empty fruit bunch', *IOP Conf. Ser.: Mater. Sci. Eng.*, vol. 778, p. 012140, May 2020, doi: 10.1088/1757-899X/778/1/012140.

[150] E. Stylianou *et al.*, 'Bioprocess development using organic biowaste and sustainability assessment of succinic acid production with engineered Yarrowia lipolytica strain', *Biochemical Engineering Journal*, vol. 174, p. 108099, Oct. 2021, doi: 10.1016/j.bej.2021.108099.

[151] A. Shaji, Y. Shastri, V. Kumar, V. V. Ranade, and N. Hindle, 'Economic and Environmental Assessment of Succinic Acid Production from Sugarcane Bagasse', *ACS Sustainable Chem. Eng.*, vol. 9, no. 38, pp. 12738–12746, Sep. 2021, doi: 10.1021/acssuschemeng.1c02483.

[152] R. Dickson *et al.*, 'Sustainable bio-succinic acid production: superstructure optimization, techno-economic, and lifecycle assessment', *Energy Environ. Sci.*, vol. 14, no. 6, pp. 3542–3558, 2021, doi: 10.1039/D0EE03545A.

[153] S. Bello, D. Ladakis, S. González-García, G. Feijoo, A. Koutinas, and M. T. Moreira, 'Renewable carbon opportunities in the production of succinic acid applying attributional and consequential modelling',

Chemical Engineering Journal, vol. 428, p. 132011, Jan. 2022, doi: 10.1016/j.cej.2021.132011.

[154] H. H. Khoo, L. L. Wong, J. Tan, V. Isoni, and P. Sharratt, 'Synthesis of 2-methyl tetrahydrofuran from various lignocellulosic feedstocks: Sustainability assessment via LCA', *Resources, Conservation and Recycling*, vol. 95, pp. 174–182, Feb. 2015, doi: 10.1016/j.resconrec.2014.12.013.

[155] S. González-García, B. Gullón, S. Rivas, G. Feijoo, and M. T. Moreira, 'Environmental performance of biomass refining into high-added value compounds', *Journal of Cleaner Production*, vol. 120, pp. 170–180, May 2016, doi: 10.1016/j.jclepro.2016.02.015.

[156] J. Sadhukhan and E. Martinez-Hernandez, 'Material flow and sustainability analyses of biorefining of municipal solid waste', *Bioresource Technology*, vol. 243, pp. 135–146, Nov. 2017, doi: 10.1016/j.biortech.2017.06.078.

[157] V. Isoni, D. Kumbang, P. N. Sharratt, and H. H. Khoo, 'Biomass to levulinic acid: A techno-economic analysis and sustainability of biorefinery processes in Southeast Asia', *Journal of Environmental Management*, vol. 214, pp. 267–275, May 2018, doi: 10.1016/j.jenvman.2018.03.012.

[158] H. H. Khoo, R. M. Eufrasio-Espinosa, L. S. C. Koh, P. N. Sharratt, and V. Isoni, 'Sustainability assessment of biorefinery production chains: A combined LCA-supply chain approach', *Journal of Cleaner Production*, vol. 235, pp. 1116–1137, Oct. 2019, doi: 10.1016/j.jclepro.2019.07.007.

[159] K. K. Kapanji, S. Farzad, and J. F. Görgens, 'Life cycle and sustainability assessments of biorefineries producing glucaric acid, sorbitol or levulinic acid annexed to a sugar mill', *Journal of Cleaner Production*, vol. 295, p. 126339, May 2021, doi: 10.1016/j.jclepro.2021.126339.

[160] J. Hong, J. Zhou, and J. Hong, 'Environmental and economic impact of furfuralcohol production using corncob as a raw material', *Int J Life Cycle Assess*, vol. 20, no. 5, pp. 623–631, May 2015, doi: 10.1007/s11367-015-0854-2.

[161] J. K. Raman and E. Gnansounou, 'LCA of bioethanol and furfural production from vetiver', *Bioresource Technology*, vol. 185, pp. 202–210, Jun. 2015, doi: 10.1016/j.biortech.2015.02.096.

[162] V. Aristizábal-Marulanda, J. A. Poveda-Giraldo, and C. A. Cardona Alzate, 'Comparison of furfural and biogas production using pentoses as platform', *Science of The Total Environment*, vol. 728, p. 138841, Aug. 2020, doi: 10.1016/j.scitotenv.2020.138841.

[163] H. Schöppe, P. Kleine-Möllhoff, and R. Epple, 'Energy and Material Flows and Carbon Footprint Assessment Concerning the Production of HMF and Furfural from a Cellulosic Biomass', *Processes*, vol. 8, no. 1, p. 119, Jan. 2020, doi: 10.3390/pr8010119.

[164] A. S. Putra, R. Noguchi, T. Ahamed, A. Nakagawa-Izumi, and H. Ohi, 'Development of integrated oil palm empty fruit bunches (EFB)-based dissolving pulp and furfural production: a consequential LCA approach',

Int J Life Cycle Assess, vol. 26, no. 1, pp. 175–188, Jan. 2021, doi: 10.1007/s11367-020-01833-6.

[165] M. A. Thompson, A. Mohajeri, and A. Mirkouei, 'Comparison of pyrolysis and hydrolysis processes for furfural production from sugar beet pulp: A case study in southern Idaho, USA', *Journal of Cleaner Production*, vol. 311, p. 127695, Aug. 2021, doi: 10.1016/j.jclepro.2021.127695.

[166] C.-M. Lam, I. K. M. Yu, S.-C. Hsu, and D. C. W. Tsang, 'Life-cycle assessment on food waste valorisation to value-added products', *Journal of Cleaner Production*, vol. 199, pp. 840–848, Oct. 2018, doi: 10.1016/j.jclepro.2018.07.199.

[167] S. Bello, I. Salim, P. Méndez-Trelles, E. Rodil, G. Feijoo, and M. T. Moreira, 'Environmental sustainability assessment of HMF and FDCA production from lignocellulosic biomass through life cycle assessment (LCA)', *Holzforschung*, vol. 73, no. 1, pp. 105–115, Dec. 2018, doi: 10.1515/hf-2018-0100.

[168] C. Isola *et al.*, 'Life cycle assessment of photodegradable polymeric material derived from renewable bioresources', *Journal of Cleaner Production*, vol. 142, pp. 2935–2944, Jan. 2017, doi: 10.1016/j.jclepro.2016.10.177.

[169] M. N. García González, P. Börjesson, M. Levi, and S. Turri, 'Development and Life Cycle Assessment of Polyester Binders Containing 2,5-Furandicarboxylic Acid and Their Polyurethane Coatings', *J Polym Environ*, vol. 26, no. 9, pp. 3626–3637, Sep. 2018, doi: 10.1007/s10924-018-1234-3.

[170] S. Bello, P. Méndez-Trelles, E. Rodil, G. Feijoo, and M. T. Moreira, 'Towards improving the sustainability of bioplastics: Process modelling and life cycle assessment of two separation routes for 2,5-furandicarboxylic acid', *Separation and Purification Technology*, vol. 233, p. 116056, Feb. 2020, doi: 10.1016/j.seppur.2019.116056.

[171] H. Kim, J. Choi, J. Park, and W. Won, 'Production of a sustainable and renewable biomass-derived monomer: conceptual process design and techno-economic analysis', *Green Chem.*, vol. 22, no. 20, pp. 7070–7079, 2020, doi: 10.1039/D0GC02258F.

[172] J. Hong, Y. Zhang, X. Xu, and X. Li, 'Life cycle assessment of corn- and cassava-based ethylene production', *Biomass and Bioenergy*, vol. 67, pp. 304–311, Aug. 2014, doi: 10.1016/j.biombioe.2014.05.014.

[173] C. Liptow, A.-M. Tillman, and M. Janssen, 'Life cycle assessment of biomass-based ethylene production in Sweden — is gasification or fermentation the environmentally preferable route?', *Int J Life Cycle Assess*, vol. 20, no. 5, pp. 632–644, May 2015, doi: 10.1007/s11367-015-0855-1.

[174] M. Yang, X. Tian, and F. You, 'Manufacturing Ethylene from Wet Shale Gas and Biomass: Comparative Technoeconomic Analysis and Environmental Life Cycle Assessment', *Ind. Eng. Chem. Res.*, vol. 57, no. 17, pp. 5980–5998, May 2018, doi: 10.1021/acs.iecr.7b03731.

[175] B. Alonso-Fariñas, A. Gallego-Schmid, P. Haro, and A. Azapagic, 'Environmental assessment of thermo-chemical processes for bio-ethylene production in comparison with bio-chemical and fossil-based ethylene', *Journal of Cleaner Production*, vol. 202, pp. 817–829, Nov. 2018, doi: 10.1016/j.jclepro.2018.08.147.

[176] Z. Zhao, K. Chong, J. Jiang, K. Wilson, X. Zhang, and F. Wang, 'Low-carbon roadmap of chemical production: A case study of ethylene in China', *Renewable and Sustainable Energy Reviews*, vol. 97, pp. 580–591, Dec. 2018, doi: 10.1016/j.rser.2018.08.008.

[177] A. Somoza-Tornos, A. Gonzalez-Garay, C. Pozo, M. Graells, A. Espuña, and G. Guillén-Gosálbez, 'Realizing the Potential High Benefits of Circular Economy in the Chemical Industry: Ethylene Monomer Recovery via Polyethylene Pyrolysis', *ACS Sustainable Chem. Eng.*, vol. 8, no. 9, pp. 3561–3572, Mar. 2020, doi: 10.1021/acssuschemeng.9b04835.

[178] R. Akmalina and M. G. Pawitra, 'Life cycle assessment of ethylene production from empty fruit bunch', *Asia-Pac J Chem Eng*, vol. 15, no. 3, May 2020, doi: 10.1002/apj.2436.

[179] J. B. J. H. van Duuren, B. Brehmer, A. E. Mars, G. Eggink, V. A. P. M. dos Santos, and J. P. M. Sanders, 'A limited LCA of bio-adipic acid: Manufacturing the nylon-6,6 precursor adipic acid using the benzoic acid degradation pathway from different feedstocks', *Biotechnol. Bioeng.*, vol. 108, no. 6, pp. 1298–1306, Jun. 2011, doi: 10.1002/bit.23074.

[180] R. Aryapratama and M. Janssen, 'Prospective life cycle assessment of bio-based adipic acid production from forest residues', *Journal of Cleaner Production*, vol. 164, pp. 434–443, Oct. 2017, doi: 10.1016/j.jclepro.2017.06.222.

[181] A. Corona, M. J. Biddy, D. R. Vardon, M. Birkved, M. Z. Hauschild, and G. T. Beckham, 'Life cycle assessment of adipic acid production from lignin', *Green Chem.*, vol. 20, no. 16, pp. 3857–3866, 2018, doi: 10.1039/C8GC00868J.

[182] J. B. J. H. Duuren *et al.*, 'Limited life cycle and cost assessment for the bioconversion of lignin-derived aromatics into adipic acid', *Biotechnology and Bioengineering*, vol. 117, no. 5, pp. 1381–1393, May 2020, doi: 10.1002/bit.27299.

[183] B. Choe, S. Lee, and W. Won, 'Coproduction of butene oligomers and adipic acid from lignocellulosic biomass: Process design and evaluation', *Energy*, vol. 235, p. 121278, Nov. 2021, doi: 10.1016/j.energy.2021.121278.

[184] B. Choe, S. Lee, H. Lee, J. Lee, H. Lim, and W. Won, 'Integrated strategy for coproducing bioethanol and adipic acid from lignocellulosic biomass', *Journal of Cleaner Production*, vol. 311, p. 127849, Aug. 2021, doi: 10.1016/j.jclepro.2021.127849.

[185] A. T. Ubando, C. B. Felix, and W.-H. Chen, 'Biorefineries in circular bioeconomy: A comprehensive review', *Bioresource Technology*, vol. 299, p. 122585, 2020, doi: https://doi.org/10.1016/j.biortech.2019.122585.

[186] S. A. Miller and G. A. Keoleian, 'Framework for Analyzing Transformative Technologies in Life Cycle Assessment', *Environ. Sci. Technol.*, vol. 49, no. 5, pp. 3067–3075, Mar. 2015, doi: 10.1021/es505217a.

[187] Y. Yao and E. Masanet, 'Life-cycle modeling framework for generating energy and greenhouse gas emissions inventory of emerging technologies in the chemical industry', *Journal of Cleaner Production*, vol. 172, pp. 768–777, 2018, doi: https://doi.org/10.1016/j.jclepro.2017.10.125.

[188] E. G. Hertwich *et al.*, 'Integrated life-cycle assessment of electricity-supply scenarios confirms global environmental benefit of low-carbon technologies', *Proc Natl Acad Sci USA*, vol. 112, no. 20, pp. 6277–6282, May 2015, doi: 10.1073/pnas.1312753111.

[189] O. Platnieks, S. Gaidukovs, V. K. Thakur, A. Barkane, and S. Beluns, 'Bio-based poly (butylene succinate): Recent progress, challenges and future opportunities', *European Polymer Journal*, vol. 161, p. 110855, 2021, doi: https://doi.org/10.1016/j.eurpolymj.2021.110855.

[190] K. J. Jem and B. Tan, 'The development and challenges of poly (lactic acid) and poly (glycolic acid)', *Advanced Industrial and Engineering Polymer Research*, vol. 3, no. 2, pp. 60–70, 2020, doi: https://doi.org/10.1016/j.aiepr.2020.01.002.

[191] 'ISO 14044 - Environmental management — Life cycle assessment — Requirements and guidelines'. International Organization for Standardization, Jul. 2006. [Online]. Available: https://www.iso.org/standard/38498.html

[192] European Commission. Joint Research Centre. Institute for Environment and Sustainability, *International Reference Life Cycle Data System (ILCD) Handbook: general guide for life cycle assessment: detailed guidance.* LU: Publications Office, 2010. Accessed: Jan. 19, 2022. [Online]. Available: https://data.europa.eu/doi/10.2788/38479

[193] R. Heijungs *et al.*, 'System Expansion and Substitution in LCA: A Lost Opportunity of ISO 14044 Amendment 2', *Frontiers in Sustainability*, vol. 2, 2021, Accessed: Jul. 05, 2022. [Online]. Available: https://www.frontiersin.org/articles/10.3389/frsus.2021.692055

[194] International Organization for Standarization, Ed., 'ISO 14044:2006/AMD 2:2020 Environmental management — Life cycle assessment — Requirements and guidelines — Amendment 2'. Sep. 2020. [Online]. Available: https://www.iso.org/standard/76122.html

[195] B. P. Weidema, M. Pizzol, J. Schmidt, and G. Thoma, 'Attributional or consequential Life Cycle Assessment: A matter of social responsibility', *Journal of Cleaner Production*, vol. 174, pp. 305–314, Feb. 2018, doi: 10.1016/j.jclepro.2017.10.340.

[196] R. Heijungs and M. A. J. Huijbregts, 'A Review of Approaches to Treat Uncertainty in LCA', presented at the International Congress on Environmental Modelling and Software, Osnabrük, Germany, 2004, p.

9. [Online]. Available: https://scholarsarchive.byu.edu/iemssconference/2004/all/197

[197] C. R. Bojacá and E. Schrevens, 'Parameter uncertainty in LCA: stochastic sampling under correlation', *Int J Life Cycle Assess*, vol. 15, no. 3, pp. 238–246, Mar. 2010, doi: 10.1007/s11367-010-0150-0.

[198] M. A. J. Huijbregts, W. Gilijamse, A. M. J. Ragas, and L. Reijnders, 'Evaluating Uncertainty in Environmental Life-Cycle Assessment. A Case Study Comparing Two Insulation Options for a Dutch One-Family Dwelling', *Environ. Sci. Technol.*, vol. 37, no. 11, pp. 2600–2608, Jun. 2003, doi: 10.1021/es020971.

[199] A. Mahmood, V. Varabuntoonvit, J. Mungkalasiri, T. Silalertruksa, and S. H. Gheewala, 'A Tier-Wise Method for Evaluating Uncertainty in Life Cycle Assessment', *Sustainability*, vol. 14, no. 20, p. 13400, Oct. 2022, doi: 10.3390/su142013400.

[200] B. P. Weidema and M. S. Wesnæs, 'Data quality management for life cycle inventories—an example of using data quality indicators', *Journal of Cleaner Production*, vol. 4, no. 3, pp. 167–174, 1996, doi: https://doi.org/10.1016/S0959-6526(96)00043-1.

[201] N. Thonemann, A. Schulte, and D. Maga, 'How to Conduct Prospective Life Cycle Assessment for Emerging Technologies? A Systematic Review and Methodological Guidance', *Sustainability*, vol. 12, no. 3, p. 1192, Feb. 2020, doi: 10.3390/su12031192.

[202] M. Guo and R. J. Murphy, 'LCA data quality: Sensitivity and uncertainty analysis', *Science of The Total Environment*, vol. 435–436, pp. 230–243, Oct. 2012, doi: 10.1016/j.scitotenv.2012.07.006.

[203] B. A. Wender *et al.*, 'Anticipatory life-cycle assessment for responsible research and innovation', *Journal of Responsible Innovation*, vol. 1, no. 2, pp. 200–207, 2014, doi: 10.1080/23299460.2014.920121.

[204] F. Piccinno, R. Hischier, S. Seeger, and C. Som, 'From laboratory to industrial scale: a scale-up framework for chemical processes in life cycle assessment studies', *Journal of Cleaner Production*, vol. 135, pp. 1085–1097, 2016, doi: https://doi.org/10.1016/j.jclepro.2016.06.164.

[205] T. Bicalho, I. Sauer, A. Rambaud, and Y. Altukhova, 'LCA data quality: A management science perspective', *Journal of Cleaner Production*, vol. 156, pp. 888–898, 2017, doi: https://doi.org/10.1016/j.jclepro.2017.03.229.

[206] Directorate-General for Environment, 'COMMISSION RECOMMENDATION (EU) 2021/2279 on the use of the Environmental Footprint methods to measure and communicate the life cycle environmental performance of products and organisations'. Dec. 15, 2021. [Online]. Available: https://eur-lex.europa.eu/legal-content/EN/TXT/?uri=CELEX%3A32021H2279

[207] M. A. J. Huijbregts *et al.*, 'ReCiPe 2016 v1.1 A harmonized life cycle impact assessment method at midpoint and endpoint level Report I: Characterization'. *The International Journal of Life Cycle Assessment*, vol. 22, pp. 138-147, 2017, doi: 10.1007/s11367-016-1246-y

[208] J. B. Guinée and E. Lindeijer, *Handbook on Life Cycle Assessment: Operational Guide to the ISO Standards*, vol. 7. in Eco-Efficiency in Industry and Science. Springer Netherlands, 2002. [Online]. Available: https://books.google.es/books?id=Q1VYuV5vc8UC

[209] O. Jolliet *et al.*, 'IMPACT 2002+: A new life cycle impact assessment methodology', *Int J LCA*, vol. 8, no. 6, p. 324, Nov. 2003, doi: 10.1007/BF02978505.

[210] J. Bare, 'Tool for the Reduction and Assessment of Chemical and Other Environmental Impacts (TRACI) TRACI version 2.1 User's Guide'. U.S. EPA Office of Research and Development, 2014.

[211] L. Meyer, S. Brinkman, L. van Kesteren, N. Leprince-Ringuet, and F. van Boxmeer, 'IPCC, 2014: Climate Change 2014: Synthesis Report. Contribution of Working Groups I, II and III to the Fifth Assessment Report of the Intergovernmental Panel on Climate Change'. 2014.

[212] E. Calvo Buendía *et al.*, '2019 Refinement to the 2006 IPCC Guidelines for National Greenhouse Gas Inventories'. 2019. [Online]. Available: https://www.ipcc-nggip.iges.or.jp/public/2019rf/index.html

[213] P. A. Arias *et al.*, 'Technical Summary. In Climate Change 2021: The Physical Science Basis. Contribution of Working Group I to the Sixth Assessment Report of the Intergovernmental Panel on Climate Change', pp. 33–114, 2021, doi: 10.1017/9781009157896.002.

[214] R. F. M. Teixeira, D. Maia de Souza, M. P. Curran, A. Antón, O. Michelsen, and L. Milà i Canals, 'Towards consensus on land use impacts on biodiversity in LCA: UNEP/SETAC Life Cycle Initiative preliminary recommendations based on expert contributions', *Journal of Cleaner Production*, vol. 112, pp. 4283–4287, Jan. 2016, doi: 10.1016/j.jclepro.2015.07.118.

[215] M. Damiani, T. Sinkko, C. Caldeira, D. Tosches, M. Robuchon, and S. Sala, 'Critical Review of Methods and Models for Biodiversity Impact Assessment and Their Applicability in the LCA Context'. Rochester, NY, Nov. 17, 2022. doi: 10.2139/ssrn.4279734.

[216] E. I. Wiloso, R. Heijungs, G. Huppes, and K. Fang, 'Effect of biogenic carbon inventory on the life cycle assessment of bioenergy: challenges to the neutrality assumption', *Journal of Cleaner Production*, vol. 125, pp. 78–85, Jul. 2016, doi: 10.1016/j.jclepro.2016.03.096.

[217] W. Liu *et al.*, 'Analysis of the Global Warming Potential of Biogenic CO_2 Emission in Life Cycle Assessments', *Sci Rep*, vol. 7, no. 1, p. 39857, Feb. 2017, doi: 10.1038/srep39857.

[218] R. Garcia, R. A. F. Alvarenga, S. Huysveld, J. Dewulf, and K. Allacker, 'Accounting for biogenic carbon and end-of-life allocation in life cycle assessment of multi-output wood cascade systems', *Journal of Cleaner Production*, vol. 275, p. 122795, Dec. 2020, doi: 10.1016/j.jclepro.2020.122795.

[219] C. Liptow, M. Janssen, and A.-M. Tillman, 'Accounting for effects of carbon flows in LCA of biomass-based products—exploration and

evaluation of a selection of existing methods', *Int J Life Cycle Assess*, vol. 23, no. 11, pp. 2110–2125, Nov. 2018, doi: 10.1007/s11367-018-1436-x.

[220] A. Levasseur, P. Lesage, M. Margni, and R. Samson, 'Biogenic Carbon and Temporary Storage Addressed with Dynamic Life Cycle Assessment', *Journal of Industrial Ecology*, vol. 17, no. 1, pp. 117–128, Feb. 2013, doi: 10.1111/j.1530-9290.2012.00503.x.

[221] A. Levasseur, P. Lesage, M. Margni, L. Deschênes, and R. Samson, 'Considering Time in LCA: Dynamic LCA and Its Application to Global Warming Impact Assessments', *Environ. Sci. Technol.*, vol. 44, no. 8, pp. 3169–3174, Apr. 2010, doi: 10.1021/es9030003.

[222] A. Ventura, 'Conceptual issue of the dynamic GWP indicator and solution', *Int J Life Cycle Assess*, Feb. 2022, doi: 10.1007/s11367-022-02028-x.

[223] P. Pawelzik *et al.*, 'Critical aspects in the life cycle assessment (LCA) of bio-based materials – Reviewing methodologies and deriving recommendations', *Resources, Conservation and Recycling*, vol. 73, pp. 211–228, Apr. 2013, doi: 10.1016/j.resconrec.2013.02.006.

[224] European Commission. Directorate-General for Enterprise and Industry, *Taking bio-based from promise to market: measures to promote the market introduction of innovative bio-based products*. BE: European Commission, 2009. Accessed: Mar. 03, 2022. [Online]. Available: https://data.europa.eu/doi/10.2769/34881

[225] D. Tonini, L. Hamelin, and T. F. Astrup, 'Environmental implications of the use of agro-industrial residues for biorefineries: application of a deterministic model for indirect land-use changes', *GCB Bioenergy*, vol. 8, no. 4, pp. 690–706, 2016, doi: https://doi.org/10.1111/gcbb.12290.

[226] B. Wicke, P. Verweij, H. van Meijl, D. P. van Vuuren, and A. P. Faaij, 'Indirect land use change: review of existing models and strategies for mitigation', *Biofuels*, vol. 3, no. 1, pp. 87–100, Jan. 2012, doi: 10.4155/bfs.11.154.

[227] V. Daioglou *et al.*, 'Progress and barriers in understanding and preventing indirect land-use change', *Biofuels, Bioproducts and Biorefining*, vol. 14, no. 5, pp. 924–934, 2020, doi: https://doi.org/10.1002/bbb.2124.

[228] J. H. Schmidt, B. P. Weidema, and M. Brandão, 'A framework for modelling indirect land use changes in Life Cycle Assessment', *Journal of Cleaner Production*, vol. 99, pp. 230–238, Jul. 2015, doi: 10.1016/j.jclepro.2015.03.013.

[229] A. C. Hetherington, A. L. Borrion, O. G. Griffiths, and M. C. McManus, 'Use of LCA as a development tool within early research: challenges and issues across different sectors', *The International Journal of Life Cycle Assessment*, vol. 19, no. 1, pp. 130–143, Jan. 2014, doi: 10.1007/s11367-013-0627-8.

[230] S. Cucurachi, C. van der Giesen, and J. Guinée, 'Ex-ante LCA of Emerging Technologies', *Procedia CIRP*, vol. 69, pp. 463–468, 2018, doi: 10.1016/j.procir.2017.11.005.

[231] J. A. Bergerson *et al.*, 'Life cycle assessment of emerging technologies: Evaluation techniques at different stages of market and technical maturity', *Journal of Industrial Ecology*, vol. 24, no. 1, pp. 11–25, Feb. 2020, doi: 10.1111/jiec.12954.

[232] A. Azapagic and R. Clift, 'The application of life cycle assessment to process optimisation', *Computers & Chemical Engineering*, vol. 23, no. 10, pp. 1509–1526, Dec. 1999, doi: 10.1016/S0098-1354(99)00308-7.

[233] C. Pieragostini, M. C. Mussati, and P. Aguirre, 'On process optimization considering LCA methodology', *Journal of Environmental Management*, vol. 96, no. 1, pp. 43–54, Apr. 2012, doi: 10.1016/j.jenvman.2011.10.014.

[234] J. Steimel, M. Harrmann, G. Schembecker, and S. Engell, 'Model-based conceptual design and optimization tool support for the early stage development of chemical processes under uncertainty', *Computers & Chemical Engineering*, vol. 59, pp. 63–73, Dec. 2013, doi: 10.1016/j.compchemeng.2013.06.017.

[235] G. Guillen-Gosalbez, A. Caballero, and L. Jimenez, 'Application of Life Cycle Assessment to the Structural Optimization of Process Flowsheets', *Industrial & Engineering Chemistry Research*, vol. 47, no. 3, pp. 777–789, Jan. 2008, doi: https://doi.org/10.1021/ie070448+.

[236] G. Guillén-Gosálbez, F. You, Á. Galán-Martín, C. Pozo, and I. E. Grossmann, 'Process systems engineering thinking and tools applied to sustainability problems: current landscape and future opportunities', *Current Opinion in Chemical Engineering*, vol. 26, pp. 170–179, Dec. 2019, doi: 10.1016/j.coche.2019.11.002.

[237] N. Itsubo and A. Inaba, 'A new LCIA method: LIME has been completed', *The International Journal of Life Cycle Assessment*, vol. 8, no. 5, pp. 305–305, Sep. 2003, doi: 10.1007/BF02978923.

[238] TNO Biobased and Circular Technologies, 'Phyllis2 - Database for the physico-chemical composition of (treated) lignocellulosic biomass, micro- and macroalgae, various feedstocks for biogas production and biochar'. Accessed: Aug. 08, 2023. [Online]. Available: https://phyllis.nl/

[239] 'International - U.S. Energy Information Administration (EIA)'. Accessed: May 05, 2024. [Online]. Available: https://www.eia.gov/international/analysis/country/CHN

[240] 'Dominican Republic - Countries & Regions', IEA. Accessed: May 05, 2024. [Online]. Available: https://www.iea.org/countries/dominican-republic/energy-mix

[241] L. Tomas da Rocha, H. Kim, C. Lee, and S.-M. Jung, 'Mechanism of NO_x Formation from Nitrogen in the Combustion of the Coals Used in Sintering Process', *Metall Mater Trans B*, vol. 51, no. 5, pp. 2068–2078, Oct. 2020, doi: 10.1007/s11663-020-01923-8.

[242] A. K. Singh, R. E. Masto, B. Hazra, J. Esterle, and P. K. Singh, 'Environmental Effects of Coal and Biomass Ash Generation', in *Ash*

from Coal and Biomass Combustion, Eds., Cham: Springer International Publishing, 2020, pp. 91–114. doi: 10.1007/978-3-030-56981-5_4.

[243] S. A. Sharifi, M. Zaeimdar, S. A. Jozi, and R. Hejazi, 'Effects of Soil, Water and Air Pollution with Heavy Metal Ions Around Lead and Zinc Mining and Processing Factories', *Water Air Soil Pollut*, vol. 234, no. 12, p. 760, Dec. 2023, doi: 10.1007/s11270-023-06758-y.

[244] J. Yang, J. Sun, R. Wang, and Y. Qu, 'Treatment of drilling fluid waste during oil and gas drilling: a review', *Environ Sci Pollut Res*, vol. 30, no. 8, pp. 19662–19682, Feb. 2023, doi: 10.1007/s11356-022-25114-x.

[245] S. Dahija, S. Pilić, and R. Bešta-Gajević, 'Speciation, Mobilization, and Toxicity of Cadmium in Soil–Microbe–Plant System: An Overview', in *Cadmium Toxicity Mitigation*, A. K. Jha and N. Kumar, Eds., Cham: Springer Nature Switzerland, 2024, pp. 31–61. doi: 10.1007/978-3-031-47390-6_2.

[246] M. Pazalja *et al.*, 'Heavy metals content in ashes of wood pellets and the health risk assessment related to their presence in the environment', *Sci Rep*, vol. 11, no. 1, p. 17952, Sep. 2021, doi: 10.1038/s41598-021-97305-4.

[247] Olli Sippula, *Fine particle formation and emissions in biomass combustion*. in Report series in Aeropsol Science, no. 108. Kuopio, Finland: University of Eastern Finland, 2010. Accessed: May 15, 2024. [Online]. Available: https://www.researchgate.net/publication/266564189_fine_particle_formation_and_emissions_in_biomass_combustion

[248] 'Process Design Center (PDC)', Process Design Center. Accessed: May 24, 2024. [Online]. Available: https://www.process-design-center.com/who-we-are/

[249] G. D. Ulrich, *Chemical Engineering Process Design and Economics: A Practical Guide*. Process Publishing, 2004.

[250] S. Ceschin, A. Bellini, and M. Scalici, 'Aquatic plants and ecotoxicological assessment in freshwater ecosystems: a review', *Environ Sci Pollut Res*, vol. 28, no. 5, pp. 4975–4988, Feb. 2021, doi: 10.1007/s11356-020-11496-3.

[251] C. Meili, N. Jungbluth, and J. Annaheim, 'Life cycle inventories of crude oil extraction', ESU-services Ltd., Schaffhausen, Switzerland, 2022. [Online]. Available: https://esu-services.ch/data/public-lci-reports/

[252] O. P. Missen *et al.*, 'Love is in the Earth: A review of tellurium (bio)geochemistry in surface environments', *Earth-Science Reviews*, vol. 204, p. 103150, May 2020, doi: 10.1016/j.earscirev.2020.103150.

[253] F. M. Makuei and G. Senanayake, 'Extraction of tellurium from lead and copper bearing feed materials and interim metallurgical products – A short review', *Minerals Engineering*, vol. 115, pp. 79–87, Jan. 2018, doi: 10.1016/j.mineng.2017.10.013.

[254] 'Cuarto Inventario Forestal Nacional', Ministerio para la Transición Ecológica y el Reto Demográfico. Accessed: Mar. 25, 2024. [Online]. Available:

https://www.miteco.gob.es/es/biodiversidad/temas/inventarios-nacionales/inventario-forestal-nacional/cuarto_inventario.html

[255] A. Sultana and A. Kumar, 'Optimal configuration and combination of multiple lignocellulosic biomass feedstocks delivery to a biorefinery', *Bioresource Technology*, vol. 102, no. 21, pp. 9947–9956, Nov. 2011, doi: 10.1016/j.biortech.2011.07.119.

[256] W. Li, H. Sun, G. Wang, W. Sui, L. Dai, and C. Si, 'Lignin as a green and multifunctional alternative to phenol for resin synthesis', *Green Chem.*, vol. 25, no. 6, pp. 2241–2261, Mar. 2023, doi: 10.1039/D2GC04319J.

[257] L. Hu, H. Pan, Y. Zhou, and M. Zhang, 'Methods to improve lignin's reactivity as a phenol substitute and as replacement for other phenolic compounds: A brief review.', *BioResources*, vol. 6, no. 3, pp. 3515–3525, 2011.

FIGURES LIST

INTRODUCTION

METHODOLOGY

CHAPTER I (LCA REVIEW)

CHAPTER II (BENCHMARK TECHNOLOGIES)

CHAPTER III (FRACTIONATION TECHNOLOGY)

TABLES LIST

INTRODUCTION

METHODOLOGY

CHAPTER I (LCA REVIEW)

CHAPTER II (BENCHMARK TECHNOLOGIES)

CHAPTER III (FRACTIONATION TECHNOLOGY)

PUBLICATIONS LIST

PUBLICATIONS IN THE SCOPE OF THE THESIS

Blanco-Cejas J., Martín S., Linares M., Iglesias J., Moreno J. *Life cycle assessment applied to bio-based platform molecules: Critical review of methodological practices*. Journal of Cleaner Production 414, 137513 (2023).

GLOSSARY OF TERMS AND ABBREVIATIONS

METHODOLOGY

$C_i^{\propto}$	*Concentration of component i to the stoichiometric factor of the specie*
$-r_i$	*Reaction rate of component i*
A	*Pre-exponential factor on Arrhenius equation*
E_A	*Molar energy of activation*
R	*Universal gas constant*
$K_{f\text{-}r}$	*Kinetic constant of the forward and reverse reactions*
K_i	*Adsorption equilibrium constant for species i*

CHAPTER II (BENCHMARK TECHNOLOGIES)

CBP	*Chinese Batch Process*
QOP	*Quaker Oats Process*
LPS	*Low-Pressure Steam*
MPS	*Medium-Pressure Steam*
HPS	*High-Pressure Steam*

ENVIRONMENTAL FOOTPRINT 3.1 MIDPOINT INDICATORS

AC	*Acidification (mol H^+ eq.)*
GWP100	*Global Warming Potential (kg CO_2 eq.)*
FWET	*Freshwater Ecotoxicity (CTUe)*
ADPf	*Abiotic Depletion Potential, fossil consumption (MJ)*
FWEP	*Freshwater Eutrophication (kg P eq.)*
MEP	*Marine Eutrophication (kg N eq.)*
TEP	*Terrestrial Eutrophication (mol N eq.)*
HTc	*Human Toxicity, cancer effects (CTUh)*
HTnc	*Human Toxicity, non-cancer effects (CTUh)*
IR	*Ionising Radiation (kBq U235 eq.)*
LU	*Land Use (dimensionless)*

ADPm	*Abiotic Depletion Potential, minerals/metals (kg Sb eq.)*
ODP	*Ozone Depletion Potential (kg CFC-11 eq.)*
PMF	*Particulate Matter Formation (disease incidences)*
POF	*Photochemical Ozone Formation (kg NMVOC eq.)*
WU	*Water Use, deprivation (m^3 world eq.)*

CHAPTER III (FRACTIONATION TECHNOLOGY)

FTP	*Fractionation Process*

OPTIMIZATION MODEL: SETS

I :=	{*i: farming sites*}
J :=	{*j: production plants sites*}
K :=	{*k: market sites*}
T :=	{*t: conventional technologies sites*}
P :=	{*p: products commercialized*}
E :=	{*e: environmental endpoints*}
B :=	{*b: biomass type*}
V :=	{*v: transport type*}

OPTIMIZATION MODEL: SUBSETS

$FR_{i,j,v}$:=	{*i,b: transport routes forbidden for biomass b from sites i*}
$FR_{j,k,v}$:=	{*j,p: transport routes forbidden for products p from plants j*}
$FR_{t,k,p,v}$ =	{*t,p: transport routes forbidden for products p from conventional plants t*}

OPTIMIZATION MODEL: PARAMETERS

$\bar{F}_{ib}^{bms}$	*Biomass production upper bound [ton·y⁻¹, wet basis]*
$LOSS_b^{hrv}$	*Biomass b losses during harvesting [ton·y⁻¹, wet basis]*
$LOSS_b^{chp}$	*Biomass b losses during chipping [ton·y⁻¹, wet basis]*
CC_b	*Carbon content of biomass b [t carbon per ton of biomass (wt.%), dry basis]*

M^{CO2}	*Molecular weight of CO_2 [g·mol⁻¹]*
M^{C}	*Molecular weight of carbon [g·mol⁻¹]*
$LOSS^{tp}$	*Biomass losses during transportation from i to j [ton·y⁻¹, wet basis]*
CAP_{j}^{plt}	*Capacity of each plant j to assimilate an input of biomass b [ton·y⁻¹]*
$OPPLANTS$	*Operating plants upper bound*
$CV_{b,p}$	*Yields matrix of products p from biomass type b [%]*
$\bar{F}_{tp}^{cnv}$	*Capacity of each conventional site p to produce a product p [ton·y⁻¹]*
DD_{kp}^{mkt}	*Demand of each product p in each market k [ton·y⁻¹]*
UC_{b}^{hrv}	*Price of 1 ton of biomass b harvested in i [€·t⁻¹]*
UC_{ib}^{chp}	*Price of 1 ton of chips produced at i [€·t⁻¹]*
UC_{v}^{tp}	*Unitary costs of vehicles v use [€·tkm⁻¹]*
D_{vij}^{i}	*Distance between nodes i and j by transport v [Km]*
CFD_{v}^{chp}	*Correction factor of capacity to density*
$OPEX^{plt}$	*Operating costs of each plant j [€·t⁻¹, per ton of input chips]*
D_{vjk}^{j}	*Distance between nodes j and k by transport v [Km]*
D_{vtk}^{t}	*Distance between nodes t and k by transport v [Km]*
UC_{p}^{cvprd}	*Unitary cost of conventional products [€·t⁻¹]*
UC_{p}^{prd}	*Unitary cost (negative) of alternative products [€·t⁻¹]*
IMP_{be}^{chp}	*Impact vector of chipping biomass b [impact·t⁻¹]*
IMP_{ve}^{tp}	*Impact vector of vehicles use [impact·tkm⁻¹]*
IMP_{ibe}^{iloss}	*Impact vector of emissions from biomass oxidation at i [impact·t⁻¹]*
IMP_{ibe}^{jloss}	*Impact vector of emissions from biomass oxidation at j [impact·t⁻¹]*
IMP_{e}^{plt}	*Impact vector of plant j operation [impact·t-1 of chips]*
IMP_{pe}^{cvprd}	*Impact vector of products p [impact·t⁻¹]*

OPTIMIZATION MODEL: VARIABLES

f_{ib}^{grw}	*Biomass b available in region i [t·y⁻¹, wet basis]*
f_{ib}^{hrv}	*Biomass b harvested in region i after losses [t·y⁻¹, wet basis]*
em_{ib}^{lshrv}	*Emissions of oxidized biomass b lost during harvesting at i [t of CO_2·y⁻¹]*
f_{ib}^{chp}	*Chips of biomass b in region i after losses [t·y⁻¹, wet basis]*
em_{ib}^{lschp}	*Emissions of oxidized biomass b lost during chipping at i [t of CO_2·y⁻¹]*
tp_{ijbv}^{chp}	*Biomass b transported from i to j via v in form of chips [t·y⁻¹, wet basis]*
$f_{j,b}^{chpav}$	*Chips available at plants j [t·y⁻¹, wet basis]*
em_{jb}^{lstp}	*Emissions of biomass b lost during transport from i to j [t of CO_2·y⁻¹]*
f_{j}^{chpt}	*Total amount of chips at plants j [t·y⁻¹, wet basis]*
BAU_j	*Discrete variable to allow / neglect each plant j operation*
f_{jp}^{plt}	*Products p available as outputs in each plant j [t·y⁻¹]*
tp_{jkpv}^{prd}	*Products p transported from j to k in v [t·y⁻¹]*
f_{kp}^{pmkt}	*Products available at final demand sites from j [t·y⁻¹]*
f_{tp}^{cvprd}	*Products p available at conventional sites t [t·y⁻¹]*
tp_{tkpv}^{cvprd}	*Products p transported from t to k in v [t·y⁻¹]*
f_{tp}^{cvmkt}	*Products available at final demand sites from t [t·y⁻¹]*
co_{ib}^{bms}	*Cost of the purchased biomass b in i [€·y⁻¹]*
co_{ib}^{chp}	*Cost of chipping biomass b in each location i [€·y⁻¹]*
co_{ijbv}^{itp}	*Total cost of transportation of chips from i to j [€·y⁻¹]*
co_{j}^{plt}	*Total cost of plant j operation [€·y⁻¹]*
co_{jkpv}^{jtp}	*Total cost of transportation of products p from j to k [€·y⁻¹]*
co_{tkpv}^{ttp}	*Total cost of transportation of products p from t to k [€·y⁻¹]*

co_{pk}^{cvmkt}	*Total cost of conventional products purchase [€·y⁻¹]*
co_{pk}^{pmkt}	*(Negative) costs of selling products from j [€·y⁻¹]*
co	*Total cost function [€·y⁻¹]*
ei_{ibe}^{chp}	*Impact of biomass b harvesting and chipping at i [imact·y⁻¹]*
ei_{ijvbe}^{itp}	*Environmental impact of transportation of chips from i to j [impact·y⁻¹]*
ei_{ibe}^{iloss}	*Impact of emissions from oxidized biomass b losses at i impact ·y-1]*
ei_{ibe}^{jloss}	*Impact of emissions from oxidized biomass b losses at j impact ·y-1]*
ei_{j}^{plt}	*Environmental impact of plant j operation [impact·y⁻¹]*
ei_{jkpve}^{jtp}	*Environmental impact of transportation of chips from j to k [impact·y⁻¹]*
ei_{tkpve}^{ttp}	*Environmental impact of transportation of chips from t to k [impact·y⁻¹]*
ei_{pk}^{cvmkt}	*Environmental impact of purchasing conventional products [impact·y⁻¹]*
ei_{RD}	*Resources depletion function*
ei_{EQ}	*Ecosystem quality function*
ei_{HH}	*Human health function*

ReCiPe2016 MIDPOINT INDICATORS

TAP	*Terrestrial Acidification potential (Kg SO_2 - eq.)*
GWP100	*Global Warming Potential (kg CO_2 eq.)*
FETP	*Freshwater Ecotoxicity Potential (Kg 1,4-DCB - eq.)*
METP	*Marine Ecotoxicity Potential (Kg 1,4-DCB - eq.)*
TETP	*Terrestrial Ecotoxicity Potential (Kg 1,4-DCB - eq.)*
FFP	*Fossil Fuel Potential (Kg oil - eq.)*
FEP	*Freshwater Eutrophication Potential (Kg P - eq.)*
MEP	*Marine Eutrophication Potential (Kg N - eq.)*
HTPc	*Human Toxicity Potential, cancer (Kg 1,4-DCB - eq.)*
HTPnc	*Human Toxicity Potential, non-cancer (Kg 1,4-DCB - eq.)*

IRP	*Ionising Radiation (Kg Co-60 - eq.)*
LOP	*Agricultural Land Occupation Potential (m^2 crop - eq.)*
SOP	*Surplus Ore Potential (Kg Cu - eq.)*
ODP	*Ozone Depletion Potential (Kg CFC-11 - eq.)*
PMFP	*Particulate Matter Formation- Potential (Kg PM2.5 - eq.)*
HOFP	*Photochemical Oxidant Formation Potential, humans (Kg NO_x - eq.)*
EOFP	*Photochemical Oxidant Formation Potential, ecosystems (Kg NO_x - eq.)*
WCP	*Water Consumption Potential [m^3]*

APPENDIX

CHAPTER II (BENCHMARK TECHNOLOGIES)

A. Streams composition and conditions in the QOP and CBP

Tables A1 and A2 show the composition and conditions of the main input and output streams of the QOP and CBP respectively. Only the streams providing the most relevant information for reproducibility purposes are shown for clarity. The mass flows are referred to the production of 20,000 tonne/year of furfural, unlike Tables 5.3 and 5.4 shown in the text, which are normalised to 1 tonne of furfural for LCA reasons.

Table A 1. Mass flow rate and conditions of main input/output streams in the QOP.

	Stream				
	catalyst	**scb**	**spent**	**carbox**	**furfural**
Temp. (°C)	25	25	153.1	99.6	92.4
Pressure (bar)	1.01	1.01	5.1	1.01	0.2
Solids fraction	0	0.93	0.55	0	0
Mass flow rate (kg/h) per component					
Cellulose		6551.8	6352.9		
Xylan		5962	49.5		
Arabinan		808.26	11		
Lignin		1599.7	1554.3		
Ash		1272	1272.1		
Acetyl		648.6	0.1		
Formyl		6.7	6.7		
Tar 1			1094.7		
Tar 2			1121		
Glucose			221	<0.1	
Xylose			228.3	<0.1	
Arabinose			32	<0.1	
Xylose intermediates			14.9	<0.1	
Acetic acid			112.9	488	<0.1
Formic acid			0		
Water	4515.5	1344.3	8279.8	41030	12.6
Sulphuric acid	377.4		376.3	1.1	
Furfural			184.5	42.8	2506.9

Table A 2. Mass flow rate of main input/output streams in the CBP.

	Stream					
	water	**H_2SO_4**	**biomass**	**spent**	**carbox**	**furfural**
Temp. (°C)	25	25	25	159.9	99.6	92.4
Pressure (bar)	1.01	1.01	1.01	6.1	1.01	0.2
Solids fraction	0	0	0.87	0.28	0	0
Mass flow rate (kg/h) per component						
Cellulose			9604.3	8322.4		
Xylan			5971.25	11		
Arabinan			809.7	1.5		
Lignin			3544	3544		
Ash			661.6	661.6		
Acetyl			652.1	0.1		
Formyl			7.1	7.1		
Tar 1				1674		
Tar 2				265.1		
Glucose				1424.4	<0.1	
Xylose				141.3	<0.1	
Arabinose				19.2	<0.1	
Xylose intermediates				9.1	<0.1	
Acetic acid				206.4	415.7	<0.1
Formic acid						
Methanol						
Water	28153.6		3187.5	35383	61377.3	12.6
Sulphuric acid		477.3		476.5	0.8	
Furfural				379.7	45.6	2507.5

CHAPTER III (FRACTIONATION TECHNOLOGY)

B. Streams composition and conditions in the FTP

The composition and conditions of the most relevant streams in the FTP are shown in Tables A3 to A5. All streams are referred to a plant with a processing capacity of 25 tonnes per hour of eucalyptus chips. The results are presented in three tables. The first table presents the inputs to the process, namely GVL makeup, water makeup, sulphuric acid, quicklime, and biomass. The second table presents data on the waste streams, including tars, acetic acid, calcium sulphate, and calcium oxide. The final table presents data on the plant products (cellulose, lignin, furfural, and low-grade lignin).

Table A 3. Mass flow rate and conditions of main input streams in the FTP. S1 and S2 refer to fresh addition of GVL and water, respectively.

	Stream				
	S1 (GVL)	**S2 (H_2O)**	**S3 (H_2SO_4)**	**S7 (biomass)**	**S73 (quicklime)**
Temp. (°C)	25	25	25		
Pressure (bar)	1.01	1.01	1.01		
V_{frac}	0	0	0		
Solids fraction	0	0	0		
Mass flow rate (tonne/h) per component					
GVL	0.58				
Water		0.75			
H_2SO_4			0.98		
Biomass				25	
CaO					0.57

Table A 4. Mass flow rate and conditions of main waste streams in the FTP. S44 and S49 are avoided in the final process concept.

	Stream				
	S44 (water)	**S49 (acetic)**	**S59 (tars)**	**S76 (CaO)**	**S82 ($CaSO_4$)**
Temp. (°C)	*Not required*		225	40	91.6
Pressure (bar)			21	1	1.2
V_{frac}			0	0	0
Solids fraction			0	1	1
Mass flow rate (tonne/h) per component					
Tars	*Not required*		1.15		
CaO				0.02	
$CaSO_4$					1.35

Table A 5. Mass flow rate and conditions of main product streams in the FTP.

	Stream			
	S17 (cellulose)	**S25 (lignin)**	**S71 (furfural)**	**S91 (lignin, lg)**
Temp. (°C)	27.3	33.6	167.8	242.6
Pressure (bar)	1.01	1.01	1.2	0.1
V_{frac}	0	0	0	0
Solids fraction	0.73	0	0	0
Mass flow rate (tonne/h) per component				
GVL	0.47	0.01	0.02	
Water	5.49	0.05		
Cellulose	10.69			
Glucose				0.2
Galactose				0.1
Mannose				0.06
Xylose	0.01			
Lignin	0.01	4.6		2.04
Extractives				0.01
Soluble ash				0.1
Non-soluble ash	0.03			
H_2SO_4	0.04	0.01		
Furfural			1.71	
HMF				0.28
Levulinic Acid				0.06

C. I/O Tables for Fractionation products

The table of inputs and outputs is presented for furfural, cellulose, and lignin in the fractionation process. The inventories were obtained using the subdivision method described in Section 6.3.I.

Table A 6. I/O inventory for cellulose, lignin and furfural.

Material/Utility	Unit	Cellulose	Lignin	Furfural
MP Steam		2.99	9.05	32.94
HP Steam		2.65	2.52	18.95
Cooling Water		3.02	1077.61	9.52
Electricity		20.69	19.65	73.33
Biomass		1.18	1.12	2.93
GVL	ton·ton(prod)$^{-1}$	0.03	0.03	0.07
Sulphuric Acid		0.05	0.04	0.12
Calcium Oxide		0.03	0.03	0.07
CO_2 (absorbed)		0.16	0.15	0.4
Wastewater		1.04	0.99	2.6
Product		1.00	1.00	1.00

D. Biomass abundance

The abundance of the different eucalyptus species was obtained from the Fourth National Forest Inventory of Spain. The results presented correspond to the annual tonnes ($\cdot 10^3$) of biomass available after discounting the current uses of this resource.

Table A 7. Biomass abundance per species and region.

	Eucalyptus globulus	*Eucalyptus nitens*	*Eucalyptus camadulensis*
A Corunha	1259.7	15.4	15.4
Asturias	653.4		
Cantabria	312.2		
Extremadura	4.9		119.4
Lugo	816.3	24.7	
Basque country	135.8	12.5	
Pontevedra	468.1		

E. Products demand

Table A3 presents the demand for the three products produced by the fractionation process, disaggregated by country. The demand is expressed in tonnes ($\cdot 10^3$) per year and is calculated following the methodology described in the main text.

Table A 8. Demand of cellulose, lignin and furfural in tonne/year, disaggregated by country.

	Cellulose	**Lignin (phenol)**	**Furfural**
Austria	20.92	39.77	
Belgium	7.83	74.81	20.82
Bulgaria	15.50	1.36	4.12E-04
Croatia	10.08	0.58	
Czechia		85.84	0.01
Denmark	21.57	7.48	
Estonia	1.16		
France	41.99		0.37
Germany			0.45
Greece	37.72	5.39	
Hungary	10.08	1.79	
Iceland		0.08	
Ireland			0.01
Italy	165.30	71.73	1.17
Latvia	2.79	11.10	
Lithuania	11.84		
Luxembourg	1.94	1.08	
Malta	1.94	0.05	
Netherlands		229.69	1.99
Norway	3.90	9.43	
Poland	129.12	101.71	0.48
Portugal	19.73	20.21	
Romania	38.38	6.41	5.93E-04
Slovakia	9.91	12.63	
Slovenia	31.69	14.46	
Spain	135.24		0.61
Switzerland		21.67	0.01